Adapting mechanistic isotope models to trace the geographical origin of agricultural products

Inauguraldissertation

zur

Erlangung der Würde eines Doktors der Philosophie

vorgelegt der

Philosophisch-Naturwissenschaftlichen Fakultät

der Universität Basel

von

Florian Cueni

2022

Genehmigt von der Philosophisch-Naturwissenschaftlichen Fakultät
Auftrag von

Prof. Dr. Ansgar Kahmen

Prof. Dr. Walter Salzburger

Prof. Dr. Jason B. West

Basel, den 15.12.2020

Prof. Dr. Martin Spiess
Dekan

Table of Contents

General introduction

"Italian police break mafia ring exporting fake olive oil to U.S." (Reuters 2017), "Big egg-fraud: Spanish instead of Swiss quail eggs" (SRF 2016), "Origin deception - Strawberry labeling-fraud" (DlF 2016) - news headlines similar to these are sadly not uncommon and all encompass a crime broadly known as food fraud. Food fraud is more specifically defined as the economically motivated and intentional act of deceptively adulterating food or food ingredients and thereby betraying consumers (Spink and Moyer 2011; van Ruth et al. 2017; European Commission 2018). The number of identified cases of food fraud might have increased in the last century, be it due to better analysis methods or the improved control of supply chains, however, food fraud is not a phenomenon of the recent human history. Food fraud has likely been practiced since mankind started trading food, and documented cases of food fraud date back several thousand years (Johnson 2014). Today, counterfeit food products are considered to make up 10 % to 30 % of all food sold worldwide, still, most cases of food fraud are not discovered (Johnson 2014; Manning 2016). The cost of food fraud is estimated to annually sum up to $10 to $40 billion (Johnson 2014; PwC and SSAFE 2016; Manning 2016). Usually, food fraud relates to false labelling of products, predominantly concerning the geographical origin. (Tähkäpää et al. 2015; European Commission 2019).

To counteract food fraud and regulate the indication of the origin of food, in recent years, different laws have been passed on the mandatory provision of the country of origin, mainly concerning the major ingredients of food or unprocessed food products (European Commission 2020a). In the European Union (EU) provenance declaration of such products is for example ruled by the regulation (EU) No 1169/2011, in the USA by the "Country of Origin Labeling" (COOL) law (U.S. Department of Agriculture 2020) (European Commission 2020a). Moreover, the globalization of food markets led to an increase in the variability and availability of food products from different countries and continents around the world. Consumers are thus increasingly interested in the geographic origin of food, which has been found to be the major information influencing consumers' decisions (Danezis et al. 2016; Bitzios et al. 2017). The reasons therefore are manifold but can often be related to the quality of food, good or bad, associated with certain regions (Camin et al. 2017). The proof of the geographic origin of food is thus getting

increasingly important for food quality control, to assure agreement with legislation, and for consumer protection (Drivelos and Georgiou 2012; Aung and Chang 2014). This raises the interest in tools and methods allowing the verification of the geographic origin of food (Danezis et al. 2016).

These days, different analytical techniques for the verification of the origin of food have been developed and are used in food quality control. These include the application of NMR, chromatography, or since more recently, the application of genomics and proteomics, which are rapidly replacing more traditional approaches (Danezis et al. 2016). The leading analytic method used for origin analysis of foodstuff is, however, stable isotope analysis. Routinely applied in food quality control laboratories worldwide, stable isotope analysis has been successfully used in many cases of food fraud (Rossmann et al. 1996; Rossmann 2001; Gonzalvez et al. 2009; Cerling et al. 2016; Camin et al. 2017; Carter and Chesson 2017).

But what exactly are stable isotopes? The term "isotope" describes versions of the same element, only differing in their number of neutrons. Stable isotopes, compared to unstable, short-living, radioactive isotopes, do not decay and can, for example, be used in forensic applications. Stable isotopes of an element naturally occur in different abundances. In oxygen for example, the light ^{16}O stable isotope is the most common, occurring with 99.7630 %, while the heavier ^{17}O and ^{18}O stable isotopes are only found in 0.0375 % and 0.1995 % of the cases, respectively (Hoefs 2009). Due to the differing element weights of stable isotopes, this ratio of natural abundance is changing through chemical and physical processes, which leads to product specific isotope ratios that can be used for forensic analysis (Cerling et al. 2016). The ratios of the abundance of stable isotopes are expressed in delta (δ) notation and shown in per mil (‰), as a ratio of the heavy over the light isotope of the sample (R_{sample}) in relation to the same ratio of an international standard ($R_{standart}$). Stable isotope ratios are calculated using following equation (Eqn. 1) where for the example of oxygen R is the $^{18}O/^{16}O$ ratio (Coplen 2011):

Equation 1: $\delta_{sample} = (R_{sample}/R_{standard}) - 1$, ‰

The application of stable isotopes to verify the geographic origin of food is particularly suited for agricultural products. The ratios of the

abundance of stable isotopes, here after called the stable isotope composition, of plants' tissue water and organic compounds reflect location specific, robust isotopic fingerprints (Carter and Chesson 2017). The isotopic composition of oxygen and hydrogen for example is influenced by the distinct geography and climate of the plant's growing location (Dansgaard 1964; Bowen 2010), the underlying geology is the major driver of the composition of sulfur (Krouse 1989), and agricultural practices influence the nitrogen isotope composition found in plants (Bateman et al. 2007). The isotopic fingerprints of agricultural products have, amongst others, been used for the origin determination of cereals (Goitom Asfaha et al. 2011; Luo et al. 2015), olive oil (Camin et al. 2010), and coffee (Santato et al. 2012).

For the origin analysis of agricultural products, especially the oxygen ($\delta^{18}O$) and hydrogen ($\delta^{2}H$) isotope composition of a plant's tissue water and organic compounds is used, because, as stated before, they directly reflect a plant's geographic origin (Carter and Chesson 2017). This is, since the $\delta^{18}O$ and $\delta^{2}H$ values of precipitation show distinct temporal and geographic patterns (Dansgaard 1964; Bowen 2010). These patterns are also reflected in $\delta^{18}O$ and $\delta^{2}H$ values of a plant's leaf water, and its organic compounds, such as cellulose or leaf wax *n*-alkanes (Epstein et al. 1977; Sternberg et al. 1986; Yakir and DeNiro 1990; Sachse et al. 2012). However, the $\delta^{18}O$ and $\delta^{2}H$ values plant's leaf water and organic compounds not only reflect the isotope composition of precipitation but are also strongly influenced by the plant's growing season climate (Barbour et al. 2000; Barbour 2007). The $\delta^{18}O$ and $\delta^{2}H$ values of plants' tissue water and organic compounds, therefore, carry distinct information of a plant's growing location, and the growing season specific climate conditions. Especially the $\delta^{18}O$ and $\delta^{2}H$ values of plant organic compounds, have thus been established as critical climatic indicators across space and time (Treydte et al. 2006; Sachse et al. 2012), and more importantly for this thesis, they are routinely used in forensic origin analyses (Rossmann 2001; Cerling et al. 2016; Camin et al. 2017; Carter and Chesson 2017).

Forensic origin analyses with stable isotopes are usually done on a comparative basis, where the isotope composition of a suspicious fraudulent sample with uncertain origin, is compared to the isotope compositions authentic reference samples of known origin (Carter and Chesson 2017). This allows for simple analyses of the results, and thus is easily understood by laypeople like customers or judges in court (Carter and Chesson 2017). Other

applications use geostatistical spatial modelling (e.g. kriging) to interpolate the isotopic composition of a product over a large geographic region (West et al. 2007; Chesson et al. 2014; Chiocchini et al. 2016). Such applications allow for predictions of the geographic origin of suspicious samples, also in regions where no reference material has been collected (Cerling et al. 2016). However, for the geostatistical, spatial modelling approach, the collection of big reference data sets with samples distributed evenly over the large geographic region, is essential. The collection of authentic reference samples for both approaches is expensive and takes a lot of effort to organize and conduct, especially over bigger geographical scales.

In the past decades, mechanistic plant physiological stable isotope models have been developed that allow the prediction of $\delta^{18}O$ and $\delta^{2}H$ values of plant leaf water and plant organic compounds based on environmental and physiological input variables (Sternberg and DeNiro 1983; Flanagan et al. 1991; Flanagan and Ehleringer 1991; Farquhar and Lloyd 1993; Roden et al. 1999; Roden and Ehleringer 1999a; Barbour and Farquhar 2000; Farquhar et al. 2007). In many cases such models may be adapted for use with only temperature and vapor pressure as external input variables, and can therefore be used to calculate the $\delta^{18}O$ and $\delta^{2}H$ values of plant water or tissues for a given geographic location based on climate data. Plant physiological stable isotope models have thereby been applied to spatial scale and been used to model the geographic distribution of $\delta^{18}O$ and $\delta^{2}H$ values of plant leaf water or the cellulose of cotton (West et al. 2008, 2010; Kahmen et al. 2013). Through similar spatial applications, plant physiological stable isotope models could help to validate the geographic origin of a sample based on the comparison between simulated and measured $\delta^{18}O$ and $\delta^{2}H$ values of plant organic compounds. They could thus act as an alternative for predicting the geographic origin of agricultural plant products, while also expanding the potential geographic reach with which these methods could be applied to evaluate possible growth locations of a suspicious sample, independent of authentic reference samples.

The aim of mechanistic plant physiological stable isotope models is to simulate $\delta^{18}O$ and $\delta^{2}H$ values of plant tissue water or organic compounds. The Craig-Gordon model (Craig and Gordon 1965), which was developed to mathematically describe the isotopic enrichment of standing water bodies and was later modified for plants (Dongmann et al. 1974; Farquhar and Lloyd

1993) is the base for most modelling process for $\delta^{18}O$ and $\delta^{2}H$ values in plants. It describes how evaporative conditions (air temperature and vapor pressure) lead to ^{18}O- and ^{2}H-enrichment of water within leaves (Farquhar and Lloyd 1993; Roden et al. 1999). The Craig-Gordon model however usually overpredicts measured bulk leaf water $\delta^{18}O$ and $\delta^{2}H$ values (Cernusak et al. 2005; Kahmen et al. 2008). This deviation of Craig-Gordon-model predictions from measured values can be corrected for with the so called two-pool modification to the Craig-Gordon model (Leaney et al. 1985; Yakir 1989). This modification accounts for the overestimation of the Craig-Gordon model, by separating the bulk leaf water into an evaporatively enriched fraction at the site of evaporation (calculated by the Craig-Gordon model) (Flanagan et al. 1991; Yakir et al. 1994) and an unenriched water fraction equal to the source water of the plant.

As described before, the $\delta^{18}O$ and $\delta^{2}H$ values in organic compounds in of plants generally reflect the $\delta^{18}O$ and $\delta^{2}H$ values of the bulk leaf water (Sternberg et al. 1986; Yakir and DeNiro 1990; Roden and Ehleringer 1999a). However, fractionation effects alter the $\delta^{18}O$ and $\delta^{2}H$ values of the bulk leaf water that are found in organic material of plants. These isotope fractionations can be grouped into processes associated with the primary carbon fixation during the light reaction of photosynthesis, and post-photosynthetic processes leading to oxygen and hydrogen exchange with medium water during carbohydrate synthesis. This results in organic tissue of plants to be generally enriched in ^{18}O but depleted in ^{2}H compared to leaf water (Sternberg and DeNiro 1983; Yakir and DeNiro 1990; Luo and Sternberg 1992; Yakir 1992; Roden et al. 1999; Barbour and Farquhar 2000; Sternberg and Ellsworth 2011; Cormier et al. 2018). Model additions to the basic two-pool modified Craig-Gordon model which simulates the leaf-water of plants, allow for the prediction of the $\delta^{18}O$ and $\delta^{2}H$ values of cellulose or bulk organic compounds of plants, by accounting for the isotope fractionations and the exchange of oxygen and hydrogen with medium water during carbohydrate synthesis (Roden and Ehleringer 1999a; Barbour and Farquhar 2000).

Widespread application of plant physiological stable isotope models for origin identification of agricultural products is, however, yet pending. This is, since for precise model simulations of the $\delta^{18}O$ and $\delta^{2}H$ values of tissue water and organic compounds of plants, the essential model parameters describing the evaporative enrichment of leaf water, the two-pool factor accounting for the modelled leaf water overestimation, and the parameters

accounting for the exchange of oxygen and hydrogen during carbohydrate synthesis have to be carefully constrained. While an increasing number of studies have done this for leaf water (Allison 1985; Walker et al. 1989; Flanagan et al. 1991; Roden and Ehleringer 1999b; Song et al. 2015), and leaf or stem organic compounds (Barbour et al. 2000; Helliker and Ehleringer 2002; Barbour et al. 2004; Kahmen et al. 2011; Cheesman and Cernusak 2016), these parameters have yet to be experimentally determined for the tissue water or organic compounds of agricultural products. Moreover, to accurately simulate the spatial distribution of $\delta^{18}O$ and $\delta^{2}H$ values of tissue water or organic compounds of an agricultural product during a certain growing season, the exact type and timing of model input variables, responsible for the variability in the plant $\delta^{18}O$ and $\delta^{2}H$ values, need to be determined. This is for the climate (temperature and vapor pressure) during the growing season, as well as for the precipitation events determining the plant's source water $\delta^{18}O$ and $\delta^{2}H$ values. For such careful evaluations big, and spatially and timely heterogenous reference data sets are needed to compare different model simulations against, to define the most appropriate type and timing of model input variables required for the most accurate results.

The objective of my doctoral studies presented in this thesis, was to adapt the Craig-Gordon based stable isotope models for agricultural products, and to apply the models to a spatial scale, in order to use them as a further, logistically simple and low-cost method, for predicting the geographic origin of agricultural products.

In the first chapter of the thesis, we investigated whether a Craig-Gordon based isotope model can be employed to simulate the $\delta^{18}O$ and $\delta^{2}H$ values of tissue water and organic compounds of fruits (i.e. strawberries and raspberries). We assessed how the key model parameters for simulating tissue water and plant organic compounds in fruit differed from those of leaves. Moreover, we examined how the model needed to be parametrized for different evaporative environments. We thus conducted a controlled growth chamber experiment.

In the second chapter, we defined the variability in leaf water and grain tissue $\delta^{18}O$ and $\delta^{2}H$ values of different cereal species, cereals being the most important source of food for humans (FAO 2003). This allowed us to adapt the key model parameters of Craig-Gordon based isotope models for

cereals, and to describe the main drives of species-specific differences between cereals. We therefore grew seven different cereal species in the botanical garden of the University of Basel.

In the third chapter, we studied the variability in leaf water and grain tissue $\delta^{18}O$ and $\delta^{2}H$ values between varieties within one cereal species, winter wheat (*Triticum aestivum* L.), one of the main cereals worldwide (FAO 2020) and representing over 50 % of European cereal production (European Commission 2020b). Variety variability within species is important to assess, since for origin analysis, different varieties of the same species, possibly differing in their $\delta^{18}O$ and $\delta^{2}H$ values, are usually used in the same reference data sets. This could induce unwanted variability and reduce the precision of origin assignments. The samples used in this chapter of the thesis were grown in winter wheat variety experiments, established across Switzerland by the Swiss Institute for Sustainability Sciences (ISS) Agroscope.

In the fourth and final chapter, we applied the newly adapted isotope model for strawberries (Chapter 1) to a spatial scale and tested whether it could be used for origin analysis. We therefore carefully evaluated the type of isotopic and climatic input variables, with respect to their necessary spatial resolution and temporal integration, needed for the most accurate prediction of strawberry $\delta^{18}O$ values across Europe. This was achieved by validating our model predictions across space and time, with a unique Europe-wide strawberry $\delta^{18}O$ reference dataset, containing of 154 authentic reference samples that have been collected across Europe from 2007 to 2017. The samples of this exceptional dataset were provided by the industrial partner of this thesis, Agroisolab GmbH in Jülich, Germany.

The chapters of this thesis represent independent manuscripts, that are either published in or prepared for submission to internationally acknowledged, peer-reviewed journals. The manuscripts of the chapters thus comply with the guidelines of these different journals. Therefore, the formatting and citation style differs among the single chapters, and each chapter does have its own reference section. Co-authors of each chapter are named on the respective manuscript title pages. The literature cited in this general introduction can be found at the end of the thesis, together with the references of the Concluding discussion.

Chapter 1

Constraining parameter uncertainty for predicting oxygen and hydrogen isotope values in fruit

Florian Cueni*[1,2], Daniel B. Nelson[1], Marco M. Lehmann[3], Markus Boner[2], Ansgar Kahmen[1]

[1]University of Basel, Department of Environmental Sciences – Botany, Schönbeinstrasse 6, 4056 Basel, Switzerland
[2]Agroisolab GmbH, Professor-Rehm-Strasse 6, 52428 Jülich, Germany
[3]Forest dynamics, Swiss Federal Institute for Forest, Snow and Landscape Research (WSL), Zürcherstrasse 111, 8903 Birmensdorf, Switzerland
* Corresponding author: f.cueni.plantphys@gmail.com

This chapter is published in the ***Journal of Experimental Botany***.

DOI: https://doi.org/10.1093/jxb/erac180

Abstract
Understanding $\delta^{18}O$ and $\delta^{2}H$ values of agricultural products like fruit is of particular scientific interest in plant physiology, ecology, and forensic studies. Applications of mechanistic stable isotope models to predict $\delta^{18}O$ and $\delta^{2}H$ values of water and organic compounds in fruit, however, are hindered by a lack of empirical parameterizations and validations. We addressed this lack of data by experimentally evaluating model parameter values required to model $\delta^{18}O$ and $\delta^{2}H$ values of water and organic compounds in berries and leaves from strawberry and raspberry plants grown at different relative humidities. Our study revealed substantial differences between leaf and berry isotope values, consistent across the different RH treatments. We demonstrated that existing isotope models can reproduce water and organic $\delta^{18}O$ and $\delta^{2}H$ values for leaves and berries. Yet, these simulations require organ-specific model parameterization to accurately predict $\delta^{18}O$ and $\delta^{2}H$ values of leaf and berry tissue and water pools. We quantified these organ-specific model parameters for both species and RH conditions. Depending on the required model accuracy, species- and environment-specific model parameters may be justified. The parameter values determined in this study thus facilitate applications of stable isotope models where understanding $\delta^{18}O$ and $\delta^{2}H$ values of fruit is of scientific interest.

Introduction

The oxygen and hydrogen stable isotope composition of plants ($\delta^{18}O$ and $\delta^{2}H$ values, respectively) are valuable tools for a variety of ecological, plant physiological, paleoclimate, and forensic applications. Most investigations assessing controls on $\delta^{18}O$ and $\delta^{2}H$ values in plants have addressed variability in leaves or tree rings. In contrast, very few studies have assessed how $\delta^{18}O$ and $\delta^{2}H$ values of fruit vary in comparison to leaves and in response to environmental forcing. This lack of information limits the interpretation of $\delta^{18}O$ and $\delta^{2}H$ values in fruit, for example, in physiological or agronomic studies investigating the carbon and water dynamics of fruit. In addition, a better mechanistic understanding of the drivers of $\delta^{18}O$ and $\delta^{2}H$ values in fruit would allow these values to be employed in ecological investigations or in forensic applications, where $\delta^{18}O$ and $\delta^{2}H$ values can provide critical information for fruit origin identification (Bricout and Koziet, 1987; Rossmann *et al.*, 1996; Rossmann, 2001; West *et al.*, 2007; Gonzalvez *et al.*, 2009; Camin *et al.*, 2017; Bitter *et al.*, 2020).

Two prominent studies have investigated the isotopic composition of water in fruit (Dunbar and Wilson, 1983; Förstel and Hützen, 1984). Förstel and Hützen (1984) found that fruit water was isotopically similar to soil water, while Dunbar and Wilson (1983) found higher values in fruit tissue water than source water. To our knowledge, no study has yet assessed how $\delta^{18}O$ and $\delta^{2}H$ values of organic compounds or bulk tissue in fruit vary in comparison to other plant organs. Recent detailed investigations have demonstrated that post-photosynthetic biochemical transformations and allocation processes influence the $\delta^{18}O$ and, in particular, the $\delta^{2}H$ values of carbohydrates in plants (Gessler *et al.*, 2007, 2014; Cormier *et al.*, 2018, 2019). As fruit are a larger carbon sink tissue than leaves (e.g. Hoch, 2005), and not the primary site of photosynthesis, it is likely that $\delta^{18}O$ and $\delta^{2}H$ values of organic materials in fruit deviate from those of more commonly investigated leaves. Similarly, since the physical location, timing and rate of production, and associated processes that shape $\delta^{18}O$ and $\delta^{2}H$ values of fruit also differ from those that are relevant for tree-ring tissue, $\delta^{18}O$ and $\delta^{2}H$ values of organic materials in fruit may also differ from those of tree-rings, which are comparatively well-understood.

Key environmental and plant physiological drivers that explain variability $\delta^{18}O$ and $\delta^{2}H$ values in leaf water have been identified (Cernusak *et al.*, 2016), and controls on $\delta^{18}O$ and $\delta^{2}H$ values in plant-derived organic

compounds are increasingly well understood (Barbour and Farquhar, 2000; Gessler *et al.*, 2007; Kahmen *et al.*, 2013; Song *et al.*, 2014; Gamarra *et al.*, 2016; Lehmann *et al.*, 2017, 2020*b*,*a*; Cormier *et al.*, 2018, 2019). This has allowed the development of mechanistic isotope models, which have become critical tools for predicting and interpreting leaf water and plant-derived organic compound $\delta^{18}O$ and $\delta^{2}H$ values in a diverse range of applications (Sternberg and DeNiro, 1983; Flanagan and Ehleringer, 1991; Flanagan *et al.*, 1991; Farquhar and Lloyd, 1993; Roden *et al.*, 1999; Roden and Ehleringer, 1999; Barbour and Farquhar, 2000; Farquhar *et al.*, 2007). These models depend, on the one side, on the availability of accurate and precise environmental and physiological input variables, which include, for example, atmospheric humidity and temperature that directly determine the extent of evaporative ^{18}O- and ^{2}H-enrichment of leaf water. On the other hand, these models also depend on precise characterization of model parameters that determine the extent to which evaporatively ^{18}O- and ^{2}H-enriched leaf water is diluted by source water, and the extent to which biochemical isotopic fractionations and isotopic exchange processes between organic compounds and tissue water shape the ultimate $\delta^{18}O$ and $\delta^{2}H$ values of cellulose or plant bulk material. Given the lack of studies that have addressed the isotope composition of fruit, it is also unclear if leaf or tree-ring-derived values for model parameters can be employed to predict and interpret $\delta^{18}O$ and $\delta^{2}H$ values of water or organic compounds in fruit with existing stable isotope models.

The overall objective of this study was to determine whether $\delta^{18}O$ and $\delta^{2}H$ values of water or organic compounds in fruit differ in a predictable manner from those of leaves. In particular, we tested if values for model parameters that are necessary for predicting isotope values in fruit with existing stable isotope models differ from those of leaves, and if these parameter values differ among species and across different environments. Specifically, we addressed the following questions with a controlled growth chamber experiment:

1) How do $\delta^{18}O$ and $\delta^{2}H$ values of tissue water compare between leaves and fruit?
2) Do model parameter values for simulating plant water $\delta^{18}O$ and $\delta^{2}H$ values, i.e. the dilution of ^{18}O- and ^{2}H-enriched tissue water by source water, differ between leaves and fruit and are the values of these parameters consistent across different evaporative environments?

3) How do $\delta^{18}O$ and $\delta^{2}H$ values of different organic compound pools compare between leaves and fruit?
4) Do model parameter values for simulating plant organic compound $\delta^{18}O$ and $\delta^{2}H$ values, i.e. the biosynthetic isotopic fractionation from tissue water to sugars and the fraction of O and H atoms that undergo exchange with tissue water during cellulose formation, differ between leaves and fruit, and are the values of these parameters consistent across different evaporative environments?

Materials and methods

Oxygen and hydrogen isotope models

Mechanistic oxygen and hydrogen isotope models for tissue water in transpiring plant-organs (e.g. leaves) are built on the Craig-Gordon model (Craig and Gordon 1965). The model was originally developed to mathematically describe the evaporatively driven ^{18}O- and ^{2}H-enrichment of water surfaces of standing bodies of water. The model was later modified to quantitatively describe how transpiration causes ^{18}O- and ^{2}H-enrichment of leaf water (Dongmann et al., 1974; Flanagan and Ehleringer, 1991; Flanagan et al., 1991; Farquhar and Lloyd, 1993; Roden et al., 1999). The Craig-Gordon model modified for the simulation of ^{18}O- and ^{2}H-enrichment of the leaf water above source water takes the form:

Equation 1: $\Delta_{e\ leaf} = (1 + \varepsilon^{+}) [(1 + \varepsilon_k) (1 - e_a/e_i) + e_a/e_i (1 + \Delta_{Vapor})] - 1$

where $\Delta_{e\ leaf}$ is the isotopic enrichment of the water at the evaporative site in leaves above source water, and refers to either the oxygen or hydrogen isotope value (this shorthand applies throughout the remaining text), ε^{+} is the liquid-vapor equilibrium isotopic fractionation for water, ε_k is the kinetic isotopic fractionation of diffusion through the stomata and boundary layer, e_a/e_i is the ratio of atmospheric vapor pressure to intercellular vapor pressure in the leaf, and Δ_{Vapor} is the isotopic enrichment of ambient water vapor above source water. The values for ε^{+} and ε_k are element-specific, and can be derived according to the equations provided by Majoube (1971) for ε^{+} and by Farquhar *et al.* (1989) for ε_k with values from Merlivat (1978). The isotopic fractionation from diffusion was scaled to incorporate the effects of stomatal resistance and boundary layer resistance (Farquhar *et al.*, 1989; Cernusak *et al.*, 2016). To account for effects of source water $\delta^{18}O$ and $\delta^{2}H$ values leaf water $\delta^{18}O$ and $\delta^{2}H$ values at the site of enrichment (δ_{e_leaf}) can be calculated as:

Equation 2: $\delta_{e\_leaf} = \delta_{source\ water} + \Delta_{e\_leaf} (1 + \delta_{source\ water})$

where and $\delta_{source\ water}$ are the $\delta^{18}O$ or $\delta^{2}H$ values of the plant's source water.

The Craig-Gordon model typically overestimates measured leaf water $\delta^{18}O$ and $\delta^{2}H$ values, as the model simulates heavy isotope enrichment at the evaporative front in the leaf (Leaney *et al.*, 1985; Yakir *et al.*, 1990;

Flanagan *et al.*, 1991; Roden *et al.*, 2015). This is in contrast to measured leaf water $\delta^{18}O$ and $\delta^{2}H$ values that typically reflect bulk leaf water, which includes water from the evaporative front as well as a given fraction of non-^{18}O and ^{2}H enriched source water that is contained in leaves (see Supplementary Fig. S1 for CG-overestimation of data used in this study). There are two widely applied modifications to the Craig-Gordon model that account for this isotopic heterogeneity of bulk leaf water. One approach includes a Péclet effect in the model to describe the advection of unenriched source water towards the sites of evaporation opposed by back diffusion of enriched water from those sites (Farquhar and Lloyd, 1993; Barbour *et al.*, 2004; Kahmen *et al.*, 2011). The alternative approach divides leaf water into two distinct pools, a ^{18}O- and ^{2}H-enriched pool representing the evaporative front and a evaporatively non-^{18}O- and ^{2}H-enriched source water pool in the leaf (Leaney *et al.*, 1985; Yakir *et al.*, 1990). We used the two-pool model modification in our study to correct for these effects. In mathematical terms, the two-pool model is:

Equation 3: $\delta_{leaf\ water} = (1 - f_{xylem})\ \delta_{e\ leaf} + f_{xylem} * \delta_{source\ water}$

Where $\delta_{leaf\ water}$ is the isotope value for bulk leaf water, and f_{xylem} (or $f_{xylem\ oxygen}$ or $f_{xylem\ hydrogen}$) is a fitting parameter that accounts for the fraction of unenriched source water, (Flanagan *et al.*, 1991), in this study fitted separately for oxygen and hydrogen. See results and discussion for further explanations.

The $\delta^{18}O$ and $\delta^{2}H$ values of sugars in leaves are usually assumed to be in isotopic equilibrium with bulk leaf water and reflect its $\delta^{18}O$ and $\delta^{2}H$ values plus additional isotope fractionation effects that occur during the assimilation of carbohydrate sources (Sternberg *et al.*, 1986; Yakir and DeNiro, 1990; Roden and Ehleringer, 1999). For oxygen, ^{18}O-enrichment occurs when carbonyl-group oxygen exchanges with leaf tissue water during the assimilation of simple individual carbohydrates (trioses and hexoses) (Sternberg and DeNiro, 1983). In the model this is accounted for by the parameter $\varepsilon_{wc\ source}$:

Equation 4: $\delta^{18}O_{sugars} = \delta^{18}O_{leaf\ water} + \varepsilon_{wc\ source}$

Several studies have estimated $\varepsilon_{wc\ source}$ to be around +27 ‰ (Sternberg *et al.*, 1986; Yakir and DeNiro, 1990; Yakir, 1992; Barbour and Farquhar, 2000;

Cernusak *et al.*, 2003*a*; Sternberg and Ellsworth, 2011). Recently, higher values have been also suggested in a compound-specific analysis of sucrose, glucose, and fructose in grasses (Lehmann et al., 2017), and $\varepsilon_{wc\ source}$ has been shown to exponentially decrease with increasing temperature (Sternberg and Ellsworth, 2011).

To form cellulose in sink tissues, sucrose molecules are broken down into individual hexose molecules. One of the five oxygen atoms in each hexose that is ultimately incorporated into cellulose can exchange with the surrounding water as being part of a carbonyl group (Barbour, 2007). In addition, three out of the five atoms can exchange with local water via triose phosphate in the futile cycle (Hill *et al.*, 1995). This exchange is described in the cellulose $\delta^{18}O$ model (Eq. 5) as $\varepsilon_{wc\ sink}$. As $\varepsilon_{wc\ sink}$ cannot be directly measured, its values are typically believed to be identical to the ones for $\varepsilon_{wc\ source}$ (i.e. +27 ‰) (Sternberg *et al.*, 1986; Farquhar *et al.*, 2007). As water in developing leaf cells has been shown to mainly reflect source water (Liu *et al.*, 2017), the exchange of oxygen atoms during the formation of cellulose leads to a dampening of the originally ^{18}O-enriched leaf water and sugar signal in cellulose $\delta^{18}O$ values. The model that accounts for these effects is as follows (Barbour and Farquhar, 2000):

Equation 5: $\delta^{18}O_{cellulose} = f_o p_x * (\delta^{18}O_{source\ water} + \varepsilon_{wc\ sink}) + (1-f_o p_x) * (\delta^{18}O_{leaf\ water} + \varepsilon_{wc\ source})$

where $\delta^{18}O_{cellulose}$ is the oxygen isotopic composition of cellulose, the parameter f_o describes the fraction of oxygen atoms that exchange with surrounding water during the breakdown of sucrose to hexose and during the futile cycle (often described as p_{ex} in other studies), and the parameter p_x accounts for the fraction of unenriched source water in the developing cell (Barbour and Farquhar, 2000). As it is challenging to independently determine f_o, it is often merged with p_x to the combined parameter $f_o p_x$. Previous studies have found leaf $f_o p_x$ values in grasses, crops, and trees to range from 0.25 to 0.54 (Barbour *et al.*, 2000*a*, 2004; Helliker and Ehleringer, 2002; Kahmen *et al.*, 2011; Cheesman and Cernusak, 2016).

Many studies report $\delta^{18}O$ values of bulk dried plant tissue rather than pure cellulose. Bulk dry tissue of plants is composed of carbohydrates and a blend of different chemical compounds such as lignin, lipids, and proteins, which are reported to be ^{18}O-depleted compared to carbohydrates

(Schmidt *et al.*, 2001). Therefore, bulk dried plant tissue has generally been found to have lower $\delta^{18}O$ values than the corresponding cellulose, ranging from -1.4 ‰ to -9.5 ‰ (Barbour *et al.*, 2000*a*; Barbour and Farquhar, 2000; Cernusak *et al.*, 2005), however, more positive $\delta^{18}O$ values (+1.4 ‰) have also been observed in bulk dried tissue of fully developed leaves of Tasmanian blue gum (Cernusak *et al.*, 2005). To describe the difference between cellulose and bulk tissue $\delta^{18}O$ values, Barbour and Farquhar (2000) introduced the model parameter $\varepsilon_{cp\ oxygen}$ describing the difference between bulk dried plant tissue and cellulose. Thus, the $\delta^{18}O$ values of bulk dried plant tissue can be determined with the following equation:

Equation 6: $\delta^{18}O_{bulk} = [f_o p_x * (\delta^{18}O_{source\ water} + \varepsilon_{wc\ sink}) + (1-f_o p_x) * (\delta^{18}O_{leaf\ water} + \varepsilon_{wc\ source})] + \varepsilon_{cp\ oxygen}$

Hydrogen in carbohydrates is bound to carbon or to oxygen in hydroxyl groups. Carbon-bound hydrogen in cellulose does not exchange with surrounding water after biosynthesis, but some hydrogen in hydroxyl groups does (Epstein *et al.*, 1976). For cellulose, a large fraction (ca. 80 %) of the hydroxyl hydrogen engages in hydrogen bonding to link parallel polysaccharide chains, and the hydrogen in these bridging positions is also non-exchangeable with water or vapor at temperatures lower than 100 ºC (Meier-Augenstein *et al.*, 2014). This bridging hydrogen pool is ca. 25 % of the total non-exchangeable hydrogen pool, with the larger component being the carbon-bound hydrogen (Meier-Augenstein *et al.*, 2014). Meaningful environmental and physiological information is thus only contained in the $\delta^{2}H$ values of hydrogen that does not exchange with water or vapor under normal conditions, which is the focus of subsequent discussion.

For carbon-bound hydrogen in carbohydrates, such as cellulose, hydrogen isotope fractionations can be grouped into photosynthetic (autotrophic), and post-photosynthetic (heterotrophic) processes (Roden *et al.*, 1999; Cormier *et al.*, 2018). The large, negative autotrophic fractionation (ε_{HA}; -171 ‰; Yakir & DeNiro, 1990) occurs when photolysis of water molecules produces hydrogen that reacts with NADP+ to form NADPH (Nicotinamide adenine dinucleotide phosphate) (Luo *et al.*, 1991). In the Calvin-Cycle, this ^{2}H-depleted NADPH is then incorporated into organic compounds as glyceraldehyde-3-phosphate (GAP) (Yakir, 1992; Cormier *et al.*, 2018). The heterotrophic fractionation (ε_{HH}) occurs during post-

photosynthetic processes, including cellulose biosynthesis. It begins with triosephosphate (TP) – hexosephosphate (HP) exchange in the futile cycle and subsequent processes leading to the ^{2}H-enrichment of the TP and HP pools from which carbohydrates are then synthesized (Buchanan *et al.*, 2015; Cormier *et al.*, 2018). The combined effect of post-photosynthetic processes leads to a ^{2}H-enrichment that has been determined as either +158 ‰ (Yakir and DeNiro, 1990), or to vary between +144 ‰ and +166 ‰ (Luo and Sternberg, 1992) for cellulose. The combined controls on δ^2H values of carbon-bound non-exchangeable hydrogen of cellulose ($\delta^2H_{cellulose}$) are described by (Roden and Ehleringer, 1999) in the following equation:

Equation 7: $\delta^2H_{cellulose} = f_H p_x * (\delta^2H_{source\ water} + \varepsilon_{HH}) + (1-f_H p_x) * (\delta^2H_{leaf\ water} + \varepsilon_{HA})$

where the parameter f_H is the proportion of carbon-bound hydrogen that undergoes exchange with surrounding water, and the parameter p_x is the proportion of unenriched source water in the cell where cellulose is synthesized. Like oxygen, $f_H p_x$ values are typically determined as a combined parameter, with observed values between 0.34 and 0.4 (Yakir and DeNiro, 1990; Luo and Sternberg, 1992).

For bulk dried plant tissue δ^2H values, the additional effects due to the blend of different compounds contained in a sample that differ in their individual δ^2H values from cellulose, also need to be accounted for (Ziegler, 1989). Although not developed for hydrogen, we followed the same approach as proposed by Barbour and Farquhar (2000) for oxygen. Here, the model parameter $\varepsilon_{cp\ hydrogen}$ describes the difference between δ^2H values of bulk dried plant tissue and cellulose:

Equation 8: $\delta^2H_{bulk} = [f_H p_x * (\delta^2H_{source\ water} + \varepsilon_{HH}) + (1-f_H p_x) * (\delta^2H_{leaf\ water} + \varepsilon_{HA})] + \varepsilon_{cp\ hydrogen}$

Experimental setup

Strawberry (*Fragaria* × *ananassa* "Thulana") and raspberry (*Rubus idaeus* "autumn bliss") plants were grown concurrently for 14 weeks in three climate-controlled chambers to test how δ^2H and $\delta^{18}O$ values of water and organic compounds from leaves and berries varied in response to imposed environmental conditions. We applied constant low (36 %), moderate (55 %),

and high (72 %) relative humidity (RH) treatments in the chambers to create differences in leaf water evaporative enrichment. Day/night temperatures were fixed at 25 °C (8:00 to 22:00) and 18 °C (23:00 to 7:00), respectively, with a one-hour transition phase between the two states. LED-panels supplied light from approximately 80 cm above the plants, resulting in intensities from 350 to 600 µmol/m^2/s depending on location. The red:far-red ratio was set to 6:1 to promote flowering (Samuolienė *et al.*, 2010).

Sixty plants of each species were grown in total (twenty plants per species and growth chamber). Juvenile strawberry plants and mature, leafless raspberry plants were purchased in January 2018 from a nursery near Basel. The experiment was initiated with leafless plants to ensure that all utilized plant materials were produced under controlled experimental conditions. Strawberry plants were grown in 2-liter pots and raspberry plants in 5.5-liter pots, and both were manually pollinated.

Plants were watered three times per week using water from two 510 L tanks, which were covered to ensure constant source water isotope composition. To enhance differences in leaf water δ^2H values between treatments, the tank water was modified to have a δ^2H value +120 ‰ (Gamarra, Sachse, & Kahmen, 2016), while $\delta^{18}O$ values were left unmodified (-10.5 ‰). Evaporative ^{18}O- and ^2H-enrichment of soil water in the pots was limited by covering the soil with aluminum foil and gravel. Soil water $\delta^{18}O$ and δ^2H values were determined once at the very end of the experiment and showed minimal evaporative ^{18}O or ^2H enrichment, with the largest effects observed in the low relative humidity treatment with an increase of + 0.9 ‰ for $\delta^{18}O$, and + 5.3 ‰ for δ^2H. Water vapor from each chamber was periodically sampled using a cryogenic vapor trap to monitor the isotopic composition (Kahmen et al., 2008).

Ambient temperature and relative humidity of each chamber was monitored every 15 minutes using three evenly spaced sensors per chamber (HOBO Pro V2 temp/RH, Onset Computer Corporation, Bourne, USA), which were suspended and maintained at the height of the growing plants. Midday stomatal conductance was assessed every second week using a leaf porometer (Decagon SC-1 Porometer, Decagon Devices, Pullman, USA). On a sampling day, conductance was measured on eight leaves per species from randomly selected plants in each chamber. Leaf temperature was measured using an infrared thermometer (Voltcraft Conrad Electronic AG, Wollreau, Switzerland).

Sampling

Following an initial growth period of four weeks, midday samples were collected on six occasions for $\delta^{18}O$ and $\delta^{2}H$ analyses of leaf and berry water. Mature leaf samples were collected every other week over a ten-week period, while ripe berries were collected weekly over a six-week period. For each collection date, seven leaf and/or seven berry samples were collected per chamber. Immediately after sampling, the leaf midvein was removed and the remaining leaf blade or berry was sealed in a glass vial (Labco exetainer; 12 ml; Lampeter, Wales) and stored at -20 °C.

For $\delta^{18}O$ analyses of bulk sugars, leaf and berry samples were collected once, 10 weeks after the start of the experiment. Two neighboring leaves or berries were collected per plant (seven plants per species and treatment). The samples were immediately microwaved to stop enzyme activity (Landhäusser *et al.*, 2018) and sugar metabolism, then oven-dried at 60 °C for at least 48 h.

Leaf samples for $\delta^{18}O$ and $\delta^{2}H$ analyses of bulk material and α-cellulose were collected once at the end of the treatment, with seven samples per chamber/species. Each sample consisted of two leaves from randomly selected plants, which were dried at 60 °C for at least 48 h. As plants produced fewer fruits than leaves, organic material from the fruits was obtained from the samples collected for water extraction (see above).

All dried samples were milled using a laboratory mixer mill (Retsch MM440, Retsch GmbH, Haan, Germany).

Tissue water extraction, α-cellulose and bulk sugar purification

Leaf and berry water was cryogenically extracted after Newberry et al. (2017a). α-Cellulose was purified after Gaudinski et al. (2005). Briefly, approximately 100 mg of dry sample material was sealed in filter bags (Ankom F57, Ankom Technology, Macedon, USA). Lipids were removed by Soxhlet extraction for 24 h using 2:1 toluene:ethanol followed by 24 h with ethanol. Lignin was removed using 1.4 % sodium chlorite and acetic acid (pH = 4) in an ultrasonic bath at 70 °C for 24 h. Hemicellulose was removed with 15 % sodium hydroxide in an ultrasonic bath to yield purified α-cellulose.

Sugars were purified following Lehmann et al. (2020, 2017). Powdered samples (ca. 60 mg) were suspended in water, shaken, and heated to dissolve water-soluble carbohydrates (WSC), which were removed after

centrifugation and kept frozen until further processing. Sugars were purified by elution with Milli-Q water through three stacked Dionex OnGuard II Ion-exchange cartridges (1 cc, Thermo Fisher Scientific, Bremen, Germany). The first cartridge contained a styrene based, strong sulfonic acid resin in the H^+ form to remove cations (H-cartridge), the second removed highly retained anions using styrene based, strong base anion exchange resin in the HCO_3^- form (A-cartridge), and the third used a polyvinylpyrrolidone (PVP) polymer to remove phenolic compounds, azo compounds, humic acids, and amino acids (P-cartridge).

Isotope analyses

Water $\delta^{18}O$ and $\delta^{2}H$ values were measured as described in (Newberry *et al.*, 2017) using a high-temperature conversion/elemental analyzer (TC/EA) coupled to a Delta V Plus isotope ratio mass spectrometer (IRMS) through a ConFlo IV interface (Thermo Fisher Scientific, Bremen, Germany) in the Stable Isotope Ecology Laboratory at the University of Basel. These data, as well as all other isotope data presented in this study were normalized to the VSMOW-SLAP scale using at least two calibrated in-house standards. The long-term precision was determined for each type of isotope measurement as one standard deviation of repeated analyses of lab quality control material. For $\delta^{18}O$ and $\delta^{2}H$ values in water these were 0.2 ‰ and 0.7 ‰, respectively.

Bulk dried tissue and α-cellulose $\delta^{18}O$ values were analyzed using a Flash IRMS operated in pyrolysis mode with a glassy carbon reactor coupled to a Delta V Plus IRMS through a ConFlo IV interface (Thermo Fisher Scientific, Bremen, Germany). Samples were purged with helium for at least 3 hours directly prior to analysis using a Costech Zero-Blank Autosampler (NC Technologies Srl, Milan, Italy). Analytical precision was 0.2 ‰.

The $\delta^{2}H$ values of the non-exchangeable hydrogen of bulk dried tissue and α-cellulose were analyzed using a TC/EA coupled with the same IRMS used for $\delta^{18}O$ analyses. The reactor used chromium packing to avoid hydrogen isotope fractionation due to residual sample nitrogen (Gehre *et al.*, 2015). The H3+ factor was calculated before each set of analyses and was stable and within specification. Analytical precision was 1.3 ‰.

In order to correct measured $\delta^{2}H$ values for the contribution of exchangeable hydrogen, aliquots of each sample were measured in two separate analytical runs. Prior to each, the samples were dried under vacuum (1 h), equilibrated with water with a known $\delta^{2}H$ value (1 h), and then dried

again under vacuum (1 h) (Soto *et al.*, 2017), with all steps done at 70 °C using a Uni-prep autosampler (Wassenaar et al. 2015; Eurovector, Milan, Italy). Equilibration water volume was 50 µL, and the δ^2H values of the two waters were +45.2 ‰ and -189.3 ‰. Results from the two sets of analyses were then used to calculate the δ^2H value of the non-exchangeable H-pool (Soto *et al.*, 2017). A matrix-similar cellulose triacetate quality control sample, which does not contain exchangeable H, was measured with each set of analyses to ensure that no sorption occurred. Any isotopic fractionation associated with the equilibration between the vapor from the injected water and the exchangeable hydrogen in samples was corrected for using wood standards with known non-exchangeable hydrogen δ^2H values that were purchased from the United States Geological Survey (USGS 54/55/56), where the values were determined using a low temperature dual water equilibration procedure (Qi *et al.*, 2016). Analytical precision for non-exchangeable H was 0.9 ‰ for pure cellulose and 1.3 ‰ for bulk plant quality control materials. The average fraction of exchangeable hydrogen determined for this pure cellulose was 3.3 %, which is close to the theoretical value of 6 in 120 hydrogen positions being freely available for exchange under normal conditions (Meier-Augenstein *et al.*, 2014).

Bulk sugar $\delta^{18}O$ analyses were performed following Lehmann et al. (2020) at WSL (Swiss Federal Institute for Forest Snow and Landscape Research, Birmensdorf, Switzerland). Samples were analyzed on a Vario PYRO cube (Elementar, Hanau, Germany), which was coupled to a Delta Plus XP IRMS (Thermo Fisher Scientific, Bremen, Germany) through a ConFlo III interface. Analytical precision was 0.2 ‰.

Model parameter estimation

Values for model parameters f_{xylem}, $\varepsilon_{wc\ source}$, $f_{O}p_x$, $\varepsilon_{cp\ oxygen}$, $f_{H}p_x$, and $\varepsilon_{cp\ hydrogen}$ were estimated by fitting the respective models described in equations 1 - 8 to measured $\delta^{18}O$ and δ^2H values. This was done for each water, sugar, cellulose, or bulk dried tissue $\delta^{18}O$ and δ^2H value obtained from the sample as described below. After these initial determinations, mean parameter values were calculated for each organ, species, and treatment. The mean environmental and physiological input data that were used to fit the models to the samples from the different organs, species and treatments are provided in Supplementary Table S1.

Values for f_{xylem} in leaves were determined from equation 3, with measured input values for $\delta_{leaf\ water}$ and $\delta_{source\ water}$. $\delta_{e\ leaf}$ values were calculated with equation 2 with values of $\Delta_{e\ leaf}$ obtained from equation 1 and measured values of $\delta_{source\ water}$. To calculate values for f_{xylem} in berries, analogous to the leaves, first the berry water at the evaporative front ($\delta_{e\ berry}$) was estimated with equation 1 and 2, however, using berry specific input parameter values for stomatal conductance (Supplementary Table S1A). f_{xylem} for berries was subsequently calculated using equation 3 but using $\delta_{e\ berry}$ instead of $\delta_{e\ leaf}$ and measured bulk berry water ($\delta_{berry\ water}$) instead of leaf water ($\delta_{leaf\ water}$).

Equilibrium and kinetic isotopic fractionation factors for O and H were calculated using stomatal and boundary layer resistance, and tissue temperature (Supplementary Table S1A). Stomatal resistance was derived from average leaf stomatal conductance measurements for each organ, species, and treatment. Berry stomatal conductance was set to 0.1 mol/m^{2}s in order to account for cuticular water loss (Blanke, 1988). Boundary layer resistance was set for leaves and berries to 1 m^{2}s/mol (Sachse *et al.*, 2009). Measured leaf and berry tissue temperatures did generally not differ from the mean daytime growing chamber air temperature and were thus set to 25 °C for the calculations. Before using in the model, measured values for source water and water vapor $\delta^{18}O$ and $\delta^{2}H$ values, tissue temperature, and relative humidity were averaged to single means for each treatment (Supplementary Table S1A).

Values for the model parameter $\varepsilon_{wc\ source}$ were calculated for each leaf and berry sample by solving equation 4 using input variables displayed in Supplementary Table S1B. Leaf water $\delta^{18}O$ values were used as input variables for leaves and berries since berry sugars are initially produced at the sites of photosynthesis (i.e. the leaves) and then exported to the berries.

Values for the model parameter $f_o p_x$ were determined by solving equation 5, using input variables displayed in Supplementary Table S1B. The calculation of $f_o p_x$ also requires values for $\varepsilon_{wc\ source}$ and $\varepsilon_{wc\ sink}$ as input variables. $\varepsilon_{wc\ source}$ values that we calculated for sugars recovered from leaves and berries (see above) slightly deviated from literature value of +27 ‰, and between leaves and berries. These $\varepsilon_{wc\ source}$ values thus reflect the measured isotopic fractionation associated with the exchange of carbonyl-oxygen with tissue water during the biosynthesis of source carbohydrates. $\varepsilon_{wc\ sink}$ becomes relevant when carbonyl oxygen in sugars exchanges with tissue water during the formation of cellulose (Eqn. 5). As the magnitude of the isotopic

fractionation that is associated with this process cannot be directly measured, it remained unclear if the $\varepsilon_{wc\ source}$ values that we determined empirically for the biosynthesis of sugars - and that slightly deviate from literature values - are also valid for the formation of cellulose i.e. $\varepsilon_{wc\ sink}$. To account for this uncertainty in our calculation of $f_o p_x$, we followed three different approaches for determining $f_o p_x$: *Scenario i*: We ignored our empirically determined $\varepsilon_{wc\ source}$ values and set $\varepsilon_{wc\ source}$ and $\varepsilon_{wc\ sink}$ to +27 ‰ based on reported values in the literature (Sternberg and DeNiro 1983; Yakir and DeNiro 1990; Yakir 1992). *Scenario ii*: We used mean $\varepsilon_{wc\ source}$ values for each species that we calculated from measured leaf sugar $\delta^{18}O$ values as described above, reflecting the measured species-specific isotopic fractionation occurring during the carbonyl-oxygen exchange with tissue water during sugar biosynthesis. We used the same values for $\varepsilon_{wc\ sink}$ with the assumption that these values are identical both for the formation of source (sugars) and sink (cellulose) carbohydrates. *Scenario iii*: We used species and organ-specific values for $\varepsilon_{wc\ source}$ and $\varepsilon_{wc\ sink}$. This scenario was equal to *Scenario ii* for leaf tissues. For berry tissues, however, this approach resulted in different $\varepsilon_{wc\ source}$ and $\varepsilon_{wc\ sink}$ values. $\varepsilon_{wc\ source}$ values were determined from leaf sugars for a respective species, and were thus equal to those from *Scenario ii*. For $\varepsilon_{wc\ sink}$, we used $\varepsilon_{wc\ source}$ values determined from measured berry sugar $\delta^{18}O$ values, assuming that these values already account for some post-photosynthetic exchange of carbonyl oxygen in berry sink tissue. This scenario necessarily reappropriates some of the difference between cellulose and sugar $\delta^{18}O$ values from $f_o p_x$ and assigns it to the modified $\varepsilon_{wc\ sink}$ value. We deemed this worthy of consideration, given that we directly measured the $\delta^{18}O$ of berry sugar, which should be the direct precursor of cellulose synthesized in a berry, and therefore also allowed us a direct means to calculate a distinct $\varepsilon_{wc\ sink}$ value. In addition, we used mean $\delta^{18}O$ values of measured leaf water ($\delta^{18}O_{leaf\ water}$) for calculating $f_o p_x$ for leaves as well as for calculating $f_o p_x$ for berries, since sugars used for synthesis of organic compounds in leaves and berries originate from leaves and their $\delta^{18}O$ values should accordingly be driven by leaf rather than berry water.

Values for the model parameter $f_H p_x$ were determined by solving equation 7, using input variables from Supplementary Table S1C. For the heterotrophic and autotrophic fractionation factors (ε_{HH} and ε_{HA}) we used the reported values of +158 ‰ and -171 ‰, respectively (Yakir and DeNiro, 1990). Apart from the different fractionation factors, $f_H p_x$ values were

calculated analogous to the "*scenario i*" approach used for $f_o p_x$ values, with isotopic fractionation factors (ε_{HH} and ε_{HA}) prescribed based on literature values. As for oxygen, mean δ^2H values for leaf water ($\delta^2H_{leaf\ water}$) were used for determining $f_H p_x$ for leaves as well as from berries for the same reasons as explained above. Importantly, our measurements of $\delta^2H_{cellulose}$ values account for all non-exchangeable hydrogen including ca. 25 % non C-bound but bridging hydrogen. The here calculated $f_H p_x$ values might therefore deviate from "true" $f_H p_x$ values that describe the exchange of only C-bound hydrogen and additionally capture variability in non C-bound but bridging hydrogen.

The model parameters $\varepsilon_{cp\ oxygen}$ and $\varepsilon_{cp\ hydrogen}$ were determined by solving equations 6 and 8, respectively, using the measured cellulose $\delta^{18}O$ and δ^2H values, as averages per species, treatment and organ, and the individual measured bulk dried tissue $\delta^{18}O$ and δ^2H values (Supplementary Table S1B and S1C).

Data analysis

Statistical analyses were done using R version 3.5.3. Type I statistical error was set to $\alpha = 0.05$. The relationships among groups were determined using analysis of variance (ANOVA) with Tukey's honest significant difference (HSD) post-hoc tests, with significance level set to $p = 0.05$. Errors are reported as one standard deviation (SD) of the mean.

Results

Growth chamber conditions

Air temperature in all growth chambers was 25 ± 0.4 °C during the day (8:00 to 22:00), and 18 ± 0.5 °C at night (23:00 to 7:00). Observed RH values ranged from 34 % to 39 % (mean = 36 % ± 5%), 53 % to 58 % (mean = 55 % ± 3%), and 70 % to 77 % (mean = 72 % ± 3%) in the low, medium, and high RH treatments, respectively. Irrigation water $\delta^{18}O$ values were -10.5 ± 0.11 ‰ (Fig. 1, Supplementary Table S1A), while $\delta^{2}H$ values were + 120 ± 0.9 ‰ (Fig. 2, Supplementary Table S1A). The water vapor isotopic composition varied over the course of each day, with low, medium, and high RH treatment $\delta^{18}O$ values ranging from -18 ‰ to -21 ‰, -17 ‰ to -19 ‰, and -16 ‰ to -18 ‰, respectively (Fig. 1, Supplementary Table S1A, Supplementary Fig. S2), and $\delta^{2}H$ values ranging from -17 ‰ to -45 ‰, 0 ‰ to -45 ‰, and -80 ‰ to -110 ‰, respectively (Fig. 2, Supplementary Table S1A, Supplementary Fig. S2).

Oxygen isotopes in plant samples

Berry and leaf tissue water $\delta^{18}O$ values were constant throughout the experiment (Supplementary Fig. S3A). We therefore discuss temporally averaged values from each organ, species, and treatment. The $\delta^{18}O$ values of berry water were significantly lower than those of leaf water in both species for a given treatment (Fig. 1, Supplementary Table S2, Supplementary Table S3). Bulk tissue water $\delta^{18}O$ values did not differ between the two species for either organ (Fig. 1, Supplementary Table S3). Bulk tissue water $\delta^{18}O$ values of strawberries and raspberries were highest at low RH, and lowest at high RH in both organs (Fig. 1, Supplementary Table S2, Supplementary Table S3). The offsets between leaf and berry water $\delta^{18}O$ values decreased, however, with increasing RH from 8.4 ‰ to 4.4 ‰ (Fig. 1, Supplementary Table S3).

The $\delta^{18}O$ values of organic material in leaves and berries were always higher than corresponding tissue water values (Fig. 1). Among organic fractions, there was a general pattern that bulk sugar $\delta^{18}O$ values were the highest, followed by cellulose and then bulk dried tissue (Fig. 1, Supplementary Table S2). This was consistent for both organs and species (Fig. 1, Supplementary Table S3). Bulk dried tissue $\delta^{18}O$ values were similar between berries and leaves of plants grown in the same treatment (Fig. 1, Supplementary Table S3) and the observed statistical differences were largely due to small differences between leaves and berries in strawberries grown at

high RH (Tukey's HSD: $p<0.05$). Statistically significant differences in $\delta^{18}O$ values of bulk dried tissue material were found between species (Supplementary Table S3), but these too were small, and were mostly driven by higher leaf and berry values in raspberries at low RH (Tukey's HSD: $p<0.05$). Raspberry berry cellulose $\delta^{18}O$ values were higher than those in leaves grown under the same conditions, but strawberry berry cellulose $\delta^{18}O$ values were lower than those in leaves grown under the same conditions (Fig. 1). Significant, yet relatively small differences in cellulose $\delta^{18}O$ values were observed between species (Fig. 1, Supplementary Table S3). Bulk sugar $\delta^{18}O$ values also differed significantly between organs with slightly higher $\delta^{18}O$ values in leaves compared to berries. Cellulose, bulk sugar, and bulk tissue $\delta^{18}O$ values of leaves and berries were significantly affected by the RH treatments, with generally higher $\delta^{18}O$ values at low RH and lower values at high RH (Fig. 1, Supplementary Table S3).

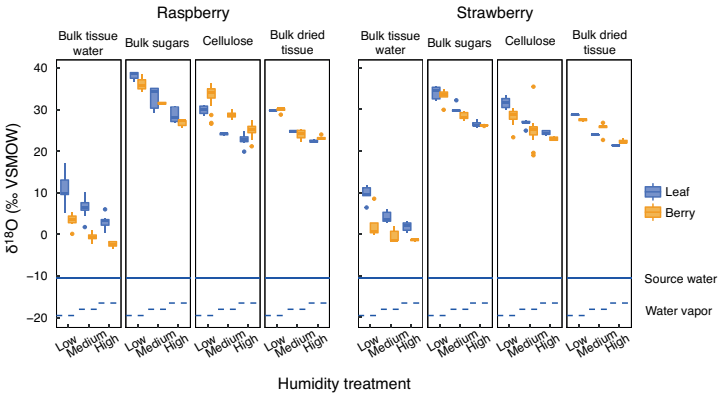

Figure 1: Raspberry and strawberry leaf and berry oxygen isotope ($\delta^{18}O$) values from mean bulk tissue water (n=7 per organ of each species in each treatment), mean bulk sugars (n=5 per organ of each species in each treatment), mean cellulose (n=7 per organ of each species in each treatment) and mean bulk dried tissue material (n=7 per organ of each species in each treatment) (boxplot data, mean values ± SD Supplementary Table S2). Data are separated by different relative humidity treatments (low, medium, and high RH) and species (strawberry and raspberry). Solid blue horizontal line represents source water $\delta^{18}O$ value, which was kept constant at $\delta^{18}O$ = -10.5 ‰ over the whole experiment, dashed blue horizontal lines represent ambient water vapor $\delta^{18}O$ values in the growing chambers. Results of ANOVAs showing the effects of species, organ, and treatment on the $\delta^{18}O$ values of the different compounds analyzed shown in Supplementary Table S3.

Hydrogen isotopes in plant samples

As for oxygen, temporally averaged δ^2H values are presented for each organ, species, and treatment (Supplementary Fig. S3B). Leaf water and berry water δ^2H values did not differ for plants grown under the same RH conditions (Supplementary Table S4). Bulk tissue water δ^2H values differed between species but the effects were small. Bulk tissue water δ^2H values of strawberry and raspberry leaves and berries were the highest at low RH and the lowest at high RH (Fig. 2). Compared to the source water, bulk tissue waters were ^2H-enriched in the low RH treatment, similar in the medium RH treatment, and ^2H-depleted in the high RH treatment (Fig. 2). This pattern was the result of ^2H-enriched source water that we used in the experiment and different degrees of ^2H-exchange between water and vapor supplied by the growth chamber humidity control system (Flanagan *et al.*, 1991).

In contrast to oxygen, δ^2H values of non-exchangeable hydrogen of organic compounds in leaves and berries were always ^2H-depleted relative to the plant's source water and bulk tissue water (Fig. 2, Supplementary Table S2). Among organic fractions, there was a general pattern that cellulose δ^2H values were always higher than δ^2H values of bulk dried tissue for a given organ, species, and treatment (Fig. 2). Bulk dried tissue δ^2H values differed significantly between berries and leaves of plants grown under the same RH treatments, where berries were generally more ^2H-enriched than leaves (Fig. 2, Supplementary Table S4). Significant differences in δ^2H values of bulk dried tissue were also found between species (Supplementary Table S4). Berry cellulose δ^2H values in both species were higher than leaf cellulose values in each RH treatment, but cellulose δ^2H values did not differ between species grown under the same RH conditions (Supplementary Table S4; Tukey's HSD $p>0.05$). Like in oxygen, we observed a consistent RH effect in both organs and species for each compound class, with the highest δ^2H values at low RH, and the lowest values at high RH (Fig. 2, Supplementary Table S3).

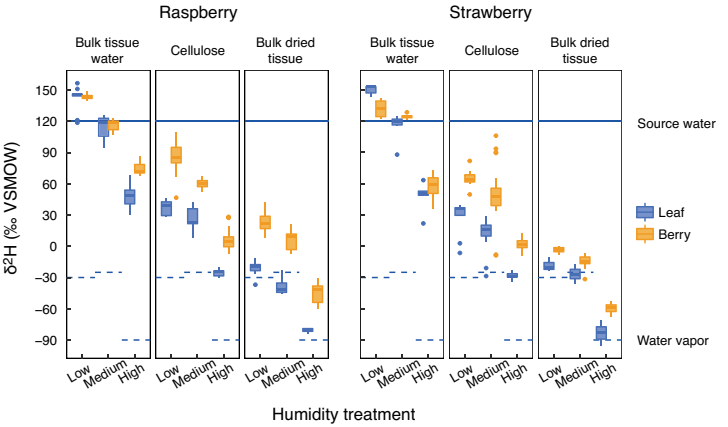

Figure 2: Raspberry and strawberry berry and leaf hydrogen isotope (δ^2H) values from mean bulk tissue water (n=7 per organ of each species in each treatment), mean cellulose (n=7 per organ of each species in each treatment), and mean bulk dried tissue material (n=7 per organ of each species in each treatment) (boxplot data, values ± SD Supplementary Table S2). Data are separated by different relative humidity treatments (low, medium, and high relative humidity) and species (strawberry and raspberry). Solid blue horizontal line represents source water δ^2H value, which was artificially kept constant at δ^2H = +120 ‰ over the whole experiment, dashed blue horizontal lines represent ambient water vapor δ^2H values in the growing chambers. Results of ANOVAs showing the effects of species, organ, and treatment on the δ^2H values of the different compounds analyzed shown in Supplementary Table S4.

Model parameter values for leaf water

Craig-Gordon predicted leaf and berry tissue water $\delta^{18}O$ and δ^2H values ($\delta^{18}O_{e\ leaf}$ & $\delta^{18}O_{e\ berry}$), as expected, overestimated the observed $\delta^{18}O$ and δ^2H enrichment of bulk tissue water (Supplementary information Fig. S1). The calculated f_{xylem} values for oxygen, that correct this overestimation, were 0.26 ± 0.11 for leaves and 0.53 ± 0.09 for berries, when averaged across species and treatments (Equation 3, Fig. 3A and Supplementary Table S1A). f_{xylem} values were thus significantly higher in berries than in leaves but did not differ between the two species (Fig. 3A, Supplementary Table S5). The f_{xylem} values also differed among treatments (Supplementary Table S5), trending towards slightly lower f_{xylem} values at higher humidity (Fig. 3A).

For hydrogen, calculated f_{xylem} values did not differ between leaves and berries, and were highly variable, in several cases yielding physically impossible values (> 1) (Equation 3, Fig. 3B). The large spread in calculated f_{xylem} values occurred because the leaf water and artificially enriched source

water (+120 ‰) were not in equilibrium and instead had similar δ^2H values, especially in the medium RH treatment (Fig. 2). Thus, small changes in the leaf water isotopic composition, even within instrumental error, led to large changes in the calculated relative contribution of source water (f_{xylem}) to the total tissue water, due only to the similarity in mixing model end member δ^2H values. Therefore, no further evaluations of the hydrogen-derived f_{xylem} values were made.

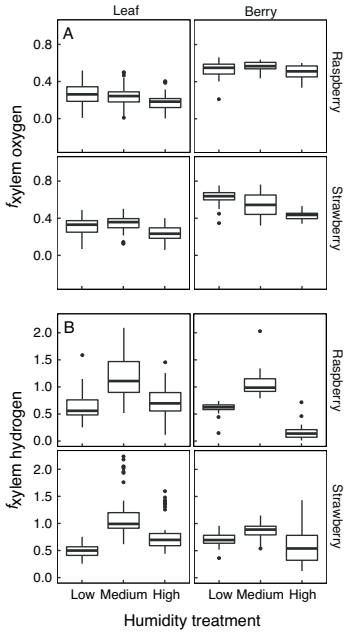

Figure 3 A): Parameter values for the fraction of unenriched source water (f_{xylem}) required for the two-pool modification to the Craig-Gordon leaf water isotope model. **A)** Values for the oxygen isotope model for bulk tissue water of leaves and berries, separated by species (raspberry/strawberry), organ (leaf/berry), and treatment (low, medium, and high relative humidity). **B)** As in **(A)**, but for the hydrogen isotope model. Results of ANOVAs showing the effects of species, organ, and treatment on f_{xylem} (oxygen and hydrogen) shown in Supplementary Table S5.

Model parameters values for sugar, cellulose, and bulk tissue

Across all organs, species, and treatments we obtained a mean $\varepsilon_{wc\ source}$ value of 25.0 ‰ ± 1.7 for bulk sugars (Equation 4). The $\varepsilon_{wc\ source}$ values were slightly higher for leaves (25.7 ‰ ± 1.8) than berries (24.3 ‰ ± 1.2) and higher for raspberries (25.5 ‰ ± 1.8) than strawberries (24.5 ‰ ± 1.4) (Fig. 4, Supplementary Table S1B). The humidity treatments had no effect on $\varepsilon_{wc\ source}$ values of strawberries or raspberries in either organ (Fig. 4, Supplementary Table S6).

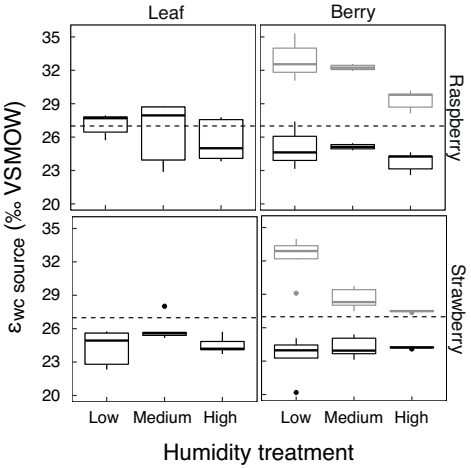

Figure 4: $\varepsilon_{wc\ source}$ values for bulk sugar $\delta^{18}O$ values, separated by species (raspberry/strawberry), organ (berry/leaf), and treatment (low, medium, and high relative humidity). For berry sugar $\delta^{18}O$ values, the $\varepsilon_{wc\ source}$ values are shown as calculated relative to the respective mean leaf water (black boxplot, *scenario i* in methods) as well as the mean berry water (light grey boxplot). The established $\varepsilon_{wc\ source}$ value of +27 ‰ is shown as a dashed horizontal line for reference. Results of ANOVAs showing the effects of species, organ, and treatment on $\varepsilon_{wc\ source}$ shown in Supplementary Table S6.

When averaged across species and treatments, the mean $f_o p_x$ value for leaf cellulose was 0.39 ± 0.13, if an $\varepsilon_{wc\ source}$ and $\varepsilon_{wc\ sink}$ value of +27 ‰ was used (*scenario i*), and 0.30 ± 0.16 when using species average $\varepsilon_{wc\ source}$ and $\varepsilon_{wc\ sink}$ values (*scenario ii*) or species- and sink tissue-specific $\varepsilon_{wc\ source}$ and $\varepsilon_{wc\ sink}$ values (*scenario iii*). The latter two scenarios yield identical $f_o p_x$ values for leaves because input data for $\varepsilon_{wc\ source}$ and $\varepsilon_{wc\ sink}$ were identical (Equation 5; Fig. 5, Supplementary Table S1B). For cellulose in berries, the corresponding $f_o p_x$ values averaged across species and treatments were 0.31 ± 0.13 (*scenario i*), 0.25 ± 0.13 (*scenario ii*), and 0.23 ± 0.12 (*scenario iii*) (Fig. 5). $f_o p_x$ values differed significantly between organs and species but species differences were small when using fixed $\varepsilon_{wc\ source}$ and $\varepsilon_{wc\ sink}$ values of +27 ‰ in the model (Fig. 5, Supplementary Table S7). $f_o p_x$ values were higher in leaves than in berries for raspberries but lower in leaves than in berries for strawberries (Fig. 5). $f_o p_x$ values also differed among treatments, where $f_o p_x$

values of cellulose trended towards slightly higher values with increasing RH in raspberries but not in strawberries (Fig. 5).

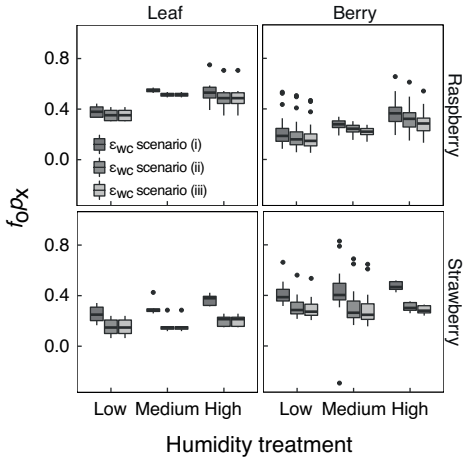

Figure 5: Values for post-photosynthetic exchange parameters for cellulose ($f_{O}p_{x}$) required to fit oxygen isotope model results to observations for different possible $\varepsilon_{wc\ source}$ values (*scenario i*: +27 ‰; *scenario ii*: species-specific mean $\varepsilon_{wc\ source}$ and $\varepsilon_{wc\ sink}$ values calculated from measured $\delta^{18}O$ values of leaf water and the bulk sugars of leaves; *scenario iii*: species-, and organ-specific mean $\varepsilon_{wc\ source}$ and $\varepsilon_{wc\ sink}$ values calculated from measured $\delta^{18}O$ values of leaf water and the bulk sugars of leaves or berries). Values separated by species (raspberry/strawberry), organ (berry/leaf), treatment (low, medium, and high RH), and the three different ε_{wc}-scenarios. Results of ANOVAs showing the effects of species, organ, and treatment on $f_{O}p_{x}$ shown in Supplementary Table S7.

Across all organs, species, and treatments we obtained a mean $\varepsilon_{cp\ oxygen}$ value of (-2.06 ‰ ± 2.00 ‰) (Fig. 6). The obtained $\varepsilon_{cp\ oxygen}$ values were significantly more negative for berries (-2.24 ‰ ± 2.06 ‰) than for leaves (-1.53 ‰ ± 1.72 ‰) (Fig. 6, Supplementary Table S8). Interestingly, $\varepsilon_{cp\ oxygen}$ differences between leaves and berries were species dependent, with higher values in leaves than berries for raspberries and lower values in leaves than berries in strawberries (Fig. 6, Supplementary Table S8). No effect of treatment was observed for $\varepsilon_{cp\ oxygen}$ values in organs, species or treatments (Fig.6).

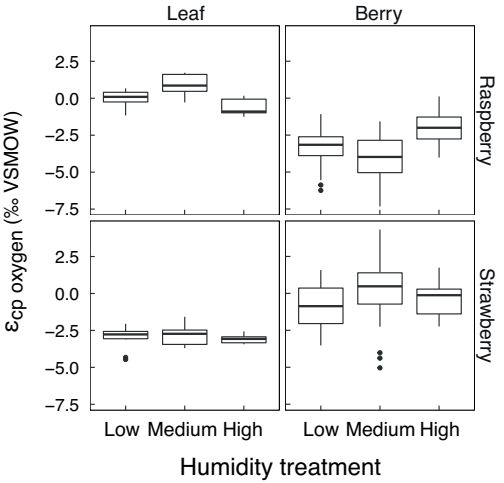

Figure 6: Difference of cellulose and bulk dried tissue $\delta^{18}O$ values ($\varepsilon_{cp\ oxygen}$), separated by species (raspberry/strawberry), organ (berry/leaf), and treatment (low, medium, and high relative humidity). Results of ANOVAs showing the effects of species, organ, and treatment on $\varepsilon_{cp\ oxygen}$ shown in Supplementary Table S8.

For the simulation of δ^2H values of the non-exchangeable hydrogen in cellulose, the mean f_Hp_x values obtained averaged across species and treatments were 0.22 ± 0.04 for leaves, and 0.34 ± 0.05 for berries (Fig. 7). The f_Hp_x values differed significantly between organs, between species, and among treatments (Supplementary Table S9). The f_Hp_x values decreased with increasing RH in berries, and increased with increasing RH in leaves (Fig. 7).

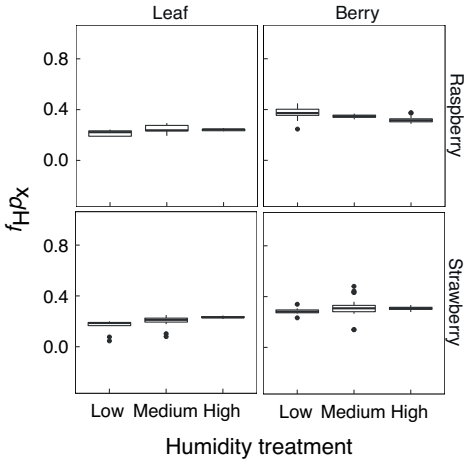

Figure 7: Post-photosynthetic exchange parameters for cellulose (f_{Hpx}) required to fit hydrogen isotope model results to observations. Values separated by species (raspberry/strawberry), organ (berry/leaf), treatment (low, medium, and high RH). Results of ANOVAs showing the effects of species, organ, and treatment on f_{Hpx} shown in Supplementary Table S9.

For bulk dried tissue, the mean $\varepsilon_{cp\ hydrogen}$ values obtained across species and treatments were -49.8 ‰ ± 9.9 ‰ for leaves and -54.4 ‰ ± 9.1 ‰ for berries. $\varepsilon_{cp\ hydrogen}$ values differed significantly between organs, and treatments (Fig. 8, Supplementary Table S10). The $\varepsilon_{cp\ hydrogen}$ values, however, were similar between species (Supplementary Table S10).

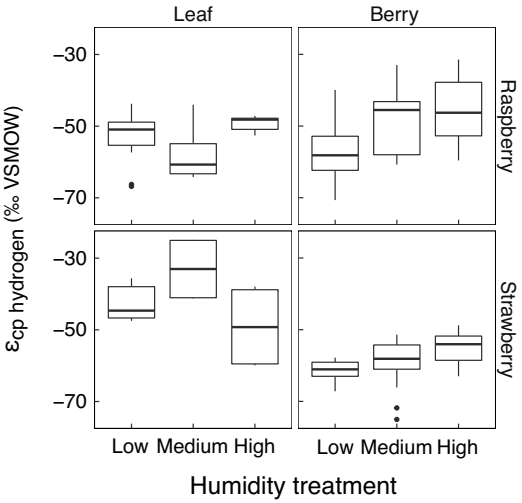

Figure 8: Difference of cellulose and bulk dried tissue δ^2H values ($\varepsilon_{cp\ hydrogen}$), separated by species (raspberry/strawberry), organ (berry/leaf), and treatment (low, medium, and high relative humidity). Results of ANOVAs showing the effects of species, organ, and treatment on $\varepsilon_{cp\ hydrogen}$ shown in Supplementary Table S10.

Discussion

This study demonstrates how water and different organic compounds differ in their $\delta^{18}O$ and $\delta^{2}H$ values between berries and leaves, and how these differences vary in two different species and in different environments. All plant water compartments and organic compound classes followed the same general and expected large-scale pattern, with organic $\delta^{18}O$ values being generally higher than source and leaf water $\delta^{18}O$ values for leaves and berries but organic $\delta^{2}H$ values being generally lower than source and leaf water $\delta^{2}H$ values for leaves and berries. For water and different organic compounds, isotope values for O and H generally decreased as RH values increased (Figs. 1 & 2). Most importantly, we found that leaves and berries differed substantially in their water $\delta^{18}O$ values but only slightly in their organic $\delta^{18}O$ values. In contrast, leaves and berries did not differ in their water $\delta^{2}H$ values but in their organic $\delta^{2}H$ values. These observations were consistent across species and environmental treatments. We discuss these patterns in the following sections and evaluate if general and typically available leaf-derived values for model parameters or alternatively organ, species or environmentally specific model parameters are required for applying existing stable isotope models for the simulation and interpretation of fruit $\delta^{18}O$ and $\delta^{2}H$ values.

Leaf and berry water $\delta^{18}O$ and $\delta^{2}H$ values

We found $\delta^{18}O$ values of berry water being consistently higher than source water values but less ^{18}O-enriched than leaf water (Fig. 1), agreeing with Dunbar and Wilson (1983) and Sanchez-Bragado et al. (2019). Although berries generally carry a low number of functional stomata (Konarska, 2013), there is still some exchange of berry water with the atmosphere (e.g. through remaining stomata and possible cuticular water loss (Blanke, 1988)), leading to the evaporative ^{18}O-enrichment of berry water compared to source water. In addition, ^{18}O-enrichement of berry water compared to source water might derive from filling of the developing fruit via the phloem. Since phloem sap originates in leaves, it carries ^{18}O-enriched leaf water (Barbour and Farquhar, 2000; Cernusak *et al.*, 2005), and the observed berry water $\delta^{18}O$ values are most probably a mixture of phloem derived leaf water with source water. Despite being ^{18}O-enriched compared to source water, berries had consistently lower $\delta^{18}O$ values than leaves. The reason for this could be the generally lower number of stomata in berries compared to leaves, which results in berries

being less well coupled to the atmosphere than leaves and reducing the possibility of evaporative ^{18}O-enrichment of berry tissue water. In addition, the ratio of berry surface area to berry volume is much larger than the surface to volume ratio in leaves. As such, water in berries that becomes ^{18}O-enriched at the (few) sites of evaporation ($\delta_{e\ berry}$) is diluted by a substantially larger body of unenriched vein water compared to leaves. This phenomenon is reflected by the bigger f_{xylem} values of berries compared to leaves that we found in our study.

The larger fraction of unenriched source water in bulk tissue water in berries compared to leaves led to mean $f_{xylem\ oxygen}$ values that ranged from 0.43 to 0.61 in berries, but only from 0.17 to 0.34 in leaves (Fig. 3). To our knowledge, no previous estimates of f_{xylem} values exist for fruit, but values for leaves have been reported from 0.10 to 0.33 (Allison, 1985; Leaney *et al.*, 1985; Walker *et al.*, 1989; Flanagan *et al.*, 1991; Cernusak *et al.*, 2003*a*; Song *et al.*, 2015), although higher values have also been observed (Cernusak *et al.*, 2016). The increase of relatively ^{18}O-depleted source water in bulk tissue water with decreasing RH (correlation of $f_{xylem\ oxygen}$ with RH) could be explained with the Péclet-theory, where higher transpiration rates under low RH lead to larger flux of source water into the leaf (Cernusak and Kahmen, 2013). In the two-pool correction of the Craig-Gorgon model this increase of source water is reflected in bigger f_{xylem} values. Already in 1991, Flanagan et al. observed this pattern in green bean (*Phaseolus vulgaris* L.), as have many subsequent investigations (Barbour and Farquhar, 2000; Barbour *et al.*, 2000*b*; Cernusak *et al.*, 2005; Song *et al.*, 2015; Bögelein *et al.*, 2017).

The patterns observed for leaf and berry water δ^{18}O values should also hold for leaf and berry water δ^{2}H values. However, as indicated above, plants received ^{2}H-enriched source water while water vapor in the chambers was -150 to -210 per mil depleted indicating that source water and vapour were not in equilibrium. In this setting, the strongly ^{2}H-depleted water vapor has limited the expected evaporatively ^{2}H-enrichment of leaf water, resulting in leaf water δ^{2}H values that were similar or even ^{2}H-depleted compared to berry water δ^{2}H values. The leaf and berry water δ^{2}H values observed in this study thus deviate from what we would have expected in conditions where source water δ^{2}H values and water vapor δ^{2}H values are in isotopic equilibrium and where offsets between leaf and berry water δ^{2}H values should have been similar to the ones observed for δ^{18}O values.

Leaf and berry $\delta^{18}O$ values of organic components

Sugars had the highest $\delta^{18}O$ values of all measured compounds, followed by cellulose, then bulk dried material (Fig. 1). This suggests that following sucrose synthesis, oxygen exchange with the surrounding cell water occurs. It also suggests that non-carbohydrate components in bulk dried material must have lower $\delta^{18}O$ values than bulk sugars and cellulose (Barbour *et al.*, 2000*a*; Schmidt *et al.*, 2001; Farquhar *et al.*, 2007; Lehmann *et al.*, 2017).

The $\varepsilon_{wc\ source}$ values obtained for bulk sugars in leaves were lower than the canonical value of +27 ‰ (Sternberg and DeNiro 1983; Yakir and DeNiro 1990; Yakir 1992), but still within previously reported variability (Schmidt *et al.*, 2001; Sternberg and Ellsworth, 2011; Lehmann *et al.*, 2017). Differences in sugar $\delta^{18}O$ values between leaves and berries were much smaller than differences in leaf and berry water $\delta^{18}O$ values. The small differences between leaf and berry bulk sugar $\delta^{18}O$ values are reflected in $\varepsilon_{wc\ source}$ values that were only slightly lower for berries than for leaves in both species (Fig. 4, Supplementary Table S6). In general, these relatively small differences in sugar $\delta^{18}O$ and $\varepsilon_{wc\ source}$ values between leaves and berries suggests that berries act mostly as sink tissue for leaf-derived carbohydrates, where sugars that originate in leaves and carry foliar $\delta^{18}O$ values are allocated to berries without strong alteration. The small differences in sugar $\delta^{18}O$ and $\varepsilon_{wc\ source}$ values that we did observe between leaves and berries reflect several processes altering berry sugar $\delta^{18}O$ values. These may relate to the breakdown of transitory starch in leaves and phloem loading at night when transpiration is not occurring, which would result in incorporation of leaf water oxygen with lower $\delta^{18}O$ values into the newly formed monomers (Smith *et al.*, 2003; Weise *et al.*, 2004; Gessler *et al.*, 2007). These monomers, and the sucrose that they primarily comprise, are then exported to sink tissue such as berries, resulting in accumulation of compounds with lower $\delta^{18}O$ values. Also, changes in $\delta^{18}O$ values of sugars during transport in phloem sap can take place in companion cells, which take up sugars from sieve cells, breakdown sugars to triose or monomers, and thus allow exchange with surrounding water (Gessler *et al.*, 2007, 2014). In addition, post-photosynthetic exchange with the less ^{18}O enriched berry water can occur in the berry (Fig. 1, Supplementary Table S3) (Yakir and DeNiro, 1990; Roden and Ehleringer, 1999; Roden, 2000; Barbour *et al.*, 2004). Finally, different sugars (i.e. sucrose, fructose, glucose) show different degrees of ^{18}O-enrichment (Lehmann *et al.*, 2017), so

some of the differences between leaf and berry sugar $\delta^{18}O$ values may relate to molecular composition.

Cellulose $\delta^{18}O$ values differed significantly between leaves and berries. Interestingly, the direction of this effect was different between raspberries and strawberries (Fig. 1). The species-specific differences in cellulose $\delta^{18}O$ values between leaves and berries were also reflected in the $f_o p_x$ values. Namely, in raspberries, where berry cellulose was ^{18}O-enriched compared to leaf cellulose, $f_o p_x$ values were generally lower for berries than for leaves, but in strawberries the opposite pattern was observed (Fig. 5). $f_o p_x$ values that we obtained for the different organs, species and treatments were in the range of previous work (0.22 to 0.38) (Barbour *et al.*, 2000*a*, 2004; Barbour and Farquhar, 2000; Helliker and Ehleringer, 2002; Cernusak *et al.*, 2005). The choice of $\varepsilon_{wc\ source}$ and $\varepsilon_{wc\ sink}$ values (*scenarios i* to *iii*, see methods) influences the corresponding $f_o p_x$ values, which can explain variability in $f_o p_x$ values for a given organ, species, or treatment. In the first two scenarios, values for $\varepsilon_{wc\ source}$ and $\varepsilon_{wc\ sink}$ are identical, so possible sink effects in $\varepsilon_{wc\ sink}$ are not accounted for and are thus incorporated into the fitted $f_o p_x$ values. For berries in the third approach (*scenario iii*), this exchange is incorporated in the $\varepsilon_{wc\ sink}$ value.

Given that the $\delta^{18}O$ values of cellulose result from mixing and exchange between sugars and contacted water pools (Eqn. 4), we expected the effect of decreasing RH on $\delta^{18}O$ values to be smaller for cellulose than for bulk sugar $\delta^{18}O$ values, assuming that RH treatment did not affect $f_o p_x$ values. Surprisingly, we detected similar RH effects on cellulose and bulk sugar $\delta^{18}O$ values. Out of a mathematical necessity and irrespective of the chosen $\varepsilon_{wc\ source}$ and $\varepsilon_{wc\ sink}$ values, this resulted in $f_o p_x$ values that increased with increasing humidity for both leaves and berries. This finding is in contrast to Cheesman and Cernusak (2016), who found $f_o p_x$ to decrease with increasing humidity. Our finding of variable $f_o p_x$ values suggests that the fraction of unenriched source water (p_x) or of carbonyl oxygen in cellulose that exchanges (f_o) changes with organ, species, and environment (RH). However, Liu et al. (2017) showed that for monocot leaves, changing VPD does not alter the amount of source water in the leaf growth-and-differentiation zone where cellulose is synthesized, and that this water is isotopically similar to source water, which would imply a constant p_x. Gessler et al. (2013) have shown species-specific differences in f_o and in an earlier study they observed it to change with different transpiration rates (Gessler *et al.*, 2009). A change in f_o

can also result from different primary substrates (i.e. starch) available for cellulose synthesis and thus different biosynthetic pathway utilization (Luo and Sternberg, 1992; Sternberg *et al.*, 2006). Thirdly, the turnover rate of non-structural carbohydrates (NSC) has been shown to have a positive relationship with f_o (Song *et al.*, 2014). In their study, Song et al. (2014) also reported an increase in f_o with increasing RH, supporting our hypothesis but contrasting Cheesman and Cernusak (2016).

Bulk dried tissue $\delta^{18}O$ values were lower than sugar $\delta^{18}O$ values and similar to, but in cases, lower than cellulose $\delta^{18}O$ values. Interestingly, a consistent offset between bulk dried tissue and cellulose $\delta^{18}O$ values, described by the model parameter $\varepsilon_{cp\ oxygen}$, was observed for berries but not leaves in raspberries, while for strawberries, a similar consistent offset was observed for leaves but not berries (Fig. 1 and Fig. 6). Raspberry berries and strawberry leaves and berries produce a substantial amount of organic acids, mainly malate and citric acid, which can account for 20-25 % of the total dry weight (Andersen, 2011). Organic acid $\delta^{18}O$ values are typically about 10 ‰ lower than those of cellulose and sugars (Schmidt *et al.*, 2001), possibly explaining the patterns observed. This, and the fact that other compounds present in bulk dried tissue, like lignin or lipids which also show lower $\delta^{18}O$ values than carbohydrates (Schmidt *et al.*, 2001), can explain why we generally observed the lowest $\delta^{18}O$ values in bulk dried tissue. These results agree with previous works (Barbour *et al.*, 2000*a*; Barbour and Farquhar, 2000; Cernusak *et al.*, 2005), which have found whole leaf tissue $\delta^{18}O$ values to be generally lower than those of cellulose. The $\varepsilon_{cp\ oxygen}$ values that we obtained for the different organs, species and treatments were in the range of these previous studies (1.4 ‰ to -9.5 ‰). The authors of these studies also suggested that offsets between cellulose and bulk dried tissue $\delta^{18}O$ values might vary with different chemical compositions of leaves, different tissues, different species, different developmental stages, and for plants grown under differing conditions.

Leaf and berry δ^2H values of organic components

Non-exchangeable hydrogen of cellulose was always ^2H-depleted compared to source water, which can be explained by the broadly characterized autotrophic and heterotrophic fractionation processes during cellulose synthesis (Yakir and DeNiro, 1990). δ^2H values of non-exchangeable hydrogen of bulk tissue were even lower than cellulose values (Fig. 2). This

suggests the presence of additional compounds that are strongly ^{2}H-depleted. These are most likely cuticle or membrane lipids, which are strongly ^{2}H-depleted compared to source water (Ziegler, 1989; Chikaraishi and Naraoka, 2003; Kahmen *et al.*, 2013; Cormier *et al.*, 2018). The offset between bulk dried tissue and cellulose $\delta^{2}H$ values, expressed through the model parameter $\varepsilon_{cp\ hydrogen}$, was similar for berries and for leaves in raspberries but lower for berries compared to leaves in strawberries (Fig. 2 and Fig. 8).

Cellulose and dry bulk tissue $\delta^{2}H$ values of non-exchangeable hydrogen were significantly higher in berries compared to leaves, which contrasted with the rather similar leaf and berry organic $\delta^{18}O$ values. This pattern is consistent with previous work that has shown that carbon sink tissues are ^{2}H-enriched compared to the source (Ziegler, 1989; Augusti *et al.*, 2008; Gamarra and Kahmen, 2015; Newberry *et al.*, 2015; Gebauer *et al.*, 2016; Cormier *et al.*, 2018). It has been proposed that the lower carbon supply compared to source tissues leads to reduced Calvin cycle activity, smaller triose phosphate and hexose phosphate pools, and thus faster cycling of the pools (Cormier *et al.*, 2018). This increases the likelihood of exchange between carbon-bound hydrogen and source water, which is ^{2}H-enriched compared to the substrate (Luo and Sternberg, 1992; Augusti *et al.*, 2006). Sink tissue can also become ^{2}H-enriched if low carbohydrate supplies are counteracted by up-regulation of the oxidative pentose phosphate pathway, which enriches its products in ^{2}H (Hermes *et al.*, 1982; Cormier *et al.*, 2019). As for oxygen, cellulose, and bulk dried tissue $\delta^{2}H$ values differed significantly between the RH treatments, reflecting the patterns observed in the leaf water $\delta^{2}H$ values (Fig. 2).

Our study shows that values for $f_{H}p_{x}$ differ between leaves and berries (Roden and Ehleringer, 1999). This finding is based on an assumed heterotrophic fractionation factor ε_{HH} of +158 ‰ (Yakir and DeNiro, 1990), and an autotrophic fractionation factor ε_{HA} of -171 ‰ (Yakir and DeNiro, 1990), with $f_{H}p_{x}$ describing the proportion of carbon bound hydrogen that exchanges with source water during assimilation of cellulose (Fig. 7). Although for cellulose, our calculated $f_{H}p_{x}$ values fall within the range of previously suggested values (Yakir and DeNiro, 1990; Luo and Sternberg, 1992), they were generally higher for berries than for leaves (Fig. 7). This suggests carbohydrate export from the site of production in the leaf and exchange with source water during berry formation, primarily occurring

during triose phosphate isomerization and interconversion between the product fructose-6-P and glucose-6-P (Roden and Ehleringer, 1999).

Importantly and as already explained above, the $\delta^2H_{cellulose}$ values we present here account for all non-exchangeable hydrogen including ca. 25 % non C-bound but bridging hydrogen. The f_Hp_x values we present here can therefore deviate from "true" f_Hp_x values that only describe the exchange of only C-bound hydrogen. Given that the overall patterns in δ^2H values of organic material in source (leaves) and sink (berries) tissue that we report are consistent with previous reports, we argue that larger f_Hp_x values in berries compared to leaves are yet consistent with our current understanding of δ^2H values of organic material from autotrophic and heterotrophic plant material (Ziegler, 1989; Augusti *et al.*, 2008; Newberry *et al.*, 2015; Gebauer *et al.*, 2016; Gamarra *et al.*, 2016; Cormier *et al.*, 2018).

Implications of model parameter variability for simulation of $\delta^{18}O$ and δ^2H values in leaves and berries

We show that the $\delta^{18}O$ and δ^2H values of water or organic compounds in leaves and berries can differ substantially from each other, but that the direction and magnitude of these differences depends on the element (O or H) and the substance (water, organics) under consideration. Our study also shows that mechanistic isotope models that were originally developed for leaves can be parameterized to simulate variability of $\delta^{18}O$ and δ^2H values of berries. Yet, values for crucial model parameters f_{xylem}, ε_{wc}, f_Op_x, $\varepsilon_{cp\ oxygen}$, f_Hp_x, and $\varepsilon_{cp\ hydrogen}$ can vary between leaves and berries, depending on species and environment. The parameter values obtained in our study can be used to facilitate applications of existing stable isotope models for fruit, for example in forensic studies, where the models can help constrain $\delta^{18}O$ and δ^2H values to provide critical information about the geographical origin of such products (Bricout and Koziet, 1987; Rossmann *et al.*, 1996; Rossmann, 2001; West *et al.*, 2007; Gonzalvez *et al.*, 2009; Camin *et al.*, 2017; Bitter *et al.*, 2020). However, the reported variability in model parameters between organs, species and environmental conditions raises questions about the extent to which generalized model parameters can be used for such simulations of the $\delta^{18}O$ and δ^2H values of fruit or leaves of different species in different environments. We therefore evaluated the effect of variability in model parameters averaged across species and treatments on prediction errors in the different environments, by calculating general model parameters for water and

organic material that are averaged across species and treatments. For comparability between studies, for $f_o p_x$ we used "*scenario i*" (see methods). We then imposed a ± 10 % change in each model parameter and determined the effect (i.e. error) on model predicted $\delta^{18}O$ and $\delta^{2}H$ values caused by this change.

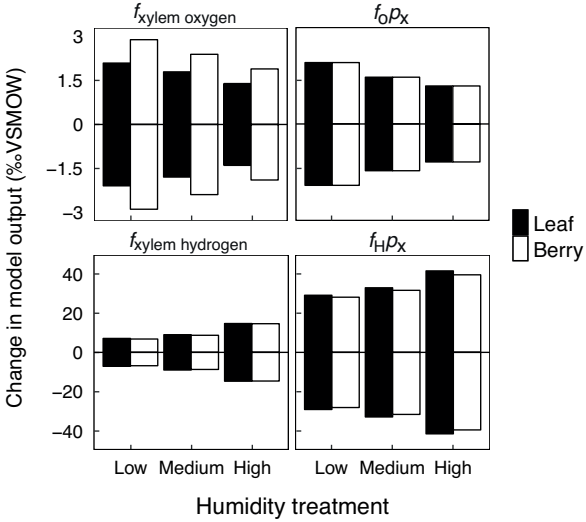

Figure 9: Resulting change of the tissue water, or cellulose $\delta^{18}O$ or $\delta^{2}H$ values by changing the tissue specific mean model parameter (f_{xylem}, $f_o p_x$, and $f_H p_x$) by ± 10 %. For $f_o p_x$ we used "*scenario i*" (see methods). Separated by model parameter, organ (berry/leaf), and treatment (low, medium, and high relative humidity).

In general, this simple sensitivity analysis shows that a 0.1 error in model input variables can have effects between ± 1.3 ‰ and ± 2.9 ‰ for predicted water or organic $\delta^{18}O$ values and between ± 6.8 ‰ and ± 44.6 ‰ for predicted water or organic $\delta^{2}H$ values (Fig. 9). Given that our study shows that f_{xylem} differs by much more than 0.1 between leaves and berries we advise that model applications utilize organ-specific f_{xylem} values rather than generalized f_{xylem} when simulating the $\delta^{18}O$ and $\delta^{2}H$ of leaves or berries. Differences in the model parameters $\varepsilon_{wc\ source}$ and $f_o p_x$, were not particularly large between leaves and berries, so using parameter values in model applications that are generalized across organs, species and environments might be possible. With an average difference of 3.0 ‰ the values of $\varepsilon_{cp\ oxygen}$,

however, varied substantially between organs in dependency of the species, suggesting the use of organ and species-specific values. Values for $f_{\mathrm{H}}p_{\mathrm{x}}$, and $\varepsilon_{\mathrm{cp\ hydrogen}}$ again differed between leaves and berries, depending on the species used in our study, so especially for strawberries, the use of organ-specific values in model applications is advisable. In addition to organ effects, our study shows effects of species and environment on all model parameters. Depending on the scope of a study and on the required minimum model prediction error it might be necessary to include species-specific model parameters that are constrained for a given environment, but the RH-driven differences among the parameter values were generally low compared to the difference between organs, so they may also potentially be neglected in certain scenarios. In any case we advise that studies that employ existing stable isotope models for the simulation and interpretation of leaf and berry $\delta^{18}O$ and $\delta^{2}H$ values should also estimate the effects on model parameter uncertainty in sensitivity analyses. The values for the model parameters f_{xylem}, $\varepsilon_{\mathrm{wc\ source}}$, $f_{\mathrm{O}}p_{\mathrm{x}}$, $\varepsilon_{\mathrm{cp\ oxygen}}$, $f_{\mathrm{H}}p_{\mathrm{x}}$, and $\varepsilon_{\mathrm{cp\ hydrogen}}$ that we report here for leaves and berries in two different species across different environmental settings thereby serve as an important reference for the possible range over which these parameters can vary, while our overall approach of adapting plant physiological isotope models for fruit serves as an important proof of concept that can be used to guide future research.

Supplementary data

Supplementary data are available at *JXB* online and after the references of this chapter.

Figure S1: Mean values (± SD) of the difference between the Craig-Gordon predicted and measured leaf and berry water $\delta^{18}O$ and $\delta^{2}H$ values.

Figure S2: Boxplots of growth chamber water vapor $\delta^{18}O$ and $\delta^{2}H$ values.

Figure S3: Leaf and berry tissue water $\delta^{18}O$ and $\delta^{2}H$ values (mean ± SD) shown for each sampling day over the course of the experiment.

Table S1: Values of model input variables used for the calculation of the model parameters f_{xylem}, ε_{wc}, $f_{o}p_{x}$, $\varepsilon_{cp\ oxygen}$, $f_{H}p_{x}$, and $\varepsilon_{cp\ hydrogen}$, as well as the resulting parameters values.

Table S2: Mean measured $\delta^{18}O$ and $\delta^{2}H$ values (±SD) of tissue water and the different organic fractions.

Table S3: ANOVAs showing the effects of species, organ, and treatment on the $\delta^{18}O$ values of tissue water, bulk sugars, cellulose, and bulk dried tissue.

Table S4: ANOVAs showing the effects of species, organ, and treatment on the $\delta^{2}H$ values of tissue water, cellulose, and bulk dried tissue.

Table S5: ANOVAs showing the effects of species, organ, and treatment on f_{xylem}.

Table S6: ANOVAs showing the effects of species, organ, and treatment on ε_{wc} for bulk sugars.

Table S7: ANOVAs showing the effects of species, organ, and treatment on $f_{o}p_{x}$.

Table S8: ANOVAs showing the effects of species, organ, and treatment on $\varepsilon_{cp\ oxygen}$.

Table S9: ANOVAs showing the effects of species, organ, and treatment on $f_{H}p_{x}$.

Table S10: ANOVAs showing the effects of species, organ, and treatment on $\varepsilon_{cp\ hydrogen}$.

Data availability statement

The data supporting the findings of this study are available within the paper, within its supplementary materials published online, and from the corresponding author, (F.C.), upon request.

Acknowledgements

We thank the two anonymous reviewers who provided helpful comments on an earlier version of this manuscript, Svenja Förster for her support with sample preparation and analysis, Melanie Egli for her help with sugar purification, and Dr. Meisha M. Holloway-Phillips for her valuable inputs. The present work was (i) supported by PlantHUB - European Industrial Doctorate funded by the European Commission's Horizon 2020 research and innovation program under the Marie Skłodowska-Curie grant agreement No 722338. The program is managed by the Zurich-Basel Plant Science Center. It was further supported by (ii) the ERC consolidator grant No 724750 - HYDROCARB, and (iii) by the "Freiwillige Akademische Gesellschaft Basel" (FAG). MML was supported by the Ambizione grant (PZ00P2_179978) from the Swiss National Science Foundation.

Author Contribution

F.C., D.B.N., and A.K. conceptualized the study. F.C. led the formal analysis in collaboration with D.B.N. and A.K.. M.L. provided the measurements of the bulk sugars. F.C., D.B.N., and A.K. prepared the original draft of the paper. All authors reviewed and edited the paper.

References

Allison GB. 1985. The relationship between deuterium and oxygen-18 delta values in leaf water. Chemical Geology **58**, 145–156.

Andersen G. 2011. *Der kleine 'Souci-Fachmann-Kraut', Lebensmitteltabelle für die Praxis*. Stuttgrat: Wissenschaftliche Verlagsgesellschaft Stuttgart.

Augusti A, Betson TR, Schleucher J. 2006. Hydrogen exchange during cellulose synthesis distinguishes climatic and biochemical isotope fractionations in tree rings. New Phytologist **172**, 490–499.

Augusti A, Betson TR, Schleucher J. 2008. Deriving correlated climate and physiological signals from deuterium isotopomers in tree rings. Chemical Geology **252**, 1–8.

Barbour MM. 2007. Stable oxygen isotope composition of plant tissue: a review. Functional Plant Biology **34**, 83–94.

Barbour MM, Farquhar GD. 2000. Relative humidity- and ABA-induced variation in carbon and oxygen isotope ratios of cotton leaves. Plant, Cell & Environment **23**, 473–485.

Barbour MM, Fischer RA, Sayre KD, Farquhar GD. 2000*a*. Oxygen isotope ratio of leaf and grain material correlates with stomatal conductance and grain yield in irrigated wheat. Australian Journal of Plant Physiology **27**, 625–637.

Barbour MM, Roden JS, Farquhar GD, Ehleringer JR. 2004. Expressing leaf water and cellulose oxygen isotope ratios as enrichment above source water reveals evidence of a Péclet effect. Oecologia **138**, 426–435.

Barbour MM, Schurr U, Henry BK, Wong SC, Farquhar GD. 2000*b*. Variation in the Oxygen Isotope Ratio of Phloem Sap Sucrose from Castor Bean. Evidence in Support of the Péclet Effect. Plant Physiology **123**, 671–680.

Bitter NQ, Fernandez DP, Driscoll AW, Howa JD, Ehleringer JR. 2020. Distinguishing the region-of-origin of roasted coffee beans with trace element ratios. Food Chemistry **320**, 126602.

Blanke MM. 1988. Stomatal and Cuticular Transpiration of the Cap and Berry of Grape. Journal of Plant Physiology **132**, 250–253.

Bögelein R, Thomas FM, Kahmen A. 2017. Leaf water 18O and 2H enrichment along vertical canopy profiles in a broadleaved and a conifer forest tree. Plant Cell and Environment **40**, 1086–1103.

Bricout J, Koziet J. 1987. Control of the authenticity of orange juice by isotopic analysis. Journal of Agricultural and Food Chemistry **35**, 758–760.

Buchanan B, Gruissem W, Vickers K, Jones R. 2015. *Biochemistry and molecular biology of plants*. New York, NY, USA: John Wiley & Sons.

Camin F, Boner M, Bontempo L, Fauhl-Hassek C, Kelly SD, Riedl J, Rossmann A. 2017. Stable isotope techniques for verifying the declared geographical origin of food in legal cases. Trends in Food Science & Technology **61**, 176–187.

Cernusak LA, Barbour MM, Arndt SK, *et al.* 2016. Stable isotopes in leaf water of terrestrial plants. Plant Cell and Environment **39**, 1087–1102.

Cernusak LA, Farquhar GD, Pate JS. 2005. Environmental and physiological controls over oxygen and carbon isotope composition of Tasmanian blue gum, Eucalyptus globulus. Tree Physiology **25**, 129–146.

Cernusak LA, Kahmen A. 2013. The multifaceted relationship between leaf water 18O enrichment and transpiration rate. Plant Cell and Environment **36**, 1239–1241.

Cernusak LA, Wong SC, Farquhar GD. 2003*a*. Oxygen isotope composition of phloem sap in relation to leaf water in Ricinus communis. Functional Plant Biology **30**, 1059.

Cernusak LA, Wong SC, Farquhar GD. 2003*b*. Oxygen isotope composition of phloem sap in relation to leaf water in Ricinus communis. Functional Plant Biology **30**, 1059–1070.

Cheesman AW, Cernusak LA. 2016. Infidelity in the outback : climate signal recorded in Δ18O of leaf but not branch cellulose of eucalypts across an Australian aridity gradient. Tree Physiology **37**, 554–564.

Chikaraishi Y, Naraoka H. 2003. Compound-specific δD – δ^{13}C analyses of *n*-alkanes extracted from terrestrial and aquatic plants. Phytochemistry **63**, 361–371.

Cormier M-A, Werner RA, Leuenberger MC, Kahmen A. 2019. ^{2}H-enrichment of cellulose and *n*-alkanes in heterotrophic plants. Oecologia **189**, 365–373.

Cormier M-A, Werner RA, Sauer PE, Gröcke DR, Leuenberger MC, Wieloch T, Schleucher J, Kahmen A. 2018. ^{2}H-fractionations during the biosynthesis of carbohydrates and lipids imprint a metabolic signal on the δ^{2}H values of plant organic compounds. New Phytologist **218**, 479–491.

Craig H, Gordon LI. 1965. Deuterium and oxygen 18 variations in the ocean and the marine atmosphere. In: Tongiorgi E, ed. Proceedings of the conference on stable isotopes in oceanographic studies and paleotemperatures. Piza, Italy: Laboratory of Geology and Nuclear Science. Pisa IT, 9–130.

Dongmann G, Nürnberg HW, Förstel H, Wagener K. 1974. On the Enrichment of $H_2{}^{18}O$ in the Leaves of Transpiring Plants. Radiation and Environmental Biophysics **11**, 41–52.

Dunbar J, Wilson AT. 1983. Oxygen and Hydrogen Isotopes in Fruit and Vegetable Juices. Plant Physiology **72**, 725–727.

Epstein S, Yapp CJ, Hall JH. 1976. The Determination of the D/H Ratio of Non-Exchangable Hydrogen in Cellulose Extracted from Aquatic and Land Plants. Earth and Planetary Science Letters **30**, 241–251.

Farquhar GD, Cernusak LA, Barnes B. 2007. Heavy Water Fractionation during Transpiration. Plant Physiology **143**, 11–18.

Farquhar GD, Hubick KT, Condon AG, Richards RA. 1989. Carbon Isotope Fractionation and Plant Water-Use Efficiency. In: Rundel, P.W., Ehleringer, J.R., Nagy, K.A., eds. Stable Isotopes in Ecological Research. Ecological Studies. New York, NY: Springer New York, 21–40.

Farquhar GD, Lloyd J. 1993. Carbon and Oxygen Isotope Effects in the Exchange of Carbon Dioxide between Terrestrial Plants and the Atmosphere. In: James R. Ehleringer, Anthony E. Hall, Graham D. Farquhar, eds. Stable Isotopes and Plant Carbon-water Relations. Elsevier, 47–70.

Flanagan LB, Comstock JP, Ehleringer JR. 1991. Comparison of Modeled and Observed Environmental Influences on the Stable Oxygen and Hydrogen Isotope Composition of Leaf Water in Phaseolus vulgaris L. Plant Physiology **96**, 588–596.

Flanagan LB, Ehleringer JR. 1991. Stable isotope composition of stem and leaf water : applications to the study of plant water use. Functional Ecology **5**, 270–277.

Förstel H, Hützen H. 1984. Stabile Sauerstoffisotope als natürliche Markierung von Weinen. Die Weinwirtschaft Technik **3**, 71–76.

Gamarra B, Kahmen A. 2015. Concentrations and δ^2H values of cuticular n-alkanes vary significantly among plant organs, species and habitats in grasses from an alpine and a temperate European grassland. Oecologia **178**, 981–998.

Gamarra B, Sachse D, Kahmen A. 2016. Effects of leaf water evaporative 2H-enrichment and biosynthetic fractionation on leaf wax n-alkane δ2H values in C3 and C4 grasses. Plant Cell and Environment **39**, 2390–2403.

Gaudinski JB, Dawson TE, Quideau S, Schuur EAG, Roden JS, Trumbore SE, Sandquist DR, Oh S-W, Wasylishen RE. 2005. Comparative Analysis of Cellulose Preparation Techniques for Use with

^{13}C,^{14}C, and ^{18}O Isotopic Measurements. Analytical Chemistry **77**, 7212–7224.

Gebauer G, Preiss K, Gebauer AC. 2016. Partial mycoheterotrophy is more widespread among orchids than previously assumed. New Phytologist **211**, 11–15.

Gehre M, Renpenning J, Gilevska T, Qi H, Coplen TB, Meijer HAJ, Brand WA, Schimmelmann A. 2015. On-Line Hydrogen-Isotope Measurements of Organic Samples Using Elemental Chromium: An Extension for High Temperature Elemental-Analyzer Techniques. Analytical Chemistry **87**, 5198–5205.

Gessler A, Brandes E, Buchmann N, Helle G, Rennenberg H, Barnard RL. 2009. Tracing carbon and oxygen isotope signals from newly assimilated sugars in the leaves to the tree-ring archive. Plant Cell and Environment **32**, 780–795.

Gessler A, Brandes E, Keitel C, Boda S, Kayler ZE, Granier A, Barbour M, Farquhar GD, Treydte K. 2013. The oxygen isotope enrichment of leaf-exported assimilates – does it always reflect lamina leaf water enrichment? New Phytologist **200**, 144–157.

Gessler A, Ferrio JP, Hommel R, Treydte K, Werner RA, Monson RK. 2014. Stable isotopes in tree rings: Towards a mechanistic understanding of isotope fractionation and mixing processes from the leaves to the wood. Tree Physiology **34**, 796–818.

Gessler A, Peuke AD, Keitel C, Farquhar GD. 2007. Oxygen isotope enrichment of organic matter in *Ricinus communis* during the diel course and as affected by assimilate transport. New Phytologist **174**, 600–613.

Gonzalvez A, Armenta S, de la Guardia M. 2009. Trace-element composition and stable-isotope ratio for discrimination of foods with Protected Designation of Origin. TrAC - Trends in Analytical Chemistry **28**, 1295–1311.

Helliker BR, Ehleringer JR. 2002. Differential ^{18}O enrichment of leaf cellulose in C3 versus C4 grasses. Functional Plant Biology **29**, 435.

Hermes JD, Roeske CA, O'Leary MH, Cleland WW. 1982. Use of multiple isotope effects to determine enzyme mechanisms and intrinsic isotope effects. Malic enzyme and glucose 6-phosphate dehydrogenase. Biochemistry **21**, 5106–5114.

Hill SA, Waterhouse JS, Field EM, Switsur VR, Ap Rees T. 1995. Rapid recycling of triose phosphates in oak stem tissue. Plant Cell and Environment

18, 931–936.
Hoch G. 2005. Fruit-bearing branchlets are carbon autonomous in mature broad-leaved temperate forest trees. Plant Cell and Environment **28**, 651–659.
Kahmen A, Hoffmann B, Schefuß E, Arndt SK, Cernusak LA, West JB, Sachse D. 2013. Leaf water deuterium enrichment shapes leaf wax *n*-alkane δD values of angiosperm plants II: Observational evidence and global implications. Geochimica et Cosmochimica Acta **111**, 50–63.
Kahmen A, Sachse D, Arndt SK, Tu KP, Farrington H, Vitousek PM, Dawson TE. 2011. Cellulose $\delta^{18}O$ is an index of leaf-to-air vapor pressure difference (VPD) in tropical plants. Proceedings of the National Academy of Sciences **108**, 1981–1986.
Kahmen A, Simonin K, Tu KP, Merchant A, Callister A, Siegwolf R, Dawson TE, Arndt SK. 2008. Effects of environmental parameters, leaf physiological properties and leaf water relations on leaf water δ18O enrichment in different Eucalyptus species. Plant Cell and Environment **31**, 738–751.
Konarska A. 2013. The structure of the fruit peel in two varieties of Malus domestica Borkh. (Rosaceae) before and after storage. Protoplasma **250**, 701–714.
Landhäusser SM, Chow PS, Turin Dickman L, *et al.* 2018. Standardized protocols and procedures can precisely and accurately quantify non-structural carbohydrates. Tree Physiology **38**, 1764–1778.
Leaney FW, Osmond CB, Allison GB, Ziegler H. 1985. Hydrogen-isotope composition of leaf water in C3 and C4 plants: its relationship to the hydrogen-isotope composition of dry matter. Planta **164**, 215–220.
Lehmann MM, Egli M, Brinkmann N, Werner RA, Saurer M, Kahmen A. 2020*a*. Improving the extraction and purification of leaf and phloem sugars for oxygen isotope analyses. Rapid Communications in Mass Spectrometry **34**, e8854.
Lehmann MM, Gamarra B, Kahmen A, Siegwolf RTW, Saurer M. 2017. Oxygen isotope fractionations across individual leaf carbohydrates in grass and tree species. Plant Cell and Environment **40**, 1658–1670.
Lehmann MM, Goldsmith GR, Mirande-Ney C, Weigt RB, Schönbeck L, Kahmen A, Gessler A, Siegwolf RTW, Saurer M. 2020*b*. The 18 O-signal transfer from water vapour to leaf water and assimilates varies among plant species and growth forms. Plant Cell and Environment **43**, 510–523.
Liu HT, Schäufele R, Gong XY, Schnyder H. 2017. The δ 18 O and δ 2 H

of water in the leaf growth-and-differentiation zone of grasses is close to source water in both humid and dry atmospheres. New Phytologist **214**, 1423–1431.

Luo Y-H, Sternberg L. 1992. Hydrogen and Oxygen Isotopic Fractionation During Heterotrophic Cellulose Synthesis. Journal of Experimental Botany **43**, 47–50.

Luo Y-H, Sternberg L, Suda S, Kumazawa S, Mitsui A. 1991. Extremely Low D/H Ratios of Photoproduced Hydrogen by Cyanobacteria. Plant Cell Physiology **32**, 897–900.

Majoube M. 1971. Fractionnement en oxygène 18 et en deutérium entre l'eau et sa vapeur. Journal de Chimie Physique **68**, 1423–1436.

Meier-Augenstein W, Kemp HF, Schenk ER, Almirall JR. 2014. Discrimination of unprocessed cotton on the basis of geographic origin using multi-element stable isotope signatures. Rapid Communications in Mass Spectrometry **28**, 545–552.

Merlivat L. 1978. Molecular diffusivities of $H_2{}^{16}O$, $HD^{16}O$, and $H_2{}^{18}O$ in gases. The Journal of Chemical Physics **69**, 2864–2871.

Newberry SL, Kahmen A, Dennis P, Grant A. 2015. *n*-Alkane biosynthetic hydrogen isotope fractionation is not constant throughout the growing season in the riparian tree *Salix viminalis*. Geochimica et Cosmochimica Acta **165**, 75–85.

Newberry SL, Nelson DB, Kahmen A. 2017. Cryogenic vacuum artifacts do not affect plant water-uptake studies using stable isotope analysis. Ecohydrology **10**, e1892.

Qi H, Coplen TB, Jordan JA. 2016. Three whole-wood isotopic reference materials, USGS54, USGS55, and USGS56, for δ^2H, $\delta^{18}O$, $\delta^{13}C$, and $\delta^{15}N$ measurements. Chemical Geology **442**, 47–53.

Roden JS. 2000. A mechanistic model for interpretation of hydrogen and oxygen isotope ratios in tree-ring cellulose. **64**, 21–35.

Roden JS, Ehleringer JR. 1999. Hydrogen and oxygen isotope ratios of tree-ring cellulose for riparian trees grown long term under hydroponycally environments. Oecologia **121**, 467–477.

Roden J, Kahmen A, Buchmann N, Siegwolf R. 2015. The enigma of effective path length for 18 O enrichment in leaf water of conifers. Plant Cell and Environment **38**, 2551–2565.

Roden JS, Lin G, Ehleringer JR. 1999. A mechanistic model for interpretation of hydrogen and oxygen isotope ratios in tree-ring cellulose.

Geochimica et Cosmochimica Acta **64**, 21–35.
Rossmann A. 2001. Determination of Stable Isotope Ratios in Food Analysis. Food Reviews International **17**, 347–381.
Rossmann A, Schmidt HL, Reniero F, Versini G, Moussa I, Merle MH. 1996. Stable carbon isotope content in ethanol of EC data bank wines from Italy, France and Germany. Zeitschrift für Lebensmittel-Untersuchung und -Forschung **203**, 293–301.
Sachse D, Kahmen A, Gleixner G. 2009. Organic Geochemistry Significant seasonal variation in the hydrogen isotopic composition of leaf-wax lipids for two deciduous tree ecosystems (*Fagus sylvativa* and *Acer pseudoplatanus*). Organic Geochemistry **40**, 732–742.
Samuolienė G, Brazaitytė A, Urbonavičiūtė A. 2010. The effect of red and blue light component on the growth and development of frigo strawberries. Zemdirbyste-Agriculture **97**, 99–104.
Sanchez-Bragado R, Serret MD, Marimon RM, Bort J, Araus JL. 2019. The hydrogen isotope composition δ^2H reflects plant performance. Plant Physiology **180**, 793–812.
Schmidt HL, Werner RA, Roßmann A. 2001. ^{18}O pattern and biosynthesis of natural plant products. Phytochemistry **58**, 9–32.
Smith AM, Zeeman SC, Thorneycroft D, Smith SM. 2003. Starch mobilization in leaves. Journal of Experimental Botany **54**, 577–583.
Song X, Farquhar GD, Gessler A, Barbour MM. 2014. Turnover time of the non-structural carbohydrate pool influences δ18O of leaf cellulose. Plant Cell and Environment **37**, 2500–2507.
Song X, Loucos KE, Simonin KA, Farquhar GD, Barbour MM. 2015. Measurements of transpiration isotopologues and leaf water to assess enrichment models in cotton. New Phytologist **1**, 637–646.
Soto DX, Koehler G, Wassenaar LI, Hobson KA. 2017. Re-evaluation of the hydrogen stable isotopic composition of keratin calibration standards for wildlife and forensic science applications. Rapid Communications in Mass Spectrometry **31**, 1193–1203.
Sternberg L, DeNiro M. 1983. Biogeochemical implications of the isotopic equilibrium fractionation factor between the oxygen atoms of acetone and water. Geochimica et Cosmochimica Acta **47**.
Sternberg L, DeNiro MJ, Savidge RA. 1986. Oxygen Isotope Exchange between Metabolites and Water during Biochemical Reactions Leading to Cellulose Synthesis. Plant Physiology **82**, 423–427.

Sternberg L, Ellsworth PFV. 2011. Divergent Biochemical Fractionation, Not Convergent Temperature, Explains Cellulose Oxygen Isotope Enrichment across Latitudes (HYH Chen, Ed.). PLOS ONE **6**, e28040.

Sternberg L, Pinzon MC, Anderson WT, Jahren HA. 2006. Variation in oxygen isotope fractionation during cellulose synthesis: intramolecular and biosynthetic effects. Plant Cell and Environment **29**, 1881–1889.

Walker CD, Leaney FW, Dighton JC, Allison GB. 1989. The influence of transpiration on the equilibration of leaf water with atmospheric water vapour. Plant Cell and Environment **12**, 221–234.

Wassenaar LI, Hobson KA, Sisti L. 2015. An online temperature-controlled vacuum-equilibration preparation system for the measurement of δ2H values of non- exchangeable-H and of δ18O values in organic materials by isotope-ratio mass spectrometry. Rapid Communications in Mass Spectrometry **29**, 397–407.

Weise SE, Weber APM, Sharkey TD. 2004. Maltose is the major form of carbon exported from the chloroplast at night. Planta **218**, 474–482.

West JB, Ehleringer JR, Cerling TE. 2007. Geography and vintage predicted by a novel GIS model of wine $\delta^{18}O$. Journal of Agricultural and Food Chemistry **55**, 7075–7083.

Yakir D. 1992. Variations in the natural abundance of oxygen-18 and deuterium in plant carbohydrates. Plant Cell and Environment **15**, 1005–1020.

Yakir D, DeNiro MJ. 1990. Oxygen and Hydrogen Isotope Fractionation during Cellulose Metabolism in Lemna gibba L. Plant Physiology **93**, 325–332.

Yakir D, DeNiro MJ, Gat JR. 1990. Natural deuterium and oxygen-18 enrichment in leaf water of cotton plants grown under wet and dry conditions: evidence for water compartmentation and its dynamics. Plant Cell and Environment **13**, 49–56.

Ziegler H. 1989. Hydrogen Isotope Fractionation in Plant Tissues. In: Rundel P.W., Ehleringer J.R., Nagy K.A. , eds. Stable Isotopes in Ecological Research. Ecological Studies (Analysis and Synthesis). New York: Springer, 105–123.

Supplementary Data

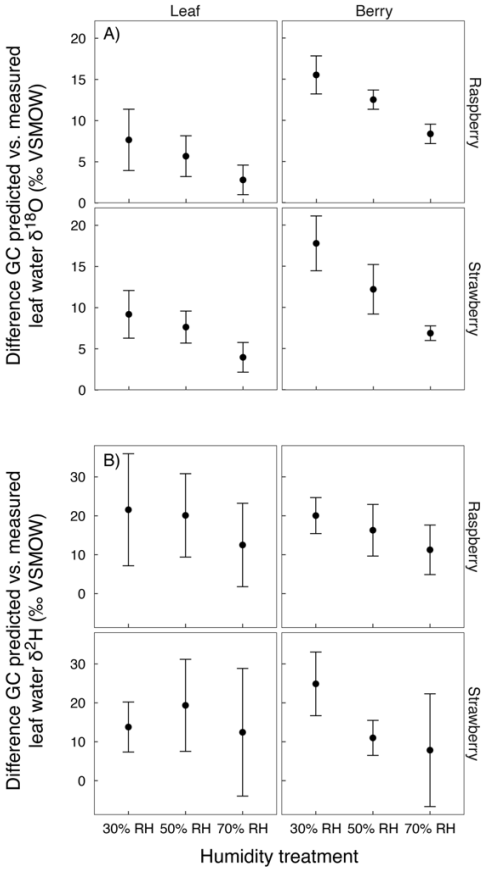

Supplementary data Figure S1: A) Mean values (± SD) of the difference between the Craig-Gordon (GC) predicted leaf water $\delta^{18}O$ values ($\delta^{18}O_{e\ leaf}$) modelled using Equations 1 and 2 and the measured bulk leaf water $\delta^{18}O$ values ($\delta^{18}O_{leaf\ water}$). Values separated by species (raspberry/strawberry), organ (berry/leaf), and treatment (low, medium, and high relative humidity). **B)** As in (A), but for leaf and berry $\delta^{2}H$ values rather than oxygen.

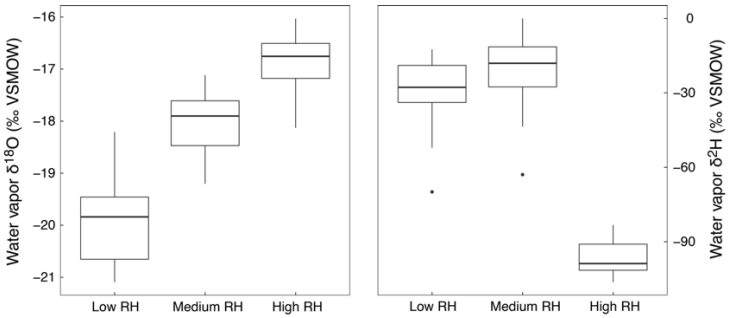

Supplementary data Figure S2: Boxplots showing the range the isotopic composition of water vapor (oxygen/hydrogen) inside the three different relative humidity growth chambers (low, medium, and high RH), assessed using a cryogenic air vapor trap in two-hourly intervals at eight different days during the experiment.

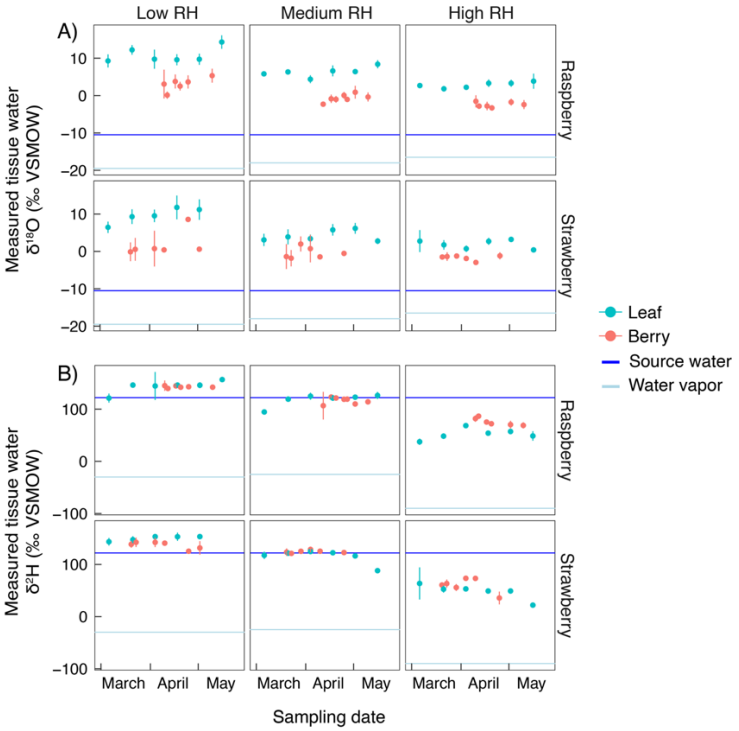

Supplementary data Figure S3: A) Raspberry and strawberry leaf and berry bulk tissue water oxygen isotope ($\delta^{18}O$) values (mean ± SD) collected at six sampling days over the course of the experiment (n=7 per sampling day, per organ of each species in each treatment). **B)** As in (A), but for leaf and berry hydrogen isotope ($\delta^{2}H$) rather than oxygen. Data are separated by different relative humidity treatments (low, medium, and high RH) and species (strawberry and raspberry). Dark blue horizontal line represents source water $\delta^{18}O$ and $\delta^{2}H$ value, which was kept constant at $\delta^{18}O$ = -10.5 ‰, and $\delta^{2}H$ = +120 ‰ over the whole experiment, light blue horizontal lines represent ambient water vapor $\delta^{18}O$ and $\delta^{2}H$ values in the growing chambers.

Supplementary data Table S1: Values of model input variables used for the calculation of the model parameters f_{xylem}, ε_{wc}, $f_o p_x$, $\varepsilon_{cp\ oxygen}$, $f_H p_x$, and $\varepsilon_{cp\ hydrogen}$, as well as the resulting parameters values. Values averaged across species (strawberry, raspberry), organ (leaf, berry) and treatment (low, medium, and high RH), and shown as means ± SD. Input variables where measured values obtained in this study were used for the calculations are indicated as bold text of the table column headers. **A)** Values for the calculation of f_{xylem} using equations 1, 2 and 3. **B)** Values for the calculation of $f_o p_x$, and $\varepsilon_{cp\ oxygen}$ using equations 5 and 6. Using reported values of ε_{wc} for *scenario i*, and $\varepsilon_{wc\ source\ /\ sink}$ calculated using bulk sugar $\delta^{18}O$ values (eqn. 4) of leaves or leaves and berries, respectively (*scenario ii* and *iii*, see methods) measured in this study. **C)** Values for the calculation of $f_H p_x$, and $\varepsilon_{cp\ hydrogen}$ using equations 7 and 8 with reported values of ε_{HH} and ε_{AH}.

A)	Organ	RH treatment	**Air Temp (°C)**	**RH (%)**	**Source water $\delta^{18}O$ (‰)**	**Source water δ^2H (‰)**	**Water vapor $\delta^{18}O$ (‰)**	**Water vapor δ^2H (‰)**	**Tissue temp. (°C)**	r_b (m^2s/ mol)	**g_s (mol/m^{2}s)**	**Tissue water $\delta^{18}O$ (‰)**	**Tissue water δ^2H (‰)**	$f_{xylem\ oxygen}$	$f_{xylem\ hydrogen}$
Strawberry	Leaf	Low	25 ± 0.4	36 ± 5	- 10.5 ± 0.11	120 ± 0.9	-19.84 ± 0.83	-29.07 ± 12.45	25 ± 0.5	1	0.32 ± 0.12	9.73 ± 2.87	150.3 ± 7.2	0.31 ± 0.09	0.53 ± 0.12
		Medium		55 ± 3			-18.02 ± 0.52	-21.09 ± 13.86			0.40 ± 0.13	4.18 ± 1.93	115.1 ± 13.2	0.34 ± 0.09	1.23 ± 0.44
		High		72 ± 3			-16.89 ± 0.54	-96.57 ± 5.94			0.35 ± 0.11	1.95 ± 1.78	48.5 ± 18.4	0.24 ± 0.08	0.79 ± 0.30
	Berry	Low	25 ± 0.4	36 ± 5	- 10.5 ± 0.11	120 ± 0.9	-19.84 ± 0.83	-29.07 ± 12.45	25 ± 0.5	1	0.1	0.77 ± 3.11	138.7 ± 8.5	0.61 ± 0.11	0.73 ± 0.15
		Medium		55 ± 3			-18.02 ± 0.52	-21.09 ± 13.86				-0.19 ± 2.91	124.4 ± 4.9	0.54 ± 0.13	0.92 ± 0.17
		High		72 ± 3			-16.89 ± 0.54	-96.57 ± 5.94				-1.45 ± 0.92	55.6 ± 15.9	0.43 ± 0.05	0.61 ± 0.38
Raspberry	Leaf	Low	25 ± 0.4	36 ± 5	- 10.5 ± 0.11	120 ± 0.9	-19.84 ± 0.83	-29.07 ± 12.45	25 ± 0.5	1	0.32 ± 0.12	11.06 ± 3.68	141.6 ± 16.1	0.26 ± 0.13	0.67 ± 0.27
		Medium		55 ± 3			-18.02 ± 0.52	-21.09 ± 13.86			0.29 ± 0.15	6.37 ± 2.45	114.2 ± 12.0	0.25 ± 0.11	1.26 ± 0.39
		High		72 ± 3			-16.89 ± 0.54	-96.57 ± 5.94			0.36 ± 0.15	3.02 ± 1.78	48.4 ± 12.0	0.17 ± 0.09	0.73 ± 0.28

Berry	Low	25 ± 0.4	36 ± 5	- 10.5 ± 0.11	120 ± 0.9	-19.84 ± 0.83	-29.07 ± 12.45	25 ± 0.5	1	0.1	3.14 ± 2.29	143.3 ± 5.21	0.53 ± 0.08	0.64 ± 0.09
	Medium		55 ± 3			-18.02 ± 0.52	-21.09 ± 13.86				-0.74 ± 1.16	118.5 ± 7.4	0.56 ± 0.05	1.11 ± 0.24
	High		72 ± 3			-16.89 ± 0.54	-96.57 ± 5.94				-2.53 ± 1.17	75.1 ± 7.1	0.51 ± 0.07	0.16 ± 0.12

B)	Organ	RH treatment	**Source water $\delta^{18}O$ (‰)**	**Leaf water $\delta^{18}O$ (‰)**	**Cellulose $\delta^{18}O$ (‰)**	**Bulk dried tissue $\delta^{18}O$ (‰)**	$\varepsilon_{wc\ source}$ (‰)	$\varepsilon_{wc\ sink}$ (‰)	**Bulk sugar $\delta^{18}O$ (‰)**	$f_o p_x$	$\varepsilon_{cp\ oxygen}$ (‰)
Scenario i											
Strawberry	Leaf	Low	- 10.5 ± 0.11	9.73 ± 2.87	31.59 ± 1.43	28.58 ± 0.82	27	27		0.25 ± 0.07	-3.04 ± 0.83
		Medium		4.18 ± 1.93	26.65 ± 0.98	23.86 ± 0.72				0.31 ± 0.07	-2.82 ± 0.73
		High		1.95 ± 1.78	24.38 ± 0.58	21.33 ± 0.27				0.37 ± 0.05	-3.08 ± 0.27
	Berry	Low	- 10.5 ± 0.11	9.73 ± 2.87	28.23 ± 2.08	27.47 ± 1.63	27	27		0.42 ± 0.10	-0.77 ± 1.65
		Medium		4.18 ± 1.93	25.01 ± 3.37	25.12 ± 2.31				0.42 ± 0.23	0.11 ± 2.34
		High		1.95 ± 1.78	23.04 ± 0.47	22.66 ± 1.35				0.47 ± 0.04	-0.39 ± 1.36

Raspberry	Leaf	Low	- 10.5 ± 0.11	11.06 ± 3.68	29.85 ± 1.09	29.82 ± 0.61	27	27		0.38 ± 0.05	-0.03 ± 0.61
		Medium		6.37 ± 2.45	24.11 ± 0.36	25.02 ± 0.71				0.55 ± 0.02	0.91 ± 0.72
		High		3.02 ± 1.78	22.67 ± 1.63	22.06 ± 0.56				0.54 ± 0.12	-0.61 ± 0.56
	Berry	Low		11.06 ± 3.68	33.56 ± 2.02	30.23 ± 1.11				0.21 ± 0.09	-3.37 ± 1.12
		Medium		6.37 ± 2.45	28.73 ± 0.70	24.69 ± 1.60				0.28 ± 0.04	-4.08 ± 1.61
		High		3.02 ± 1.78	25.03 ± 1.23	23.02 ± 0.96				0.37 ± 0.09	-2.03 ± 0.97
Scenario ii							$\varepsilon_{wc\ source}$ (‰)	$\varepsilon_{wc\ sink}$ (‰)			
Strawberry	Leaf	Low	- 10.5 ± 0.11	9.73 ± 2.87	31.59 ± 1.43	28.58 ± 0.82	24.94	24.94	34.04 ± 1.60	0.15 ± 0.07	-3.04 ± 0.83
		Medium		4.18 ± 1.93	26.65 ± 0.98	23.86 ± 0.72			30.17 ± 1.16	0.17 ± 0.07	-2.82 ± 0.73
		High		1.95 ± 1.78	24.38 ± 0.58	21.33 ± 0.27			26.48 ± 0.78	0.20 ± 0.05	-3.08 ± 0.27
	Berry	Low		9.73 ± 2.87	28.23 ± 2.08	27.47 ± 1.63			34.04 ± 1.60	0.32 ± 0.10	-0.77 ± 1.65
		Medium		4.18 ± 1.93	25.01 ± 3.37	25.12 ± 2.31			30.17 ± 1.16	0.28 ± 0.23	0.11 ± 2.34
		High		1.95 ± 1.78	23.04 ± 0.47	22.66 ± 1.35			26.48 ± 0.78	0.31 ± 0.04	-0.39 ± 1.36

Raspberry	Leaf	Low	- 10.5 ± 0.11	11.06 ± 3.68	29.85 ± 1.09	29.82 ± 0.61	26.41	26.41	38.19 ± 0.98	0.35 ± 0.05	-0.03 ± 0.61
		Medium		6.37 ± 2.45	24.11 ± 0.36	25.02 ± 0.71			32.82 ± 2.81	0.51 ± 0.02	0.91 ± 0.72
		High		3.02 ± 1.78	22.67 ± 1.63	22.06 ± 0.56			28.68 ± 1.89	0.50 ± 0.12	-0.61 ± 0.56
	Berry	Low		11.06 ± 3.68	33.56 ± 2.02	30.23 ± 1.11			38.19 ± 0.98	0.18 ± 0.09	-3.37 ± 1.12
		Medium		6.37 ± 2.45	28.73 ± 0.70	24.69 ± 1.60			32.82 ± 2.81	0.24 ± 0.04	-4.08 ± 1.61
		High		3.02 ± 1.78	25.03 ± 1.23	23.02 ± 0.96			28.68 ± 1.89	0.33 ± 0.09	-2.03 ± 0.97
Scenario iii							$\varepsilon_{wc\ source}$ (‰)	$\varepsilon_{wc\ sink}$ (‰)			
Strawberry	Leaf	Low	- 10.5 ± 0.11	9.73 ± 2.87	31.59 ± 1.43	28.58 ± 0.82	24.94	24.94	34.04 ± 1.60	0.15 ± 0.07	-3.04 ± 0.83
		Medium		4.18 ± 1.93	26.65 ± 0.98	23.86 ± 0.72			30.17 ± 1.16	0.17 ± 0.07	-2.82 ± 0.73
		High		1.95 ± 1.78	24.38 ± 0.58	21.33 ± 0.27			26.48 ± 0.78	0.20 ± 0.05	-3.08 ± 0.27
	Berry	Low		9.73 ± 2.87	28.23 ± 2.08	27.47 ± 1.63			33.14 ± 1.91	0.30 ± 0.10	-0.77 ± 1.65
		Medium		4.18 ± 1.93	25.01 ± 3.37	25.12 ± 2.31	24.94	23.97	28.44 ± 0.96	0.26 ± 0.22	0.11 ± 2.34
		High		1.95 ± 1.78	23.04 ± 0.47	22.66 ± 1.35			26.18 ± 0.08	0.29 ± 0.03	-0.39 ± 1.36

Raspberry	Leaf	Low	- 10.5 ± 0.11	11.06 ± 3.68	29.85 ± 1.09	29.82 ± 0.61	26.41	26.41	38.19 ± 0.98	0.35 ± 0.05	-0.03 ± 0.61
		Medium		6.37 ± 2.45	24.11 ± 0.36	25.02 ± 0.71			32.82 ± 2.81	0.51 ± 0.02	0.91 ± 0.72
		High		3.02 ± 1.78	22.67 ± 1.63	22.06 ± 0.56			28.68 ± 1.89	0.50 ± 0.12	-0.61 ± 0.56
	Berry	Low		11.06 ± 3.68	33.56 ± 2.02	30.23 ± 1.11			36.09 ± 1.71	0.17 ± 0.09	-3.37 ± 1.12
		Medium	- 10.5 ± 0.11	6.37 ± 2.45	28.73 ± 0.70	24.69 ± 1.60	26.41	24.65	31.51 ± 0.26	0.22 ± 0.04	-4.08 ± 1.61
		High		3.02 ± 1.78	25.03 ± 1.23	23.02 ± 0.96			26.81 ± 0.87	0.29 ± 0.08	-2.03 ± 0.97

C)	Organ	RH treatment	**Source water δ^2H (‰)**	**Leaf water δ^2H (‰)**	**Cellulose δ^2H (‰)**	**Bulk dried tissue δ^2H (‰)**	ε_{HH} (‰)	ε_{HA} (‰)	f_{HPx}	$\varepsilon_{cp\ hydrogen}$ (‰)
Strawberry	Leaf	Low	120 ± 0.9	150.3 ± 7.2	29.4 ± 15.0	-18.3 ± 6.1	158	-171	0.17 ± 0.05	-42.6 ± 5.74
		Medium		115.1 ± 13.2	10.4 ± 18.6	-26.6 ± 10.4			0.20 ± 0.06	-33.1 ± 9.31
		High		48.5 ± 18.4	-28.3 ± 3.6	-83.3 ± 13.7			0.23 ± 0.01	-49.1 ± 12.2
	Berry	Low	120 ± 0.9	150.3 ± 7.2	65.2 ± 7.6	-3.5 ± 3.4	158	-171	0.29 ± 0.02	-61.4 ± 3.00
		Medium		115.1 ± 13.2	50.7 ± 24.7	-15.4 ± 7.4			0.32 ± 0.08	-59.0 ± 6.56
		High		48.5 ± 18.4	1.9 ± 7.1	-59.9 ± 5.9			0.31 ± 0.02	-55.2 ± 5.29
Raspberry	Leaf	Low	120 ± 0.9	141.6 ± 16.1	37.6 ± 6.8	-21.4 ± 7.8	158	-171	0.22 ± 0.02	-52.7 ± 6.95
		Medium		114.2 ± 12.0	26.3 ± 11.0	-37.9 ± 8.7			0.25 ± 0.03	-57.3 ± 7.73
		High		48.4 ± 12.0	-25.5 ± 3.2	-80.7 ± 2.6			0.24 ± 0.01	-49.3 ± 2.29
	Berry	Low	120 ± 0.9	141.6 ± 16.1	87.0 ± 9.9	23.0 ± 8.3	158	-171	0.38 ± 0.03	-57.2 ± 7.40
		Medium		114.2 ± 12.0	60.2 ± 4.0	6.5 ± 11.1			0.35 ± 0.01	-48.0 ± 9.94
		High		48.4 ± 12.0	5.0 ± 7.1	-45.9 ± 9.4			0.32 ± 0.02	-45.4 ± 8.38

Supplementary data Table S2: Mean measured $\delta^{18}O$ and $\delta^{2}H$ values with standard deviation, of tissue water and the different organic fractions measured in the study, separated by species (raspberry/strawberry), organ (berry/leaf) and treatment (low, medium, and high relative humidity). Means calculated over six sampling days, and seven samples per day, species, organ and treatment (n=42 per organ of each species in each treatment).

			$\delta^{18}O$ (‰ VSMOW)				$\delta^{2}H$ (‰ VSMOW)		
Plant	RH treatment	Part	Tissue water ± SD	Cellulose ± SD	Dried tissue ± SD	Sugars ± SD	Tissue water ± SD	Cellulose ± SD	Dried tissue ± SD
Raspberry	Low	berry	3.14 ± 2.29	33.56 ± 2.02	30.23 ± 1.11	36.09 ± 1.71	143.3 ± 5.2	87.0 ± 9.9	23.0 ± 8.3
Raspberry	Medium	berry	-0.74 ± 1.16	28.73 ± 0.70	24.69 ± 1.60	31.51 ± 0.26	118.5 ± 7.4	60.2 ± 4.0	6.5 ± 11.1
Raspberry	High	berry	-2.53 ± 1.17	25.03 ± 1.23	23.02 ± 0.96	26.81 ± 0.87	75.1 ± 7.1	5.0 ± 7.1	-45.9 ± 9.4
Strawberry	Low	berry	0.82 ± 3.29	28.23 ± 2.08	27.47 ± 1.63	33.14 ± 1.91	137.8 ± 9.2	65.2 ± 7.6	-3.5 ± 3.4
Strawberry	Medium	berry	-0.17 ± 2.97	25.01 ± 3.37	25.12 ± 2.31	28.44 ± 0.96	124.4 ± 5.0	50.7 ± 24.7	-15.4 ± 7.4
Strawberry	High	berry	-1.32 ± 0.88	23.04 ± 0.47	22.66 ± 1.35	26.18 ± 0.08	53.7 ± 16.2	1.9 ± 7.1	-59.9 ± 5.9
Raspberry	Low	leaf	11.06 ± 3.68	29.85 ± 1.09	29.82 ± 0.61	38.19 ± 0.98	141.6 ± 16.1	37.6 ± 6.8	-21.4 ± 7.8
Raspberry	Medium	leaf	6.37 ± 2.45	24.11 ± 0.36	25.02 ± 0.71	32.82 ± 2.81	114.2 ± 12.0	26.3 ± 11.0	-37.9 ± 8.7
Raspberry	High	leaf	3.02 ± 1.78	22.67 ± 1.63	22.06 ± 0.56	28.68 ± 1.89	48.4 ± 12.0	-25.5 ± 3.2	-80.7 ± 2.6
Strawberry	Low	leaf	9.73 ± 2.87	31.59 ± 1.43	28.58 ± 0.82	34.04 ± 1.60	150.3 ± 7.2	29.4 ± 15.0	-18.3 ± 6.1
Strawberry	Medium	leaf	4.18 ± 1.93	26.65 ± 0.98	23.86 ± 0.72	30.17 ± 1.16	115.1 ± 13.2	10.4 ± 18.6	-26.6 ± 10.4
Strawberry	High	leaf	1.95 ± 1.78	24.38 ± 0.58	21.33 ± 0.27	26.48 ± 0.78	48.5 ± 18.4	-28.3 ± 3.6	-83.3 ± 13.7

Supplementary data Table S3: ANOVAs showing the effects of species (raspberry vs. strawberry), organ (leaves vs. berries) and treatment (low, medium, and high RH) on the $\delta^{18}O$ values of tissue water, bulk sugars, cellulose, and bulk dried tissue.

		Df	Sum Sq	Mean Sq	F value	P
Tissue water $\delta^{18}O$	Species	1	7.3	7.3	1.3331	0.249
	Organ	1	4526.6	4526.6	822.877	< 0.001
	Treatment	2	4103.5	2051.7	372.9796	< 0.001
	Species:Treatment	2	4.5	2.2	0.4058	0.667
	Species:Organ	1	51.1	51.1	9.2926	< 0.01
	Organ:Treatment	2	208.9	104.4	18.9835	< 0.001
	Species:Organ:Treatment	2	65.9	33	5.9906	< 0.01
	Residuals	506	2783.5	5.5		
Bulk sugars $\delta^{18}O$	Species	1	102.08	102.08	48.4122	< 0.001
	Organ	1	28.04	28.04	13.2987	< 0.001
	Treatment	2	696.22	348.11	165.0916	< 0.001
	Species:Tratment	2	11.95	5.98	2.8337	0.069
	Species:Organ	1	2.31	2.31	1.0934	0.301
	Organ:Treatment	2	0.59	0.29	0.1398	0.869
	Species:Organ:Treatment	2	2.77	1.38	0.6559	0.524
	Residuals	48	101.21	2.11		
Cellulose $\delta^{18}O$	Species	1	100.44	100.44	41.0222	< 0.001
	Organ	1	83.42	83.42	34.069	< 0.001
	Treatment	2	1330.03	665.02	271.6016	< 0.001
	Species:Tratment	2	2.41	1.21	0.493	0.613
	Species:Organ	1	70.2	70.2	28.6722	< 0.001
	Organ:Treatment	2	8.15	4.08	1.6649	0.195
	Species:Organ:Treatment	2	1.92	0.96	0.3927	0.676
	Residuals	88	215.47	2.45		
Bulk	Species	1	127.29	127.29	74.7944	< 0.001
	Organ	1	40.07	40.07	23.5445	< 0.001

Treatment	2	1696.61	848.31	498.4554	< 0.001
Species:Treatment	2	33.14	16.57	9.735	< 0.001
Species:Organ	1	0.14	0.14	0.084	0.772
Organ:Treatment	2	10.45	5.22	3.0691	< 0.05
Species:Organ:Treatment	2	14.56	7.28	4.278	< 0.05
Residuals	85	314.85	1.7		

Supplementary data Table S4: ANOVAs showing the effects of species (raspberry vs. strawberry), organ (leaves vs. berries) and treatment (low, medium, and high RH) on the δ^2H values of tissue water, cellulose, and bulk dried tissue.

		Df	Sum Sq	Mean Sq	F value	P
Tissue water δ^2H	Species	1	68407	68407	519.1849	< 0.001
	Organ	1	258	258	1.9549	0.163
	Treatment	4	1156914	289229	2195.1366	< 0.001
	Species:Tratment	2	5369	2685	20.3762	< 0.001
	Species:Organ	1	3873	3873	29.3966	< 0.001
	Organ:Treatment	4	11484	2871	21.7891	< 0.001
	Species:Organ:Treatment	2	3066	1533	11.6355	< 0.001
	Residuals	543	71545	132		
Cellulose δ^2H	Species	1	13412	13412	105.8152	< 0.001
	Organ	1	99285	99285	783.3406	< 0.001
	Treatment	2	323137	161568	1274.7434	< 0.001
	Species:Tratment	2	3122	1561	12.3147	< 0.001
	Species:Organ	1	4	4	0.0335	0.855
	Organ:Treatment	2	1509	754	5.9511	< 0.01
	Species:Organ:Treatment	2	1060	530	4.1806	< 0.05
Bulk	Species	1	16685	16685	199.5769	< 0.001

Organ	1	33297	33297	398.288	< 0.001
Tratment	2	76088	38044	455.0731	< 0.001
Species:Treatment	2	198	99	1.185	0.31
Species:Organ	1	3467	3467	41.4653	< 0.001
Organ:Treatment	2	218	109	1.3015	0.277
Species:Organ:Treatment	1	2	2	0.0242	0.877

Supplementary data Table S5: ANOVAs showing the effects of species (raspberry vs. strawberry), organ (leaves vs. berries) and treatment (low, medium, and high RH) on f_{xylem} (oxygen and hydrogen).

		Df	Sum Sq	Mean Sq	F value	P
$f_{xylem\ oxygen}$	Species	1	0	0	0.0012	0.972
	Organ	1	9.3898	9.3898	1044.3834	< 0.001
	Treatment	2	0.6103	0.3052	33.9415	< 0.001
	Species:Treatment	2	0.0294	0.0147	1.6333	0.196
	Species:Organ	1	0.1571	0.1571	17.4763	< 0.001
	Organ:Treatment	2	0.0088	0.0044	0.4911	0.612
	Species:Organ:Treatment	2	0.1432	0.0716	7.9632	< 0.001
	Residuals	506	4.5493	0.009		
$f_{xylem\ hydrogen}$	Species	1	1.468	1.4681	19.525	< 0.001
	Organ	1	8.15	8.1505	108.3959	< 0.001
	Treatment	2	35.026	17.5132	232.9147	< 0.001
	Species:Treatment	2	3.101	1.5503	20.6177	< 0.001
	Species:Organ	1	0.456	0.4558	6.062	0.014
	Organ:Treatment	2	5.197	2.5985	34.5589	< 0.001
	Species:Organ:Treatment	2	1.343	0.6715	8.9301	< 0.001
	Residuals	507	38.122	0.0752		

Supplementary data Table S6: ANOVAs showing the effects species of (raspberry vs. strawberry), organ (leaves vs. berries) and treatment (low, medium, and high RH) on $\varepsilon_{wc\ source}$ for bulk sugars (for berry bulk sugars, only $\varepsilon_{wc\ source}$ values to leaf water).

		Df	Sum Sq	Mean Sq	F value	P
$\varepsilon_{wc\ source}$	Species	1	17.408	17.4078	8.2556	0.006
	Organ	1	28.042	28.0416	13.2987	< 0.001
	Treatment	2	8.193	4.0965	1.9428	0.154
	Species:Treatment	2	10.173	5.0866	2.4123	0.100
	Species:Organ	1	2.306	2.3055	1.0934	0.301
	Organ:Treatment	2	0.59	0.2949	0.1398	0.870
	Species:Organ:Treatment	2	2.766	1.383	0.6559	0.524
	Residuals	48	101.212	2.1086		

Supplementary data Table S7: ANOVAs showing the effects species of (raspberry vs. strawberry), organ (leaves vs. berries) and treatment (low, medium, and high RH) on $f_o p_x$.

		Df	Sum Sq	Mean Sq	F value	P
$f_o p_x$ ε_{wc} = 27‰	Species	1	0.31507	0.31507	25.9079	<0.001
	Organ	1	0.07738	0.07738	6.3627	0.013
	Treatment	2	0.62259	0.3113	25.5976	<0.001
	Species:Treatment	2	0.05117	0.02559	2.1039	0.126
	Species:Organ	1	0.60641	0.60641	49.8641	<0.001
	Organ:Treatment	2	0.01911	0.00956	0.7858	0.458
	Species:Organ:Treatment	2	0.00905	0.00452	0.372	0.690
	Residuals	151	1.83634	0.01216		
$f_o p_x$ ε_{wc} mean of	Species	1	0.00104	0.00104	0.0856	0.770
	Organ	1	0.07557	0.07557	6.2137	0.0138
	Treatment	2	0.40823	0.20411	16.784	< 0.001
	Species:Treatment	2	0.1131	0.05655	4.6499	0.011
	Species:Organ	1	0.60641	0.60641	49.8641	< 0.001
	Organ:Treatment	2	0.01911	0.00956	0.7858	0.458
	Species:Organ:Treatment	2	0.00905	0.00452	0.372	0.690
	Residuals	151	1.83634	0.01216		
$f_o p_x$ ε_{wc} per species and organ	Species	1	0.00014	0.00014	0.0133	0.908
	Organ	1	0.13995	0.13995	13.2127	< 0.001
	Treatment	2	0.30301	0.15151	14.3038	< 0.001
	Species:Treatment	2	0.09054	0.04527	4.2738	0.016
	Species:Organ	1	0.63268	0.63268	59.7322	< 0.001
	Organ:Treatment	2	0.02313	0.01157	1.0919	0.338
	Species:Organ:Treatment	2	0.00732	0.00366	0.3457	0.708
	Residuals	151	1.5994	0.01059		

Supplementary data Table S8: ANOVAs showing the effects species of (raspberry vs. strawberry), organ (leaves vs. berries) and treatment (low, medium, and high RH) on $\varepsilon_{cp\ oxygen}$ for bulk dried tissue $\delta^{18}O$ values.

		Df	Sum Sq	Mean Sq	F value	P
$\varepsilon_{cp\ oxygen}$	Species	1	64.28	64.277	36.9795	< 0.001
	Organ	1	7.23	7.227	4.1580	0.043
	Treatment	2	26.23	13.116	7.5456	0.001
	Species:Treatment	2	29.43	14.713	8.4647	< 0.001
	Species:Organ	1	293.66	293.663	168.9487	< 0.001
	Organ:Treatment	2	19.21	9.607	5.5269	0.005
	Species:Organ:Treatment	2	20.76	10.379	5.9713	0.003
	Residuals	185	321.56	1.738		

Supplementary data Table S9: ANOVAs showing the effects species of (raspberry vs. strawberry), organ (leaves vs. berries) and treatment (low, medium, and high RH) on f_{HIPx}.

		Df	Sum Sq	Mean Sq	F value	P
f_{HIPx}	Species	1	0.19728	0.19728	161.5472	< 0.001
	Organ	1	0.53335	0.53335	436.7471	< 0.001
	Treatment	2	0.24756	0.12378	101.3578	< 0.001
	Species:Treatment	2	0.11091	0.05545	45.4093	< 0.001
	Species:Organ	1	0.00382	0.00382	3.1305	0.078
	Organ:Treatment	2	0.10596	0.05298	43.3827	< 0.001
	Species:Organ:Treatment	2	0.00391	0.00195	1.5997	0.204
	Residuals	311	0.37979	0.00122		

Supplementary data Table S10: ANOVAs showing the effects species of (raspberry vs. strawberry), organ (leaves vs. berries) and treatment (low, medium, and high RH) on $\varepsilon_{cp\ hydrogen}$ for bulk dried tissue δ^2H values.

		Df	Sum Sq	Mean Sq	F value	P
$\varepsilon_{cp\ hydrogen}$	Species	1	41.9	41.87	0.7661	0.383
	Organ	1	726	726	13.2824	< 0.001
	Treatment	2	2022	1011.01	18.4969	< 0.001
	Species:Treatment	2	464.5	232.23	4.2487	0.016
	Species:Organ	1	2265.6	2265.58	41.4498	< 0.001
	Organ:Treatment	2	582.7	291.36	5.3305	0.006
	Species:Organ:Treatment	2	731.3	365.66	6.6900	0.002
	Residuals	164	8964	54.66		

Chapter 2

Variation of the oxygen isotope composition in leaves and grains of different cereal species and their implication for the parameterization of isotope models

Florian Cueni*[1,2], Daniel B. Nelson[1], Ansgar Kahmen[1]

[1]University of Basel, Department of Environmental Sciences – Botany, Schönbeinstrasse 6, 4056 Basel, Switzerland
[2]Agroisolab GmbH, Professor-Rehm-Strasse 6, 52428 Jülich, Germany
* Corresponding author: f.cueni.plantphys@gmail.com

Abstract

The leading method used for the geographic origin determination of agricultural products is stable isotope analysis. The recently proposed application of plant physiological isotope models for origin analysis promises to predict the oxygen isotopic signature of a product of interest at any given time point for any region where model input data is available. However, such applications require a careful model parameterization. In this study we tested if model parameters for simulating leaf water $\delta^{18}O$ values (f_{xylem}) and bulk dry leaf and grain $\delta^{18}O$ values ($p_x p_{ex} c$) are universal or species specific for different cereal species grown in the same environment. We found that leaf water $\delta^{18}O$ values of different cereal species differed among each other and that these differences are reflected in the model parameter f_{xylem}. Variation in f_{xylem} was, however, comparably small so that we can suggest the use of a common f_{xylem} value for the simulation of cereal leaf water d $\delta^{18}O$ values. We also found that, the bulk dried tissue $\delta^{18}O$ values were generally ^{18}O enriched compared to tissue water $\delta^{18}O$ values and that this was more so in grains than in leaves (Fig. 2). Differences between leaf and grain $\delta^{18}O$ values can partly be explained by different times of the growing season when these organs are synthesized. More importantly, however, we also found for $p_x p_{ex} c$ to be lower for grains than for leaves suggesting that less exchange of oxygen with source water in grains explains why grains are ^{18}O-enriched compared to leaves. Importantly, bulk dried tissue $\delta^{18}O$ values differed significantly among species, in particular for grains, which can also be mostly explained by species-specific differences in $p_x p_{ex} c$. The results of our study suggest that for using plant physiological stable isotope models for the origin analysis of cereal grains a careful selection of the key model parameters f_{xylem} and $p_x p_{ex} c$ is crucial. For f_{xylem} using a general value of 0.23 that is largely independent of the cereal species studied is suggested. In contrast, our study revealed that $p_x p_{ex} c$ can differ substantially among the different cereals so that species-specific values for $p_x p_{ex} c$ are recommended for a successful application of plant-physiological stable isotope models simulating bulk dried cereal grain $\delta^{18}O$ values for leaves and in particular for grains.

Introduction

The stable oxygen isotope composition ($\delta^{18}O$) in plant material is an important source of eco-hydrological information. The $\delta^{18}O$ values of a plant's tissue water reflect the $\delta^{18}O$ values of precipitation as well as the evaporative environment of the plant (Epstein et al. 1977; Sternberg et al. 1986; Yakir and DeNiro 1990), both of which show distinct temporal and geographic patterns (Dansgaard 1964; Bowen 2010). Moreover, the $\delta^{18}O$ values in organic molecules in plants have been found to generally reflect the $\delta^{18}O$ values of the bulk leaf water, with additional variation that is due to fractionation effects that occur during the primary assimilation of carbohydrates and post-photosynthetic processes (Sternberg et al. 1986; Yakir and DeNiro 1990; Roden and Ehleringer 1999).

The increasing understanding of key environmental and plant physiological drivers that explain this variability in leaf water (Cernusak et al. 2016), and plant organic compounds $\delta^{18}O$ values (Barbour and Farquhar 2000; Gessler et al. 2007; Song et al. 2014; Lehmann et al. 2017; Lehmann et al. 2020b; Lehmann et al. 2020a), have been incorporated into semi-mechanistic isotope models for leaf water and organic $\delta^{18}O$ values. These models have become indispensable tools for predicting and interpreting leaf water and plant-derived organic compound $\delta^{18}O$ values in a diverse range of applications, including ecology, plant physiology, and paleoclimatology (Sternberg and DeNiro 1983; Flanagan and Ehleringer 1991; Flanagan et al. 1991; Farquhar and Lloyd 1993; Roden et al. 1999; Roden and Ehleringer 1999; Barbour and Farquhar 2000; Farquhar et al. 2007).

Important uncertainties with regard to key model parameters still exist so that model applications require a case-by-case model parameterization which often limits their generalized application. For $\delta^{18}O$ values in leaf water, uncertainties exist in particular for the model parameters f_{xylem}, which is the fraction of unenriched source water in the leaf (Flanagan et al. 1991). For $\delta^{18}O$ values in plant organic material uncertainties exist in particular for the model parameters $p_x p_{ex}$ which describes the fraction of ^{18}O that exchanges with oxygen from source water during the synthesis of higher carbohydrates such as starch or cellulose and the transport of derived organic compounds with the surrounding plant water. Values of f_{xylem} have been reported to range from 0.10 to 0.33 (Allison 1985; Leaney et al. 1985; Walker et al. 1989; Flanagan et al. 1991; Cernusak et al. 2003; Song et al. 2015), and even higher values have been observed (Cernusak et al. 2016). This variability

in f_{xylem} has been mainly attributed to differences in transpiration rates and leaf anatomical features (Song et al. 2013; Roden et al. 2015). In addition, studies on plant cellulose $\delta^{18}O$ values, have reported $p_x p_{ex}$ values to range from 0.22 to 0.38 (Barbour et al. 2000a; Barbour and Farquhar 2000; Helliker and Ehleringer 2002; Barbour et al. 2004; Cernusak et al. 2005). Differences in $p_x p_{ex}$ values have been reported to be relative humidity driven (Cheesman and Cernusak 2016; Hirl et al. 2020) and dependent on different biosynthetic pathways used between species (Luo and Sternberg 1992; Sternberg et al. 2006).

An important requirement for a generalized application of oxygen isotope models, is to know if key model parameters are similarly expressed among species within constrained phylogenetic and functional groups. As such assessments of parameter variability are missing species-specific model parameterization are still necessary, which often limits the application of the models for the interpretation of oxygen isotope values in plants. Overcoming this limitation was the objective of this study. For this purpose, we analyzed the $\delta^{18}O$ values of different cereal species that are grown in a a common garden experiment at the University of Basel and assessed how variability in the $\delta^{18}O$ values among the investigated species translated into different expressions of the model parameters f_{xylem} and $p_x p_{ex}$. We chose cereals for our study because cereals are the most important food source for humans (FAO 2003) with a global cereal production of 2,711 million tons in 2019/2020 (FAO 2020). In the past, the stable isotope composition of cereals been used for the evaluation of crop performance (Barbour and Farquhar 2000; Condon et al. 2002; Farquhar et al. 2007; Cabrera-Bosquet et al. 2009; Araus et al. 2013), or for forensic applications like origin analysis (Goitom Asfaha et al. 2011; Luo et al. 2015). The interpretation of oxygen isotopes for either application is, however, associated with large uncertainty given uncertainties in parameter variability as explained above. Within the general context of our study we addressed the following specific questions:

1. How do tissue water $\delta^{18}O$ values compare among different cereal species that are grown in a common environment?
2. How do bulk dried tissue $\delta^{18}O$ values for leaves and grains compare among different cereal species that are grown in a common environment?

3. How does species specific variability in the model parameters f_{xylem} and $p_x p_{ex}$ explain the observed species-specific variability in leaf and and grain $\delta^{18}O$ values?

Methods

Experimental setup

Five winter crops and two summer crops were grown in a common garden experiment to investigate how the $\delta^{18}O$ values of tissue water and the $\delta^{18}O$ values bulk dried tissue of cereal leaves and grains compare among the seven different cereal species. Each species was grown in a 0.35 by 2.3 meter plot, in the botanical garden of the University of Basel, Switzerland. The investigated species were the common crops winter wheat (*Triticum aestivum* L.), spelt (*Triticum aestivum* subsp. *spelta* L.), winter barley (*Hordeum vulgare* L.), summer barley (*Hordeum vulgare* L. var. "Ayer 6"), oat (*Avena sativa* L.), as well as the related ancient species jointed goatgrass (*Aegilops cylindrica*), durum wheat (*Triticum turgidum* L.). Crops were sown in late November 2017, except for the two summer crops (summer barley and oat), which were sown in early spring 2018. We grew ca. 200 individual plants per crop species.

Ambient air temperature and relative humidity were monitored every 15 minutes using two sensors (HOBO Pro V2 temp/RH, Onset Computer Corporation, Bourne, USA) evenly spaced on the plot. The sensors were fixed on wooden poles one meter above the ground. To avoid direct sunlight hitting the sensors, they were shaded using white plastic flower pots, with air vents were cut into the sidewalls allowing for air circulation (for results see Supporting information Fig. 2). During dry periods in spring the plots were irrigated with local tap water.

The growth stages of crops were assessed after Tottman and Broad (1987) every second week. This was the start of booting, inflorescence emergence, and milk development, which were defined as the "beginning of grain ripening".

Sample collection

The $\delta^{18}O$ values of the precipitation water (including irrigation water) were assessed in 10-day intervals using two rain water collectors built after Prechsl et al. (2014).

Starting at the three-leaf stadium, samples for leaf water $\delta^{18}O$ (and $\delta^{2}H$, data only shown in Supporting information) were collected once every second week (for exact dates see Supporting information Table 1). In total, samples for leaf water were taken two to five times over the course of the experiment, dependent on the onset of leaf senescence at the end of the season.

For oat, samples for leaf water were collected only twice, for summer barley three times. Grain samples for tissue water analysis were collected once or twice prior to grain maturity for each species. For oat, no grains were collected for tissue water analysis due to a low number of plants that germinated. Five randomly selected leaf or grain samples were collected per species. For grain tissue water analysis, individual grains from one ear were collected per sample. After harvesting, leaves and grains were immediately sealed in a 12 mL gas-tight glass vial (Labco exetainers 12 mL, Labco, Lampeter, Wales, UK) and stored at -20 °C until extraction. Sampling was always done during the afternoon on sunny days.

By the end of the season, leaves and grains of mature, harvestable plants were collected for bulk dried tissue stable oxygen isotope analysis (for sampling dates see Supporting information Table 2). Five randomly selected leaf or grains samples were collected for each species. After harvesting, the samples were dried at 60 °C for at least 48 h. All dried samples for bulk dried tissue analysis were milled to a fine powder using mixer mill (Retsch MM440, Retsch GmbH, Haan, Germany).

Leaf physiological measurements

At each sampling day (see section above), midday stomatal conductance was measured, using a leaf porometer (Decagon SC-1 Porometer, Decagon Devices, Pullman, USA). The measurements were conducted between 12:30 and 16:00, on five healthy and sun exposed leaves per species. Each stomatal conductance measurement was followed by the assessment of the leaf temperature using a non-contact infrared thermometer (Voltcraft Conrad Electronic AG, Wollreau, Switzerland). Based on measurements, we found no difference in leaf temperature between the species, leaf temperature turned out to be 115 % of the midday air temperature (Supporting information Table 3).

Tissue water extraction

Tissue water from leaves and grains was cryogenically extracted after Newberry et al. (2017a). For the water extraction the exetainer tubes with the samples were heated in a water bath to 90 °C and the water evaporated from the sample was trapped in a glass u-tube submerged in liquid nitrogen at -196 °C, with the exetainer-u-tube system under constant vacuum (< 1.33 Pa). The extractions were run for two and a half hours. After extraction the u-tubes

were sealed and the samples were left to thaw and then transferred into 2 mL glass vials, sealed, and stored at 4 °C until analysis.

Isotope analysis

Water $\delta^{18}O$ (and $\delta^{2}H$) values were measured using the instrumental configuration as described in (Newberry et al. 2017b). Briefly, this used a TC/EA (high-temperature conversion/elemental analyzer) that was coupled to a Delta V Plus isotope ratio mass spectrometer (IRMS) through a ConFlo IV interface (Thermo Electron Corporation, Bremen, Germany) in the Stable Isotope Laboratory of the plant physiological ecology group of the University of Basel, Basel, Switzerland. Data were normalized to the VSMOW-SLAP scale using two calibrated in-house standards and are reported in delta notation (Vienna Standard Mean Ocean Water, and Standard Light Antarctic Precipitation, respectively). The long-term precision of the lab's quality control standard for $\delta^{18}O$ and $\delta^{2}H$ values in water were 0.24 ‰ and 0.7 ‰, respectively.

For the measurement of the bulk dried tissue $\delta^{18}O$ values, dried bulk material powder was oven dried for at least two days, after which ~ 0.5 mg was weighed into silver capsules, and then stored in a desiccator prior to analysis. Analyses were performed using a Flash IRMS operated in pyrolysis mode using a glassy carbon reactor configuration coupled to a Delta V Plus isotope ratio mass spectrometer through a ConFlo IV interface (Thermo Fisher Scientific, Bremen, Germany). At the beginning of each analytical run the samples were equilibrated with the pyrolysis reactor under constant helium flow for at least 3 hours using a Costech Zero-Blank Autosampler (NC Technologies Srl, Milan, Italy). $\delta^{18}O$ values were normalized to the VSMOW-SLAP scale using calibrated in-house standards and are reported in delta notation. Long term analytical precision was monitored through repeat analysis of an additional quality control sample, and was 0.20 ‰.

Stable isotope ratios are all expressed in delta (δ) notation and shown in per mil (‰) as ratio of the heavy over the light isotope of the sample (R_{sample}) in relation to the same ratio of the international standard ($R_{standard}$) using the following equation (Eqn. 1) where R is the $^{2}H/^{1}H$ or $^{18}O/^{16}O$ ratio (Coplen 2011):

Equation 1: $\delta_{sample} = (R_{sample}/R_{standard}) - 1$, ‰

Determination of model parameters

The model parameters f_{xylem} and $p_x p_{ex}$ were determined by fitting existing isotope models to measured values of leaf water and bulk $\delta^{18}O$ values using measured environmental variables. Oxygen isotope models for plant material are based on the Craig-Gordon model (Craig and Gordon 1965), and have been modified for plants (Dongmann et al. 1974; Farquhar and Lloyd 1993). The baseline model describes how evaporation leads to ^{18}O enrichment of water within leaves (Flanagan and Ehleringer 1991; Flanagan et al. 1991; Farquhar and Lloyd 1993; Roden et al. 1999) (Eqn 2):

Equation 2: $\delta^{18}O_{e\_leaf} = \delta^{18}O_{source\ water} + \varepsilon^{+} + \varepsilon_k + [(\delta^{18}O_V - \delta^{18}O_{source\ water}) - \varepsilon_k] * e_a/e_i$

$\delta^{18}O_{e\_leaf}$ is the isotopic composition of the water at the evaporative site in leaves, $\delta^{18}O_{source\ water}$ is the isotopic composition of plant source water, ε^{+} is the liquid-vapor equilibrium fractionation for water, ε_k is the kinetic fractionation factor accounting for diffusion through the stomata and boundary layer, $\delta^{18}O_V$ is the isotopic composition of ambient vapor, and e_a/e_i is the atmospheric vapor pressure (e_a) in relation to the intercellular vapor pressure in the leaf (e_i) (Bottinga and Craig 1969; Majoube 1971; Farquhar et al. 1989).

The model does not account for the constant flux of unenriched source water into the leaf, thus usually overestimates measured leaf water $\delta^{18}O$ values (Allison 1985; Walker et al. 1989; Yakir et al. 1990; Flanagan et al. 1991). This can be accounted for by incorporating the so called Péclet-effect into the calculations (Farquhar and Lloyd 1993; Barbour et al. 2004; Kahmen et al. 2011; Cernusak and Kahmen 2013), or by a two-pool modification of the model (Leaney et al. 1985; Yakir et al. 1990). To avoid overparameterization, the simpler two-pool model is sufficient for most applications, and thus used in this study (Cernusak et al. 2016; Bögelein et al. 2017). It divides bulk leaf water into an ^{18}O-enriched fraction ($\delta^{18}O_{e\_leaf}$) and a source water fraction ($\delta^{18}O_{source\ water}$). The parameter f_{xylem} describes how big the fraction of the source water in the bulk leaf water is ($\delta^{18}O_{\ leaf\ water}$) (Flanagan et al. 1991) (Eqn. 3):

Equation 3: $\delta^{18}O_{\ leaf\ water} = (1 - f_{xylem}) * \delta^{18}O_{\ e\_leaf} + (f_{xylem} * \delta^{18}O_{\ source\ water})$

During the primary assimilation of carbohydrates (trioses and hexoses) fractionations occur when carbonyl-group oxygen exchanges with leaf tissue water (Sternberg and DeNiro 1983). This leads to an ^{18}O-enrichment (ε_{wc}) of ~ +27 ‰ of primary carbohydrates compared to leaf water (Cueni et al. in review; Sternberg and DeNiro 1983; Yakir and DeNiro 1990; Yakir 1992; Sternberg and Ellsworth 2011; Lehmann et al. 2017). To form cellulose from primary assimilates, sucrose molecules are broken down to glucose and then re-joined, allowing some of the carbonyl oxygen to undergo further exchange with water in the developing cell. This causes the same fractionation of ~ +27 ‰ (ε_{wc}), as during primary carbohydrate assimilation (Sternberg and DeNiro 1983; Farquhar et al. 2007). The extent to which this fractionation is expressed on the resulting compounds depends, however, on the fraction of source water and ^{18}O enriched leaf water at the location of biosynthesis and the fraction of oxygen in sucrose that exchange with medium water during the biosynthesis of cellulose. These processes can mathematically be described as in Equation 4 (Roden and Ehleringer 1999; Barbour and Farquhar 2000):

Equation 4: $\delta^{18}O_{cellulose} = p_x p_{ex} * (\delta^{18}O_{source\ water} + \varepsilon_{wc}) + (1- p_x p_{ex}) * (\delta^{18}O_{leaf\ water} + \varepsilon_{wc})$

$\delta^{18}O_{cellulose}$ is the oxygen isotopic composition of cellulose, and p_{ex} is the fraction of carbonyl oxygen in cellulose that exchanges with the surrounding water during biosynthesis, and p_x is the proportion of unenriched source water in the cell where cellulose is synthesized (Barbour and Farquhar 2000). The values for p_x or p_{ex} are usually not determined individually, but combined as $p_x p_{ex}$ (Barbour et al. 2004). The bulk dried tissue material investigated in this study, besides cellulose, also contains other compounds such as lignin, lipids, and proteins. To simulate bulk dried tissue $\delta^{18}O$ values, the effect of these different compounds on the $\delta^{18}O$ values needs be incorporated by adding the model parameter c. However, $p_x p_{ex}$ and c cannot be determined individually, thus they are merged to the parameter $p_x p_{ex} c$:

Equation 5: $\delta^{18}O_{bulk} = p_x p_{ex} c *(\delta^{18}O_{source\ water} + \varepsilon_{wc}) + (1- p_x p_{ex} c) * (\delta^{18}O_{leaf\ water} + \varepsilon_{wc})$

We calculated the model parameters f_{xylem} and $p_x p_{ex} c$ on an individual basis for leaves and grains of each species using equation 3 and 5 (values for f_{xylem} were only determined for leaves). f_{xylem} values were calculated for samples of each collection date. For the calculation, $\delta^{18}O_{e\_leaf}$ was determined using equation 2 with equilibrium and kinetic fractionation factors calculated using stomatal conductance (mean values per sampling day and species), boundary layer resistance (1 m^2s/mol (Sachse et al. 2009)), and leaf temperature (115 % of the midday air temperature). Source water values were assumed to equal the measured precipitation $\delta^{18}O$ values (preceding two measurement, ca. 20 days (Brinkmann et al. 2019)) and vapor was set to be in equilibrium with precipitation water. Relative humidity was entered into the model as sampling time values (afternoon). Values for all model input data can be found in the supporting information Table 3.

Values for $p_x p_{ex} c$ were calculated using equation 5. For calculating $p_x p_{ex} c$ in leaves, species-specific mean $\delta^{18}O$ values of measured leaf water during the leaf formation period in April were used for $\delta^{18}O_{leaf\ water}$. Values $\delta^{18}O_{source\ water}$ we used mean source water from March and April, the time of leaf formation. For calculating $p_x p_{ex} c$ in grains, species-specific mean $\delta^{18}O$ values of measured leaf water during the species-specific growth stages of grain filling were used $\delta^{18}O_{leaf\ water}$. Leaf water values were used since sugars used for the synthesis of organic compounds in grains were originally produced in the leaves. For $\delta^{18}O_{source\ water}$, species-specific mean $\delta^{18}O$ values of measured precipitation water during the growth stages of heading to grain filling were used. The model parameter ε_{wc}, describing the enrichment of ^{18}O during the assimilation of primary organic compounds is described was set to be +27 ‰ (Sternberg and DeNiro 1983; Yakir and DeNiro 1990; Yakir 1992). Values for all model input data can be found in the supporting information table 4.

Statistical analysis

Statistical analyses were done using the statistical package R version 3.5.3 (R Core Team (2019). R: A language and environment for statistical computing. R Foundation for Statistical Computing, Vienna, Austria. URL: https://www.R-project.org/). Assumptions for the statistical tests (constant variance of residuals, normal distribution of residuals, same influence of all measurements) were tested with graphical residual diagnostics, using quantile-quantile and residuals vs. fitted plots. The type I error of all statistical

tests was set to $\alpha = 0.05$. The relationships among the different species and organs within one fraction (tissue water, bulk dried tissue) were compared using an analysis of variance (ANOVA) with a Tukey's honest significant difference (HSD) post-hoc test to find significant differences between individual groups, with the significance level set to $p = 0.05$.

Results

Tissue water

Over the course of the growing season the precipitation water $\delta^{18}O$ values increased by about 4 ‰, from -8.68 ‰ (± 0.18 ‰, n = 2) in early April to -4.75 ‰ (± 0.00 ‰, n = 2) in early July, at the end of the experiment (Fig. 1). Bulk leaf water was always enriched in ^{18}O compared to precipitation water (Fig. 1). Over the course of the growing season leaf water $\delta^{18}O$ values generally increased. On average, the increase in leaf water $\delta^{18}O$ values (mean slope over all species = 0.07 ‰) was similar as in precipitation water $\delta^{18}O$ values (slope = 0.07 ‰, Fig. 1). The mean leaf water $\delta^{18}O$ values for a given species ranged from 9.33 ‰ (durum wheat) to 13.18 ‰ (jointed goat grass) and differed significantly among species (Table 1). This difference was largely driven by jointed goatgrass, while the leaf water $\delta^{18}O$ values of the other species were rather similar.

The mean grain water $\delta^{18}O$ value for a given species ranged from -1.98 ‰ (winter barley) to 9.33 ‰ (jointed goat grass). Grain water $\delta^{18}O$ values were always lower than the corresponding leaf water $\delta^{18}O$ values with large and significant species-specific differences. Grain water $\delta^{18}O$ values similar to leaf water for jointed goatgrass and spelt but substantially lower that leaf water $\delta^{18}O$ values for the remaining species (Fig. 1). In fact, grain water $\delta^{18}O$ values of durum wheat, and summer barley and winter barley were almost similar to those of source water (Fig. 1).

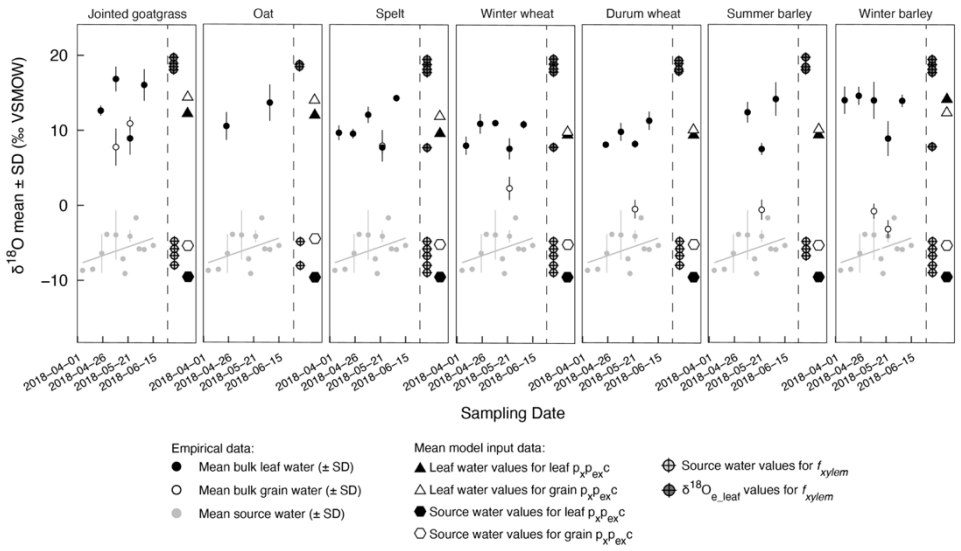

Figure 1: Bulk tissue water $\delta^{18}O$ values (mean ±SD) of leaves and grains (n = 5) for seven different cereal species collected throughout the 2018 growing season. Source water $\delta^{18}O$ values (mean± SD) and linear regression shown in grey. Values of leaf water $\delta^{18}O_{e\_leaf}$ and source water $\delta^{18}O$ used as model input data for the calculation of f_{xylem} (Eqn. 3) are shown as crossed points for each species, see also supporting information Table 3. Organ and species-specific $\delta^{18}O$ values of leaf water used as model input data for the calculation of $p_x p_{ex} c$ (Eqn. 5) are shown as triangles and source water values shown as hexagons, see supporting information Table 4 for details.

Table 1: ANOVAs showing the effect of species on the $\delta^{18}O$ values of leaf water and the modelled value $\delta^{18}O_{e\_leaf}$ (Equation 2).

Leaf water $\delta^{18}O$					
	Df	Sum Sq	Mean Sq	F value	P
Species	6	289.1	49.69	9.19	<0.001
Residuals	129	873.6	6.77		
$\delta^{18}O_{e\_leaf}$					
	Df	Sum Sq	Mean Sq	F value	P
Species	6	172	28.63	2.586	0.021
Residuals	129	1429	11.07		

Bulk dried tissue

Dried bulk tissue $\delta^{18}O$ values for a given species ranged from 24.15 ‰ to 26.04 ‰ for leaves and from 26.18 ‰ to 31.87 ‰ for grains and varied significantly among species (Fig. 2, Tukey's HSD $p < 0.05$) (Fig. 2). Grain bulk dried tissue $\delta^{18}O$ values were always significantly higher than leaf bulk dried tissue $\delta^{18}O$ values for a given species (Fig. 2, Table 2). We found no significant relationship between the bulk dried tissue $\delta^{18}O$ values of leaves and grains (Fig. 2b). We also did not find a significant relationship between the species mean leaf water $\delta^{18}O$ values and bulk dry tissue $\delta^{18}O$ values for leaves or grains (Fig. 3). We found, however, a strong and significant linear relationship between the start of the grain ripening time in the year and bulk dried tissue $\delta^{18}O$ values of grain ($r^2 = 0.89$, $p = 0.02$) (Fig. 4).

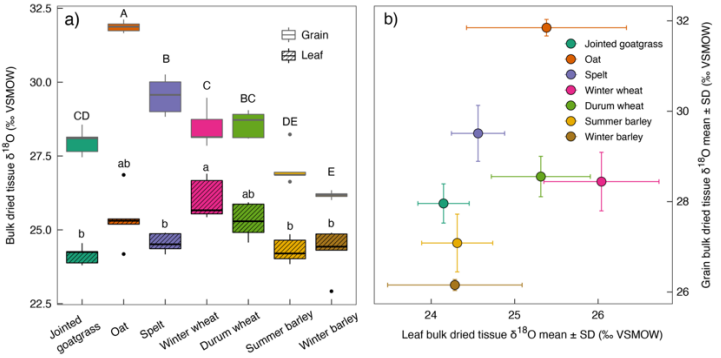

Figure 2: a) Bulk dried tissue $\delta^{18}O$ values of leaves (black outlined boxplot) and ripe grains (grey outlined boxplot) of 7 different cereal species collected at the end of the 2018 growing season (n = 5). For both organs (leaves and grains), significant differences among species are indicated in letters (lower case for leaves, upper case for grains). **b)** Correlation between the bulk dried tissue $\delta^{18}O$ values of cereal leaves and grains (mean ± SD; n = 5) for the seven species (r = 0.50, p = 0. 26).

Table 2: ANOVAs showing the effects of species (jointed goatgrass, oat, spelt, winter wheat, durum wheat, summer barley, and winter barley), and organ (leaves vs. grains) on the $\delta^{18}O$ values of bulk dried tissue.

Bulk dried tissue $\delta^{18}O$					
	Df	Sum Sq	Mean Sq	F value	P
Species	6	77.51	12.92	40.9	<0.001
Organ	1	235.41	235.41	745.5	<0.001
Species:Organ	6	38.32	6.39	20.2	<0.001
Residuals	56	17.68	0.32		

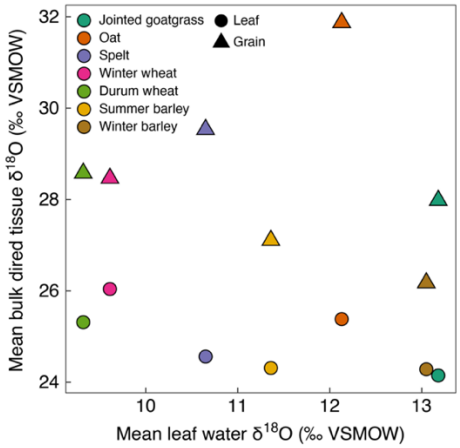

Figure 3: Relationship between leaf water $\delta^{18}O$ values (n = 10 to 25, dependent on the sampling days for each species, see Fig. 1) and bulk dried tissue $\delta^{18}O$ values of cereal leaves (full circle) and grains (open circle) (n = 5) across the seven species. (Correlation coefficients for leaves: r = -0.69, p = 0.08; for grains: r = -0.18, p = 0.70)

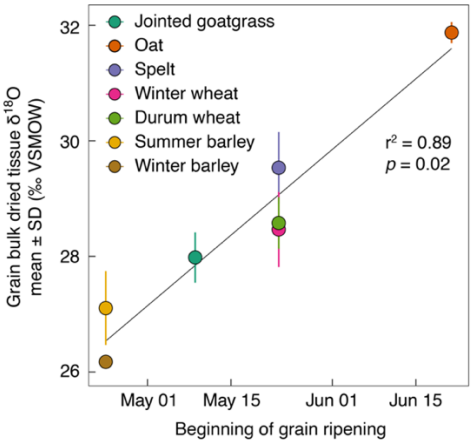

Figure 4: Bulk dried tissue $\delta^{18}O$ values (mean ±SD, n=5) of ripe grains of 7 different cereal species collected at the end of the 2018 growing season as a function of the beginning of fruit ripening of the individual species.

Leaf water f_{xylem} and bulk dried tissue $p_x p_{ex} c$ *values*

The species means of the calculated leaf water $\delta^{18}O$ values at the site of evaporation ($\delta^{18}O_{e\_leaf}$) ranged from 16.14 ‰ to 18.60 ‰ (Fig. 1). The values differed significantly among the species (Fig. 1, Table 1). The species means of the calculated f_{xylem} values ranged from 0.09 (winter barley) to 0.36 (summer barley) and differed significantly among species (Fig. 5, Table 3). The across species average f_{xylem} value obtained in this study was 0.23 (SD ± 0.19).

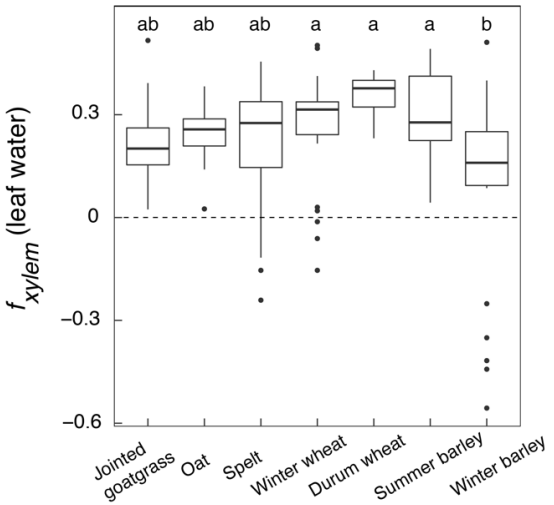

Figure 5: The fraction of unenriched source water (f_{xylem}) in leaf water for seven different cereal species collected once during the 2018 growing season (n = 5 per species and sampling day, in total 2 to 5 sampling days per species, see Fig.1).

Table 3: ANOVAs showing the effects of species (jointed goatgrass, oat, spelt, winter wheat, durum wheat, summer barley, and winter barley), on the f_{xylem} values for bulk leaf water $\delta^{18}O$ values.

f_{xylem} **(leaf water)**					
	Df	Sum Sq	Mean Sq	F value	P
Species	6	0.884	0.147	4.502	<0.001
Residuals	129	4.222	0.033		

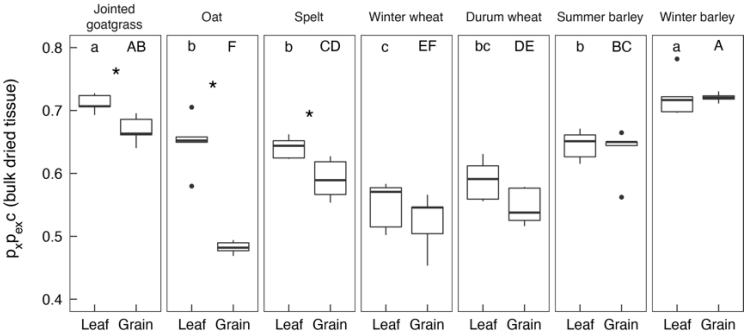

Figure 6: $p_xp_{ex}c$ values for bulk dried tissue $\delta^{18}O$ values of ripe grains and leaves for seven different cereal species collected at the end of the 2018 growing season (n = 5). Significant differences between grain and leaf $p_xp_{ex}c$ values within a species indicated with *, significant differences among species are indicated in letters, lower case for leaves, upper case for grains.

Table 4: ANOVAs showing the effects of species (jointed goatgrass, oat, spelt, winter wheat, durum wheat, summer barley, and winter barley), and organ (leaves vs. grains) on $p_xp_{ex}c$ values for bulk dried tissue $\delta^{18}O$ values of leaves and ripe grains.

$p_xp_{ex}c$					
	Df	Sum Sq	Mean Sq	F value	P
Species	6	0.283	0.047	50.91	<0.001
Organ	1	0.042	0.042	44.87	<0.001
Species:Organ	6	0.045	0.008	8.12	<0.001
Residuals	56	0.052	0.001		

The species means for the calculated $p_xp_{ex}c$ values ranged among species from 0.55 to 0.72 for leaves and from 0.48 to 0.72 for grains (Fig. 6), and differed significantly among species (Fig. 6, Table 4). Across all species, the mean $p_xp_{ex}c$ values was 0.64 (SD ± 0.06) for leaves and 0.60 (SD ± 0.08) for grains. The values differed significantly between organs and among species (Fig. 5, Table 4). We found strong linear relationship between the start of the grain ripening time and species mean $p_xp_{ex}c$ values, indicating lower $p_xp_{ex}c$ values in grains that formed later in the season ($r^2 = 0.75$, $p < 0.001$) (Fig. 7).

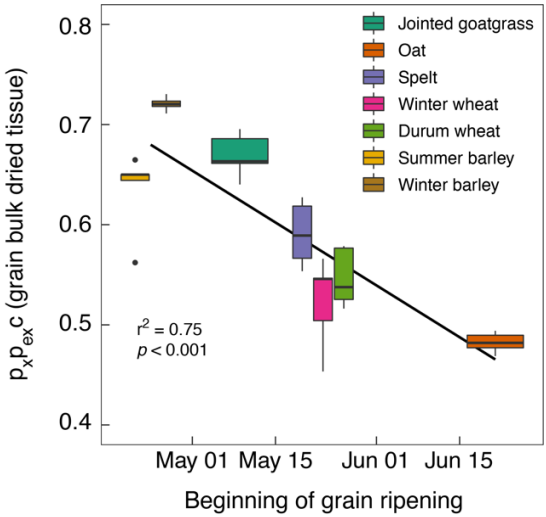

Figure 7: $p_xp_{ex}c$ values for bulk dried tissue $\delta^{18}O$ values of ripe grains of 7 different cereal species collected at the end of the 2018 growing season (n = 5) plotted versus the beginning of grain ripening of the individual species. Linear regression over all species shown as black line.

Discussion

The results of our study show that leaf water $\delta^{18}O$ values of different cereal species that were grown in a common environment varied (Fig. 1 and Table 1). These differences are reflected in the model parameter f_{xylem} rather than in $\delta^{18}O_{e\_leaf}$ (Fig. 1, Fig. 4 and Table 1, Table 3). We also found that compared to tissue water $\delta^{18}O$ values, the bulk dried tissue $\delta^{18}O$ values were generally ^{18}O enriched and more so in grains than in leaves (Fig. 2). Differences between leaves and grains were also found for $p_x p_{ex} c$, with lower values for grains. Importantly, bulk dried tissue $\delta^{18}O$ values differed significantly among species. The difference among species was smaller for leaves than for grains (Fig. 2). The model parameter $p_x p_{ex} c$ also differed significantly among species (Fig. 5). Moreover, the bulk dried tissue $\delta^{18}O$ values of grains correlated significantly with grain ripening time (Fig. 3).

$\delta^{18}O$ values of leaf and grain tissue water

Measured bulk leaf water $\delta^{18}O$ values in our study were consistently enriched in ^{18}O compared to the precipitation water (Fig. 1, for hydrogen Supporting information Fig. 1). This confirms that evaporative conditions lead to ^{18}O enrichment of leaf water, as has been described in many studies before (Dongmann et al. 1974; Flanagan and Ehleringer 1991; Flanagan et al. 1991; Farquhar and Lloyd 1993; Roden et al. 1999; Barbour and Farquhar 2000; Barbour et al. 2000b; Cernusak et al. 2005; Cernusak and Kahmen 2013; Song et al. 2015; Bögelein et al. 2017). The general increase of leaf water $\delta^{18}O$ values over time reflects the observed increases in source water $\delta^{18}O$ values over the course of the season. Among the species studied, we observed a range of 3.85 ‰ among the mean leaf water values. This range across species is lower than the ranges reported in previous studies investigating leaf water ^{18}O-enrichment of similar species grown in common environments (Helliker and Ehleringer 2000; Terwilliger et al. 2002; Kahmen et al. 2008).

The observed differences in the leaf tissue water $\delta^{18}O$ values among species can on the one hand be rooted in species-specific differences in evaporative ^{18}O-enrichment at the sites of evaporation, due to physiological and leaf energy balance differences among species. These effects are integrated in the basic Craig-Gordon model, that simulates the ^{18}O-enrichment at the sites of evaporation ($\delta^{18}O_{e\_leaf}$) as a function of atmospheric conditions (Eqn.2). Modelled $\delta^{18}O_{e\_leaf}$ values showed significant differences (Table 1), suggesting that physiological and leaf energy balance differences contribute

to the observed variability in leaf water $\delta^{18}O$ values. Physiological and leaf energy balance differences among the investigated species could come from, e.g., differences in plant height or leaf form that allow for different exposure to the atmosphere and therefore different leaf temperatures and stomatal conductance (g_s) (Helliker and Ehleringer 2000; Helliker and Ehleringer 2002). This in turn influences the equilibrium and kinetic fractionation during evaporation of leaf water and thus results in differing degrees of leaf water ^{18}O-enrichment ($\delta^{18}O_{e\_leaf}$) among the species. We found, for example, jointed goat grass and summer barley, both plants with narrow leaves, to generally have a lower g_s, ca. 0.03 mol/m^{2}s. These small differences resulted in slightly higher, but not significantly different $\delta^{18}O_{e\_leaf}$ values in jointed goat grass and summer barley compared to the other species (Tukey's HSD $p > 0.05$, Fig. 1, Supporting information Table 3). The small differences (Table 1, $p = 0.021$) that we found among the species in the initial ^{18}O-enrichment leaf water were caused by the low values from the first sampling date (10th of April), where only spelt, winter wheat, and winter barley were analysed (Supporting information Table 3), and may therefore largely be a sampling artifact.

On the other hand, and most important in our study, differences in the bulk leaf water $\delta^{18}O$ values also reflect differences of the dilution of evaporatively enriched leaf water ($\delta^{18}O_{e\_leaf}$) with non-^{18}O-enriched source water (Cernusak and Kahmen 2013). This effect is driven by large transpiration rates and leaf anatomical features that separate different water pools in leaves (Roden et al. 2015). In monocots (e.g. cereals), it has been shown that the flux of source water in leaves gets progressively enriched in ^{18}O with from the base of the leaf towards the tip, resulting in higher bulk leaf water $\delta^{18}O$ values in longer leaves (Helliker and Ehleringer 2000; Farquhar and Gan 2003). These processes are described as the "Péclet-effect" or as f_{xylem} in the two pool model that we apply (Farquhar and Lloyd 1993; Barbour et al. 2000b; Farquhar and Gan 2003; Barbour et al. 2004; Barbour 2007; Kahmen et al. 2008). Calculated f_{xylem} values among species varied significantly (Fig. 4, Table 3). We found that f_{xylem} was high for durum wheat and low for jointed goat grass and winter barley (Fig. 4). Some of the f_{xylem} values of winter barley, and also winter wheat and spelt, (first picking date at 10th of April) were even negative (Fig. 4). It shows that low transpiration due to low g_s, low air temperature, and high RH, in combination with the long leaves of spelt, winter wheat, and winter barley, led to a strong progressive leaf water ^{18}O-

enrichment along the leaf blade, which the Craig-Gordon model underpredicted (Supporting information Table 3). This circumstance has been described before for grasses (Helliker and Ehleringer 2000). In general, however, we found that the variability in f_{xylem} values among species was small, with most falling close to the overall mean of 0.23, which corresponds well with the reported values by literature (0.10 to 0.33) (Allison 1985; Leaney et al. 1985; Walker et al. 1989; Flanagan et al. 1991; Cernusak et al. 2003; Song et al. 2015). This suggests that general f_{xylem} values can be applied for simulating leaf water $\delta^{18}O$ values of most cereal species.

Comparing the tissue water $\delta^{18}O$ values of leaves to grains, we found that cereal grain water was generally ^{18}O-enriched compared to those of the source water (Fig.1). This agrees with the findings of Sanchez-Bragado et al. (2019), Cernusak et al. (2016), Barbour et al. (2000), and Cernusak et al. (2002). Importantly, however, bulk grain water was generally less ^{18}O-enriched than the corresponding bulk leaf water, sampled on the same day (Fig. 1). This was largely consistent across the seven species studied, except for jointed goatgrass and spelt, and also agrees with results from a recent study on durum wheat (Sanchez-Bragado et al. 2019). Compared to leaves, cereal grains are generally not exposed to evaporative enrichment because they have few stomata on the pericarp (Barlow et al. 1980), even though ripening grains have a photosynthetically active layer of aleurone (Caley et al. 1990). Moreover, reducing possible transpirational water loss are the ear bracts of grains (Bort et al. 1996). The intermediate grain water $\delta^{18}O$ values, which are lower than those of leaf water but higher than those of source water, indicates that this water pool carries both an unenriched source water signal as well as one influenced by evaporatively enriching conditions. This influence on the isotope composition of grain water might be direct, via a slight evaporative water loss from the grain. However, more importantly, the enrichment of water in cereal grains can be explained by water transport from leaves to grains, during filling of the developing grains via the phloem. Since phloem sap originates from leaves, it carries the ^{18}O-enriched bulk leaf water signal (Barbour and Farquhar 2000; Cernusak et al. 2005). For tomatoes, water filling the fruit has been shown to consist of up to 85-92 % of phloem sap during growth, and 98-99 % during maturity (Ho et al. 1987). Our results suggest that grain water is the result of mixing of ^{18}O and ^{2}H-enriched phloem water from the leaves, with relatively depleted source water (Cernusak et al. 2016; Sanchez-Bragado et al. 2019). The large variability in grain tissue water

$\delta^{18}O$ values (11.31 ‰) compared to leaves (3.85 ‰), is likely due to physiological differences among the species that allow for different amounts of unenriched source water to dilute the phloem $\delta^{18}O$ values. For winter barley, for example, the grain water $\delta^{18}O$ values were almost identical to the source water values (Fig. 1).

$\delta^{18}O$ values in bulk organic material

We found that the $\delta^{18}O$ values in bulk dried leaf and grain material were always ^{18}O-enriched compared to leaf water $\delta^{18}O$ values of the respective species. This ^{18}O-enrichment is due to the exchange of the carbonyl-group oxygen with cell water, leading to ^{18}O-enriching fractionation processes (~ +27 ‰), either during the primary assimilation of carbohydrates or during the synthesis of higher carbohydrates (Cueni et al. in review; Sternberg and DeNiro 1983; Yakir and DeNiro 1990; Yakir 1992; Sternberg and Ellsworth 2011; Lehmann et al. 2017). The variability in the bulk dried tissue $\delta^{18}O$ values of leaves and grains was, however, higher (range = 7.72 ‰) compared to the variability in the mean leaf water $\delta^{18}O$ values (range = 3.85 ‰) (Fig. 4). This is because the variability in cereal organic material is not only driven by the variability in leaf water directly, but also incorporates information about the timing of carbohydrate synthesis in the growing season and the leaf and source water pools used, as well as species-specific differences in the biosynthesis of the carbohydrates

The leaves of all cereal species that we used for bulk dried tissue $\delta^{18}O$ analysis developed throughout the month of April. The leaf water $\delta^{18}O$ values used for the assimilation of primary sugars in the month of April differed among species with a range of 5 ‰ (Fig. 1, Supporting information table 4). The plant's source water that exchanges oxygen during the formation of higher carbohydrates in the leaves can, however, be assumed to be similar for all species for the time of leaf formation in April (Fig. 1, Supporting information table 4). This suggests that varying degrees of leaf water ^{18}O-enrichment may have been the primary driver of observed variability in the leaf bulk dried tissue $\delta^{18}O$ values. On the other hand, variability in bulk dried leaf $\delta^{18}O$ values can also derive from physiological differences during carbohydrate synthesis, summarized in the model parameter $p_x p_{ex} c$. This parameter describes the fraction of unenriched source water present in the total pool of surrounding water (p_x), the fraction of carbonyl oxygen that exchanges with this pool during carbohydrate synthesis and the transport of derived

organic compounds with the surrounding plant water (p_{ex}), as well as other compounds present in bulk dried tissue (c). The $p_x p_{ex} c$ values for leaves differed significantly among the investigated species (Fig. 5, Table 4). A difference in p_x among different cereal species is, however, unlikely, since water in developing cells has been found to primarily reflect the isotope composition of source water (Barbour et al. 2002; Liu et al. 2017). The main drivers varying $p_x p_{ex} c$ values between species are thus changes in p_{ex} or c. Gessler et al. (2013) have shown species-specific differences in p_{ex}, for example occurring during the breakdown of transitory starch in the leaf, or during transport in phloem sap (Smith et al. 2003; Weise et al. 2004; Gessler et al. 2007; Gessler et al. 2014).Variability in p_{ex} can also result from different primary substrates (i.e. starch) available for carbohydrate synthesis and thus different biosynthetic pathways used between the species (Luo and Sternberg 1992; Sternberg et al. 2006). Moreover, the turnover rate of non-structural carbohydrates (NSC), that might differ between species due to differing photosynthetic activity and thus differences in carbon supply, has been shown to have a positive relationship with p_{ex} (Song et al. 2014). The mean value of $p_x p_{ex} c$ that we found across all species was 0.64 (SD ± 0.06). This is higher than $p_x p_{ex} c$ values reported for cellulose (0.25 to 0.54) (Barbour et al. 2000a; Helliker and Ehleringer 2002; Barbour et al. 2004; Kahmen et al. 2011; Cheesman and Cernusak 2016), and could reflect the fact that bulk dried tissue contains other compounds like lignin, lipids, or proteins in addition to carbohydrates, and is thus generally less ^{18}O-enriched than cellulose (Barbour and Farquhar 2000), accounted for by the parameter c.

To quantify how much of the observed across species variability in the bulk dried leaf $\delta^{18}O$ values in our study was derived from the different leaf water $\delta^{18}O$ values among the species, as opposed to species-specific values in $p_x p_{ex} c$, we simulated the bulk dried leaf $\delta^{18}O$ values using species specific $p_x p_{ex} c$ values, but an overall mean leaf water value (10.76 ‰). We found that in doing so, the simulated values bulk dried leaf $\delta^{18}O$ values had a range of 3.45 ‰, which is larger than the observed range of 1.89 ‰. This increase in variability suggests that the variability in leaf bulk dried tissue is strongly driven by species-specific differences in $p_x p_{ex} c$. However, it also shows that differences in leaf water $\delta^{18}O$ values among the species counteract the variability, and mute the observed differences in bulk dried leaf $\delta^{18}O$ values among the species.

Compared to the $\delta^{18}O$ values of bulk dried leaves, the $\delta^{18}O$ values in dried grain tissues were always higher within the same species. Grains act as carbohydrate sinks, so grain organic material carries the ^{18}O-enriched signal from sugars imported from the leaves. However, grain filling occurs later in the season than leaf formation (Tottman and Broad 1987). Thus, the sugars forming the organic material in grains are synthesized from leaf water with higher $\delta^{18}O$ values than leaf water present during the formation of leaves themselves. In addition, source water $\delta^{18}O$ values also increased over the course of the season, which would have provided a more 18O-rich pool for exchange pool for higher carbohydrate synthesis during grain filling compared to source water pool available during leaf formation (Fig. 1 and Supporting information Table 4). This explains grain bulk dried tissue being more ^{18}O-enrichend compared to leaves (Fig. 2), and agrees with studies investigating carbon allocation in sink tissues (e.g. grains), which has been shown to vary temporally compared to leaves (Cernusak et al. 2002). Moreover, we found $p_x p_{ex} c$ values to be lower for grains compared to leaves (Fig. 5, Table 4). This suggests that a smaller fraction of source water (p_x) and/or a smaller fraction of oxygen that exchanges with source water (p_{ex}) can as well explain grains to be generally ^{18}O-enriched compared to leaves. Values for p_{ex} have been shown to increase with increasing RH (Song et al. 2014). We observed a slight decrease in RH during the experiment (Supporting information Fig. 2). This might have resulted in higher p_{ex} during the development of leaves under a higher RH in spring, compared to grains in early summer, thus resulting in slightly higher $p_x p_{ex} c$ values for leaves of the same species (Fig. 5).

The $\delta^{18}O$ values of grains differed significantly among species and much more so than for leaves (Figure 2, Table 2). This can on the one hand be explained by the strong correlation of bulk dried grain $\delta^{18}O$ values with the beginning of the grain ripening time in the year ($r^2 = 0.89$) (Fig. 4), and thus different leaf water and source water pools, with differing $\delta^{18}O$ values that are imprinted into the grain organic matter of different species. On the other hand, we also found, that for grains, $p_x p_{ex} c$ values were significantly different among the species (Fig. 5, Table 2). The difference in $p_x p_{ex} c$ values between species, can be explained by the same mechanisms as described for leaves. The magnitude of difference in the $p_x p_{ex} c$ values among the grains of the different species is, however, that big (range between species means 0.2), that we doubt that the RH between the different grain ripening times are the major influence

on the difference, as for leaves compared grains of the same species. Rather, it reflects species-specific variability in $p_x p_{ex} c$ (Fig. 6). With a mean value of 0.60, the $p_x p_{ex} c$ values for grains were also higher than reported in the literature, mainly due to the same reasons as explained for leaves.

It is unclear, how much of the variability in the bulk dried $\delta^{18}O$ values in grains can be attributed to external factors relating to seasonal changes in temperature, humidity, and source water $\delta^{18}O$ values and their influence on the plant-relevant water pools, versus variability driven by internal species-specific effects related to differences in carbohydrate synthesis among species. To assess the degree to which this variability (range = 5.69 ‰) could be explained by species-specific $p_x p_{ex} c$ values as opposed to seasonal changes in the available water pools, we modeled grain $\delta^{18}O$ values using fixed tissue and source water $\delta^{18}O$ values. We did so by using species-specific $p_x p_{ex} c$ values, but instead of species- /ripening time-specific leaf and source water values, we used an overall mean leaf water (10.6 ‰) and source water value (-5.5 ‰). These calculated bulk dried grain $\delta^{18}O$ values varied with a range of 4.74 ‰. This accounted for 83 % of the range observed across species in our samples, suggesting that the differences in bulk dried $\delta^{18}O$ values in grains among the species were mainly driven by differences in the synthesis of carbohydrates ($p_x p_{ex} c$). However, the timing of grain ripening and consequent shifting of the source and leaf water $\delta^{18}O$ values was not negligible.

Conclusion

The results of our study promote the potential of using plant physiological stable isotope models for the origin analysis of cereal grains. However, we also showed that careful parametrizations of the key model parameters f_{xylem}, and $p_x p_{ex} c$ are crucial. For f_{xylem} the differences among most of the species were small. For the application of plant physiological stable isotope models to simulate cereal leaf water $\delta^{18}O$ values, this in turn means that a general leaf water model for cereals could be used, mostly independent of the cereal species studied. The $p_x p_{ex} c$ values among the different cereals, however, were strongly species-specific and explained a large fraction of the species-specific variability in bulk dried grain $\delta^{18}O$ values that we observed in this study. Moreover, we also found the source and leaf water needed for an accurate simulation of the bulk dried grain $\delta^{18}O$ values to strongly correlate with the species-specific time of grain ripening. Thus, for a successful

application of plant-physiological stable isotope models simulating bulk dried cereal grain $\delta^{18}O$ values for origin analysis, it is crucial to use species-specific $p_x p_{ex} c$ values, as well as water input values specific to the grain ripening time.

Acknowledgements
We would like to Svenja Förster for her support with the sample preparation and analysis, and the team of the botanical garden Basel for providing us with the space to grow the plants and helping us whenever in need. The present work was supported by PlantHUB - European Industrial Doctorate funded by the European Commission's Horizon 2020 research and innovation program under the Marie Skłodowska-Curie grant agreement No 722338. The program is managed by the Zurich-Basel Plant Science Center.

Literature

Allison GB (1985) The relationship between deuterium and oxygen-18 delta values in leaf water. Chem Geol 58:145–156.

Araus JL, Cabrera-Bosquet L, Serret MD, et al (2013) Comparative performance of $\delta^{13}C$, $\delta^{18}O$ and $\delta^{15}N$ for phenotyping durum wheat adaptation to a dryland environment. Funct Plant Biol 40:595. doi: 10.1071/FP12254

Barbour MM (2007) Stable oxygen isotope composition of plant tissue: a review. Funct Plant Biol 34:83–94. doi: 10.1071/FP06228

Barbour MM, Farquhar GD (2000) Relative humidity- and ABA-induced variation in carbon and oxygen isotope ratios of cotton leaves. Plant Cell Environ 23:473–485. doi: 10.1046/j.1365-3040.2000.00575.x

Barbour MM, Fischer RA, Sayre KD, Farquhar GD (2000a) Oxygen isotope ratio of leaf and grain material correlates with stomatal conductance and grain yield in irrigated wheat. Aust J Plant Physiol 27:625–637. doi: 10.1071/PP99041

Barbour MM, Roden JS, Farquhar GD, Ehleringer JR (2004) Expressing leaf water and cellulose oxygen isotope ratios as enrichment above source water reveals evidence of a Péclet effect. Oecologia 138:426–435. doi: 10.1007/s00442-003-1449-3

Barbour MM, Schurr U, Henry BK, et al (2000b) Variation in the Oxygen Isotope Ratio of Phloem Sap Sucrose from Castor Bean. Evidence in Support of the Péclet Effect. Plant Physiol 123:671–680. doi: 10.1104/pp.123.2.671

Barbour MM, Walcroft AS, Farquhar GD (2002) Seasonal variation in δ13C and δ18O of cellulose cellulose from growth rings of Pinus radiata. Plant Cell Environ 1483–1499. doi: https://doi.org/10.1046/j.0016-8025.2002.00931.x

Barlow EWR, Lee JW, Munns R, Smart MG (1980) Water Relations of the Developing Wheat Grain. Aust J Plant Physiol 7:519–25. doi: 10.1071/PP9800519

Bögelein R, Thomas FM, Kahmen A (2017) Leaf water ^{18}O and ^{2}H enrichment along vertical canopy profiles in a broadleaved and a conifer forest tree. Plant Cell Environ 40:1086–1103. doi: 10.1111/pce.12895

Bort J, Brown RH, Araus JL (1996) Refixation of respiratory CO_2 in the ears of C_3 cereals. J Exp Bot 47:1567–1575. doi: 10.1093/jxb/47.10.1567

Bottinga Y, Craig H (1969) Oxygen Isotope Fractionation Between CO_2 and Water, and the Isotopic Composition of Marina Atmospheric CO_2. Earth Planet Sci Lett 5:285–295.

Bowen GJ (2010) Isoscapes: Spatial Pattern in Isotopic Biogeochemistry. Annu Rev Earth Planet Sci 38:161–187. doi: 10.1146/annurev-earth-040809-152429

Brinkmann N, Eugster W, Buchmann N, Kahmen A (2019) Species-specific differences in water uptake depth of mature temperate trees vary with water availability in the soil. Plant Biol 21:71–81. doi: 10.1111/plb.12907

Cabrera-Bosquet L, Molero G, Nogués S, Araus JL (2009) Water and nitrogen conditions affect the relationships of $\Delta^{13}C$ and $\Delta^{18}O$ to gas exchange and growth in durum wheat. J Exp Bot 60:1633–1644. doi: 10.1093/jxb/erp028

Caley CY, Duffus CM, JEFFCOAT B (1990) Photosynthesis in the Pericarp of Developing Wheat Grains. J Exp Bot 41:303–307. doi: 10.1093/jxb/41.3.303

Cernusak LA, Barbour MM, Arndt SK, et al (2016) Stable isotopes in leaf water of terrestrial plants. Plant Cell Environ 39:1087–1102. doi: 10.1111/pce.12703

Cernusak LA, Farquhar GD, Pate JS (2005) Environmental and physiological controls over oxygen and carbon isotope composition of Tasmanian blue gum, Eucalyptus globulus. Tree Physiol 25:129–146. doi: 10.1093/treephys/25.2.129

Cernusak LA, Kahmen A (2013) The multifaceted relationship between leaf water 18O enrichment and transpiration rate. Plant Cell Environ 36:1239–1241. doi: 10.1111/pce.12081

Cernusak LA, Pate JS, Farquhar GD (2002) Diurnal variation in the stable isotope composition of water and dry matter in fruiting Lupinus angustifolius under field conditions. Plant Cell Environ 25:893–907. doi: 10.1046/j.1365-3040.2002.00875.x

Cernusak LA, Wong SC, Farquhar GD (2003) Oxygen isotope composition of phloem sap in relation to leaf water in Ricinus communis. Funct Plant Biol 30:1059. doi: 10.1071/FP03137

Cheesman AW, Cernusak LA (2016) Infidelity in the outback : climate signal recorded in $\Delta^{18}O$ of leaf but not branch cellulose of eucalypts across an Australian aridity gradient. Tree Physiol 37:554–564. doi:

10.1093/treephys/tpw121

Condon AG, Richards RA, Rebetzke GJ, Farquhar GD (2002) Improving Intrinsic Water-Use Efficiency and Crop Yield. Crop Sci 42:122. doi: 10.2135/cropsci2002.0122

Coplen TB (2011) Guidelines and recommended terms for expression of stable- isotope-ratio and gas-ratio measurement results. Rapid Commun Mass Spectrom 2538–2560. doi: 10.1002/rcm.5129

Craig H, Gordon LI (1965) Deuterium and oxygen 18 variations in the ocean and the marine atmosphere. In: Tongiorgi E (ed) Proceedings of the conference on stable isotopes in oceanographic studies and paleotemperatures. Piza, Italy: Laboratory of Geology and Nuclear Science. Pisa IT, pp 9–130

Cueni F, Nelson DB, Lehmann MM, et al Constraining parameter uncertainty for predicting oxygen and hydrogen isotope values in fruit.

Dansgaard W (1964) Stable isotopes in precipitation. Tellus 2826:436–468. doi: 10.3402/tellusa.v16i4.8993

Dongmann G, Nürnberg HW, Förstel H, Wagener K (1974) On the Enrichment of $H_2{}^{18}O$ in the Leaves of Transpiring Plants. Radiat Environ Biophys 11:41–52. doi: 10.1007/BF01323099

Epstein S, Thompson P, Ya CJ (1977) Oxygen and Hydrogen Isotopic Ratios in Plant Cellulose.

FAO (2003) World agriculture: Towards 2015/2030. An FAO Parspective. FAO, 00100 Rome

FAO (2020) Food Outlook - Biannual Report on Global Food Markets: June 2020. Food Outlook 1–142. doi: https://doi.org/10.4060/ca9509en

Farquhar GD, Cernusak LA, Barnes B (2007) Heavy Water Fractionation during Transpiration. Plant Physiol 143:11–18. doi: 10.1104/pp.106.093278

Farquhar GD, Ehleringer JR, Hubick KT (1989) Carbon Isotope Discrimination and Photosynthesis. Annu Rev Plant Physiol Plant Mol Biol 40:503–537. doi: 1040-2519/89/0601-503

Farquhar GD, Gan KS (2003) On the progressive enrichment of the oxygen isotopic composition of water along a leaf. Plant Cell Environ 26:1579–1597. doi: 10.1046/j.0016-8025.2001.00829.x-i1

Farquhar GD, Lloyd J (1993) Carbon and Oxygen Isotope Effects in the Exchange of Carbon Dioxide between Terrestrial Plants and the Atmosphere. In: n: James R. Ehleringer, Anthony E. Hall, Graham D.

Farquhar, eds. Stable Isotopes and Plant Carbon-water Relations. Elsevier, pp 47–70

Flanagan LB, Comstock JP, Ehleringer JR (1991) Comparison of Modeled and Observed Environmental Influences on the Stable Oxygen and Hydrogen Isotope Composition of Leaf Water in Phaseolus vulgaris L. Plant Physiol 96:588–596. doi: 10.1104/pp.96.2.588

Flanagan LB, Ehleringer JR (1991) Stable isotope composition of stem and leaf water : applications to the study of plant water use. Funct Ecol 5:270–277.

Gessler A, Brandes E, Keitel C, et al (2013) The oxygen isotope enrichment of leaf-exported assimilates – does it always reflect lamina leaf water enrichment? New Phytol 200:144–157. doi: 10.1111/nph.12359

Gessler A, Ferrio JP, Hommel R, et al (2014) Stable isotopes in tree rings: Towards a mechanistic understanding of isotope fractionation and mixing processes from the leaves to the wood. Tree Physiol 34:796–818. doi: 10.1093/treephys/tpu040

Gessler A, Peuke AD, Keitel C, Farquhar GD (2007) Oxygen isotope enrichment of organic matter in *Ricinus communis* during the diel course and as affected by assimilate transport. New Phytol 174:600–613. doi: 10.1111/j.1469-8137.2007.02007.x

Goitom Asfaha D, Quétel CR, Thomas F, et al (2011) Combining isotopic signatures of $n(^{87}Sr)/n(^{86}Sr)$ and light stable elements (C, N, O, S) with multi-elemental profiling for the authentication of provenance of European cereal samples. J Cereal Sci 53:170–177. doi: 10.1016/j.jcs.2010.11.004

Helliker BR, Ehleringer JR (2002) Differential ^{18}O enrichment of leaf cellulose in C3 versus C4 grasses. Funct Plant Biol 29:435. doi: 10.1071/PP01122

Helliker BR, Ehleringer JR (2000) Establishing a grassland signature in veins: ^{18}O in the leaf water of C3 and C4 grasses. Proc Natl Acad Sci 97:7894–7898. doi: 10.1073/pnas.97.14.7894

Hirl RT, Ogée J, Ostler U, et al (2020) Temperature-sensitive biochemical ^{18}O-fractionation and humidity-dependent attenuation factor are needed to predict $\delta^{18}O$ of cellulose from leaf water in a grassland ecosystem. New Phytol. doi: 10.1111/nph.17111

Ho LC, Grange RI, Glasshouse AJP (1987) An analysis of the accumulation of water and dry matter in tomato fruit. 157–162.

Kahmen A, Sachse D, Arndt SK, et al (2011) Cellulose $\delta^{18}O$ is an index of leaf-to-air vapor pressure difference (VPD) in tropical plants. Proc Natl Acad Sci 108:1981–1986. doi: 10.1073/pnas.1018906108

Kahmen A, Simonin K, Tu KP, et al (2008) Effects of environmental parameters, leaf physiological properties and leaf water relations on leaf water δ18O enrichment in different Eucalyptus species. Plant Cell Environ 31:738–751. doi: 10.1111/j.1365-3040.2008.01784.x

Leaney FW, Osmond CB, Allison GB, Ziegler H (1985) Hydrogen-isotope composition of leaf water in C3 and C4 plants: its relationship to the hydrogen-isotope composition of dry matter. Planta 164:215–220. doi: 10.1007/BF00396084

Lehmann MM, Egli M, Brinkmann N, et al (2020a) Improving the extraction and purification of leaf and phloem sugars for oxygen isotope analyses. Rapid Commun Mass Spectrom 34:e8854. doi: 10.1002/rcm.8854

Lehmann MM, Gamarra B, Kahmen A, et al (2017) Oxygen isotope fractionations across individual leaf carbohydrates in grass and tree species. Plant Cell Environ 40:1658–1670. doi: 10.1111/pce.12974

Lehmann MM, Goldsmith GR, Mirande-Ney C, et al (2020b) The 18 O-signal transfer from water vapour to leaf water and assimilates varies among plant species and growth forms. Plant Cell Environ 43:510–523. doi: 10.1111/pce.13682

Liu HT, Schäufele R, Gong XY, Schnyder H (2017) The δ 18 O and δ 2 H of water in the leaf growth-and-differentiation zone of grasses is close to source water in both humid and dry atmospheres. New Phytol 214:1423–1431. doi: 10.1111/nph.14549

Luo D, Dong H, Luo H, et al (2015) The application of stable isotope ratio analysis to determine the geographical origin of wheat. Food Chem 174:197–201. doi: 10.1016/j.foodchem.2014.11.006

Luo Y-H, Sternberg L (1992) Hydrogen and Oxygen Isotopic Fractionation During Heterotrophic Cellulose Synthesis. J Exp Bot 43:47–50. doi: 10.1093/jxb/43.1.47

Majoube M (1971) Fractionnement en oxygène 18 et en deutérium entre l'eau et sa vapeur. J Chim Phys 68:1423–1436.

Newberry SL, Nelson DB, Kahmen A (2017a) Cryogenic vacuum artifacts do not affect plant water-uptake studies using stable isotope analysis. Ecohydrology 10:e1892. doi: 10.1002/eco.1892

Newberry SL, Prechsl UE, Pace M, Kahmen A (2017b) Tightly bound soil

water introduces isotopic memory effects on mobile and extractable soil water pools. Isotopes Environ Health Stud 53:368–381. doi: 10.1080/10256016.2017.1302446

Prechsl UE, Gilgen AK, Kahmen A, Buchmann N (2014) Reliability and quality of water isotope data collected with a low-budget rain collector. Rapid Commun Mass Spectrom 28:879–885. doi: 10.1002/rcm.6852

Roden J, Kahmen A, Buchmann N, Siegwolf R (2015) The enigma of effective path length for 18 O enrichment in leaf water of conifers. Plant Cell Environ 38:2551–2565. doi: 10.1111/pce.12568

Roden JS, Ehleringer JR (1999) Hydrogen and oxygen isotope ratios of tree-ring cellulose for riparian trees grown long term under hydroponycally environments. Oecologia 121:467–477.

Roden JS, Lin G, Ehleringer JR (1999) A mechanistic model for interpretation of hydrogen and oxygen isotope ratios in tree-ring cellulose. Geochim Cosmochim Acta 64:21–35. doi: 10.1016/S0016-7037(99)00195-7

Sachse D, Kahmen A, Gleixner G (2009) Organic Geochemistry Significant seasonal variation in the hydrogen isotopic composition of leaf-wax lipids for two deciduous tree ecosystems (*Fagus sylvativa* and *Acer pseudoplatanus*). Org Geochem 40:732–742. doi: 10.1016/j.orggeochem.2009.02.008

Sanchez-Bragado R, Serret MD, Marimon RM, et al (2019) The hydrogen isotope composition δ^2H reflects plant performance. Plant Physiol 180:793–812. doi: 10.1104/pp.19.00238

Smith AM, Zeeman SC, Thorneycroft D, Smith SM (2003) Starch mobilization in leaves. J Exp Bot 54:577–583. doi: 10.1093/jxb/erg036

Song X, Barbour MM, Farquhar GD, et al (2013) Transpiration rate relates to within- and across-species variations in effective path length in a leaf water model of oxygen isotope enrichment. Plant Cell Environ 36:1338–1351. doi: 10.1111/pce.12063

Song X, Farquhar GD, Gessler A, Barbour MM (2014) Turnover time of the non-structural carbohydrate pool influences δ18O of leaf cellulose. Plant Cell Environ 37:2500–2507. doi: 10.1111/pce.12309

Song X, Loucos KE, Simonin KA, et al (2015) Measurements of transpiration isotopologues and leaf water to assess enrichment models in cotton. New Phytol 1:637–646.

Sternberg L, DeNiro M (1983) Biogeochemical implications of the isotopic equilibrium fractionation factor between the oxygen atoms of acetone

and water.

Sternberg L, DeNiro MJ, Savidge RA (1986) Oxygen Isotope Exchange between Metabolites and Water during Biochemical Reactions Leading to Cellulose Synthesis. Plant Physiol 82:423–427. doi: 10.1104/pp.82.2.423

Sternberg L, Ellsworth PFV (2011) Divergent Biochemical Fractionation, Not Convergent Temperature, Explains Cellulose Oxygen Isotope Enrichment across Latitudes. PLoS One 6:e28040. doi: 10.1371/journal.pone.0028040

Sternberg L, Pinzon MC, Anderson WT, Jahren HA (2006) Variation in oxygen isotope fractionation during cellulose synthesis: intramolecular and biosynthetic effects. Plant Cell Environ 29:1881–1889. doi: 10.1111/j.1365-3040.2006.01564.x

Terwilliger VJ, Betancourt JL, Leavitt SW, Van De water PK (2002) Leaf cellulose δD and $\delta^{18}O$ trends with elevation differ in direction among co-occurring, semiarid plant species. Geochim Cosmochim Acta 66:3887–3900. doi: 10.1016/S0016-7037(02)00964-X

Tottman DR, Broad H (1987) The decimal code for the growth stages of cereals, with illustrations. Ann Appl Biol 110:441–454. doi: https://doi.org/10.1111/j.1744-7348.1987.tb03275.x

Walker CD, Leaney FW, Dighton JC, Allison GB (1989) The influence of transpiration on the equilibration of leaf water with atmospheric water vapour. Plant Cell Environ 12:221–234. doi: 10.1111/j.1365-3040.1989.tb01937.x

Weise SE, Weber APM, Sharkey TD (2004) Maltose is the major form of carbon exported from the chloroplast at night. Planta 218:474–482. doi: 10.1007/s00425-003-1128-y

Yakir D (1992) Variations in the natural abundance of oxygen-18 and deuterium in plant carbohydrates. Plant Cell Environ 15:1005–1020. doi: 10.1111/j.1365-3040.1992.tb01652.x

Yakir D, DeNiro MJ (1990) Oxygen and Hydrogen Isotope Fractionation during Cellulose Metabolism in Lemna gibba L. Plant Physiol 93:325–332. doi: 10.1104/pp.93.1.325

Yakir D, DeNiro MJ, Gat JR (1990) Natural deuterium and oxygen-18 enrichment in leaf water of cotton plants grown under wet and dry conditions: evidence for water compartmentation and its dynamics. Plant Cell Environ 13:49–56. doi: 10.1111/j.1365-

3040.1990.tb01298.x

Supporting Information

Supporting information Table 1: Measured leaf and grain water $\delta^{18}O$ and $\delta^{2}H$ values. As averages (n = 5) (± SD) per species, organ and sampling day. All cereals were grown in individual 0.35 x 2.3 meter parcels, of the same 2.3 by 2.5 meter plot at the botanical garden of the University of Basel, Switzerland.

Species	Organ	Sampling Date	Tissue water $\delta^{18}O$ (‰ VSMOW)		Tissue water $\delta^{2}H$ (‰ VSMOW)	
			mean	SD	mean	SD
Durum wheat	leaf	2018-04-24	8.08	0.42	-10.84	2.28
Durum wheat	leaf	2018-05-09	9.79	1.19	-8.49	4.85
Durum wheat	grain	2018-05-23	-0.51	1.23	-36.14	4.57
Durum wheat	leaf	2018-05-23	8.17	0.51	-6.66	1.84
Durum wheat	leaf	2018-06-06	11.27	1.22	-1.03	2.60
Jointed goatgrass	leaf	2018-04-24	12.62	0.68	-8.46	1.65
Jointed goatgrass	grain	2018-05-09	7.76	2.48	-15.64	9.56
Jointed goatgrass	leaf	2018-05-09	16.84	1.65	12.76	6.44
Jointed goatgrass	grain	2018-05-23	10.91	0.92	-3.00	3.07
Jointed goatgrass	leaf	2018-05-23	8.92	2.18	-6.11	4.17
Jointed goatgrass	leaf	2018-06-06	16.05	2.11	11.30	6.60
Oat	leaf	2018-04-24	10.58	1.86	-15.09	3.63
Oat	leaf	2018-06-06	13.69	2.42	7.64	3.81
Spelt	leaf	2018-04-10	9.67	0.97	-6.27	1.11
Spelt	leaf	2018-04-24	9.54	0.64	-15.77	1.89
Spelt	leaf	2018-05-09	12.06	1.09	-2.49	5.15
Spelt	grain	2018-05-23	7.93	2.11	-11.89	6.95
Spelt	leaf	2018-05-23	7.70	0.85	-8.89	2.04
Spelt	leaf	2018-06-06	14.29	0.44	7.58	0.73
Summer barley	leaf	2018-05-09	12.41	1.38	0.75	4.00
Summer barley	grain	2018-05-23	-0.59	1.35	-38.09	4.29

Summer barley	leaf	2018-05-23	7.50	0.80	-7.27	1.46
Summer barley	leaf	2018-06-06	14.16	2.23	10.44	5.17
Winter barley	leaf	2018-04-10	14.01	1.82	-8.19	2.76
Winter barley	leaf	2018-04-24	14.59	1.20	-8.22	1.41
Winter barley	grain	2018-05-09	-0.79	1.00	-46.41	6.03
Winter barley	leaf	2018-05-09	13.98	2.47	4.07	8.28
Winter barley	grain	2018-05-23	-3.18	1.19	-41.97	3.96
Winter barley	leaf	2018-05-23	8.90	2.31	-5.84	6.12
Winter barley	leaf	2018-06-06	13.92	0.83	4.48	4.91
Winter wheat	leaf	2018-04-10	7.94	1.20	-10.12	2.53
Winter wheat	leaf	2018-04-24	10.86	1.32	-11.38	4.46
Winter wheat	leaf	2018-05-09	10.95	0.36	-2.94	0.96
Winter wheat	grain	2018-05-23	2.25	1.54	-28.58	4.58
Winter wheat	leaf	2018-05-23	7.53	1.41	-7.72	2.63
Winter wheat	leaf	2018-06-06	10.77	0.55	0.52	0.88

Supporting information Table 2: Measured leaf and grain bulk dried tissue $\delta^{18}O$ values. As averages (n = 5) (± SD) per species, organ. Samples were collected once at the end of the 2018 growing season. All cereals were grown in individual 0.35 x 2.3 meter parcels, of the same 2.3 by 2.5 meter plot at the botanical garden of the University of Basel, Switzerland.

Species	Organ	Bulk dried tissue $\delta^{18}O$ (‰ VSMOW)	
		mean	SD
Durum wheat	leaf	25.31	0.59
Durum wheat	grain	28.58	0.45
Jointed goatgrass	leaf	24.15	0.31
Jointed goatgrass	grain	27.98	0.43
Oat	leaf	25.38	0.96
Oat	grain	31.87	0.18
Spelt	leaf	24.56	0.32
Spelt	grain	29.53	0.62
Summer barley	leaf	24.31	0.43
Summer barley	grain	27.11	0.64
Winter barley	leaf	24.28	0.81
Winter barley	grain	26.18	0.12
Winter wheat	leaf	26.04	0.69
Winter wheat	grain	28.47	0.65

Supporting information Table 3: Craig-Gordon model input values for the determination of f_{xylem} for leaf water $\delta^{18}O$ and $\delta^{2}H$ values.

Species	Date	Source $\delta^{18}O$ (‰ VSMOW)	Air Temp. (°C)	Leaf Temp. (°C)	RH (%)	Stom. cond. (mol/m^2 s)	Bound. layer resist. (m^{2}s/mol)	$\delta^{18}O_{e\_leaf}$ (‰ VSMOW)
Durum wheat	24.04.18	-7.69	28.4	31	44	0.12	1	18.33
Durum wheat	09.05.18	-6.69	28.7	34	45	0.18	1	18.93
Durum wheat	23.05.18	-5.77	29.4	34	52	0.12	1	17.90
Durum wheat	06.06.18	-4.84	30	35	55	0.12	1	17.99
Jointed goatggrass	24.04.18	-7.69	28.4	30	44	0.09	1	18.50
Jointed goatggrass	09.05.18	-6.69	28.7	31	45	0.095	1	19.40
Jointed goatggrass	23.05.18	-5.77	29.4	33	52	0.09	1	18.06
Jointed goatggrass	06.06.18	-4.84	30	34	55	0.08	1	18.20
Oat	24.04.18	-7.69	28.4	32	44	0.12	1	18.33
Oat	06.06.18	-4.84	30	35	55	0.09	1	18.14
Spelt	10.04.18	-8.61	17.1	21	71	0.12	1	7.54
Spelt	24.04.18	-7.69	28.4	32	44	0.12	1	18.33
Spelt	09.05.18	-6.69	28.7	33	45	0.12	1	19.25
Spelt	23.05.18	-5.77	29.4	33	52	0.131	1	17.84
Spelt	06.06.18	-4.84	30	35	55	0.12	1	17.99
Summer barley	09.05.18	-6.69	28.7	32	45	0.095	1	19.40
Summer barley	23.05.18	-5.77	29.4	34	52	0.09	1	18.06
Summer barley	06.06.18	-4.84	30	34	55	0.08	1	18.20
Winter barley	10.04.18	-8.61	17.1	20	71	0.09	1	7.65
Winter barley	24.04.18	-7.69	28.4	33	44	0.1	1	18.44
Winter barley	09.05.18	-6.69	28.7	33	45	0.118	1	19.26

Winter barley	23.05.18	-5.77	29.4	35	52	0.148	1	17.75
Winter barley	06.06.18	-4.84	30	34	55	0.12	1	17.99
Winter wheat	10.04.18	-8.61	17.1	21	71	0.128	1	7.51
Winter wheat	24.04.18	-7.69	28.4	32	44	0.12	1	18.33
Winter wheat	09.05.18	-6.69	28.7	33	45	0.117	1	19.27
Winter wheat	23.05.18	-5.77	29.4	34	52	0.122	1	17.89
Winter wheat	06.06.18	-4.84	30	34	55	0.11	1	18.04

Supporting information table 4: Model input values for the determination of $p_x p_{ex} c$ for leaf and grain bulk dried tissue $\delta^{18}O$ values.

Species	Part	Leaf water timing	Leaf water $\delta^{18}O$ (‰ VSMOW)	Source water timing	Source water $\delta^{18}O$ (‰ VSMOW)
Durum wheat	leaf	April 2018	9	March and April 2018	-9.12
Jointed goatgrass	leaf	April 2018	12.6	March and April 2018	-9.12
Oat	leaf	April 2018	12.25	March and April 2018	-9.12
Spelt	leaf	April 2018	9.5	March and April 2018	-9.12
Summer barley	leaf	April 2018	9	March and April 2018	-9.12
Winter barley	leaf	April 2018	14	March and April 2018	-9.12
Winter wheat	leaf	April 2018	9	March and April 2018	-9.12
Durum wheat	grain	2018-05-10 to 2018-06-10	10	2018-04-25 to 2018-06-10	-5.4
Jointed goatgrass	grain	2018-05-01 to 2018-05-31	14.3	2018-04-15 to 2018-05-31	-5.6
Oat	grain	2018-06-10 to 2018-07-10	13.7	2018-05-25 to 2018-07-10	-4.6
Spelt	grain	2018-05-10 to 2018-06-10	12	2018-04-25 to 2018-06-10	-5.4
Summer barley	grain	2018-04-15 to 2018-05-15	10	2018-04-01 to 2018-05-15	-5.6
Winter barley	grain	2018-04-15 to 2018-05-15	12.5	2018-04-01 to 2018-05-15	-5.6
Winter wheat	grain	2018-05-10 to 2018-06-10	9.1	2018-04-25 to 2018-06-10	-5.4

Supporting information table 5: Results from the determination of model parameters, shown as species- and organ-specific mean (± SD) values for f_{xylem} and $p_x p_{ex} c$.

Species	Organ	f_{xylem} (mean)	f_{xylem} (SD)	$p_x p_{ex} c$ (mean)	$p_x p_{ex} c$ (SD)
Jointed goatgrass	leaf	0.21	0.14	0.71	0.01
Oat	leaf	0.24	0.10	0.65	0.04
Spelt	leaf	0.21	0.20	0.64	0.02
Winter wheat	leaf	0.26	0.17	0.55	0.04
Durum wheat	leaf	0.36	0.06	0.59	0.03
Summer barley	leaf	0.29	0.13	0.65	0.02
Winter barley	leaf	0.09	0.28	0.72	0.03
Jointed goatgrass	grain			0.67	0.02
Oat	grain			0.48	0.01
Spelt	grain			0.59	0.03
Winter wheat	grain			0.52	0.05
Durum wheat	grain			0.55	0.03
Summer barley	grain			0.63	0.04
Winter barley	grain			0.72	0.01

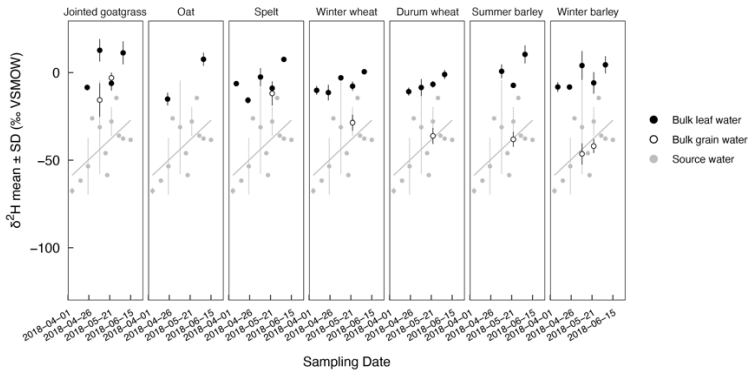

Supporting information Figure 1: Mean bulk tissue water δ^2H values (±SD) of leaves and grains (n = 5), separated by seven different cereal species collected during the 2018 growing season. Species-specific linear regression between the leaf water δ^2H values and the sampling date shown in black. Mean source water δ^2H values (±SD) and linear regression shown in grey. The source water was collected every second week with two precipitation water collectors. All cereals were grown in individual 0.35 x 2.3 meter parcels, of the same 2.3 by 2.5 meter plot at the botanical garden of the University of Basel, Switzerland.

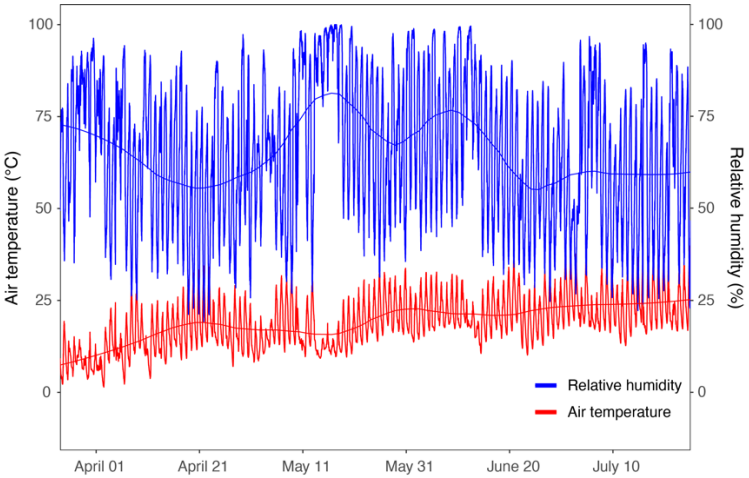

Supporting Information Figure 2: Air temperature (°C) and relative humidity (%) values measured every 15 minutes over the course of the experiment conducted in spring 2018, as means between the two sensors used (HOBO Pro V2 temp/RH, Onset Computer Corporation, Bourne, USA). The sensors were fixed on wooden poles one meter above the ground and evenly spaced on the experimental plot. Floating means between air temperature or relative humidity respectively, and time are shown as solid lines and colored accordingly.

Chapter 3

Effects of phenotypic variability on the oxygen and hydrogen isotope compositions of grains in different winter wheat varieties

Florian Cueni*[1,2], Daniel B. Nelson[1], Ansgar Kahmen[1]

[1]University of Basel, Department of Environmental Sciences – Botany, Schönbeinstrasse 6, 4056 Basel, Switzerland
[2]Agroisolab GmbH, Professor-Rehm-Strasse 6, 52428 Jülich, Germany
* Corresponding author: f.cueni.plantphys@gmail.com

This chapter is published in ***Isotopes in Environmental and Health Studies***.

DOI: https://doi.org/10.1080/10256016.2021.2002855

Abstract

Stable isotope analyses are the leading method for geographic origin determination, especially of plant based agricultural products. Origin analysis is typically done by comparing a suspicious sample to reference materials with known geographic origin. Reference materials are usually collected at the species level, assuming different varieties of a species to have comparable isotope compositions within a given location. We evaluated whether different phenotypes that are expressed in different varieties of winter wheat (*Triticum aestivum* L.), influence the oxygen ($\delta^{18}O$) and hydrogen ($\delta^{2}H$) isotope composition of plant's tissue water and organic compounds. We found that mean $\delta^{18}O$ and $\delta^{2}H$ values among winter wheat varieties did not differ significantly in leaf water, however, differed significantly in bulk dried grain tissue. The differences in bulk dried grain $\delta^{18}O$ and $\delta^{2}H$ values among varieties can be related to differences in phenotypic trait expression among varieties. Despite this substantial phenotypic variability, the overall variability of bulk dried grain $\delta^{18}O$ and $\delta^{2}H$ values among varieties was small (SD 0.54 ‰ for oxygen, 3.60 ‰ for hydrogen). We thus conclude that reference materials collected at the species level should be sufficient for geographic origin analysis of winter wheat and possibly other cereals using $\delta^{18}O$ and $\delta^{2}H$ values.

Introduction

The stable oxygen and hydrogen isotope composition of plants ($\delta^{18}O$ and $\delta^{2}H$ values, respectively) is determined by the growing site-specific geography and climate [1,2]. $\delta^{18}O$ and $\delta^{2}H$ values in plants therefore carry this regional climate-signal and have been established as a leading forensic method for geographic origin analysis [2–7]. The use of stable isotopes to verify the region-of-origin lends itself especially well to agricultural products, since plants show location-specific, robust isotopic fingerprints [6]. The $\delta^{18}O$ and $\delta^{2}H$ values of agricultural products have, for example, been used for the origin analysis of cereals [8,9], olive oil [10], and coffee [11].

Origin analysis using oxygen or hydrogen isotopes is usually based on the comparison of $\delta^{18}O$ or $\delta^{2}H$ values from a suspected fraudulent sample with those from reference materials of known geographic origin. Such comparative analyses have many benefits. Most importantly, these analyses give information based on simple differences between reference samples and the suspicious sample, and are thus easy to understand for customers or law enforcement agencies. For this comparative approach, reference sample material is usually collected for a specific species under investigation in order to account for species-specific differences in $\delta^{18}O$ and $\delta^{2}H$ values [6,12–14].

Many crop species are grown large numbers of different varieties that differ in their phenotypic expression of morphology, anatomy, phenology, and physiology. Winter wheat (*Triticum aestivum* L.), for example, which is one of the main cereals worldwide [15] and makes up more than 50 % of the cereals produced in the EU [16], is grown in varieties that show substantial phenotypic variability [17]. Such phenotypic variability may affect the isotope composition of the different varieties. Differences in drought tolerance in wheat varieties have been shown to affect the $\delta^{18}O$ and $\delta^{2}H$ values of grains [18–20]. Also, differences in plant morphology can result in different degrees of exposure to the atmosphere and different leaf temperatures, resulting in different evaporative water loss conditions, which can in turn influence the $\delta^{18}O$ and $\delta^{2}H$ values of the plant's tissue water and organic material [21,22]. From this it follows that in addition to the location-specific geographic and climatic drivers of $\delta^{18}O$ and $\delta^{2}H$ values, phenotypic variability may have an additional influence on the $\delta^{18}O$ and $\delta^{2}H$ values of crop varieties that belong to the same species [23–25]. Such variability in $\delta^{18}O$ and $\delta^{2}H$ values among crop varieties may complicate the use of reference

sample databases that are established at the species level for the comparative origin identification of agricultural products.

In this study we assessed the extent to which a large selection of winter wheat varieties that were grown in a common environment differed in their oxygen and hydrogen isotope composition. Specifically, we assessed (i) if winter wheat varieties that grew in the same locations differed in their leaf water and bulk grain $\delta^{18}O$ and $\delta^{2}H$ values. In addition, we tested (ii) if variability in $\delta^{18}O$ and $\delta^{2}H$ values among varieties is consistent in different growing locations. Finally, we (iii) determined the key morphological traits across varieties that correlate with variety $\delta^{18}O$ and $\delta^{2}H$ values. For our study, we collected leaf and grain samples from winter wheat variety trials that were established across Switzerland by the Swiss Institute for Sustainability Sciences (ISS) Agroscope.

Materials and Methods

Experimental setup

Winter wheat (*Triticum aestivum* L.) field trials were set up to test the agronomic performance of 36 different varieties in the 2017 and 2018 growing seasons across Switzerland. The field trails were organized by the Swiss Institute for Sustainability Sciences (ISS) Agroscope at 15 sites across Switzerland [17]. We obtained samples from four sites in 2017 and three sites in 2018 (Fig. 1, Table 1). The field trials at the different sites were set up in identical layouts, with the same 36 winter wheat varieties each grown on 7 to 10 m^2 plots at each site [17]. The 36 varieties used in the trials differed in the 2017 and 2018 season (Supplemental material Table 1). For both years and all sites, plants were sown between mid-October and early November in the year before the harvest.

The original goal of the field trials was to compare the yields of the different varieties, and for this purpose variety-specific plant traits were also assessed [17]. These included general information on plant morphology (e.g. plant height or plant stability), and information on overall plant and leaf health, or pathogen infestation. In addition, the yield traits were assessed as total grain weight, protein content, or based on visual checks for grain health. For the analysis presented in this paper, we used six different plant traits that were recorded for 19 of the 36 varieties of the 2017 season. These were plant height (cm), yield (q/ha, q = "quintal" = 100 kg), weight per hectolitre (kg), weight of 1000 grains (g), grain protein content (%) and the Zeleny index (ml). The Zeleny index is a measurement of the flour protein quality, which gives information about the swelling capacity of the protein and allows predictions to be made about the expected flour quality in baking. The Zeleny index is typically variety-specific and positively correlates with protein content [26,27].

Table 1: Elevation (m a.s.l.), mean annual temperature (°C), cumulative annual precipitation amount (mm), the sampling dates of the year 2017 and 2018, as well as the precipitation $\delta^{18}O$ and $\delta^{2}H$ from Piso.AI [29] for 2017 (mean May, June, and July) and 2018 (mean May and June) at the filed sites investigated in this study.

Site	Elevation (m a.s.l.)	mean annual Temp. (°C)	total annual Precip. (mm)	Sampling Date		Precip. $\delta^{18}O$ (‰ VSMOW)		Precip. $\delta^{2}H$ (‰ VSMOW)	
				2017	2018	2017	2018	2017	2018
Zollikofen	560	9.55	1075.6	07/20		-6.6		-43	
Künten	443	10.65	1100.6	07/17	06/08	-6.5	-7.2	-42	-52
Lindau	530	9.7	1117.6	07/18	06/07	-6.5	-7.2	-42	-54
Ellighausen	525	9.8	852.4	07/19	06/07	-6.4	-7.0	-42	-49

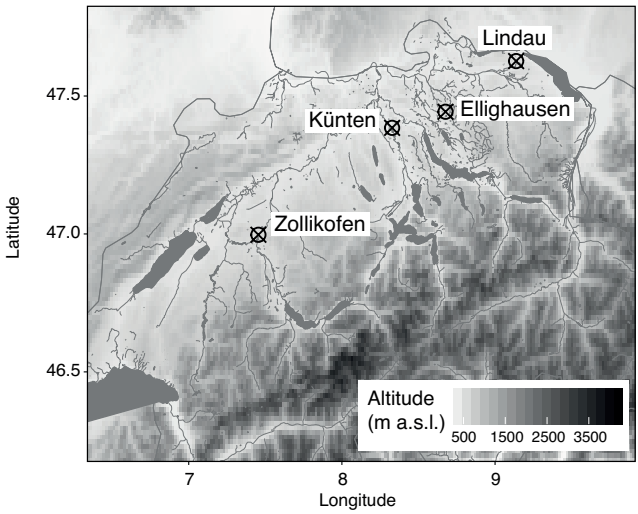

Figure 1: Map of Switzerland showing the locations of the four sites investigated in this study. Digital elevation model (GTOPO) (m a.s.l.) and major water ways used as background data.

Sample collection for isotope analysis

Samples for leaf water isotope analyses were collected at three different field sites on two different days towards the end of the 2018 wheat growing season at the time of anthesis (7th June 2018 and 8th June 2018, Table 1). From each variety (n = 36), three flag leaves of randomly selected plants in the centre of the plots were collected. Immediately after sampling the leaves were collectively put into 12 ml gas-tight glass vials (Labco exetainers 12 ml, Labco, Lampeter, Wales, UK), kept in a cooling box during transport, and then stored at -20 °C until water extraction. Sampling was conducted between 10:00 and 15:00.

Tissue water from the wheat leaves was cryogenically extracted as described by Newberry et al. (2017). The extraction ran for two hours, thereafter the frozen sample water was left to thaw. It was then transferred into 2 ml glass vials, sealed, and stored at 4 °C until analysis.

Grain samples for the bulk dried tissue oxygen and hydrogen stable isotope analyses were harvested from the 17th to the 20th of July 2017 (Table 1). The harvesting was conducted by Agroscope. We obtained grain samples from the same three sites that leaf water samples were collected from, and also from one additional site, where we did not sample for leaf water in 2018 (n = 36 for location Zollikofen, Künten and Lindau, n = 15 for location Ellighausen). In the lab, the grain samples were dried at 60 °C for at least 48 h. The dried grain samples were then milled to a fine powder using the laboratory mixer mill. Thereafter, ~0.5 mg of dried bulk material powder was weighed into silver capsules for bulk grain $\delta^{18}O$ analysis (3 mm x 5 mm; Säntis Analytical AG, Teufen, Switzerland), and stored in a desiccator until analysis. For bulk dried grain $\delta^{2}H$ analysis, ~0.5 mg of dried bulk powder was weighed into four individual silver capsules for each sample.

All values for precipitation $\delta^{18}O$ and $\delta^{2}H$ values were obtained from Piso.AI [29], a machine learning model trained on geographic and climate data that predicts monthly time series of $\delta^{18}O$ and $\delta^{2}H$ values of precipitation.

Isotope Analyses

All stable isotope analyses were performed on Delta V Plus isotope ratio mass spectrometers, which were interfaced with measurement-specific elemental analysers through ConFlo IV interfaces (Thermo Electron Corporation, Bremen, Germany). All $\delta^{2}H$ and $\delta^{18}O$ data were normalized to the VSMOW-SLAP scale (Vienna Standard Mean Ocean Water, and Standard Light

Antarctic Precipitation, respectively) with at least two calibrated in-house standards. Long-term precision for each measurement was determined through repeated analyses of quality control samples for each measurement type.

Water $\delta^{18}O$ and $\delta^{2}H$ values were measured after Newberry et al. (2017). This used a TC/EA (high-temperature conversion/elemental analyser) for conversion of the hydrogen and oxygen in water molecules to the measured H_2 and CO gases, respectively. Scale normalization was done using using calibrated in-house water standards with $\delta^{2}H$ values of -76.4 ‰ and +45.2 ‰, and $\delta^{18}O$ values of -10.7 ‰ and +4.3 ‰, respectively. Long-term precision was 0.24 ‰ and 0.7 ‰, for $\delta^{18}O$ and $\delta^{2}H$ values, respectively (n = 1247 since July 2014). Bulk dried tissue $\delta^{18}O$ values were analysed after Cueni et al. (in review). This used an EA IsoLink (in pyrolysis mode) for conversion of oxygen in organic compounds to CO gas for isotope analysis. Scale normalization was done using using calibrated in-house dimethyl-, trimethyl-, and benzoic acid standards with $\delta^{18}O$ values of +2.89 ‰, +8.91 ‰, and +23.96 ‰. Long-term precision for a separate benzoic acid quality control material was 0.20 ‰ (n = 533 since July 2016). Bulk dried tissue $\delta^{2}H$ values of non-exchangeable hydrogen atoms were also analysed after Cueni et al. (in review). This used a TC/EA operated with a chromium reduction reactor [31] for conversion of hydrogen in organic compounds to H_2 gas for isotope analysis. Scale normalization was done using two calibrated in-house caffeine standards that do not contain exchangeable hydrogen, and with $\delta^{2}H$ values of –193.6 ‰, and –4.1 ‰. Long-term precision for a cellulose triacetate quality control material, which does not contain exchangeable hydrogen, was 1.5 ‰ (n = 495 since November 2018).

We corrected the measured $\delta^{2}H$ values for the contribution from exchangeable hydrogen using a two-step water equilibration procedure performed in a Uni-prep autosampler (Eurovector, Milan, Italy; [32]) (Appendix). Sample aliquots were measured in groups of four replicates. First, two replicates were analysed after equilibration with water A ($\delta^{2}H$ = +45.2 ‰), and then on the following day, the remaining two aliquots were analysed after equilibration with water B ($\delta^{2}H$ = -189.3 ‰). The $\delta^{2}H$ value of the non-exchangeable hydrogen was than calculated from these two measurements (Appendix). Long-term precision for a bulk leaf quality control material was 1.5 ‰ (n = 260 since November 2018), and 1.0 ‰ for a pure cellulose quality control material (n = 269 since November 2018). All shown $\delta^{2}H$ values of organic

material in the following text refer to the measurement of the carbon-bound, non-exchangeable hydrogen atoms.

All stable isotope ratios are expressed delta (δ) notation and shown in per mil (‰) as the ratio of the heavy over the light isotope of the sample (R_{sample}) in relation to the same ratio of the international standard ($R_{standard}$). The stable isotope ratios are calculated using Equation 1. R is the $^{2}H/^{1}H$ or $^{18}O/^{16}O$ ratio [33]:

Equation 1: $\delta_{sample} = (R_{sample}/R_{standard}) - 1$, ‰

Statistical Analysis

Statistical analyses were done using the statistical package R version 3.5.3 (R Core Team (2019). R: A language and environment for statistical computing. R Foundation for Statistical Computing, Vienna, Austria. URL: https://www.R-project.org/). Assumptions for the statistical tests were tested with graphical residual diagnostics, using quantile-quantile and residuals vs. fitted plots. The type I error of all statistical tests was set to $\alpha = 0.05$. The relationships among the different varieties and sites, and their leaf water, or bulk dried grain material $\delta^{18}O$ and $\delta^{2}H$ values were compared using an analysis of variance (ANOVA) with a Tukey's honest significant difference (HSD) post-hoc test in order to find significant differences between individual varieties, with the significance level set to $p = 0.05$. The linear dependence between standardized $\delta^{18}O$ and $\delta^{2}H$ values of leaf water or bulk dried tissue, respectively, were assessed using the Pearson correlation (r).

Results

Leaf water $\delta^{18}O$ and $\delta^{2}H$ values

The mean leaf water of all 36 winter wheat varieties collected in June 2018 was enriched in ^{18}O and ^{2}H compared to the precipitation water at the respective site (mean May and June 2018 precipitation from Piso.AI [29] (Table 1)). We found significant differences in leaf water $\delta^{18}O$ and $\delta^{2}H$ values across the three sites (Table 3). The range of observed leaf water $\delta^{18}O$ values across the 36 varieties in the three sites was 5.15 ‰, 2.11 ‰ and 3.04 ‰, while $\delta^{2}H$ value ranges were 13.59 ‰, 4.65 ‰ and 6.39 ‰ (Fig. 2, Table 2). Varieties did not differ significantly in their leaf water $\delta^{18}O$ and $\delta^{2}H$ values at a given site (Table 3).

To assess the magnitude of the observed variability in leaf water $\delta^{18}O$ and $\delta^{2}H$ values among the different varieties, irrespective of the effects of the growing location, we standardized values by calculating the deviation of a leaf water value from the site-specific mean leaf water $\delta^{18}O$ and $\delta^{2}H$ values ($\delta_{sample} - \delta_{site\_mean}$) (Fig. 2). We then calculated from the standardized $\delta^{18}O$ and $\delta^{2}H$ values the mean $\delta^{18}O$ and $\delta^{2}H$ values for each variety across the three sites (n = 3) (Fig 2). We further calculated the grand mean across all standardized variety mean $\delta^{18}O$ and $\delta^{2}H$ values (n = 36), and the corresponding standard deviations and range across all mean variety $\delta^{18}O$ and $\delta^{2}H$ values. By definition, the resulting mean values were 0 ‰ for $\delta^{18}O$ and $\delta^{2}H$ values. The corresponding standard deviation was ±0.63 ‰ for $\delta^{18}O$ and ±1.52 ‰ for $\delta^{2}H$, with a range of 2.87 ‰ and 6.54 ‰ for $\delta^{18}O$ and $\delta^{2}H$, respectively (Fig. 2, Table 2). We also assessed the average within-variety range by determining the range of the three standardized values across the three sites for each variety, and calculated the mean across these 36 ranges. This within-variety range was 1.16 ‰ (± 0.82 ‰) for $\delta^{18}O$ and 2.57 ‰ (± 1.93 ‰) for $\delta^{2}H$ values (Table 2).

We plotted original and standardized leaf water $\delta^{18}O$ and $\delta^{2}H$ values in dual isotope space (Fig. 3). Both, original and standardized $\delta^{18}O$ and $\delta^{2}H$ values were tightly correlated. Original leaf water $\delta^{18}O$ and $\delta^{2}H$ values plotted below the local meteoric water lined obtained from Piso.AI, with slopes ranging from 1.49 to 2.33 among the three sites (Fig. 3a).

Table 2: Leaf water $\delta^{18}O$ and $\delta^{2}H$ values of 36 winter wheat varieties grown in the 2018 season at three different locations in Switzerland. Mean (± SD), lowest (Min), and highest (Max), and the across-variety range of leaf water $\delta^{18}O$ and $\delta^{2}H$ values are shown for each site. Also, the average within-variety range of the standardized $\delta^{18}O$ and $\delta^{2}H$ values are shown. Lastly, standardized across site variety mean leaf water $\delta^{18}O$ and $\delta^{2}H$ values as well as the lowest (Min), highest (Max), and the across variety range are shown (see also Fig. 2).

		Leaf water $\delta^{18}O$ (‰ VSMOW)			
Site	**Mean (± SD)**	**Min**	**Max**	**Across-variety range**	**Average within-variety range**
Künten	1.91 (± 1.14)	-1.59	3.56	5.15	
Lindau	2.37 (± 0.64)	1.21	3.32	2.11	
Ellighausen	0.56 (± 0.74)	-0.98	2.06	3.04	
Standardized individual values					1.16 (± 0.82)
Standardized across site variety means	0.00 (± 0.63)	-1.75	1.12	2.87	
		$\delta^{2}H$ (‰ VSMOW)			
Künten	-20.50 (± 2.75)	-29.18	-15.59	13.59	
Lindau	-16.99 (±1.50)	-19.03	-14.38	4.65	
Ellighausen	-24.45 (± 1.48)	-27.82	-21.43	6.39	
Standardized individual values					2.57 (± 1.93)
Standardized across site variety means	0.00 (± 1.52)	-4.53	2.01	6.54	

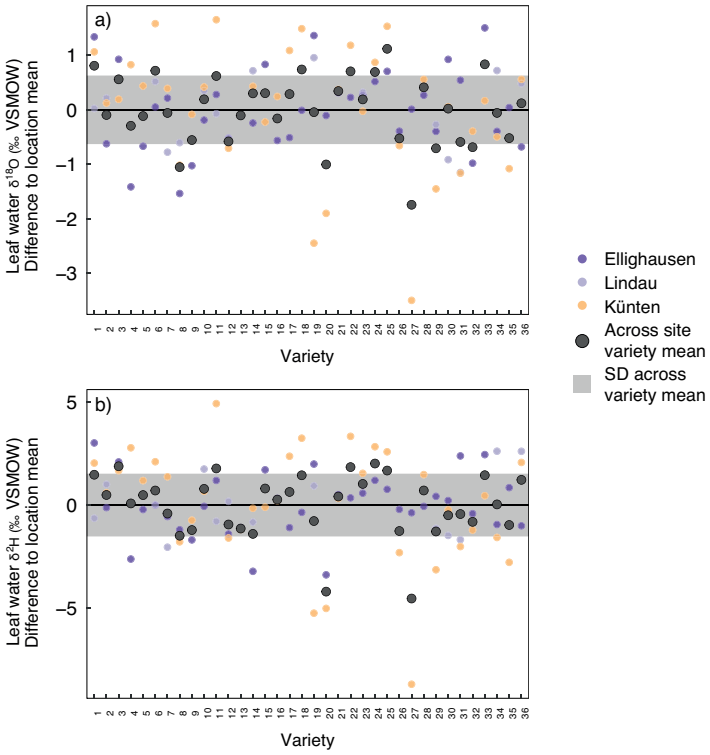

Figure 2 a): Leaf water $\delta^{18}O$ values at three growing locations for 36 winter wheat varieties. Values at each site are standardized to the site-specific mean leaf water $\delta^{18}O$ value. Mean values for each variety (averaged across sites, n = 3) are shown as black dots. The SD of all variety mean values is indicated as grey shaded area (n = 36) (see also Table 2). **b)** Leaf water $\delta^{2}H$ values standardized as described in (a).

Table 3: ANOVAs showing the effects of growing location (site) and variety on the leaf water $\delta^{18}O$ and $\delta^{2}H$ values measured in 36 winter what varieties each grown at three locations in Switzerland. Since each variety only occurs once per site, there is no variance and the interaction between site and variety could not be assessed.

Leaf water $\delta^{18}O$					
	Df	**Sum Sq**	**Mean Sq**	**F value**	**P**
Site	2	49.73	24.86	31.85	<0.001
Variety	35	31.74	0.91	1.16	0.309
Residuals	50	39.03	0.78		
Leaf water $\delta^{2}H$					
	Df	**Sum Sq**	**Mean Sq**	**F value**	**P**
Site	2	672.25	336.12	85.68	<0.001
Variety	35	179.10	5.12	1.30	0.192
Residuals	50	196.14	3.92		

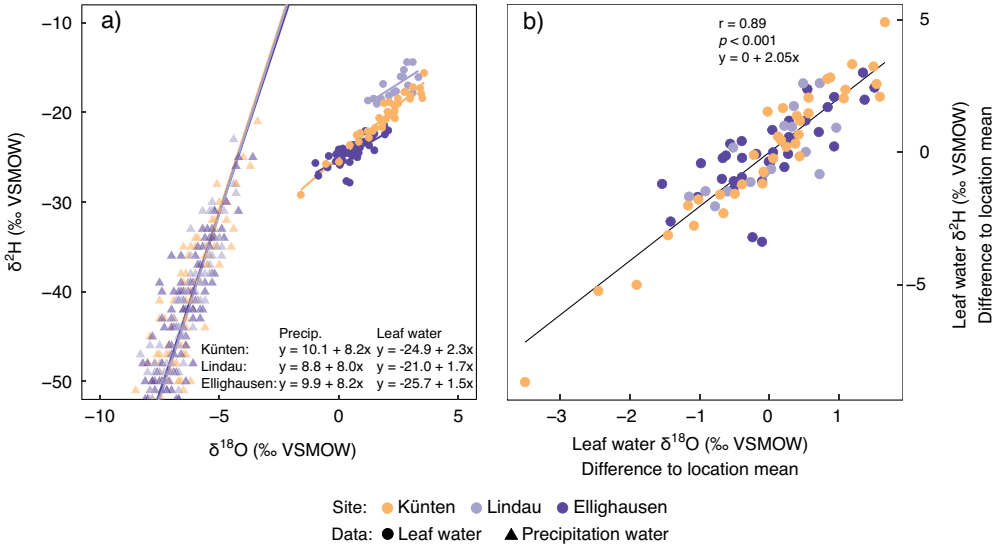

Figure 3: Correlation of the original (a) and standardized (b) leaf water $\delta^{18}O$ and $\delta^{2}H$ values of 36 different winter wheat varieties grown in a variety field trail at three different sites in Switzerland, during the 2018 season. For a) long-term (2000 to 2019) precipitation water values obtained from Piso.AI shown in triangles. In a) linear relationship and equations for leaf and precipitation water (local meteoric water line) shown for each site, in b) linear relationship independent of site shown in black.

Bulk dried grain material $\delta^{18}O$ and $\delta^{2}H$ values

Bulk dried grain material of all 36 winter wheat varieties harvested in July 2017 was enriched in ^{18}O and depleted in ^{2}H compared to the mean May, June, and July 2017 precipitation values from Piso.AI [29] at each site (Table 1 and 4). Bulk dried grain material was also generally ^{18}O enriched compared to average winter wheat leaf water $\delta^{18}O$ values and ^{2}H depleted compared to average winter wheat leaf water $\delta^{2}H$ values (Table 2 and 4). Importantly, however, leaf water and organics samples were collected in different years from different varieties and can therefore not be compared directly. We found significant differences in bulk dried grain material $\delta^{18}O$ and $\delta^{2}H$ values across the three sites (Table 5). The range of $\delta^{18}O$ values for observed bulk dried grain material across the 36 varieties in the four sites was 2.42 ‰, 2.92 ‰, 2.97 ‰, and 2.18 ‰, while $\delta^{2}H$ values ranged 15.85 ‰, 18.50 ‰, 14.15 ‰, and 13.75 ‰ (Fig. 4, Table 4). We found significant effects of variety on bulk dried grain material for $\delta^{18}O$ and $\delta^{2}H$ values (Table 5).

To assess the magnitude of the observed variability in bulk dried grain tissue $\delta^{18}O$ and $\delta^{2}H$ values among the different varieties, irrespective of the effects of the growing location, we used the same methodology that we applied to the leaf water data and standardized values by calculating the deviation of a bulk dried grain value from the site-specific mean bulk dried grain $\delta^{18}O$ and $\delta^{2}H$ values ($\delta_{sample} - \delta_{site\_mean}$) (Fig. 4). We then calculated the mean $\delta^{18}O$ and $\delta^{2}H$ values for each variety from the standardized $\delta^{18}O$ and $\delta^{2}H$ values across the four sites (n = 4) (Fig 4). We further calculated the grand mean $\delta^{18}O$ and $\delta^{2}H$ values across all standardized variety means (n = 36) and the corresponding standard deviations and range across all mean variety values. By definition the resulting mean values were 0 ‰ for $\delta^{18}O$ and $\delta^{2}H$ values. The corresponding standard deviation was ±0.54 ‰ for $\delta^{18}O$ and ±3.60 ‰ $\delta^{2}H$ with a range of 2.72 ‰ and 15.58 ‰ for $\delta^{18}O$ and $\delta^{2}H$, respectively (Fig. 4, Table 4). We also assessed the average within-variety range by determining the range of the four standardized $\delta^{18}O$ and $\delta^{2}H$ values across the four sites for each variety and calculated the mean across these 36 ranges. This within-variety range was 0.38 ‰ (± 0.18 ‰) for $\delta^{18}O$ and 4.03 ‰ (± 1.90 ‰) for $\delta^{2}H$ values (Table 4). Standardized $\delta^{18}O$ and $\delta^{2}H$ bulk dried tissue values were also significantly correlated with each other ($p < 0.001$, r = 0.48) (Fig. 5).

Table 4: Bulk dried grain $\delta^{18}O$ and $\delta^{2}H$ values of 36 winter wheat varieties grown in the 2017 season at four different locations in Switzerland. Mean (± SD), lowest (Min), and highest (Max), and the across-variety range of bulk dried grain $\delta^{18}O$ and $\delta^{2}H$ values are shown for each site. Also, the average within-variety range of the standardized $\delta^{18}O$ and $\delta^{2}H$ values are shown. Lastly, standardized across site variety mean bulk dried grain $\delta^{18}O$ and $\delta^{2}H$ values as well as the lowest (Min), highest (Max), and the across variety range are shown (see also Fig. 4).

		Bulk dried grain $\delta^{18}O$ (‰ VSMOW)			
Site	**Mean (± SD)**	**Min**	**Max**	**Across-variety range**	**Average within-variety range**
Zollikofen	28.44 (± 0.55)	27.28	29.70	2.42	
Künten	28.55 (± 0.62)	27.36	30.28	2.92	
Lindau	28.80 (± 0.52)	27.96	30.93	2.97	
Ellighausen	27.32 (± 0.62)	26.15	28.33	2.18	
Standardized individual values					0.38 (± 0.18)
Standardized across site variety means	0 (± 0.54)	-1.01	1.71	2.72	
		$\delta^{2}H$ (‰ VSMOW)			
Zollikofen	-57.67 (± 4.33)	-66.60	-50.75	15.85	
Künten	-56.67 (± 4.54)	-64.55	-46.05	18.50	
Lindau	-57.06 (± 3.67)	-64.20	-50.05	14.15	
Ellighausen	-54.61 (± 3.42)	-62.15	-48.40	13.75	
Standardized individual values					4.03 (± 1.90)
Standardized across site variety means	0 (± 3.60)	-7.82	7.76	15.58	

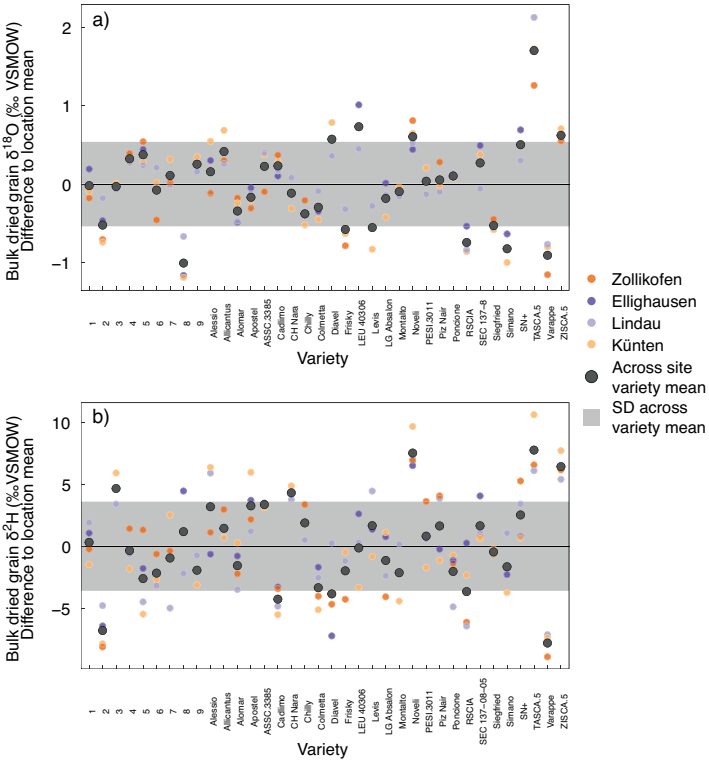

Figure 4 a): Bulk dried grain tissue $\delta^{18}O$ values at four growing locations for 36 winter wheat varieties. Values at each site are standardized to the site-specific mean bulk dried grain $\delta^{18}O$ value. Mean values for each variety (averaged across sites, n = 4) are shown as black dots. The SD of all variety mean values is indicated as grey shaded area (n = 36) (see also Table 4). **b)** As for a) but for $\delta^{2}H$ values of bulk dried grains.

Table 5: ANOVAs showing the effects of growing location (site) and variety on the bulk dried grain $\delta^{18}O$ and $\delta^{2}H$ values measured in 36 winter what varieties each grown at four different locations in Switzerland. Since each variety only occurs once per site, there is no variance and the interaction between site and variety could not be assessed.

Bulk dried grain $\delta^{18}O$

	Df	Sum Sq	Mean Sq	F value	P
Site	3	25.26	8.42	183.35	<0.001
Variety	35	31.22	0.89	19.43	<0.001
Residuals	71	3.26	0.05		

Bulk dried grain $\delta^{2}H$

	Df	**Sum Sq**	**Mean Sq**	**F value**	**P**
Site	3	189.49	63.16	8.57	<0.001
Variety	35	2964.99	84.71	11.49	<0.001
Residuals	201	1482.18	7.37		

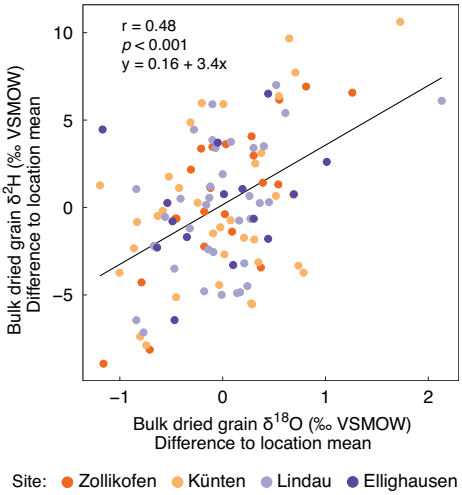

Figure 5: Correlation of the standardized bulk dried grain $\delta^{18}O$ values with the standardized bulk grain $\delta^{2}H$ values of 36 different winter wheat varieties that were grown in a variety field trail, each at four different locations in Switzerland during the 2017 season. Linear relationship independent of site shown as black line.

Six plant traits (weight per hectolitre, plant height, yield, Zeleny index and protein content) explain 85 % of the observed variability in standardized bulk dried grain $\delta^{18}O$ values (Table 6). Most of the observed variability in the standardized bulk dried grain $\delta^{18}O$ values among the varieties can be explained by the plant height (44 %), which shows a positive, significant relationship with bulk dried grain $\delta^{18}O$ values (Fig. 6a). For all other plant traits, the explanatory power of the individual trait was between 11 % and 28 % (Fig. 6). Most traits showed a significant, positive relationship with the standardized bulk dried grain $\delta^{18}O$ values, with only yield showing a significant negative correlation (Fig. 6b).

For standardized bulk dried grain $\delta^{2}H$ values, the six plant traits (weight per hectolitre, plant height, yield, Zeleny index and protein content) investigated in this study explain 62 % of the observed variability (Table 7). Most of the observed standardized bulk dried grain $\delta^{2}H$ values can be explained by weight per hectolitre (42 %), which shows a positive, significant correlation with bulk dried grain $\delta^{2}H$ values (Fig. 6c). Protein content alone can also explain 37 % of the observed variability in the standardized bulk dried grain $\delta^{2}H$ values (Fig. 6e). For all other plant traits, the explanatory power of an individual trait falls between 1 % and 21 % (Fig. 6). Five of the six traits show a positive relationship with the standardized bulk dried grain $\delta^{2}H$ values, and all are significant except for the weight of 1000 grains. For yield, the relationship with the standardized bulk dried grain $\delta^{2}H$ values is significantly negative (Fig. 6b).

Table 6: ANOVAs showing the effects of weight per hectolitre, plant height, yield, Zeleny index, and protein content on the standardized bulk dried grain $\delta^{18}O$ values, measured in 36 winter what varieties each grown at four different locations in Switzerland. Due to collinearity, not all interactions can be determined.

Standardized bulk dried grain $\delta^{18}O$ values					
	Df	**Sum Sq**	**Mean Sq**	**F value**	**P**
Weight per hectoliter	1	5.927	5.927	107.098	< 0.001
Plant height	1	3.492	3.492	63.096	< 0.001
Yield	1	0.904	0.904	16.334	< 0.001
Zeleny index	1	1.353	1.353	24.443	< 0.001
Protein content	1	0.100	0.100	1.812	0.186
Weight of 1000 grains	1	0.091	0.091	1.644	0.208
Weight per hectoliter:Plant height	1	0.669	0.669	12.095	0.001
Weight per hectoliter:Yield	1	0.021	0.021	0.377	0.543
Plant height:Yield	1	0.692	0.692	12.508	0.001
Weight per hectoliter:Zeleny index	1	0.002	0.002	0.031	0.861
Plant height:Zeleny index	1	0.575	0.575	10.386	0.003
Yield:Zeleny index	1	0.588	0.588	10.618	0.002
Weight per hectoliter:Protein content	1	1.315	1.315	23.750	< 0.001
Plant height:Protein content	1	0.326	0.326	5.892	0.020
Yield:Protein content	1	0.653	0.653	11.789	0.001
Zeleny index:Protein content	1	0.002	0.002	0.036	0.850
Weight per hectoliter:Weight of 1000 grains	1	0.257	0.257	4.648	0.038
Plant height:Weight of 1000 grains	1	0.956	0.956	17.268	< 0.001
Residuals	37	2.048	0.055		

Adjusted $r^2 = 0.85$, $p < 0.001$

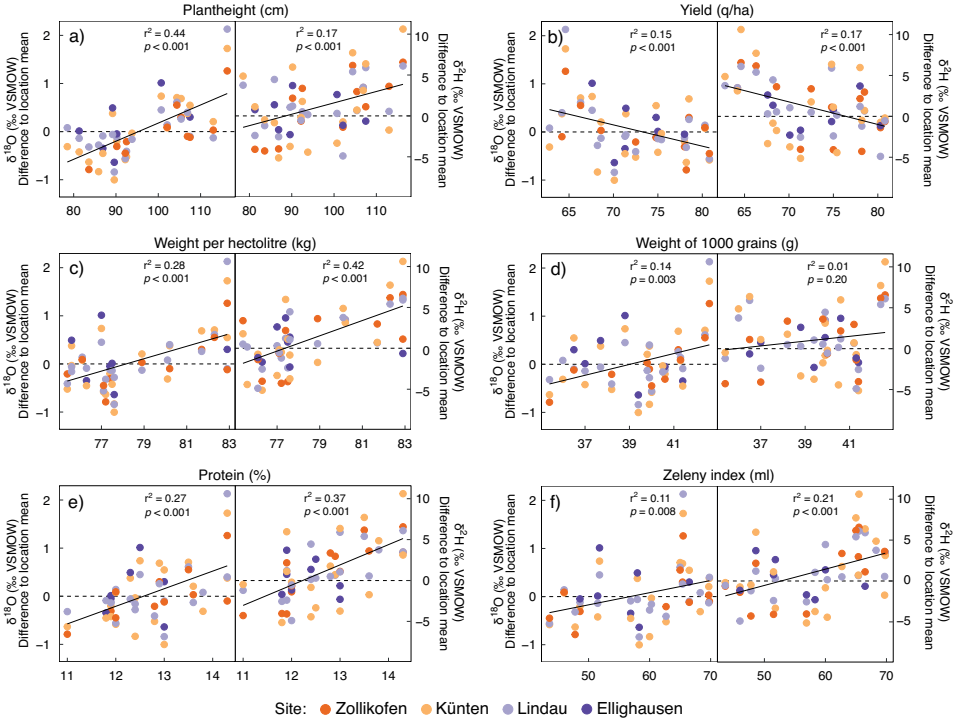

Figure 6: Relationship of **a)** plant height (cm), **b)** yield (q/ha), **c)** weight per hectolitre, **d)** weight of 1000 grains (g), **e)** protein content (%), and **f)** the Zeleny index (ml) with the standardized bulk dried grain $\delta^{18}O$ values and $\delta^{2}H$ values from the 2017 growing season. Each dot represents one winter wheat variety, separated by colour for the four variety field trail locations.

Table 7: ANOVAs showing the effects of weight per hectolitre, plant height, yield, Zeleny index, and protein content on the standardized bulk dried grain δ^2H values, measured in 36 winter what varieties each grown at four different locations in Switzerland. Due to collinearity, not all interactions can be determined.

Standardized bulk dried grain δ^2H values

	Df	Sum Sq	Mean Sq	F value	P
Weight per hectoliter	1	299.599	299.599	62.417	< 0.001
Plant height	1	0.962	0.962	0.201	0.657
Yield	1	29.513	29.513	6.149	0.018
Zeleny index	1	4.965	4.965	1.034	0.315
Protein content	1	26.995	26.995	5.624	0.023
Weight of 1000 grains	1	2.877	2.877	0.599	0.444
Weight per hectoliter:Plant height	1	4.361	4.361	0.908	0.346
Weight per hectoliter:Yield	1	9.444	9.444	1.967	0.169
Plant height:Yield	1	0.674	0.674	0.140	0.710
Weight per hectoliter:Zeleny index	1	37.027	37.027	7.714	0.008
Plant height:Zeleny index	1	13.620	13.620	2.838	0.100
Yield:Zeleny index	1	28.986	28.986	6.039	0.019
Weight per hectoliter:Protein content	1	0.725	0.725	0.151	0.700
Plant height:Protein content	1	0.139	0.139	0.029	0.866
Yield:Protein content	1	1.939	1.939	0.404	0.529
Zeleny index:Protein content	1	4.384	4.384	0.913	0.345
Weight per hectoliter:Weight of 1000 grains	1	50.778	50.778	10.579	0.002
Residuals	39	187.200	4.800		

Adjusted $r^2 = 0.62$, $p < 0.001$

Discussion

Our results show that leaf water $\delta^{18}O$ and $\delta^{2}H$ values of 36 winter wheat varieties differ significantly across the three growing locations but not among varieties at a given location. After accounting for the effects of growing location by standardizing values, the range of leaf water $\delta^{18}O$ and $\delta^{2}H$ values were 2.87 ‰ and 6.54 ‰ with standard deviations of 0.63 ‰ and 1.53 ‰, respectively. Bulk dried grain $\delta^{18}O$ and $\delta^{2}H$ values also differed significantly across growing locations, but unlike leaf water, were also significantly affected by variety at a given location. The range of standardized mean values among varieties was 2.72 ‰ for $\delta^{18}O$ and 15.58 ‰ for $\delta^{2}H$ with a standard deviation of 0.54 ‰ and 3.60 ‰, respectively. With this, the observed variability in leaf water and bulk dried grain $\delta^{18}O$ and $\delta^{2}H$ values among different winter wheat varieties was relatively low compared to other studies that have compared leaf water or organic $\delta^{18}O$ and $\delta^{2}H$ values across different species or across environmental gradients [22,34–37]. Although variety effects on bulk dried grain $\delta^{18}O$ and $\delta^{2}H$ values across the tested 36 different varieties were relatively small, we yet observed significant relationships between expressed phenotypic variability and bulk dried grain $\delta^{18}O$ and $\delta^{2}H$ values. In summary, our study suggests that variety specific effects on bulk dried grain $\delta^{18}O$ and $\delta^{2}H$ values does exist, but that these effects are small so that for the collection of reference materials for geographic origin analysis, variety-specific collections are generally not necessary.

Leaf water $\delta^{18}O$ and $\delta^{2}H$ values

The leaf water of all 36 winter wheat varieties at the three locations sampled in 2018 was ^{18}O- and ^{2}H-enriched compared to the precipitation water at each location (Table 2). This observed ^{18}O- and ^{2}H-enrichment is consistent with isotope theory and similar patterns have been demonstrated in a range of previous studies [38]. The leaf water $\delta^{18}O$ and $\delta^{2}H$ values differed among the three sampling locations (Table 3), but the precipitation water $\delta^{18}O$ and $\delta^{2}H$ values were similar among the three sampling locations (Table 1). The isotopic composition of bulk leaf water is strongly influenced by the evaporative environment of the leaf, i.e., the atmospheric humidity and air temperature [39–42]. Thus, leaf water $\delta^{18}O$ and $\delta^{2}H$ values show a strong diurnal pattern, with the highest enrichment compared to the source water at midday [34,38]. We collected the samples for the leaf water analysis on two different days. We sampled location Lindau on the first day at noon, and

Ellighausen on the same day in the afternoon, and the next day location Künten at noon. We therefore attribute the observed differences in the leaf water $\delta^{18}O$ and $\delta^{2}H$ values among the three sites to meteorological differences on the different sampling days and sampling time of the day.

When standardized across sites, the 36 wheat varieties still showed differing degrees of leaf water ^{18}O- and ^{2}H-enrichment (Fig. 2). Across standardized variety means we observed a range of 2.87 ‰ and 6.54 ‰ with a standard deviation of 0.63 ‰ and 1.52 ‰ for leaf water $\delta^{18}O$ and $\delta^{2}H$ values, respectively (Fig. 2; Table 2). Moreover, the observed variability in leaf water $\delta^{18}O$ and $\delta^{2}H$ values was closely correlated between O and H isotopes ($r = 0.89$, Fig. 3). This suggests that the observed variability, although statistically not significant among varieties, is due to differences in evaporative leaf water ^{18}O- and ^{2}H-enrichment. Unfortunately, trait data for the growing season in which we collected leaf water $\delta^{18}O$ and $\delta^{2}H$ values are not available for an in-depth analysis of the effects of phenotypic diversity on the small observed variability in leaf water $\delta^{18}O$ and $\delta^{2}H$ values. Phenotypic variability among varieties may affect leaf water evaporative ^{18}O- and ^{2}H-enrichment in different ways. Different extents of transpirational water loss among different varieties can, for example, explain the small observed differences in leaf water ^{18}O- and ^{2}H-enrichment [43]. Differences in plant height and leaf form can affect the exposure of the leaf to the atmosphere and thus leaf temperatures and the leaf to atmosphere vapor pressure deficits, which in turn influences leaf water $\delta^{18}O$ and $\delta^{2}H$ values [21,22]. Moreover, lower drought-tolerance of some varieties will lead to a lower stomatal conductance (g_s) and consequently a higher ^{18}O- and ^{2}H-enrichement of the leaf water [44]. This has been shown for wheat, where older less drought tolerant varieties displayed increased leaf water $\delta^{18}O$ and $\delta^{2}H$ values compared to modern more drought resistant varieties [18–20].

Bulk dried grain tissue $\delta^{18}O$ and $\delta^{2}H$ values

Compared to the mean leaf water $\delta^{18}O$ and $\delta^{2}H$ values of the samples collected in the 2018 growing season, the bulk dried grain material harvested in the 2017 season always showed more positive $\delta^{18}O$ values, and more negative $\delta^{2}H$ values (Fig. 4). Our data confirm that during the assimilation and synthesis of carbohydrates (i.e. starch or cellulose), isotope fractionation occurs when carbonyl-group oxygen exchanges with the surrounding water [45]. This equilibrium isotope fractionation leads to an enrichment of ^{18}O in

the carbohydrates relative to synthesis water and has been determined to be ~ +27 ‰ [24,45,46]. Our results also confirm that organic compounds were ^{2}H-depleted compared to leaf water. This can be explained by the broadly characterized isotope fractionations during the autotrophic and heterotrophic synthesis of carbohydrates, subsequently leading to a ^{2}H-depletion of carbohydrates [24,47]. Moreover, lipids making up approximately 15 % [17] of the bulk tissue are even more depleted in ^{2}H than carbohydrates [39,47–49].

Compared to the strong correlation in leaf water, we found that the variability in bulk dried grain $\delta^{18}O$ and $\delta^{2}H$ values showed a weaker correlation ($r = 0.48$, Fig. 5). This supports the interpretation that the isotope fractionation processes related to carbohydrate synthesis are only partially synchronized for O and H isotopes.

The bulk dried grain $\delta^{18}O$ and $\delta^{2}H$ values were significantly different among locations, which was largely due to the Ellighausen site that showed significantly lower $\delta^{18}O$ values (ANOVA, Tukey's HSD $p < 0.001$). This may indicate generally greater transpiration at this location and thus a less ^{18}O-enriched leaf water signal [44] that is transferred in to the grain organic material [20,24,25,50,51]. This is supported by the flatter slope between the bulk dried grain $\delta^{18}O$ and $\delta^{2}H$ values of location Ellighausen compared to the other three locations (Supplemental material Figure 1).

Standardized variety mean values of bulk dried grain tissue $\delta^{18}O$ values showed a range of 2.72 ‰ with a standard deviation of 0.54 ‰ (Fig. 4; Table 4). For hydrogen, we found a range of the standardized variety mean $\delta^{2}H$ values of 15.58 ‰ with a standard deviation of 3.60 ‰ (Fig. 4; Table 4). The observed variability in bulk dried grain tissue $\delta^{18}O$ and $\delta^{2}H$ values among different winter wheat varieties, although significant, is low compared to the variability of plant organic $\delta^{18}O$ and $\delta^{2}H$ values typically observed among species or environmental gradients [22,34–37]. Although the differences in bulk dried grain $\delta^{18}O$ and $\delta^{2}H$ values are small, we found that 85 % and 62 % of the observed variability in the standardized bulk dried grain $\delta^{18}O$ and $\delta^{2}H$ values, respectively, can be explained by the six plant traits we investigated (weight per hectolitre, plant height, yield, Zeleny index and protein content) (Table 6 and 7). We found a significant positive relationship of plant height with the bulk dried grain oxygen isotope values (Fig. 6a). As described above, different growth forms, such as plant height, result in differing degrees of transpirational water loss, and thus differences in initial leaf water enrichment

that are transferred into bulk grain material [21,22]. Our results suggest that taller plants are more closely coupled to the atmosphere, and are thus subject to stronger evaporative conditions. This in return might decrease g_s to reduce leaf water loss and thus increase the leaf water $\delta^{18}O$ values and consequently the bulk dried grain $\delta^{18}O$ values [44]. Also as stated for leaf water, monocotyledonous plants with longer leaves, which could be the case for taller plants, are subject to an increased leaf water enrichment due to a relatively smaller volume of unenriched source water in the leaf [22,44,52], which is then subsequently reflected in the bulk dried grain $\delta^{18}O$ values. Additionally, we found that yield correlated negatively with the bulk grain $\delta^{18}O$ values (Fig. 6b), agreeing with previous findings by Barbour et al. (2000). Many modern, high yielding crops show a high g_s [18–20], resulting in comparatively lower leaf water $\delta^{18}O$ values [38] that are also found in the grain $\delta^{18}O$ signal. We further observed a positive correlation of weight per hectoliter and the weight of a thousand grains with the dried bulk grain material $\delta^{18}O$ values (Fig. 6c and 6d). These measures of grain density likely correlate with the grain carbohydrate content. Carbohydrates are ^{18}O-enriched compared to other components in the bulk dried material (e.g. lipids) [53], and a higher ratio of carbohydrates relative to the total mass should thus also increase the bulk dried grain $\delta^{18}O$ values. We also found a significant positive correlation of the standardized bulk dried grain $\delta^{18}O$ values with the percentage of grain protein content (Fig. 6e) and, since Zeleny index is closely correlated to grain protein content [26,27], we also found a positive correlation of standardized bulk dried grain $\delta^{18}O$ values with the Zeleny index (Fig. 6f). Protein $\delta^{18}O$ values of plants are, however, an area with limited published data, so our findings suggest that more studies in this area would be interesting, especially for crop sciences.

Compared to oxygen, the correlation between plant height and the $\delta^{2}H$ values of the bulk dried grain material did not explain as much of the observed variability (Fig. 6a). This indicates a reduced transfer of the plant height associated leaf water ^{2}H-enrichment into the grain organic tissue [38]. Additionally, the $\delta^{2}H$ values of bulk dried grain material were negatively correlated with yield (Fig. 6b). On the one hand, this reflects the effects of g_s on yield and the leaf water isotope composition as described for oxygen. On the other hand it could further be explained that in low yielding plants, where we expect lower carbohydrate supplies in heterotrophic grain tissue, this reduced carbohydrate availability is counteracted by an up-regulation of the

oxidative pentose phosphate pathway, which enriches its products in ^{2}H [54,55]. As for oxygen, more carbohydrates in the grains should increase the bulk dried tissue $\delta^{2}H$ values of grains, which could explain the positive correlation of the $\delta^{2}H$ values with the weight per hectoliter and the weight of a thousand grains (Fig. 6c and 6d). Protein in algae have been found to be ^{2}H-depleted compared to carbohydrates [56]. We, however, found the $\delta^{2}H$ values of grains to increase with protein content (Fig. 6e). We thus assume that in heterotrophic grains, a higher amount of proteins leads to a higher recycling of compounds in the Calvin cycle and the citric acid cycle during amino acid synthesis, which allows more exchange of hydrogen with the surrounding and comparatively ^{2}H-enriched water [54]. Since grain $\delta^{2}H$ values were closely correlated to grain protein content [26,27], we speculate the same processes to hold true for the correlation with the Zeleny index (Fig. 6f).

Conclusion

The results of our study show that 36 winter wheat varieties had a relatively small range in their leaf water oxygen and hydrogen isotope compositions (SD of 0.63 and 1.52 for $\delta^{18}O$ and $\delta^{2}H$, respectively) when grown in the same location, and that the values did not differ significantly among varieties. Likewise, we found that 36 winter wheat varieties showed a small range in their bulk dried grain $\delta^{18}O$ and $\delta^{2}H$ values (SD of 0.54 and 3.60 for $\delta^{18}O$ and $\delta^{2}H$, respectively), although these values were significantly different among varieties. The small differences bulk dried grain $\delta^{18}O$ and $\delta^{2}H$ values among varieties can be related to phenotypic variability of trait expression such as plant height or weight per hectolitre. For food fraud investigations of winter wheat and possibly also other cereals, the low variability in leaf water and bulk dried grain $\delta^{18}O$ and $\delta^{2}H$ values among varieties that we observed in our study suggests that inter-variety effects are of little relevance in most cases and that that the collection of reference material at the species level is adequate.

Acknowledgements
We would like to thank Lilia Levy of Agroscope Nyon for her help with providing samples and granting access to the field trails. We also would like to thank Sandra Schmid for her help collecting the leaf samples and Svenja Förster for her support with the sample preparation and analyses.

Declaration of interest statement
The authors declare no competing interests.

Funding
This work was supported by PlantHUB - European Industrial Doctorate funded by the European Commission's Horizon 2020 research and innovation program under the Marie Skłodowska-Curie grant No 722338; the ERC consolidator under grant No 724750 – HYDROCARB; and by the 'Freiwillige Akademische Gesellschaft Basel' (FAG).

Data availability
The primary data that support the findings of this study are openly available in 'figshare' at http://doi.org/10.6084/m9.figshare.14267495.

References

[1] Dansgaard W. Stable isotopes in precipitation. Tellus. 1964;2826:436–468.

[2] Bowen GJ. Isoscapes: Spatial Pattern in Isotopic Biogeochemistry. Annu Rev Earth Planet Sci. 2010;38:161–187.

[3] Cerling TE, Barnette JE, Bowen GJ, et al. Forensic Stable Isotope Biogeochemistry. Annu Rev Earth Planet Sci. 2016;44:175–206.

[4] Camin F, Boner M, Bontempo L, et al. Stable isotope techniques for verifying the declared geographical origin of food in legal cases. Trends Food Sci Technol. 2017;

[5] Rossmann A. Determination of Stable Isotope Ratios in Food Analysis. Food Rev Int. 2001;9129.

[6] Carter JF, Chesson LA. Food Forensics: Stable Isotopes as a Guide to Authenticity and Origin. 1st Editio. Carter JF, Chesson LA, editors. Food Forensics. Boca Raton, FL: CRC Press; 2017.

[7] Cueni F, Nelson DB, Boner M, et al. Using plant physiological stable oxygen isotope models to counter food fraud. Sci Rep. 2021;11:17314.

[8] Luo D, Dong H, Luo H, et al. The application of stable isotope ratio analysis to determine the geographical origin of wheat. Food Chem. 2015;174:197–201.

[9] Goitom Asfaha D, Quétel CR, Thomas F, et al. Combining isotopic signatures of $n(^{87}Sr)/n(^{86}Sr)$ and light stable elements (C, N, O, S) with multi-elemental profiling for the authentication of provenance of European cereal samples. J Cereal Sci. 2011;53:170–177.

[10] Camin F, Archer ROL, Icolini GIN, et al. Isotopic and Elemental Data for Tracing the Origin of European Olive Oils. J Agric Food Chem. 2010;570–577.

[11] Santato A, Bertoldi D, Perini M, et al. Using elemental profiles and stable isotopes to trace the origin of green coffee beans on the global market. J Mass Spectrom. 2012;47:1132–1140.

[12] Danezis GP, Tsagkaris AS, Camin F, et al. Food authentication: Techniques, trends & emerging approaches. TrAC - Trends Anal Chem. 2016;85:123–132.

[13] Camin F, Perini M, Bontempo L, et al. Potential isotopic and chemical markers for characterising organic fruits. Food Chem. 2011;125:1072–1082.

[14] West JB, Kreuzer HW, Ehleringer JR. Approaches to Plant Hydrogen and Oxygen Isoscapes Generation. Isoscapes Underst Movement, Pattern, Process Earth Through Isot Mapp. 2010. p. 161–178.

[15] FAO. Food Outlook - Biannual Report on Global Food Markets: June 2020. Food Outlook. 2020;1–142.

[16] European Commission. Cereals, oilseeds, protein crops and rice. Prot. EU farmers Agric. Sect. through policy Mark. Interv. trade Meas. Legis. Monit. Mark. 2020.

[17] Torche J-M, Courvoisier N, Levy L. Blé d'automne 2017 - Winterweizen 2017. 1260 Nyon; 2018.

[18] Araus JL, Ferrio JP, Buxo R, et al. The historical perspective of dryland agriculture: lessons learned from 10 000 years of wheat cultivation. J Exp Bot. 2006;58:131–145.

[19] Araus JL, Cabrera-Bosquet L, Serret MD, et al. Comparative performance of $\delta^{13}C$, $\delta^{18}O$ and $\delta^{15}N$ for phenotyping durum wheat adaptation to a dryland environment. Funct Plant Biol. 2013;40:595.

[20] Sanchez-Bragado R, Serret MD, Marimon RM, et al. The hydrogen isotope composition $\delta^{2}H$ reflects plant performance. Plant Physiol. 2019;180:793–812.

[21] Helliker BR, Ehleringer JR. Differential ^{18}O enrichment of leaf cellulose in C3 versus C4 grasses. Funct Plant Biol. 2002;29:435.

[22] Helliker BR, Ehleringer JR. Establishing a grassland signature in veins: ^{18}O in the leaf water of C3 and C4 grasses. Proc Natl Acad Sci. 2000;97:7894–7898.

[23] Epstein S, Thompson P, Ya CJ. Oxygen and Hydrogen Isotopic Ratios in Plant Cellulose. Science (80-). 1977;198.

[24] Yakir D, DeNiro MJ. Oxygen and Hydrogen Isotope Fractionation during Cellulose Metabolism in Lemna gibba L. Plant Physiol. 1990;93:325–332.

[25] Sternberg L, DeNiro MJ, Savidge RA. Oxygen Isotope Exchange between Metabolites and Water during Biochemical Reactions Leading to Cellulose Synthesis. Plant Physiol. 1986;82:423–427.

[26] Agrarheute. Qualität beim Weizen: Darauf kommt es an. Agrarheute. 2015.

[27] Herzog E, Schöne F, Guddat C. Backqualität von Getreide Neue Parameter zur Charakterisierung der Backqualität von Weizen.

Thüringer Landesanstalt für Landwirtschaft. 2017;1–13.

[28] Newberry SL, Nelson DB, Kahmen A. Cryogenic vacuum artifacts do not affect plant water - uptake studies using stable isotope analysis. Ecohydrology. 2017;1–10.

[29] Nelson DB, Basler D, Kahmen A. Precipitation isotope time series predictions from machine learning applied in Europe. PNAS. 2021;118:e2024107118.

[30] Cueni F, Nelson DB, Lehmann MM, et al. Constraining parameter uncertainty for predicting oxygen and hydrogen isotope values in fruit. J Exp Bot.

[31] Gehre M, Renpenning J, Gilevska T, et al. On-Line Hydrogen-Isotope Measurements of Organic Samples Using Elemental Chromium: An Extension for High Temperature Elemental-Analyzer Techniques. Anal Chem. 2015;6.

[32] Wassenaar LI, Hobson KA, Sisti L. An online temperature-controlled vacuum-equilibration preparation system for the measurement of δ^2H values of non- exchangeable-H and of $\delta^{18}O$ values in organic materials by isotope-ratio mass spectrometry. Rapid Commun Mass Spectrom. 2015;397–407.

[33] Coplen TB. Guidelines and recommended terms for expression of stable- isotope-ratio and gas-ratio measurement results. Rapid Commun Mass Spectrom. 2011;2538–2560.

[34] Kahmen A, Simonin K, Tu KP, et al. Effects of environmental parameters, leaf physiological properties and leaf water relations on leaf water δ18O enrichment in different Eucalyptus species. Plant Cell Environ. 2008;31:738–751.

[35] Terwilliger VJ, Betancourt JL, Leavitt SW, et al. Leaf cellulose δD and $\delta^{18}O$ trends with elevation differ in direction among co-occurring, semiarid plant species. Geochim Cosmochim Acta. 2002;66:3887–3900.

[36] Cheesman AW, Cernusak LA. Infidelity in the outback : climate signal recorded in $\Delta^{18}O$ of leaf but not branch cellulose of eucalypts across an Australian aridity gradient. Tree Physiol. 2016;554–564.

[37] Kahmen A, Sachse D, Arndt SK, et al. Cellulose $\delta^{18}O$ is an index of leaf-to-air vapor pressure difference (VPD) in tropical plants. Proc Natl Acad Sci. 2011;108:1981–1986.

[38] Cernusak LA, Barbour MM, Arndt SK, et al. Stable isotopes in leaf

water of terrestrial plants. Plant Cell Environ. 2016;1087–1102.

[39] Kahmen A, Hoffmann B, Schefuß E, et al. Leaf water deuterium enrichment shapes leaf wax *n*-alkane δD values of angiosperm plants II: Observational evidence and global implications. Geochim Cosmochim Acta. 2013;111:50–63.

[40] Flanagan LB, Comstock JP, Ehieringer JR. Comparison of Modeled and Observed Environmental Influences on the Stable Oxygen and Hydrogen Isotope Composition of Leaf Water in Phaseolus vulgaris L . Plant Physiol. 1991;588–596.

[41] Flanagan LB, Ehieringer JR. Effects of Mild Water Stress and Diurnal Changes in Temperature and Humidity on the Stable Oxygen and Hydrogen Isotopic Composition of Leaf Water in Cornus stolonifera. Plant Physiol. 1991;298–305.

[42] Cernusak LA, Wong SC, Farquhar GD. Oxygen isotope composition of phloem sap in relation to leaf water in Ricinus communis. Funct Plant Biol. 2003;30:1059.

[43] Cabrera-Bosquet L, Molero G, Nogués S, et al. Water and nitrogen conditions affect the relationships of $\Delta^{13}C$ and $\Delta^{18}O$ to gas exchange and growth in durum wheat. J Exp Bot. 2009;60:1633–1644.

[44] Cernusak LA, Kahmen A. The multifaceted relationship between leaf water 18O enrichment and transpiration rate. Plant Cell Environ. 2013;1239–1241.

[45] Sternberg L, DeNiro M. Biogeochemical implications of the isotopic equilibrium fractionation factor between the oxygen atoms of acetone and water. Geochim Cosmochim Acta. 1983;47.

[46] Yakir D. Variations in the natural abundance of oxygen-18 and deuterium in plant carbohydrates. Plant Cell Environ. 1992;1005–1020.

[47] Cormier M-A, Werner RA, Sauer PE, et al. ^{2}H-fractionations during the biosynthesis of carbohydrates and lipids imprint a metabolic signal on the $\delta^{2}H$ values of plant organic compounds. New Phytol. 2018;218:479–491.

[48] Ziegler H. Hydrogen Isotope Fractionation in Plant Tissues. Rundel PW, Ehleringer JR, Nagy KA Stable Isot Ecol Res Ecol Stud (Analysis Synth. New York: Springer; 1989. p. 105–123.

[49] Chikaraishi Y, Naraoka H. Compound-specific δD – $\delta^{13}C$ analyses of *n*-alkanes extracted from terrestrial and aquatic plants.

Phytochemistry. 2003;63:361–371.

[50] Roden JS, Ehleringer JR. Hydrogen and oxygen isotope ratios of tree-ring cellulose for riparian trees grown long term under hydroponycally environments. Oecologia. 1999;121:467–477.

[51] Barbour MM, Fischer RA, Sayre KD, et al. Oxygen isotope ratio of leaf and grain material correlates with stomatal conductance and grain yield in irrigated wheat. Aust J Plant Physiol. 2000;27:625–637.

[52] Farquhar GD, Gan KS. On the progressive enrichment of the oxygen isotopic composition of water along a leaf. Plant Cell Environ. 2003;26:1579–1597.

[53] Schmidt HL, Werner RA, Roßmann A. ^{18}O pattern and biosynthesis of natural plant products. Phytochemistry. 2001;58:9–32.

[54] Cormier M-A, Werner RA, Leuenberger MC, et al. ^{2}H-enrichment of cellulose and *n*-alkanes in heterotrophic plants. Oecologia. 2019;189:365–373.

[55] Hermes JD, Roeske CA, Leary MHO, et al. Use of Multiple Isotope Effects To Determine Enzyme Mechanisms and Intrinsic Isotope Effects . Malic Enzyme and Glucose-6-phosphate. Biochemistry. 1982;5106–5114.

[56] Estep MF, Hoering TC. Stable Hydrogen Isotope Fractionations during Autotrophic and Mixotrophic Growth of Microalgae. Plant Physiol. 1981;67:474–477.

[57] Soto DX, Koehler G, Wassenaar LI, et al. Re-evaluation of the hydrogen stable isotopic composition of keratin calibration standards for wildlife and forensic science applications. Rapid Commun Mass Spectrom. 2017;31:1193–1203.

[58] Qi H, Coplen TB, Jordan JA. Three whole-wood isotopic reference materials, USGS54, USGS55, and USGS56, for $\delta^{2}H$, $\delta^{18}O$, $\delta^{13}C$, and $\delta^{15}N$ measurements. Chem Geol. 2016;442:47–53.

Appendix

Determination of δ^2H values of non-exchangeable hydrogen from dual water equilibration was facilitated with the use of a Uni-prep autosampler (Eurovector, Milan, Italy), which consists of a uniformly heated sample chamber that can be evacuated with an integrated vacuum pump, and also includes a septum port through which water can be injected [32]. The autosampler was operated at 70 °C throughout the equilibration and measurement process, and used a one-hour equilibration time [57]. Samples were initially loaded into the Uni-prep and redried under open vacuum for one hour, after which time the vacuum valve was closed, and 50 µL of water was injected into the sealed and evacuated sample carousel chamber (see methods). Following one hour of equilibration, samples were again dried for one hour under open vacuum, after which time the vacuum valve was closed, the autosampler was purged with helium, pressurized to 1.5 bar, and then opened to the TC/EA reactor. The autosampler was then left to equilibrate with the TC/EA reactor for at least three hours before starting the analyses.

Measured δ^2H values were normalized to the VSMOW-SLAP scale as described in the methods section. Following this, the resulting δ^2H values from the relatively ^2H-enriched and ^2H-depleted water equilibration sample pairs (see methods) were used to calculate the sample-specific fraction of the measured hydrogen that exchanged with the injected water during equilibration. Long term precision for the calculated non-exchangeable hydrogen δ^2H values was optimized by using three wood standards with known non-exchangeable hydrogen δ^2H values to calculate equilibration run-specific isotopic fractionation factors for each equilibration as an α value (USGS 54,55,56; [58]). The resulting α values for each wood standard were then used to calculate a mean for a given set of paired equilibration runs, and this value was used together with the previously calculated sample-specific fraction of exchangeable hydrogen to derive the non-exchangeable hydrogen δ^2H value for each sample. The calculations are summarized below.

Calculations were performed with R values, where: $R = {}^2H/{}^1H$, and $\delta^2H = (R_{sample}/R_{standard}) - 1$, and $R_{standard}$ is VSMOW (see methods).

We assume that the non-exchangeable hydrogen isotope ratio in a sample aliquot equilibrated with relatively ^2H-enriched water (EW) is equal to the non-exchangeable hydrogen isotope ratio in a sample aliquot equilibrated with

relatively ^{2}H-depleted water (DW). That is, $R_{NE} = R_{ND}$, where R_{NE} and R_{ND} represent the non-exchangeable hydrogen isotope ratios in each of these aliquots, respectively.

The measured δ^2H value of the total hydrogen yield (exchangeable + non-exchangeable) from a given sample can therefore be shown as an R value for the EW-equilibrated and DW-equilibrated samples as R_{TE} and R_{TD}, respectively, as:

$$R_{TE} = [X_N * R_{NE} + X_E * R_{EE}] / [X_N + X_E]$$

and:

$$R_{TD} = [X_N * R_{ND} + X_E * R_{ED}] / [X_N + X_E]$$

Where R_{EE} and R_{ED} are the R values of exchangeable hydrogen in the EW and DW equilibrated sample aliquots, respectively, and X_N and X_E are the quantities of non-exchangeable and exchangeable hydrogen in the total hydrogen pool, respectively. The fraction of exchangeable hydrogen in a sample, F_X, can therefore be expressed as: $F_X = X_E/(X_E+X_N)$.

Any isotopic fractionation that may occur during the equilibration process can be defined as an α_{EQ} value, where $\alpha_{EQ} = R_{EE}/R_{WE} = R_{ED}/R_{WD}$, and R_{WE} and R_{WD} are the R values for the corresponding EW and DW waters. From this, it follows that $R_{EE} = \alpha_{EQ} * R_{WE}$ and that $R_{ED} = \alpha_{EQ} * R_{WD}$.

The fraction of exchangeable hydrogen in a pair of sample aliquots, F_x, can also be calculated from previously defined terms as: $F_X = [R_{TD} – R_{TE}] / [R_{ED} – R_{EE}]$. This value can also be related to the R values of the original water used for equilibration rather than the exchanged hydrogen using the isotopic fractionation factor: $F_x = [R_{TD} – R_{TE}] / \alpha_{EQ}[R_{WD} – R_{WE}]$.

Based on the definitions of F_x and α_{EQ}, the R value of the non-exchangeable hydrogen in a sample can be calculated as:

$$R_{NE} = [R_{TE} – F_x*\alpha_{EQ} *R_{WE}] / [1 – F_x]$$
$$R_{ND} = [R_{TD} – F_x*\alpha_{EQ} *R_{WD}] / [1 – F_x]$$

In order to solve either of the two previous equations, α_{EQ} must be known, which is possible if standards that have a known non-exchangeable hydrogen δ^2H value are also analyzed. This can be achieved by substituting in definitions of F_X and α_{EQ} into either equation above and solving for α_{EQ} (shown here after starting with the R_{NE} equation):

$$\alpha_{EQ} = \frac{\left[\frac{R_{TD} - R_{TE}}{R_{WD} - R_{WE}}\right]}{\left[\left[\frac{(R_{TD} - R_{TE}) * R_{WE}}{(R_{WD} - R_{WE}) * R_{NE}}\right] - \frac{R_{TE}}{R_{NE}} + 1\right]}$$

After an α_{EQ} value is determined for each paired equilibration run based on the measured δ^2H values of the exchangeable hydrogen standards, the δ^2H value of the non-exchangeable hydrogen for each set of sample aliquots can be calculated.

Chapter 4

Using plant physiological stable oxygen isotope models to counter food fraud

Florian Cueni*[1,2], Daniel B. Nelson[1], Markus Boner[2], Ansgar Kahmen[1]

[1]University of Basel, Department of Environmental Sciences – Botany, Schönbeinstrasse 6, 4056 Basel, Switzerland
[2]Agroisolab GmbH, Professor-Rehm-Strasse 6, 52428 Jülich, Germany
* Corresponding author: f.cueni.plantphys@gmail.com

This Chapter is published in ***Scientific Reports***.

DOI: https://doi.org/10.1038/s41598-021-96722-9

Abstract

Fraudulent food products, especially regarding false claims of geographic origin, impose economic damages of $30 - $40 billion per year. Stable isotope methods, using oxygen isotopes ($\delta^{18}O$) in particular, are the leading forensic tools for identifying these crimes. Plant physiological stable oxygen isotope models simulate how precipitation $\delta^{18}O$ values and climatic variables shape the $\delta^{18}O$ values of water and organic compounds in plants. These models have the potential to simplify, speed up, and improve conventional stable isotope applications and produce temporally resolved, accurate, and precise region-of-origin assignments for agricultural food products. However, the validation of these models and thus the best choice of model parameters and input variables have limited the application of the models for the origin identification of food. In our study we test model predictions against a unique 11-year European strawberry $\delta^{18}O$ reference dataset to evaluate how choices of input variable sources and model parameterization impact the prediction skill of the model. Our results show that modifying leaf-based model parameters specifically for fruit and with product-independent, but growth time specific environmental input data, plant physiological isotope models offer a new and dynamic method that can accurately predict the geographic origin of a plant product and can advance the field of stable isotope analysis to counter food fraud.

Introduction

Food fraud, the intentional and misleading adulteration of food for economic gain [1–3], imposes an estimated annual burden of up to $40 billion [4–6]. Although most cases are not identified, it is estimated that 10 % to 30 % of all commercially sold food is fraudulent [4,5]. Improper labeling concerning the country of origin is the most common form of food fraud [7,8], which is motivated by cost reduction and maximization of profits [1]. This erodes consumer trust [3], and increases the potential for reduced quality and health risk [1,9]. Analytical tools for the independent verification of the geographical origin of food are therefore in high demand [10].

The leading methods used for the forensic assessment of geographic food origin use stable isotope analyses [11–14]. Stable isotopes are especially ideal for verifying the origin of agricultural products, since climate and topography [15,16], the underlying geology [17], and agricultural practices [18] lead to location specific isotopic fingerprints in a product [19]. Most methods using stable isotopes for the verification of geographical origins are based on the direct comparison of the isotopic fingerprint of a suspected sample to authentic reference material with known geographic origin. For such comparisons, statistical analyses are straightforward and data interpretation is easily understood by customers and law enforcement agencies [19]. Collecting authentic reference samples is, however, time consuming and expensive, especially on a global scale. Large reference datasets are therefore often geographically scattered and temporally not sufficiently resolved to account for the inter- and intra-annual variability observed in the oxygen and hydrogen isotope composition of plants, the two stable isotope ratios primarily used for origin analysis. This limitation can add substantial uncertainty in the provenance prediction of agricultural products.

In this study, we demonstrate how mechanistic plant physiological stable oxygen isotope models can be parametrized to serve as a fast, logistically simple, and low-cost alternative for predicting the geographic origin of agricultural plant products. The oxygen isotope composition ($\delta^{18}O$) of plant organic compounds is driven by the $\delta^{18}O$ values of local precipitation [20–22] and the evaporative environment of a plant, both of which show distinct geographic patterns [15,16]. If correctly parameterized, plant physiological stable isotope models can simulate how precipitation water $\delta^{18}O$ values and climatic variables jointly shape the $\delta^{18}O$ values of water inside the plant, and how these plant water $\delta^{18}O$ values are imprinted into the plant's organic materials [23,24].

Mechanistic plant physiological stable oxygen isotope models therefore have the potential to simulate the geographic variation of plant $\delta^{18}O$ values (e.g. agricultural products), to which $\delta^{18}O$ values of suspected food samples can be referenced and their purported geographic origin verified.

To demonstrate conceptually how a mechanistic plant physiological stable isotope model can be used to simulate the geographic variability in $\delta^{18}O$ values of food products, we use a unique Europe-wide strawberry $\delta^{18}O$ reference dataset that contains 154 authentic reference samples that have been collected across Europe from 2007 to 2017 (Fig. 1). We employ this dataset to validate our model predictions across space and time and to test model assumptions that we make regarding model parameters and model input variables. With this approach we test if plant physiological stable oxygen isotope models that have originally been developed for leaf water or cellulose in the leaves or stems of plants are generally applicable for identifying the geographic origin of agricultural products, or if they need to be parameterized for specific plant species and their products. In addition, we carefully evaluate the type, necessary spatial resolution, and temporal integration of isotopic (precipitation $\delta^{18}O$ values) and climatic (temperature, relative humidity) input variables that are required for the most accurate prediction of strawberry $\delta^{18}O$ values across Europe.

Results

The model that we used in our simulations is based on the two-pool adapted Craig-Gordon model [25–27]. We followed a two-step approach to determine the best possible selection of model parameters and model input variables. Firstly, we utilized different combinations of the two key physiological model parameters. These are f_{xylem}, which accounts for the dilution of ^{18}O enriched water at the site of evaporation in leaves with the plant's source water, and $p_x p_{ex}$ / $p_x p_{ex}c$, which accounts for the extent of oxygen exchange between sugars and the surrounding plant water during biosynthesis of cellulose ($p_x p_{ex}$) and other compounds ($p_x p_{ex}c$). For these model parameters we used (i) mean values obtained from the literature that were originally determined for leaf water (f_{xylem}) and leaf cellulose $\delta^{18}O$ values ($p_x p_{ex}$) across various plant species. In addition we used values that were specifically determined for (ii) leaf water (f_{xylem}) and bulk dried tissue of berries ($p_x p_{ex}c$) in berry producing plants and (iii) leaf water (f_{xylem}) and bulk dried tissue of berries ($p_x p_{ex}c$) of strawberry plants in particular [28] (see Table 1 and methods for a detailed description of the parameter selection). Since the $p_x p_{ex}c$ for strawberries and berries of other berry producing plant species have been found to be identical [28], this resulted in only one $p_x p_{ex}c$ value together with one $p_x p_{ex}$ value, that we combined with three f_{xylem} values, and therefore six differently parameterized models (Fig 2a). In a second step, we ran these six differently parameterized models with different combinations of environmental model input variables. This included different sources for precipitation $\delta^{18}O$ data and climate data as well as different time periods over which to integrate these data leading up to the actual harvest date of a sample in the field (Table 2). The combination of different model input variables resulted in 65,536 different model simulations per model parameter combination (Fig. 2a). To evaluate the differences in performance among the different model parameter and input variable choices, we calculated root mean squared error (RMSE) values based on the comparison to our reference dataset for each of the 65,536 combinations of input variables for each of the six parameter combinations.

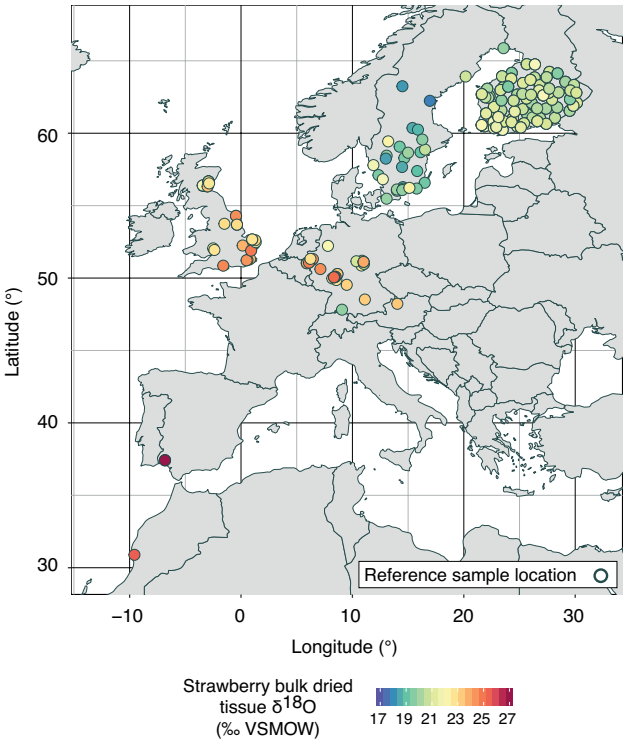

Figure 1: Map of Europe, showing the locations of the 154 authentic reference samples used for the model validation. The samples were collected between 2007 and 2017. The colored fill of the dots shows the measured $\delta^{18}O$ values of the strawberry bulk dried tissue of the reference samples. The samples were mainly collected during the main European strawberry season from May to July [76]. The map was created using the software R, version 3.5.3 (https://www.r-project.org/).

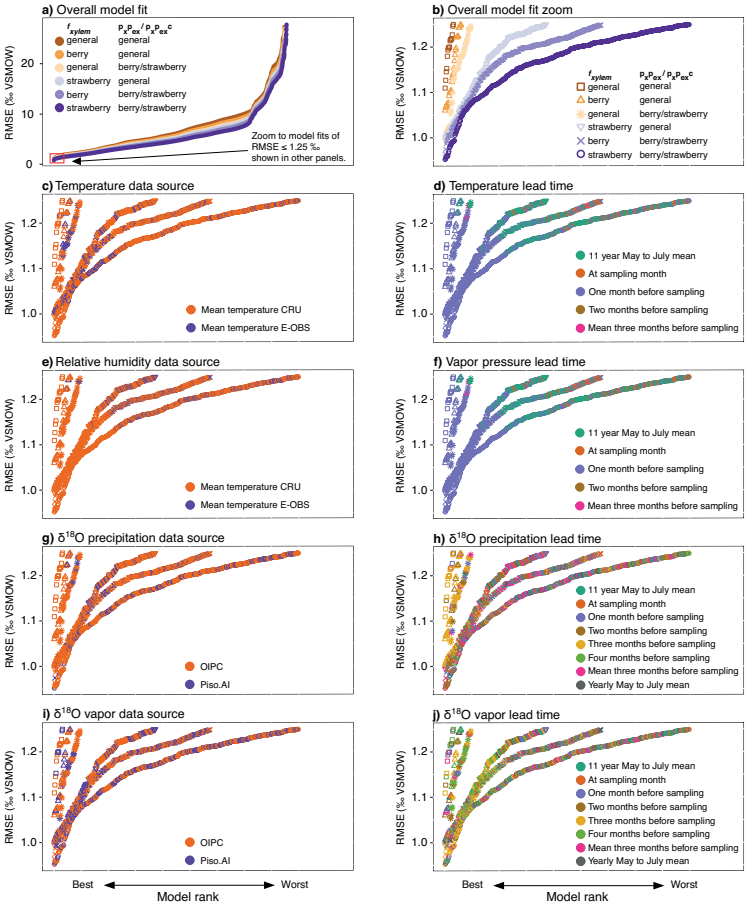

Figure 2: Model fit analysis of all possible parameter and model input data combinations. All panels show model root mean square error (RMSE) values obtained from comparison between modeled and measured bulk dried tissue $\delta^{18}O$ values (n=154) from authentic reference samples. Each dot represents the RMSE (in ‰ VSMOW) from one combination of model parameters and input data. RMSE values are ranked by best model fit. Panel **a)** shows the ranked RMSE values that are lower than 25 ‰ from the total set of 65,536 tested combinations in each of the six differently parameterized models (n ≤ 14,850 for each parameter combination). The symbols are colored according to the different model parameter combinations (f_{xylem} and $p_x p_{ex}$ / $p_x p_{ex} c$) used for the simulations, either general parameters for leaves averaged across various species using literature values ("general"), parameters that are average values for leaves (f_{xylem}) and berries ($p_x p_{ex} c$) of berry producing plants ("berry"), or

parameters specifically determined for leaves (f_{xylem}) and berries ($p_x p_{ex} c$) of strawberry plants ("strawberry"). Panels **b)-j)** only show the models with RMSE values lower than 1.25 ‰ (red square panel a). Panel **b)** shows the ranked model fits for the same model parameter and input data combinations as panel a), but introduces symbols for the different model parameter combinations used. These symbols remain the same for panels c)-j). In panels c)-j) the symbols are colored based on the model input data used for the simulation (see panel in the figures for detail as well as Supplementary Information datasets S1 to S6). Panels **c)** and **e)** compare the use of CRU[29] to E-OBS[30] input data, panels **g)**, and **i)** compare the use of OIPC[31] to Piso.AI[32] isotope data sources, and panels **d)**, **f)**, **h)**, and **j)** compare the use of different lead time intervals leading up to the sampling date of the reference material (see methods). Since the panels only show the best model fits for RMSE values of up to 1.25 ‰, for panels **d)** and **f)** some time intervals yielded RMSE values greater than the plotted range, and are thus not indicated in the legends.

We found that all six differently parameterized models were able to predict the $\delta^{18}O$ values of strawberry bulk dry material well. The best model performance was obtained using strawberry-specific model parameters, which yielded a minimum RMSE of 0.95 ‰. However, even the most general parameters still performed well, yielding a minimum RMSE of 1.11 ‰ (Fig. 2). Models that used average parameters (f_{xylem} and $p_x p_{ex} c$) for berry producing plants or parameters that are specific for strawberry plants, outperformed models that used at least one general parameter obtained from average literature values for leaves (Fig 2a and b). The overall best model results were achieved using strawberry-specific model parameters (strawberry f_{xylem} and berry/strawberry $p_x p_{ex} c$) (Fig 2a and b). The model that was parameterized with average parameters for berry producing plants (irrespective of the species) consistently showed the second-best performance (Fig 2a and b). In particular, the choice of average berry producing plant or strawberry-specific values for the model parameter f_{xylem} over general across-species averaged literature values for f_{xylem} proved to be more important for increasing the model performance than the choice of $p_x p_{ex}$ / $p_x p_{ex} c$ values (Fig. 2a).

Our analysis further revealed that the choice of model input data strongly affects the quality of model output and that this is irrespective of the model parameterization (Fig. 2c to j). Out of the 65,536 different combinations of input parameter choices we tested, models using monthly mean temperature from the climatic research unit (CRU) (0.5° grid) [29] performed better than models using data from the E-OBS dataset (0.1° grid) [30], despite the lower spatial resolution of the CRU data (Fig. 2c). Similarly, using relatively humidity values derived from CRU vapor pressure data yielded better results

than when using relative humidity data from E-OBS (Fig. 2e). The model comparisons also showed that the best predictions were obtained using temperature and vapor pressure input data for the month prior to the collection of a reference sample (Fig. 2d and f, Supplementary Information dataset S1 to S6). For precipitation $\delta^{18}O$ data, the models using monthly values from the OIPC [31] (which are not specific for a given year) generally showed a better fit (26 out of the 30 lowest RMSEs) than those using Piso.AI [32], which predicts values for specific months and years (Fig. 2g). Still, the single best fit values were based on Piso.AI derived mean of the three-month period leading up to sampling (Supplementary Information dataset S6). For vapor $\delta^{18}O$ values, however, the choice of data source showed no such clear pattern (Fig. 2i). In contrast to the temperature and vapor pressure data, the selection of the time interval prior to the collection of the reference sample resulted in no consistent best choice for precipitation and vapor $\delta^{18}O$ input variables (Fig. 2h & j).

Comparing all possible model parameter and input data choices, we found two nearly identically best performing models. These were the model that used average model input parameters for berry producing plants, which yielded an RMSE of 0.96 ‰, and the model that used strawberry-specific parameters, which yielded an RMSE of 0.95 ‰ (Fig. 2, Fig. 3). The best performing model using average parameters for berry producing plants used monthly air temperature and vapor pressure data from CRU from one month before the collection of a reference sample in a specific year, precipitation $\delta^{18}O$ values of the precipitation-weighted mean of the three-month period leading up to the harvest date of a sample from the long term mean monthly values provided by OIPC, and vapor $\delta^{18}O$ values calculated assuming isotopic equilibrium with the precipitation $\delta^{18}O$ values three month before harvest.

The map of predicted strawberry bulk dried tissue $\delta^{18}O$ values from this best performing average berry model for the example month of July 2017 shows values ranging from +31 ‰ to +16 ‰ across the European continent (Fig. 3b). The measured $\delta^{18}O$ variability within one region was generally higher than the variability captured by the model, with the largest outliers sourcing from eight locations in Germany and Sweden, which the model over or underpredicted by 2.0 ‰ to 3.5 ‰ (Fig. 3a). However, the model induced uncertainty fell mostly within the 95 % quantile of the observed within-field variability of strawberry bulk dried

tissue $\delta^{18}O$ values (± 1 ‰) which we obtained through berry samples that were collected on the same field and the same day (mainly from Germany and Finland) (Fig. 3a).

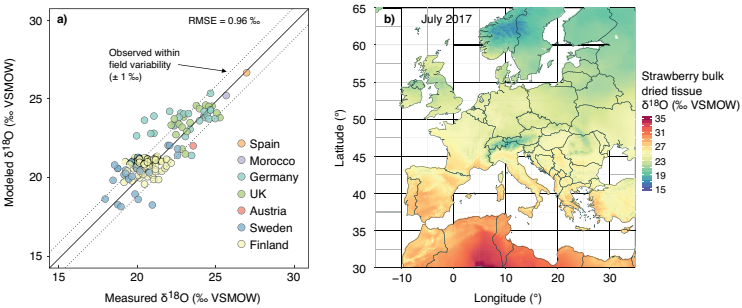

Figure 3: Results of the simulation of berry bulk dried $\delta^{18}O$ values using plant physiological isotope models. **a)** The modeled bulk dried tissue $\delta^{18}O$ values obtained from the model that was parameterized with general data for berries plotted against measured authentic bulk dried tissue reference samples $\delta^{18}O$ values (n = 154; RMSE = 0.96 ‰). Solid line represents the 1:1-line, the dashed lines show the 95 % quantile of the observed within field variability of strawberry $\delta^{18}O$ bulk dried tissue values. **b)** Map of Europe showing the expected spatial distribution of bulk dried tissue $\delta^{18}O$ values of strawberries, in this example collected in July 2017. The map was created using the software R, version 3.5.3 (https://www.r-project.org/).

Discussion

We demonstrate that a plant physiological stable oxygen isotope model that allows for the prediction of $\delta^{18}O$ values of organic compounds in leaves and wood can also serve as a powerful tool for predicting the spatial variability of $\delta^{18}O$ values in fruit. With the best choice of environmental input data, models parameterized with general across-species averaged leaf-derived values for the model parameters f_{xylem} and $p_x p_{ex}$ can predict observed data with an average RMSE of 1.11 ‰. The model that best predicted $\delta^{18}O$ values of bulk dried tissue of strawberries required model parameters specifically defined for leaves (f_{xylem}) and berries ($p_x p_{ex} c$) of strawberry plants. This model was, however, only marginally superior to the best performing model that was parameterized with average values for leaves (f_{xylem}) and berries ($p_x p_{ex} c$) of berry producing plants in general (RMSE = 0.95 ‰ vs. RMSE = 0.96 ‰). This suggests that using average parameters for berry producing plants will be sufficient for a high-quality model performance. In fact, even a model parameterization with general values obtained for leaves and averaged across various species results in a relatively good performance of the model. The robust performance of the differently parameterized models is an important outcome from this work, as it suggests a general applicability of the mechanistic plant physiological stable oxygen isotope model for simulating the spatial variability of $\delta^{18}O$ values in fruit. However, our analysis also shows that a careful choice of model input data that are specific for the year and month of sample collection – with varying lead times – is crucial for the performance of the model.

We found that model simulations using model parameters defined for berry producing plants (both average across berry producing plants and strawberry-specific) yielded model outputs that were slightly superior to those using at least one general parameter obtained from averaging leaf-derived literature values across species (Fig 2). Berries, like most other fruit, are largely heterotrophic (carbon-sink) tissues, relying on sugars imported from active photosynthetic organs (i.e. leaves). These sugars carry a climate and physiologically driven leaf water $\delta^{18}O$ signal [21,22,26,33,34]. This leaf water $\delta^{18}O$ value that is imprinted into sugars with a fixed fractionation of + 27 ‰ can be calculated by the Craig-Gordon model if the model is amended by the parameter f_{xylem} that accounts for the dilution of the evaporatively ^{18}O-enriched leaf water by the plant's source water [35]. For the two best performing models we used f_{xylem} values that were recently determined from independent growth

chamber experiments either for berry producing plants in general (0.26), or specifically for strawberry plants (0.30) [28]. These f_{xylem} values were slightly higher than mean f_{xylem} values that have been reported on average for leaves from various species in the literature (0.22) [36–40]. Higher f_{xylem} values could be the result of higher transpiration rates in berry producing plants used in agriculture than in the previously investigated plants that delivered the average f_{xylem} values of 0.22, and that included less productive wild plants with possibly lower transpiration rates.

During sugar transport from leaves via the phloem to carbon-sink tissues such as berries and during the carbohydrate synthesis in the sink tissues, some of the oxygen of the sugars exchanges with the surrounding water [41,42]. This water is ^{18}O-depleted compared to leaf water [43]. Therefore, the δ^{18}O values of sugars and carbohydrates in sink tissues differ from those of leaves [28,44]. In the model, the parameter $p_x p_{ex} c$ accounts - among others - for this effect. Our analysis shows that using $p_x p_{ex} c$ values that are specific for berries in berry producing plants improved the fit of predicted strawberry dried tissue δ^{18}O values to those of reference samples. The $p_x p_{ex} c$ value for berry bulk dried tissue that we obtained from independent growth chamber experiments (which are identical for strawberries and berries in general) [28] and used for the best performing model simulations was higher than the mean value typically reported for cellulose of leaves (0.46 vs 0.40 [45–49]). A higher $p_x p_{ex} c$ value in berries compared to the $p_x p_{ex}$ value of leaf-cellulose could be the result of increased oxygen exchange in sugar with plant source water (p_{ex}) during phloem transport from leaves to berries, as well as during carbohydrate synthesis in the berries. It could also indicate that berries typically contain more ^{18}O-depleted source water than leaves (p_x), which is in line with a recent observation in strawberries and raspberries [28]. Further, this pattern clearly shows that bulk dried tissue of berries compared to pure cellulose of leaves contains compounds with lower δ^{18}O values than cellulose itself [50], accounted for by a higher $p_x p_{ex} c$ value.

For differently parameterized models, using mean air temperature of the more coarsely spatially resolved CRU dataset (0.5° grid) resulted in an improved model fit compared to the finer resolution E-OBS dataset (0.1° grid) (Fig. 2). Other than the spatial resolution, differences between the two data sources are not evident, and the E-OBS and CRU mean temperature of the sampling month of the reference samples correlated with an r^2 of 0.98 ($y = 1.04x - 0.007$) for the sites used in this study. Although the best performing

model used precipitation $\delta^{18}O$ values from Piso.AI, which uses station coordinates and provides values for single months and years, we found model prediction skill to be generally better when using long-term monthly climatology-based precipitation $\delta^{18}O$ data from the gridded OIPC datasets as input data, as opposed to Piso.AI. It is somewhat surprising that lower spatial resolution, and climatological as opposed to contemporaneous input data generally resulted in more accurate model fits than those obtained from inputs that more closely reflect conditions at any point and time. This may relate to the fact that the exact growing location and collection date of the reference samples that we used as a validation target were often only broadly defined in the sample metadata (typically only postal codes or region names, and the month of sample delivery to the lab). This may have resulted in misassignments of climate or precipitation $\delta^{18}O$ values from neighboring nearby locations when using the more highly spatially and/or temporally resolved E-OBS and Piso.AI products, as opposed to the coarser products from CRU and OIPC. Also, when comparing Piso.AI to OIPC, Piso.AI generally produces a larger annual cycle than OIPC, so while picking the correct integration time can result in a better fit (see best preforming model), picking an incorrect one can result in bigger consequences for being wrong. Moreover, the differentiation between OIPC and Piso.AI is not only between data sources, but also between the timescales of integration. It may be the case that by averaging on interannual timescales, the monthly climatology precipitation $\delta^{18}O$ values from OIPC more accurately replicate typical $\delta^{18}O$ values of the source water that the plants use, which integrate over the timescales of the seasonal cycle due to the often long residence time of water in soil prior to plant uptake [51,52]. Both processes have the effect of smoothing out extreme $\delta^{18}O$ values that may occur in any individual month. If this explanation is correct, it also implies that predictions may be improved in the future through additional validation work using new reference samples collected with more rigorous metadata.

Our model output comparison shows that using climate input variables for the growing season of a specific year substantially improved the predictive power of the model. This is exemplified by the improvement of model predictions of the average berry parameterized model using growing season specific input data (RMSE = 0.96 ‰) compared to using 11-year average (2007 to 2017) mean growing season input data (RMSE = 1.27 ‰). Critically important for an accurate application of a plant physiological model to

simulate $\delta^{18}O$ values of bulk dried tissue for any given growing season, is also the time span before sample collection (i.e. during which a product grew) for which climatic input data are averaged before they are entered into the model. We found that using average values for air temperature and vapor pressure from one month before sampling (which is the time during which the berry grew) is the most suitable time span for which climatic input data should be averaged for simulating the $\delta^{18}O$ values in berry bulk dried tissue. The reason for improved model predictions when inter- and intra-annual variability climatic model input variable is accounted for comes from the fact that climatic drivers of leaf water and thus bulk dried tissue $\delta^{18}O$ values in plants, i.e. temperature and vapor pressure, can vary substantially from year to year and within a year. As such, leaf water $\delta^{18}O$ values also vary from year to year and within the growing season. This inter- and intra-annual variability in leaf water variability $\delta^{18}O$ values is imprinted into the $\delta^{18}O$ values of plants and can cause substantial temporal variability of plant organic $\delta^{18}O$ values at a given geographic location [46,53]. The option to simulate this variability by using climatic input variables for specific years or specific parts of the growing seasons is thus a major advantage of plant physiological stable isotope models in the origin identification of plant samples compared to the conventionally used reference datasets, which can typically not be established for a specific growing season.

We demonstrate the extent of climate induced interannual variability in bulk dried tissue $\delta^{18}O$ values of strawberries that can be captured by using growing season-specific model input variables for all locations from which authentic reference samples were collected for in this study (Fig. 4). For this purpose, we simulated bulk dried tissue $\delta^{18}O$ values for strawberries for the three growing season months (May - July) for each of the 11 years from 2007 to 2017 (33 values per site) during which the reference samples were collected (see methods for the details of this model simulation). We then determined the maximum range of values in the resulting 11-year time series for each sampling location (Fig.4). The data show interannual variability in bulk dried tissue $\delta^{18}O$ values of strawberries of up to 4.10 ‰. Interestingly, the interannual variability in bulk dried tissue $\delta^{18}O$ values of strawberries shows distinct geographical patterns with lower variability in southern and mid-range latitudes, and higher variability in northern latitudes. The apparent latitudinal pattern in site-specific predicted ranges of $\delta^{18}O$ values was linear and statistically significant ($r^2 = 0.65$, $p < 0.001$). These distinct geographic

patterns are likely due to a higher seasonal climate variability in higher latitudes. Our analysis shows, that using growing season specific climatic input variables is increasingly important for the simulation of bulk dried tissue $\delta^{18}O$ values of fruit at higher latitudes. The widely used approach of comparing suspicious samples of annually growing agricultural products to reference data, often collected over several years, cannot resolve this uncertainty, although as a compromise solution for the classic reference dataset approach, multiple reference datasets might be built up over time for different months.

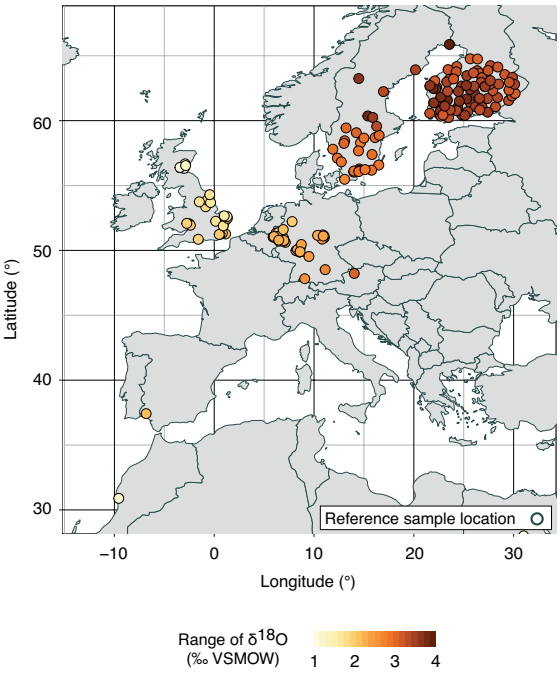

Figure 4: Map of Europe, showing locations where authentic reference samples were collected, and the range of predicted strawberry bulk dried tissue $\delta^{18}O$ values at each location for all growing season months (May to July), and years over which the sample set was collected (2007 – 2017). Predictions were made using the best berry-specific model (see text). The map was created using the software R, version 3.5.3 (https://www.r-project.org/).

Compared to climatic model input data, the temporal choice of precipitation and vapor $\delta^{18}O$ data is less important for an accurate simulation of the measured values. We show that for the best two parameterized models with the best timing of climate, any combination of precipitation and vapor oxygen isotope input, predicts the measured strawberry $\delta^{18}O$ bulk dried tissue values with an accuracy between RMSE values of 0.95 ‰ and 0.96 ‰, to 1.17 ‰ and 1.20 ‰, respectively (Fig. 2 g and i). Studies that have assessed the seasonal pattern of precipitation, soil and plant source water $\delta^{18}O$ values, have also identified lags time between precipitation and the source water $\delta^{18}O$ values of plants. It has been shown that plants use water precipitated during and, mainly for trees, prior to the growing season [51,54,55]. Our results imply that source water for strawberries integrates precipitation events before and during the berry growth, and that the model is robust to variation in precipitation and vapor $\delta^{18}O$ input data between years so that possible anomalies will not strongly influence the model's prediction power.

It is important to note that next to the quality and timing of the model input data, precise claims about the suspicious plant sample's location of origin and picking date are required for the type of specific origin analysis that our approach facilitates. In case of using the berry-specific model input parameters, a one-month error in the metadata, would reduce the model prediction power through use of misassigned input data, resulting in a 0.33 ‰ larger RMSE. Moreover, it should also be mentioned, that the model application discussed here was developed for strawberries grown in open field conditions, rather than in greenhouses. Thus, for a successful application of the model, metadata verifying the natural growing conditions of a suspicious sample is crucial.

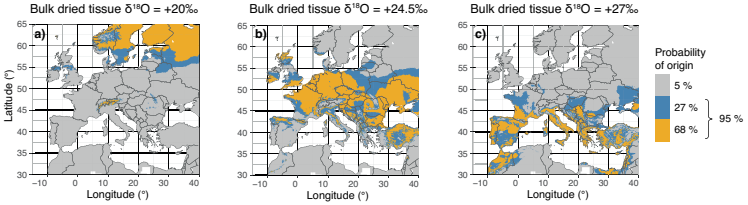

Figure 5: Prediction maps of three strawberry samples of unknown origin collected in July 2017. The prediction model is based on the best berry-specific model (Fig. 3) and shows the probability of origin (higher than 32 % in yellow, 5 % to 32 % in blue, and lower than 5 % grey). Bulk dried tissue $\delta^{18}O$ value of sample: **a)** +20 ‰ (mean Finish/Swedish sample), **b)** +24.5 ‰ (mean German sample), and **c)** +27 ‰ (mean southern European sample). Prediction maps were calculated by subtracting the $\delta^{18}O$ values of the bulk dried tissue of the suspected sample from the mapped results of the best berry-specific model. This resulted in a map showing the places that are predicted to have the same $\delta^{18}O$ values as the sample as a value of zero. The bigger the difference shown on the map, the lower the probability of provenance of the sample. Based on the prediction error of the best berry-specific model (RMSE = 0.96 ‰), the one sigma (68 %, yellow) and two sigma (95 %, yellow and blue) confidence intervals around the areas showing no difference to the $\delta^{18}O$ value of the suspected sample can be shown. The three maps were created using the software R, version 3.5.3 (https://www.r-project.org/).

To illustrate the power of the Craig-Gordon-derived plant physiological isotope model to predict the origin of an unknown sample for a given growing season, we produced prediction maps for $\delta^{18}O$ values of bulk dried tissue from three example strawberries collected in July 2017 using the best average berry model. This type of prediction map is the main product of interest for the food forensic industry because it shows all regions of possible origin of a sample of unknown provenance. The simulations show that samples from northern Europe, central Europe, and southern Europe can be clearly distinguished (Fig. 5). The assignment maps also showed that geographic regions can be distinguished within many individual countries. For example, small parts of mid-western Germany (Cologne Area) and south-western France showed similar $\delta^{18}O$ values as southern European samples (Fig. 5c).

In our study we demonstrated how plant physiological stable oxygen isotope models can produce temporally resolved, accurate, and precise region-of-origin assignments for agricultural food products. The applicability of model-based region-of-origin assignments for agricultural plant products will add several benefits for the isotope-based detection of food fraud. One major

benefit is that the model is robust and does not necessarily require a species-specific parameterization. With this, the model can be applied not only to strawberries as we show as an example here but also to other agricultural plant products or regions of the world with little change in the model parameters. This guarantees that the model can be rapidly applied to constrain the geographic origin of any type of agricultural plant product, although some degree of validation work with authentic samples would still be advisable.

Another major benefit of the model is the option to simulate year- and season-specific $\delta^{18}O$ values of a target plant product and to account as such for the potentially large temporal variability in such samples. This is often not possible when conventional reference isotope datasets are employed for origin validation. Finally, the modeling approach we present has the ability to identify all possible locations of provenance, without the need for spatially and temporally extensive reference samples across the entire potential region of origin. As such, it can also be used as a primary tool to efficiently acquire knowledge of all possible regions of origin of a suspicious sample, and in so doing provide specific advice about where to best collect new and/or additional reference samples.

Although predictions based on modeled $\delta^{18}O$ values alone are clearly not accurate enough to define the exact growth region, they are a marked improvement and complement to using a reference sample-based approach. When combined with other techniques, such as stable isotope analyses of hydrogen, nitrogen, carbon, or sulfur, which also show distinct geographical patterns depending on underlying bedrock/mineralogy or agricultural practice and have routinely been used in origin determination [11,56], and together with other authentication methods like e.g. proteomics or trace element analysis [10], the possible regions of origin may be even further constrained. These techniques can also be further refined by masking regions where a given agricultural plant product cannot be or is known not to grow. Our study therefore shows that using product independent input data (climate and precipitation stable isotope values), plant physiological isotope models offer a new and powerful tool that can help to advance the use of stable isotopes to counter food fraud.

Methods

Independent reference samples

The authentic, independent strawberry (*Fragaria* × *ananassa*) reference samples used for model validation in this study were provided by Agroisolab GmbH (Jülich, Germany). The samples were collected either directly by the company or on their behalf through authorized sample collectors between 2007 and 2017. The primary purpose of such authentic reference samples is the direct comparison between their stable isotope compositions (oxygen, hydrogen, carbon, nitrogen, or sulfur) to those of samples of suspect origin. Accompanying metadata for each reference sample included information about the geographic origin as community name, postal code, or location coordinates, and information about the month and year the strawberry sample was picked. In total, we used $\delta^{18}O$ values from 154 reference samples. Most samples were collected in the UK, Germany, Sweden, and Finland (Fig. 1). All reference samples were grown on open strawberry-fields rather than artificial greenhouse conditions. All berry samples were collected from cultivated, non-endangered plant species ("garden strawberry"), and the research conducted complies with all relevant institutional, the corresponding national, and also international guidelines and legislation.

After collection in the field, samples were stored in airtight containers and shipped directly to Agroisolab, where they were stored frozen prior to analysis. In order to analyze the oxygen stable isotope composition of the organic strawberry tissue, the lipids were solvent-extracted with dichloromethane for a at least 4h, using a Soxhlet extractor. The remaining samples were dried and milled to a fine powder. 1.5 mg of the powder was weighed into silver capsules. The silver capsules were equilibrated for at least 12 hours in a desiccator with a fixed relative humidity of 11.3 %. After a further vacuum drying the samples were measured via high-temperature furnace (Hekatech, Wegberg, Germany) in combination with an Isotope-ratio mass spectrometer (IRMS) Horizon (NU Instruments, Wrexham, UK). The pyrolysis temperature was 1530°C and the pyrolysis tube consisted of covalent-bound SiC (Agroisolab patented). The reproducibility of the measurement was better than 0.6 ‰.

Oxygen isotope model calculation

Plant physiological stable isotope models simulate the oxygen isotopic composition of leaf water or organic compounds synthesized therein as $\delta^{18}O$

values in per mil (‰), where $\delta^{18}O = (^{18}O/^{16}O)_{sample}/(^{18}O/^{16}O)_{VSMOW} - 1$, and VSMOW is Vienna Standard Mean Ocean Water as defined by the VSMOW-Standard Light Antarctic Precipitation (SLAP) scale. The Craig-Gordon model [57], which was developed to mathematically describe the isotopic enrichment of standing water bodies during evaporation and later modified for plants, is the basis for modelling plant water $\delta^{18}O$ values [23,58]. Plant source water is the baseline for the model, which is the precipitation-derived soil water that plants take up through their roots without isotope fractionation [51,59,60]. The ^{18}O enrichment of water within leaves is described by the following equation (Eqn. 1) [36,61]:

Equation 1: $\Delta^{18}O_{e\ leaf} = (1 + \varepsilon^{+}) [(1 + \varepsilon_k) (1 - e_a/e_i) + e_a/e_i (1 + \Delta^{18}O_{Vapor})] - 1$

where $\Delta^{18}O_{e\_leaf}$ is the oxygen isotopic enrichment above source of water at the evaporative site in leaves, ε^{+} is the equilibrium fractionation between liquid water and water vapor, ε_k is the kinetic fractionation associated with the diffusion through the stomata and the boundary layer. e_a/e_i is the ratio of ambient vapor pressure in the atmosphere to intercellular vapor pressure in the leaf. $\Delta^{18}O_{Vapor}$ is the isotopic composition of the ambient vapor above source water, which in this study is assumed to be in equilibrium with the source water ($\Delta^{18}O_V = - \varepsilon^{+}$) [62,63]. This assumption can be used, if the atmosphere is well mixed, and plants' source water derives from recent precipitation events. For crops, growing in the temperate climate of the mid latitudes this is usually the case, especially over the long time periods (several weeks) over which strawberries grow. If such a model is applied in other climatic zones (e.g. tropics), this assumption should, however, be reevaluated [64]. The equilibrium fractionation factor (ε^{+}) [65,66] and kinetic fractionation factor (ε_k) [67] can be calculated with the following equations (Eqn. 2 and Eqn. 3):

Equation 2:

$$\varepsilon^{+} = \left[\exp\left(\frac{1.137}{(273+T)^2} * 10^3 - \frac{0.4156}{273-T} - 2.0667 * 10^{-3}\right) - 1\right] * 1000$$

Where T is the leaf temperature in degrees Celsius. In our calculations, leaf temperature was set to 90 % of the monthly mean air temperature, which

describes a realistic leaf-energy balance scenario for well-watered crops [68,69], and also yielded the best model performance with respect to the reference data. As leaf to air temperature differences have a strong influence on leaf water $\delta^{18}O$ values, this assumption needs to be independently tested in future applications. For example, changing leaf temperature from 20°C to 22°C at a constant air temperature of 20°C and a source water $\delta^{18}O$ value of -10 ‰ will affect leaf water $\delta^{18}O$ values by +1.4 ‰.

Equation 3:

$$\varepsilon_k = \frac{28r_s + 19r_b}{r_s + r_b}$$

where r_s is the stomatal resistance and r_b is the boundary layer resistance in $m^2s/mmol$, which is the inverse of the stomatal and boundary layer conductance. For our model calculations, we consistently used stomatal conductance values of 0.4 mol/m^2s, stomatal resistance values of 1 m^2s/mol [70].

The Craig-Gordon model predicted leaf water values are often enriched in ^{18}O relative to measured bulk leaf water $\delta^{18}O$ values [26,27]. This is because the model describes the $\delta^{18}O$ values of water at the site of evaporation while measurements typically give bulk leaf water $\delta^{18}O$ values [36,71]. The two-pool modification to the Craig-Gordon model corrects for this effect by separating bulk leaf water into a pool of evaporatively enriched water at the site of evaporation ($\delta^{18}O_{e\_leaf}$ derived from the Craig-Gordon model, Eqn. 1) and a pool of unenriched plant source water ($\delta^{18}O_{source\ water}$) [25]. $\delta^{18}O_{e\_leaf}$ is calculated as follows:

Equation 4:

$$\delta^{18}O_{e\_leaf} = (\Delta^{18}O_{e\_leaf} + \delta^{18}O_{source\ water}) + (\Delta^{18}O_{e\_leaf} * \delta^{18}O_{source\ water})/1000).$$

In the two-pool modified Craig-Gordon model (Eqn. 5), the proportion of unenriched source water is described as f_{xylem} [36].

Equation 5:

$$\delta^{18}O_{leaf\ water} = (1 - f_{xylem}) * \delta^{18}O_{e\_leaf} + (f_{xylem} * \delta^{18}O_{source\ water})$$

Values for f_{xylem} in leaf water generally range from 0.10 to 0.33 [36–40] but higher values have also been observed [72]. For strawberry plants, leaf water f_{xylem} values were recently shown to vary between 0.24 and 0.34 [28].

Organic molecules in leaves generally reflect the $\delta^{18}O$ values of the bulk leaf water plus additional isotopic effects occurring during the assimilation of carbohydrates and post-photosynthetic processes [21,22,34]. The fractionations occur when carbonyl-group oxygen exchanges with leaf tissue water during the primary assimilation of carbohydrates (trioses and hexoses) [42]. This process causes ^{18}O enrichment, described as ε_{wc} [42], and has been determined to be ~ +27 ‰ [21,22,73].

During the synthesis of cellulose from primary assimilates, sucrose molecules are broken down to glucose and re-joined, allowing some of the carbonyl group oxygen to further exchange with water in the developing cell. The isotopic fractionation (ε_{wc}) during this process is assumed to be the same as in the carbonyl oxygen exchange during primary carbohydrate assimilation (~ +27 ‰) [41,42]. During the formation of cellulose, the $\delta^{18}O$ values of the primary assimilates are thus partially modified by the water in the developing cell [33]. Eqn. 6 describes this process [34]

Equation 6:

$$\delta^{18}O_{cellulose} = p_x p_{ex} *(\delta^{18}O_{source\ water} + \varepsilon_{wc}) + (1 - p_x p_{ex}) * (\delta^{18}O_{leaf\ water} + \varepsilon_{wc})$$

where $\delta^{18}O_{cellulose}$ is the oxygen isotopic composition of cellulose, p_{ex} is the fraction of carbonyl oxygen in cellulose that exchanges with the medium water during synthesis, and p_x is the proportion of unenriched source water in the bulk water of the cell where cellulose is synthesized [33]. Bulk water in developing cells where cellulose is synthesized, i.e. in the leaf growth-and-differentiation zone, has been found to primarily reflect the isotope composition of source water [43]. Therefore, p_x in equation 6 is likely larger than f_{xylem} in equation 5. For practical reasons, the parameters p_x or p_{ex} are typically not determined individually, but as the combined parameter $p_x p_{ex}$ [45]. For cellulose in leaves of grasses, crops, and trees $p_x p_{ex}$ has been found to range from 0.25 to 0.54 [45–49].

In this study as in many applied examples where plant $\delta^{18}O$ values are used for origin analysis we attempt to simulate the $\delta^{18}O$ values of dried bulk tissue. Bulk dried plant tissue ($\delta^{18}O_{bulk}$) contains in addition to carbohydrates compounds such as lignin, lipids, and proteins, which can be ^{18}O-depleted compared to carbohydrates [50]. Since this needs to be accounted for in the model, we included the parameter c into the model. As $p_x p_{ex}$ and c cannot be determined separately they are used as a combined model parameter in our approach $p_x p_{ex} c$:

Equation 7:

$$\delta^{18}O_{bulk} = p_x p_{ex} c * (\delta^{18}O_{source\ water} + \varepsilon_{wc}) + (1 - p_x p_{ex} c) * (\delta^{18}O_{leaf\ water} + \varepsilon_{wc})$$

Bulk dried tissue $\delta^{18}O$ values of strawberries in Cueni et al. (in review) did not differ statistically from pure cellulose $\delta^{18}O$ values in strawberries. Consequently, $p_x p_{ex}$ and $p_x p_{ex} c$ are identical for strawberries and ranges from 0.41 to 0.51. This approach allows the calculation of bulk dried tissue $\delta^{18}O$ values without the knowledge of cellulose $\delta^{18}O$ values, which is the case for the data set used in this study, and contrasts to the approach by Barbour & Farquhar (2000), where bulk dried tissue $\delta^{18}O$ values are assessed by an offset (ε_{cp}) to the cellulose $\delta^{18}O$ values.

Model parameter selection

To find the best values of the key model parameters for the prediction of strawberry bulk dried tissue $\delta^{18}O$ values, we used different combinations of the values for the parameters. Specifically, we compared average parameter values from the literature that were derived from leaves and parameter values that were specifically derived for berries (Cueni et al. in review) to test if a leaf-level parameterization of the model is sufficient or if a berry-specific parameterization is necessary for producing satisfying model prediction. These values were either (i) f_{xylem} and $p_x p_{ex}$ values reported in literature for leaf water and cellulose from various species that were averaged, (ii) values averaged for leaves (f_{xylem}) and berries ($p_x p_{ex} c$) of berry producing plants, or (iii) values for leaves (f_{xylem}) and berries ($p_x p_{ex} c$) specifically obtained for strawberry plants. For the general leaf-derived parameter values we used mean literature values originally obtained for leaf water and leaf cellulose $\delta^{18}O$ for different species and averaged these values (0.22 for f_{xylem} [36–40] and

0.40 for $p_x p_{ex}$ [45–49]) (Table 1). For berries (average of the values of raspberries and strawberries) the mean leaf-derived f_{xylem} value was 0.26 and the value for $p_x p_{ex}c$ was determined to be 0.46 (Table 1) (data derived from Cueni et al. in review). For strawberry plants, the leaf-derived f_{xylem} value we used was 0.30, and the value for bulk dried tissue ($p_x p_{ex}c$) was determined to be 0.46 (Table 1) (data derived from Cueni et al. in review). Since the $p_x p_{ex}c$ values of different berry species did not differ, this resulted in a total of six different model input parameter combinations.

Table 1: Values of the model parameters (f_{xylem} and $p_x p_{ex}$ / $p_x p_{ex}c$) used for the simulations of strawberry bulk dried tissue $\delta^{18}O$ values.

	f_{xylem}	$p_x p_{ex}$ / $p_x p_{ex}c$
General	0.22	0.40
Berry	0.26	0.46
Strawberry	0.30	0.46

Environmental model input data selection

In order to apply the strawberry parametrized bulk dried tissue oxygen model on a spatial scale, spatially gridded climate and precipitation isotope data layers were used as model inputs. The accurate simulation of geographically distinct $\delta^{18}O$ values, however, requires the use of the most appropriate and best available input variables. We therefore tested the importance of the temporal averaging and lead time of the input data relative to the picking date of the berry. We defined these collectively as the "integration time" of the input data. Climate of the growing season [46,53], and precipitation $\delta^{18}O$ values of rain-events prior and during the growing season [51,54,55] have been shown to shape plant tissue water and organic compound $\delta^{18}O$ values. The major objective of our study was thus a careful evaluation of the most appropriate type and integration time of model input variables needed for this kind of model simulation. Moreover, to find the best data source provided, we also used several different spatial climate and precipitation isotope datasets in our evaluations (Table 2).

Table 2: a) Table showing the different climatic (air temperature and vapor pressure) and isotope (precipitation and vapor $\delta^{18}O$) data products, b) as well as the different integration times and names used in the study used to simulate strawberry bulk dried tissue $\delta^{18}O$ values.

a) Data products	
Input variable	**Data product sources**
Climate (Air temperature, vapor pressure/ RH)	CRU, E-OBS
$\delta^{18}O$-precipitation	OIPC, Piso.AI
$\delta^{18}O$-vapor	OIPC, Piso.AI
b) Integration times	
Name	**Explanation**
At month of sampling	Value of the variable from the month of sample collection
One month before sampling	Value of the variable from one month prior to sample collection
Two months before sampling	Value of the variable from two months prior to sample collection
Three months before sampling	Value of the variable from three months prior to sample collection
Four months before sampling	Value of the variable from four months prior to sample collection
Mean three months before sampling	Average value of the variable from the three months prior to sample collection (precipitation and vapor $d^{18}O$ values are amount-weighted using CRU precipitation totals)
11-year May to July mean	Average value of the variable from the growing season (May to July) averaged over the 11-year period from which samples used in this study were collected
Yearly May to July mean	Average value of the variable from the growing season (May to July) of sample collection

Two precipitation isotope data products were compared (Table 2): (1) The mean monthly precipitation $\delta^{18}O$ grids by Bowen (2020), which are updated versions of the grids produced by Bowen and Revenaugh (2003) and Bowen et al. (2005) (Online Isotopes in Precipitation Calculator, OIPC Version 3.2). They provide global grids of monthly long-term mean precipitation isotope values. The resolution of these global grids is 5'. (2) Precipitation isotope predictions from Piso.AI (Version 1.01) [32]. This source provides values for individual months and years based on station coordinates[32]. Both data sets were on the one hand used for the precipitation $\delta^{18}O$ input data of the model, and also to extrapolate the vapor $\delta^{18}O$ values from sets (see model description above), which we treated as two individual, independent input data sets.

For the climatic drivers of the model (air temperature and vapor pressure), we used the gridded data products from the Climatic Research Unit (CRU) (TS Version 4.04) [29] and the E-OBS gridded dataset by the European Climate Assessment & Dataset (Version 22.0e) [30] (Table 2). The CRU dataset provided global gridded monthly mean air temperature, and mean vapor pressure with a resolution of 0.5°. The E-OBS dataset included European daily mean air temperature and relative humidity gridded data, with a resolution of 0.1 arc-degrees. We calculated monthly mean air temperature and relative humidity grid layers, on the basis of these daily mean air temperature and relative humidity grids, respectively.

Fruit tissue formation takes place over a period of several weeks leading up to picking date [46,53]. This results in a lead time between the date that best represents the mean climate conditions, and source water and vapor stable isotope signal influencing the isotope signal during tissue formation, and the picking date. As integration time of the input data, we therefore investigated lead times of 1, 2, 3, and 4 months, as well as the three months leading up to the picking date (Table 2). Moreover we also used more general European strawberry growing season averages [76], independent of either the sampling month (yearly May to July mean) or the sampling year (2007 to 2017 May to July mean) (Table 2). Precipitation isotope data means were calculated as amount-weighted averages using CRU mean monthly precipitation data. This means that the long term mean precipitation $\delta^{18}O$ values taken from OIPC were weighted by yearly specific CRU monthly precipitation totals for the case of the three months or growing season averages for individual years, and by average monthly precipitation totals (May, June, and July) from 2007 to 2017 for the long-term growing season calculation. The same assessment was also made using precipitation values from Piso.AI.

Validation of model with reference samples

Using the plant physiological model described above, we calculated the strawberry bulk dried tissue $\delta^{18}O$ values for the location and the growing time of each authentic reference sample. For the model input data, we tested variable combinations using each of the eight integration times described in table 2, along with all combinations of the data sources outlined in table 2. This resulted in a total of 65,536 combinations of input variables per model parameter combination (f_{xylem} and $p_x p_{ex}$ / $p_x p_{ex} c$, Table 1), yielding model

results to be evaluated against the measured reference samples. Our approach can be described with the following equation:

Equation 8: $\delta^{18}O$ plant = *f* (air temp(s,t), relative humidity(s,t), $\delta^{18}O$ precip.(s,t), $\delta^{18}O$ vapor (s,t))

Where $\delta^{18}O$ plant is the simulated $\delta^{18}O$ value of the strawberry, s is the data product for the specified input variable (Table 2), and t is the integration time of the specified variable (Table 2).

For the crucial model parameters f_{xylem} and $p_x p_{ex}$ / $p_x p_{ex}c$ we on the one hand used the values proposed for leaves by literature (for $p_x p_{ex}$), and on the other hand average of the values of raspberries and strawberries and strawberry-specific values determined from Cueni et al. (in review) (for $p_x p_{ex}c$). In all calculations an ε_{wc} value of +27 ‰ was used. To calculate mean monthly relative humidity values from the provided CRU vapor pressure data, site specific elevation was extracted from the ETOPO1 digital elevation model [77], and used to calculate the approximate atmospheric pressure. These values were then used in combination with air temperature to calculate the saturation vapor pressure after Buck (1981), in order to assess relative humidity (relative humidity = vapor pressure / saturation vapor pressure). The R-script of the model is available on "figshare", find the URL in the data availability statement.

Statistical analyses

Statistical analyses were done using the statistical package R version 3.5.3 [79]. The relationships of the range $\delta^{18}O$ values observed with latitude, and between CRU and E-OBS mean air temperature were compared with a linear regression model, and with an alpha level that was set to $\alpha = 0.05$. The results of the 65,536 models for each of the six physiological parameter combinations were compared with the measured $\delta^{18}O$ bulk dried tissue values of the authentic reference samples (n = 154) by calculation of the root mean squared error (RMSE).

Calculation of prediction maps

Prediction maps showing the regions of possible origin of a sample with unknown provenance are the product that is of interest in the food forensic industry. We calculated the prediction maps shown in Fig. 5 for three example

$\delta^{18}O$ values of strawberries collected in July 2017: (i) +20 ‰ representing a mean Finish/Swedish sample, (ii) +24.5 ‰ representing a mean German sample, and (iii) +27 ‰ representing a mean southern European sample.

The prediction maps were calculated in a two-step approach. First, we calculated a map of the expected strawberry bulk dried tissue $\delta^{18}O$ values of berries grown in July 2017. For this we used the average berry model input parameters (f_{xylem} and $p_x p_{ex} c$, Table 1), and the best fitting model input data and integration time combination, which we assessed beforehand (Fig. 2). We thus used CRU mean air temperature and vapor pressure from June 2017, precipitation $\delta^{18}O$ values from OIPC as an average from April, May and June, and vapor $\delta^{18}O$ values calculated from OIPC precipitation $\delta^{18}O$ values from April. Since using spatial maps as model input data, this calculation resulted in a mapped model result. In a second step, we calculated the prediction maps. For this we first subtracted the $\delta^{18}O$ value of the bulk dried tissue of the sample strawberry from the mapped result of the best berry-specific model. This was done for each pixel value of the map. This resulted in a map showing the difference of the sample $\delta^{18}O$ value and the predicted map $\delta^{18}O$ value for each pixel of the map. The places (pixels) that are predicted to have the same $\delta^{18}O$ value as the sample strawberry thus are represented by a value of zero. Based on the prediction error of the best berry-specific model (RMSE = 0.96 ‰), the one sigma (68 %) and two sigma (95 %) confidence intervals around the areas showing no difference to the $\delta^{18}O$ value of the suspected sample could be assessed. This means that the bigger the difference between the simulated $\delta^{18}O$ value and the sample value, the lower the probability of provenance of the sample. In other words, a difference between the sample's $\delta^{18}O$ value and the predicted $\delta^{18}O$ value of 0 ‰ to ± 0.96 ‰ equals a possible provenance of at least 68% (one sigma), and a difference between ± 0.96 ‰ and ± 1.92 ‰ reflects a possible provenance between 68% and 27 % (two sigma). Regions on the map with bigger differences than ± 1.92 ‰ represent regions of possible provenance, lower than 5 % (bigger than two sigma).

Data availability

The data that support the findings of this study are available as supplementary information of this publication and on "figshare" (dx.doi.org/10.6084/m9.figshare.15049260).

References

1. Spink, J. & Moyer, D. C. Defining the Public Health Threat of Food Fraud. *J. Food Sci.* **76**, (2011).
2. van Ruth, S. M., Huisman, W. & Luning, P. A. Food fraud vulnerability and its key factors. *Trends Food Sci. Technol.* **67**, 70–75 (2017).
3. European Commission. Agri-food fraud. *Agri-food fraud* (2018). Available at: https://ec.europa.eu/food/safety/food-fraud_en.
4. Johnson, R. Food fraud and "Economically motivated adulteration" of food and food ingredients. *Food Fraud Adulterated Ingredients Background, Issues, Fed. Action* 1–56 (2014).
5. Manning, L. Food fraud: policy and food chain. *Curr. Opin. Food Sci.* **10**, 16–21 (2016).
6. PwC & SSAFE. Food fraud vulnerability assessment. (2016).
7. European Commission. *RASFF: The Rapid Alert System for Food and Feed 2018 Annual Report*. (2019).
8. Tähkäpää, S., Maijala, R., Korkeala, H. & Nevas, M. Patterns of food frauds and adulterations reported in the EU rapid alarm system for food and feed and in Finland. *Food Control* **47**, 175–184 (2015).
9. Dasenaki, M. E. & Thomaidis, N. S. *Quality and authenticity control of fruit juices-a review*. *Molecules* **24**, (2019).
10. Danezis, G. P., Tsagkaris, A. S., Camin, F., Brusic, V. & Georgiou, C. A. Food authentication: Techniques, trends & emerging approaches. *TrAC - Trends Anal. Chem.* **85**, 123–132 (2016).
11. Camin, F. *et al.* Stable isotope techniques for verifying the declared geographical origin of food in legal cases. *Trends Food Sci. Technol.* (2017). doi:10.1016/j.tifs.2016.12.007
12. Rossmann, A. Determination of Stable Isotope Ratios in Food Analysis. *Food Rev. Int.* **9129**, (2001).
13. Rossmann, A. *et al.* Stable carbon isotope content in ethanol of EC data bank wines from Italy, France and Germany. *Z. Lebensm. Unters. Forsch.* **203**, 293–301 (1996).
14. Gonzalvez, A., Armenta, S. & de la Guardia, M. Trace-element composition and stable-isotope ratio for discrimination of foods with Protected Designation of Origin. *TrAC - Trends Anal. Chem.* **28**, 1295–1311 (2009).
15. Dansgaard, W. Stable isotopes in precipitation. *Tellus* **2826**, 436–468 (1964).

16. Bowen, G. J. Isoscapes: Spatial Pattern in Isotopic Biogeochemistry. *Annu. Rev. Earth Planet. Sci.* **38**, 161–187 (2010).
17. Krouse, H. R. Sulfur Isotope Studies of the Pedosphere and Biosphere. in *Stable Isotopes in Ecological Research* (eds. Rundel, P. W., Ehleringer, J. R. & Nagy, K. A.) 424–444 (Springer, 1989). doi:10.1007/978-1-4612-3498-2_24
18. Bateman, A. S., Kelly, S. D. & Woolfe, M. Nitrogen Isotope Composition of Organically and Conventionally Grown Crops. *J. Agric. Food Chem.* 2664–2670 (2007).
19. Carter, J. F. & Chesson, L. A. *Food Forensics: Stable Isotopes as a Guide to Authenticity and Origin*. *Food Forensics* (CRC Press, 2017). doi:10.1201/9781315151649
20. Epstein, S., Thompson, P. & Ya, C. J. Oxygen and Hydrogen Isotopic Ratios in Plant Cellulose. *Science (80-.).* **198**, (1977).
21. Yakir, D. & DeNiro, M. J. Oxygen and Hydrogen Isotope Fractionation during Cellulose Metabolism in Lemna gibba L. *Plant Physiol.* **93**, 325–332 (1990).
22. Sternberg, L., DeNiro, M. J. & Savidge, R. A. Oxygen Isotope Exchange between Metabolites and Water during Biochemical Reactions Leading to Cellulose Synthesis. *Plant Physiol.* **82**, 423–427 (1986).
23. Farquhar, G. D. & Lloyd, J. Carbon and oxygen isotope effects in the exchange of carbon dioxide between terrestrial plants and the atmosphere. *Stable Isot. Plant Carbon-water Relations* 47–70 (1993). doi:10.1016/B978-0-08-091801-3.50011-8
24. Roden, J. S., Lin, G. & Ehleringer, J. R. A mechanistic model for interpretation of hydrogen and oxygen isotope ratios in tree-ring cellulose. *Geochim. Cosmochim. Acta* **64**, 21–35 (1999).
25. Yakir, D., DeNiro, M. J. & Gat, J. R. Natural deuterium and oxygen-18 enrichment in leaf water of cotton plants grown under wet and dry conditions: evidence for water compartmentation and its dynamics. *Plant Cell Environ.* **13**, 49–56 (1990).
26. Cernusak, L. A., Farquhar, G. D. & Pate, J. S. Environmental and physiological controls over oxygen and carbon isotope composition of Tasmanian blue gum, Eucalyptus globulus. *Tree Physiol.* **25**, 129–146 (2005).
27. Kahmen, A. *et al.* Effects of environmental parameters, leaf

physiological properties and leaf water relations on leaf water δ18O enrichment in different Eucalyptus species. *Plant Cell Environ.* **31**, 738–751 (2008).

28. Cueni, F., Nelson, D. B., Lehmann, M. M., Boner, M. & Kahmen, A. Constraining parameter uncertainty for predicting oxygen and hydrogen isotope values in fruit. *J. Exp. Bot.*
29. Harris, I., Osborn, T. J., Jones, P. & Lister, D. Version 4 of the CRU TS monthly high-resolution gridded multivariate climate dataset. *Sci. Data* **7**, 1–18 (2020).
30. Cornes, R. C., van der Schrier, G., van den Besselaar, E. J. M. & Jones, P. D. An Ensemble Version of the E-OBS Temperature and Precipitation Data Sets. *J. Geophys. Res. Atmos.* **123**, 9391–9409 (2018).
31. Bowen, G. J. Gridded maps of the isotopic composition of meteoric waters. (2020). Available at: http://www.waterisotopes.org. (Accessed: 1st March 2020)
32. Nelson, D. B., Basler, D. & Kahmen, A. Precipitation isotope time series predictions from machine learning applied in Europe. *PNAS* **118**, e2024107118 (2021).
33. Barbour, M. M. & Farquhar, G. D. Relative humidity- and ABA-induced variation in carbon and oxygen isotope ratios of cotton leaves. *Plant Cell Environ.* 473–485 (2000).
34. Roden, J. S. & Ehleringer, J. R. Hydrogen and oxygen isotope ratios of tree-ring cellulose for riparian trees grown long term under hydroponycally environments. *Oecologia* **121**, 467–477 (1999).
35. Cernusak, L. A. & Kahmen, A. The multifaceted relationship between leaf water 18O enrichment and transpiration rate. *Plant Cell Environ.* 1239–1241 (2013). doi:10.1111/pce.12081
36. Flanagan, L. B., Comstock, J. P. & Ehieringer, J. R. Comparison of Modeled and Observed Environmental Influences on the Stable Oxygen and Hydrogen Isotope Composition of Leaf Water in Phaseolus vulgaris L . *Plant Physiol.* 588–596 (1991).
37. Cernusak, L. A., Wong, S. C. & Farquhar, G. D. Oxygen isotope composition of phloem sap in relation to leaf water in Ricinus communis. *Funct. Plant Biol.* **30**, 1059 (2003).
38. Allison, G. B. The relationship between deuterium and oxygen-18 delta values in leaf water. *Chem. Geol.* **58**, 145–156 (1985).

39. Walker, C. D., Leaney, F. W., Dighton, J. C. & Allison, C. S. The influence of transpiration on the equilibration of leaf water with atmospheric water vapour. *Plant Cell Environ.* 221–234 (1989).
40. Song, X., Loucos, K. E., Simonin, K. A., Farquhar, G. D. & Barbour, M. M. Measurements of transpiration isotopologues and leaf water to assess enrichment models in cotton. *New Phytol.* **1**, 637–646 (2015).
41. Farquhar, G. D., Cernusak, L. A. & Barnes, B. Heavy Water Fractionation during Transpiration. *Plant Physiol.* **143**, 11–18 (2007).
42. Sternberg, L. & DeNiro, M. Biogeochemical implications of the isotopic equilibrium fractionation factor between the oxygen atoms of acetone and water. *Geochim. Cosmochim. Acta* **47**, (1983).
43. Liu, H. T., Schäufle, R., Gong, X. Y. & Schnyder, H. The $\delta^{18}O$ and $\delta^{2}H$ of water in the leaf growth-and-differentiation zone of grasses is close to source water in both humid and dry atmospheres. *New Phytol.* 1423–1431 (2017). doi:10.1111/nph.14549
44. Sanchez-Bragado, R., Serret, M. D., Marimon, R. M., Bort, J. & Araus, J. L. The hydrogen isotope composition $\delta^{2}H$ reflects plant performance. *Plant Physiol.* **180**, 793–812 (2019).
45. Barbour, M. M., Roden, J. S., Farquhar, G. D., Ehleringer, J. R. & Farquhar, G. D. Expressing leaf water and cellulose oxygen isotope ratios as enrichment above source water reveals evidence of a Péclet effect. *Ecosyst. Ecol.* 426–435 (2004). doi:10.1007/s00442-003-1449-3
46. Barbour, M. M., Fischer, R. A., Sayre, K. D. & Farquhar, G. D. Oxygen isotope ratio of leaf and grain material correlates with stomatal conductance and grain yield in irrigated wheat. *Aust. J. Plant Physiol.* **27**, 625–637 (2000).
47. Helliker, B. R. & Ehleringer, J. R. Differential ^{18}O enrichment of leaf cellulose in C3 versus C4 grasses. *Funct. Plant Biol.* **29**, 435 (2002).
48. Cheesman, A. W. & Cernusak, L. A. Infidelity in the outback : climate signal recorded in $\Delta^{18}O$ of leaf but not branch cellulose of eucalypts across an Australian aridity gradient. *Tree Physiol.* 554–564 (2016). doi:10.1093/treephys/tpw121
49. Kahmen, A. *et al.* Cellulose $\delta^{18}O$ is an index of leaf-to-air vapor pressure difference (VPD) in tropical plants. *Proc. Natl. Acad. Sci.* **108**, 1981–1986 (2011).
50. Schmidt, H. L., Werner, R. A. & Roßmann, A. ^{18}O pattern and biosynthesis of natural plant products. *Phytochemistry* **58**, 9–32 (2001).

51. Brinkmann, N. *et al.* Employing stable isotopes to determine the residence times of soil water and the temporal origin of water taken up by *Fagus sylvatica* and *Picea abies* in a temperate forest. *New Phytol.* **219**, 1300–1313 (2018).
52. Kahmen, A., Buser, T., Hoch, G., Grun, G. & Dietrich, L. Dynamic ^{2}H irrigation pulse labelling reveals rapid infiltration and mixing of precipitation in the soil and species-specific water uptake depths of trees in a temperate forest. *Ecohydrology* 1–15 (2021). doi:10.1002/eco.2322
53. Barbour, M. M. Stable oxygen isotope composition of plant tissue: a review. *Funct. Plant Biol.* **34**, 83–94 (2007).
54. Prechsl, U. E., Burri, S., Gilgen, A. K., Kahmen, A. & Buchmann, N. No shift to a deeper water uptake depth in response to summer drought of two lowland and sub-alpine C3-grasslands in Switzerland. *Oecologia* **177**, 97–111 (2015).
55. Allen, S. T., Kirchner, J. W., Braun, S., Siegwolf, R. T. W. & Goldsmith, G. R. Seasonal origins of soil water used by trees. *Hydrol. Earth Syst. Sci.* 1199–1210 (2019).
56. Alegria, C., Antunes, C., Giovanetti, M., Abreu, M. & Máguas, C. Acorn Isotopic Composition: A New Promising Tool for Authenticity Maps of Montado's High-Value Food Products. *Molecules* **25**, 1535 (2020).
57. Craig, H. & Gordon, L. I. *Deuterium and oxygen 18 variations in the ocean and the marine atmosphere*. *Proceedings of the conference on stable isotopes in oceanographic studies and paleotemperatures. Piza, Italy: Laboratory of Geology and Nuclear Science* (1965).
58. Dongmann, G., Nürnberg, H. W., Förstel, H. & Wagener, K. On the Enrichment of $H_2{}^{18}O$ in the Leaves of Transpiring Plants. *Radiat. Environ. Biophys.* **11**, 41–52 (1974).
59. Dawson, T. E. & Ehleringer, J. R. Streamside trees that do not use stream water. *Nature* **350**, 335–337 (1991).
60. Newberry, S. L., Prechsl, U. E., Pace, M. & Kahmen, A. Tightly bound soil water introduces isotopic memory effects on mobile and extractable soil water pools on mobile and extractable soil water pools. *Isotopes Environ. Health Stud.* **6016**, (2017).
61. Flanagan, L. B. & Ehleringer, J. R. Stable isotope composition of stem and leaf water : applications to the study of plant water use. *Funct. Ecol.* **5**, 270–277 (1991).

62. Song, X., Barbour, M. M., Saurer, M. & Helliker, B. R. Examining the large-scale convergence of photosynthesis-weighted tree leaf temperatures through stable oxygen isotope analysis of multiple data sets. *New Phytol.* **192**, 912–924 (2011).
63. Brooks, J. R. & Coulombe, R. Physiological responses to fertilization recorded in tree rings: isotopic lessons from a long-term fertilization trial. *Ecol. Appl.* **19**, 1044–1060 (2009).
64. Welp, L. R. *et al.* δ18O of water vapour, evapotranspiration and the sites of leaf water evaporation in a soybean canopy. *Plant. Cell Environ.* **31**, 1214–1228 (2008).
65. Bottinga, Y. & Craig, H. Oxygen Isotope Fractionation Between CO_2 and Water, and the Isotopic Composition of Marina Atmospheric CO_2. *Earth Planet. Sci. Lett.* **5**, 285–295 (1969).
66. Majoube, M. Fractionnement en oxygène 18 et en deutérium entre l'eau et sa vapeur. *J. Chim. Phys.* **68**, 1423–1436 (1971).
67. Farquhar, G. D., Ehleringer, J. R. & Hubick, K. T. Carbon Isotope Discrimination and Photosynthesis. *Annu. Rev. Plant Physiol. Plant Mol. Biol.* **40**, 503–537 (1989).
68. Jackson, R. D., Idso, S. B., Reginato, R. J. & Pinter, P. J. Canopy temperature as a crop water stress indicator. *Water Resour. Res.* **17**, 1133–1138 (1981).
69. Jackson, R. D. Canopy Temperature and Crop Water Stress. in *Advances in Irrigation* **1**, 43–85 (ACADEMIC PRESS, INC., 1982).
70. Sachse, D., Kahmen, A. & Gleixner, G. Organic Geochemistry Significant seasonal variation in the hydrogen isotopic composition of leaf-wax lipids for two deciduous tree ecosystems (*Fagus sylvativa* and *Acer pseudoplatanus*). *Org. Geochem.* **40**, 732–742 (2009).
71. Yakir, D., Berry, J. A., Giles, L. & Osmond, C. B. Isotopic heterogeneity of water in transpiring ieaves : identification of the component that controls the δ18O of atmospheric O2 and CO2. *Plant Cell Environ.* **17**, 73–80 (1994).
72. Cernusak, L. A. *et al.* Stable isotopes in leaf water of terrestrial plants. *Plant Cell Environ.* 1087–1102 (2016). doi:10.1111/pce.12703
73. Yakir, D. Variations in the natural abundance of oxygen-18 and deuterium in plant carbohydrates. *Plant Cell Environ.* 1005–1020 (1992).
74. Bowen, G. J. & Revenaugh, J. Interpolating the isotopic composition of

modern meteoric precipitation. *Water Resour. Res.* **39**, 1–13 (2003).

75. Bowen, G. J., Wassenaar, L. I. & Hobson, K. A. Global application of stable hydrogen and oxygen isotopes to wildlife forensics. *Oecologia* **143**, 337–348 (2005).
76. Lieten, P. Strawberry Production in Central Europe. *Int. J. Fruit Sci.* **5**, 91–105 (2005).
77. NOAA. ETOPO1 Global Relief Model. *ETOPO1 is a 1 arc-minute global relief model of Earth's surface that integrates land topography and ocean bathymetry* (2020). Available at: https://www.ngdc.noaa.gov/mgg/global/. (Accessed: 1st March 2020)
78. Buck, A. L. New equations for computing vapour pressure and enhancement factor. *Journal of Applied Meteorology* **20**, 1527–1532 (1981).
79. R Core Team. R: A language and environment for statistical computing. *R Foundation for Statistical Computing, Vienna, Austria* (2019). Available at: https://www.r-project.org/.

Acknowledgements
We thank the editor for the opportunity to address the reviewers' comments, the numerous sample collectors who were responsible for collecting samples for the reference dataset over the last 13 years, and the Agroisolab team for the sample preparation and analysis. The present work was (i) supported by PlantHUB - European Industrial Doctorate funded by the European Commission's Horizon 2020 research and innovation program under the Marie Skłodowska-Curie grant agreement No 722338. The program is managed by the Zurich-Basel Plant Science Center. It was further supported by (ii) the ERC consolidator grant No 724750 - HYDROCARB, and (iii) by the "Freiwillige Akademische Gesellschaft Basel" (FAG).

Author Contributions
F.C., D.B.N., M.B. and A.K. designed the study. F.C. led the data analysis in collaboration with D.B.N. and A.K.. M.B. provided the reference dataset. F.C. wrote the initial draft of the paper. All authors revised and edited the paper.

Competing interests
The authors declare no competing interests.

Concluding discussion

The objective of my doctoral studies was to adapt a mechanistic, plant physiological oxygen and hydrogen stable isotope model, based on the Craig-Gordon model, for agricultural products. Thereby, the aim was to present a further, logistically simple and low-cost method, for predicting the geographic origin of agricultural products, using stable isotope analysis. However, since plant physiological models have yet only been parametrized for leaf water, and leaf and wood organic compounds (Allison 1985; Walker et al. 1989; Flanagan et al. 1991; Roden and Ehleringer 1999b; Barbour et al. 2000, 2004; Helliker and Ehleringer 2002; Kahmen et al. 2011; Song et al. 2015; Cheesman and Cernusak 2016), the application of plant physiological isotope models for origin analysis of agricultural products firstly requires an accurate model parameterization for such products. My co-authors and I therefore investigated the difference of the oxygen ($\delta^{18}O$) and hydrogen ($\delta^{2}H$) isotopic composition of tissue water and different organic compounds of agricultural products. This enabled us determine product specific values for the key model parameters f_{xylem}, which accounts for the fraction of unenriched source water in the leaf (Leaney et al. 1985; Yakir 1989), and $p_x p_{ex}$, and $f_H p_x$, which describe the fraction of oxygen or hydrogen, respectively, that exchange with source water during the synthesis of higher carbohydrates such as cellulose (Roden and Ehleringer 1999a; Barbour and Farquhar 2000). For the model parametrization, we grew raspberries and strawberries under controlled conditions at three different relative humidity treatments (Chapter 1), and used seven different European cereal species grown outside, in a common environment (Chapter 2). We further investigated the $\delta^{18}O$ and $\delta^{2}H$ values of different winter wheat varieties, in order to describe within species variability. (Chapter 3). Finally, we applied the newly parametrized strawberry-model to a spatial scale and determined the most suitable input variables needed for an accurate origin prediction using plant physiological stable isotope models, to be used in the food forensic industry (Chapter 4).

The results of the investigation of the tissue water $\delta^{18}O$ and $\delta^{2}H$ values of agricultural products, in our case of berries (Chapter 1) and cereals (Chapter 2), strikingly demonstrated that their values were generally higher than those of the plants' source water, but lower than the evaporatively enriched leaf water values of the same plants. These results are exciting, since

compared to leaves, berries and cereal grains only have few functional stomata (Barlow et al. 1980; Konarska 2013). Thus, their coupling to the atmosphere and thereby induced evaporative increase of the tissue water $\delta^{18}O$ and $\delta^{2}H$ values is strongly reduced to possible water loss across the cuticle, hardly explaining our results. Since our results, however, clearly showed that tissue water of berries and grains is influenced by evaporatively enriching conditions, we mainly attribute our finding to the fact that the ^{18}O and ^{2}H-enriched leaf water signal gets transferred into the developing berries and grains via the phloem. Since phloem sap originates from leaves, and to a great extent reflects ^{18}O and ^{2}H-enriched leaf water isotope values (Ho et al. 1987; Barbour and Farquhar 2000; Cernusak et al. 2005). However, since not as ^{18}O and ^{2}H-enriched as leaf water, but strongly dependent on its evaporatively driven enrichment, our results suggest that berry and cereal water can be treated as diluted bulk leaf water. Thus, the model parameter f_{xylem} is the key term that needs modification to adapt the two-pool modified Craig-Gordon model for berries and cereals, or agricultural products in general. Since accounting for a higher part of unenriched source water, diluting the leaf water signal, f_{xylem} was consistently higher for berries compared to leaves (Chapter 1).

Compared to the leaf water $\delta^{18}O$ and $\delta^{2}H$ values, the organic compounds investigated (sugars, cellulose, or bulk dried tissue) were always more enriched in ^{18}O, and more depleted in ^{2}H, independent of the organ and species (Chapters 1 to 3). The ^{18}O-enrichment of organic compounds compared to leaf water is caused by fractionation processes during the exchange of the carbonyl-group oxygen with cell water. These fractionations occur during the primary assimilation of sugars and during the synthesis of higher carbohydrates, and are ^{18}O-enriching (~ +27 ‰). (Sternberg and DeNiro 1983; Yakir and DeNiro 1990; Yakir 1992; Sternberg and Ellsworth 2011; Lehmann et al. 2017). The ^{2}H-depletion of organic compounds compared to the leaf tissue water $\delta^{2}H$ values can be explained by photosynthetic, and post-photosynthetic fractionation processes during carbohydrate assimilation and synthesis respectively, which have been shown to induce a ^{2}H-depletion of carbohydrates (Yakir and DeNiro 1990).

Most agricultural products are heterotrophic sink tissues and depend on sugars imported from the photosynthetic active leaves. These sugars carry the evaporation driven leaf water $\delta^{18}O$ and $\delta^{2}H$ values. We therefore found,

the organic material in berries but also cereal grains to generally reflect the leaf water $\delta^{18}O$ and $\delta^{2}H$ values, with additional variation due to post-photosynthetic fractionation processes (Chapter 1 to 3).

In the first chapter of the thesis, we detected that the $\delta^{18}O$ values of organic berry compounds, differed between the species and also compared to leaves. We showed that this is mainly reflecting differences related to the amount of carbonyl-oxygen that exchanges with cell water, either during sugar transport in the phloem or during carbohydrate synthesis in the berry. In strawberries this led to an increased exchange with source water, and thus lower $\delta^{18}O$ values in berries compared to leaves, reflected in the model parameter $f_o p_x$ (= $p_x p_{ex}$), that was generally higher for berries compared to leaves. For raspberries, on the other hand, this pattern was only found in the sugars, and cellulose and bulk dried tissue $\delta^{18}O$ values were enriched or similar to leaves, which hence led to similar or lower values of the model parameter $f_o p_x$ (= $p_x p_{ex}$) of berries in comparison to leaves (Chapter 1).

The bulk dried tissue $\delta^{18}O$ values of cereal grains were always higher compared to leaves, and also differed among species (Chapter 2). For one, we found that the among species variability is due to differences in carbohydrate synthesis, which is reflected in the model parameter $p_x p_{ex}$, generally differing among species. However, we also showed that $\delta^{18}O$ values of dried cereal grains are strongly influenced by the grain ripening time, and thus the different $\delta^{18}O$ values of source and leaf water pools used during grain carbohydrate synthesis (Chapter 2). Among different varieties within a single cereal species, in this study winter wheat, we, however, found the bulk dried grain $\delta^{18}O$ values to be very similar, implying biosynthetic processes (e.g. carbohydrate synthesis) to be evolutionary conserved within a species (Chapter 3).

The organic tissue $\delta^{2}H$ values in berries were always higher than the values in leaves, and generally the same between the berry species (Chapter 1). This pattern of sink tissues that are ^{2}H-enriched compared to the autotrophic source tissues is consistent with findings of previous studies, and is due to different post-photosynthetic processes in sink tissues, leading to an increased exchange of carbon-bound hydrogen with comparatively ^{2}H-enriched source water in these tissues (Ziegler 1989; Augusti et al. 2008; Newberry et al. 2015; Gebauer et al. 2016; Gamarra et al. 2016; Cormier et al. 2018). These differences between berries and leaves, required the model parameter $f_H p_x$ to be adapted for berries, with values that were generally higher

than for leaves, accounting for the increased amount of source water δ^2H signal present in sink tissue organic compounds (Chapter 1). As for oxygen, we also found the bulk dried grain δ^2H values to be very similar among the different winter wheat varieties, confirming a within species analogy of biosynthetic processes (Chapter 3).

The results of the empirical studies clearly showed that Craig-Gordon-derived isotope models originally developed for leaves and wood, can be parameterized to simulate the $\delta^{18}O$ and δ^2H values of agricultural products. Still, compared to leaves, and depending on species, the key model parameters f_{xylem}, $p_x p_{ex}$ ($=f_o p_x$), and $f_H p_x$ can significantly differ. Moreover, we also found that for an accurate simulation of the $\delta^{18}O$ and δ^2H values of agricultural products, the choice of growing time specific leaf and source water input $\delta^{18}O$ and δ^2H values is essential (Chapter 2). The RH-effects that we found to influence the model parameters of berries, however, have less impact on simulated values, especially in the range of the naturally occurring RH (Chapter 1).

Applying the model to spatial scale, we used the strawberry specific model parameters determined in chapter 1, and simulated strawberry bulk dried tissue $\delta^{18}O$ values across Europe. Comparing the results of several thousand model input data combinations, to 154 strawberry reference samples collected in Europe between 2007 and 2017, we found that model simulations using our newly defined berry-specific model parameters were superior to those using general leaf/wood parameters.

Our comparison also clearly demonstrated that using berry growing time specific climate model input variables (air temperature and vapor pressure), resulted in the best simulations. This showed the growing season climate is a major influence on the $\delta^{18}O$ values of plants' organic tissue (Barbour et al. 2000; Barbour 2007). Compared to the traditional application of reference data sets for origin analysis, this possibility to account for such seasonal climate changes, is one of the biggest benefits of using plant physiological stable isotope models in the field of food forensics. The model comparisons further showed that the timing of precipitation and vapor $\delta^{18}O$ data used for accurate simulations is less important. Our findings show that strawberries' source water is a mixture of rainwater precipitated in events several weeks prior and during the growing season, thus is not prone to short

time fluctuations in precipitation and vapor $\delta^{18}O$ values, which has also has been demonstrated in studies mainly on trees (Prechsl et al. 2015; Brinkmann et al. 2018; Allen et al. 2019).

In summary, the results of this thesis show, that mechanistic plant physiological stable isotope models offer a new, low-cost, and seasonally dynamic method to predict the origin of agricultural products. We are certain, that especially when combined with other techniques, such as stable isotope analyses of nitrogen, carbon, or sulfur (Camin et al. 2017), and other authentication methods (Danezis et al. 2016), there is a great potential in mechanistic, plant physiological stable isotope models to help to further advance the use of stable isotopes to counter food fraud.

References of the general introduction and the concluding discussion

Allen ST, Kirchner JW, Braun S, et al (2019) Seasonal origins of soil water used by trees. Hydrol Earth Syst Sci 1199–1210.

Allison GB (1985) The relationship between deuterium and oxygen-18 delta values in leaf water. Chem Geol 58:145–156.

Augusti A, Betson TR, Schleucher J (2008) Deriving correlated climate and physiological signals from deuterium isotopomers in tree rings. Chem Geol 252:1–8. doi: 10.1016/j.chemgeo.2008.01.011

Aung MM, Chang YS (2014) Traceability in a food supply chain: Safety and quality perspectives. Food Control 39:172–184. doi: 10.1016/j.foodcont.2013.11.007

Barbour MM (2007) Stable oxygen isotope composition of plant tissue: a review. Funct Plant Biol 34:83–94. doi: 10.1071/FP06228

Barbour MM, Farquhar GD (2000) Relative humidity- and ABA-induced variation in carbon and oxygen isotope ratios of cotton leaves. Plant, Cell Environ 473–485.

Barbour MM, Fischer RA, Sayre KD, Farquhar GD (2000) Oxygen isotope ratio of leaf and grain material correlates with stomatal conductance and grain yield in irrigated wheat. Aust J Plant Physiol 27:625–637. doi: 10.1071/PP99041

Barbour MM, Roden JS, Farquhar GD, et al (2004) Expressing leaf water and cellulose oxygen isotope ratios as enrichment above source water reveals evidence of a Péclet effect. Ecosyst Ecol 426–435. doi: 10.1007/s00442-003-1449-3

Barlow EWR, Lee JW, Munns R, Smart MG (1980) Water Relations of the Developing Wheat Grain. Aust J Plant Physiol 7:519–25. doi: 10.1071/PP9800519

Bateman AS, Kelly SD, Woolfe M (2007) Nitrogen Isotope Composition of Organically and Conventionally Grown Crops. J Agric Food Chem 2664–2670.

Bitzios M, Jack L, Krzyzaniak SA, Xu M (2017) Country-of-origin labelling, food traceability drivers and food fraud: Lessons from consumers' preferences and perceptions. Eur J Risk Regul 8:541–558. doi: 10.1017/err.2017.27

Bowen GJ (2010) Isoscapes: Spatial Pattern in Isotopic Biogeochemistry. Annu Rev Earth Planet Sci 38:161–187. doi: 10.1146/annurev-earth-

040809-152429

Brinkmann N, Seeger S, Weiler M, et al (2018) Employing stable isotopes to determine the residence times of soil water and the temporal origin of water taken up by *Fagus sylvatica* and *Picea abies* in a temperate forest. New Phytol 219:1300–1313. doi: 10.1111/nph.15255

Camin F, Archer ROL, Icolini GIN, et al (2010) Isotopic and Elemental Data for Tracing the Origin of European Olive Oils. J Agric Food Chem 570–577. doi: 10.1021/jf902814s

Camin F, Boner M, Bontempo L, et al (2017) Stable isotope techniques for verifying the declared geographical origin of food in legal cases. Trends Food Sci Technol. doi: 10.1016/j.tifs.2016.12.007

Carter JF, Chesson LA (2017) Food Forensics: Stable Isotopes as a Guide to Authenticity and Origin, 1st Editio. CRC Press, Boca Raton, FL

Cerling TE, Barnette JE, Bowen GJ, et al (2016) Forensic Stable Isotope Biogeochemistry. Annu Rev Earth Planet Sci 44:175–206. doi: 10.1146/annurev-earth-060115-012303

Cernusak LA, Farquhar GD, Pate JS (2005) Environmental and physiological controls over oxygen and carbon isotope composition of Tasmanian blue gum, Eucalyptus globulus. Tree Physiol 25:129–146. doi: 10.1093/treephys/25.2.129

Cheesman AW, Cernusak LA (2016) Infidelity in the outback : climate signal recorded in $\Delta^{18}O$ of leaf but not branch cellulose of eucalypts across an Australian aridity gradient. Tree Physiol 554–564. doi: 10.1093/treephys/tpw121

Chesson LA, Tipple BJ, Howa JD, et al (2014) Stable Isotopes in Forensics Applications, 2nd edn. Elsevier Ltd.

Chiocchini F, Portarena S, Ciolfi M, et al (2016) Isoscapes of carbon and oxygen stable isotope compositions in tracing authenticity and geographical origin of Italian extra-virgin olive oils. Food Chem 202:291–301. doi: 10.1016/j.foodchem.2016.01.146

Coplen TB (2011) Guidelines and recommended terms for expression of stable- isotope-ratio and gas-ratio measurement results. Rapid Commun Mass Spectrom 2538–2560. doi: 10.1002/rcm.5129

Cormier M-A, Werner RA, Sauer PE, et al (2018) ^{2}H-fractionations during the biosynthesis of carbohydrates and lipids imprint a metabolic signal on the $\delta^{2}H$ values of plant organic compounds. New Phytol 218:479–491. doi: 10.1111/nph.15016

Craig H, Gordon LI (1965) Deuterium and oxygen 18 variations in the ocean and the marine atmosphere. Pisa IT

Danezis GP, Tsagkaris AS, Camin F, et al (2016) Food authentication: Techniques, trends & emerging approaches. TrAC Trends Anal Chem 85:123–132. doi: 10.1016/j.trac.2016.02.026

Dansgaard W (1964) Stable isotopes in precipitation. Tellus 2826:436–468. doi: 10.3402/tellusa.v16i4.8993

DlF (2016) Schummelei bei der Herkunft Etikettenschwindel bei Erdbeeren.

Dongmann G, Nürnberg HW, Förstel H, Wagener K (1974) On the Enrichment of $H_2{}^{18}O$ in the Leaves of Transpiring Plants. Radiat Environ Biophys 11:41–52. doi: 10.1007/BF01323099

Drivelos SA, Georgiou CA (2012) Multi-element and multi-isotope-ratio analysis to determine the geographical origin of foods in the European Union. TrAC - Trends Anal Chem 40:38–51. doi: 10.1016/j.trac.2012.08.003

Epstein S, Thompson P, Ya CJ (1977) Oxygen and Hydrogen Isotopic Ratios in Plant Cellulose.

European Commission (2018) Agri-food fraud. In: Agri-food Fraud. https://ec.europa.eu/food/safety/food-fraud_en.

European Commission (2019) RASFF: The Rapid Alert System for Food and Feed 2018 Annual Report.

European Commission (2020a) Origin Labeling. https://ec.europa.eu/food/safety/labelling_nutrition/labelling_legislation/origin-labelling_en. Accessed 1 Oct 2020

European Commission (2020b) Cereals, oilseeds, protein crops and rice. In: Prot. EU farmers Agric. Sect. through policy Mark. Interv. trade Meas. Legis. Monit. Mark. https://ec.europa.eu/info/food-farming-fisheries/plants-and-plant-products/plant-products/cereals_en. Accessed 26 Sep 2020

FAO (2003) World agriculture: Towards 2015/2030. An FAO Parspective. FAO, 00100 Rome

FAO (2020) Food Outlook - Biannual Report on Global Food Markets: June 2020. Food Outlook 1–142. doi: https://doi.org/10.4060/ca9509en

Farquhar GD, Cernusak LA, Barnes B (2007) Heavy Water Fractionation during Transpiration. Plant Physiol 143:11–18. doi: 10.1104/pp.106.093278

Farquhar GD, Lloyd J (1993) Carbon and oxygen isotope effects in the

exchange of carbon dioxide between terrestrial plants and the atmosphere. Stable Isot Plant Carbon-water Relations 47–70. doi: 10.1016/B978-0-08-091801-3.50011-8

Flanagan LB, Comstock JP, Ehieringer JR (1991) Comparison of Modeled and Observed Environmental Influences on the Stable Oxygen and Hydrogen Isotope Composition of Leaf Water in Phaseolus vulgaris L . Plant Physiol 588–596.

Flanagan LB, Ehleringer JR (1991) Stable isotope composition of stem and leaf water : applications to the study of plant water use. Funct Ecol 5:270–277.

Gamarra B, Sachse D, Kahmen A (2016) Effects of leaf water evaporative ^{2}H-enrichment and biosynthetic fractionation on leaf wax *n*-alkane δ^{2}H values in C3 and C4 grasses. Plant Cell Environ 39:2390–2403. doi: 10.1111/pce.12789

Gebauer G, Preiss K, Gebauer AC (2016) Letters Partial mycoheterotrophy is more widespread among orchids than previously assumed. New Phytol 11–15.

Goitom Asfaha D, Quétel CR, Thomas F, et al (2011) Combining isotopic signatures of $n(^{87}Sr)/n(^{86}Sr)$ and light stable elements (C, N, O, S) with multi-elemental profiling for the authentication of provenance of European cereal samples. J Cereal Sci 53:170–177. doi: 10.1016/j.jcs.2010.11.004

Gonzalvez A, Armenta S, de la Guardia M (2009) Trace-element composition and stable-isotope ratio for discrimination of foods with Protected Designation of Origin. TrAC - Trends Anal Chem 28:1295–1311. doi: 10.1016/j.trac.2009.08.001

Helliker BR, Ehleringer JR (2002) Differential ^{18}O enrichment of leaf cellulose in C3 versus C4 grasses. Funct Plant Biol 29:435. doi: 10.1071/PP01122

Ho LC, Grange RI, Glasshouse AJP (1987) An analysis of the accumulation of water and dry matter in tomato fruit. 157–162.

Hoefs J (2009) Stable Isotope Geochemistry. Springer Berlin Heidelberg, Berlin, Heidelberg

Johnson R (2014) Food fraud and “Economically motivated adulteration” of food and food ingredients. Food Fraud Adulterated Ingredients Background, Issues, Fed Action 1–56.

Kahmen A, Hoffmann B, Schefuß E, et al (2013) Leaf water deuterium

enrichment shapes leaf wax *n*-alkane δD values of angiosperm plants II: Observational evidence and global implications. Geochim Cosmochim Acta 111:50–63. doi: 10.1016/j.gca.2012.09.004

Kahmen A, Sachse D, Arndt SK, et al (2011) Cellulose $\delta^{18}O$ is an index of leaf-to-air vapor pressure difference (VPD) in tropical plants. Proc Natl Acad Sci 108:1981–1986. doi: 10.1073/pnas.1018906108

Kahmen A, Simonin K, Tu KP, et al (2008) Effects of environmental parameters, leaf physiological properties and leaf water relations on leaf water $\delta^{18}O$ enrichment in different Eucalyptus species. Plant, Cell Environ 31:738–751. doi: 10.1111/j.1365-3040.2008.01784.x

Konarska A (2013) The structure of the fruit peel in two varieties of Malus domestica Borkh. (Rosaceae) before and after storage. Protoplasma. doi: 10.1007/s00709-012-0454-y

Krouse HR (1989) Sulfur Isotope Studies of the Pedosphere and Biosphere. In: Rundel PW, Ehleringer JR, Nagy KA (eds) Stable Isotopes in Ecological Research. Springer, New York, NY, pp 424–444

Leaney FW, Osmond CB, Allison GB, et al (1985) Hydrogen-isotope composition of leaf water in C3 and C4 plants: its relationship to the hydrogen-isotope composition of dry matter. 215–220.

Lehmann MM, Gamarra B, Kahmen A, et al (2017) Oxygen isotope fractionations across individual leaf carbohydrates in grass and tree species. Plant, Cell Environ 40:1658–1670. doi: 10.1111/pce.12974

Luo D, Dong H, Luo H, et al (2015) The application of stable isotope ratio analysis to determine the geographical origin of wheat. Food Chem 174:197–201. doi: 10.1016/j.foodchem.2014.11.006

Luo Y-H, Sternberg L (1992) Hydrogen and Oxygen Isotopic Fractionation During Heterotrophic Cellulose Synthesis. J Exp Bot 43:47–50. doi: 10.1093/jxb/43.1.47

Manning L (2016) Food fraud: policy and food chain. Curr Opin Food Sci 10:16–21. doi: 10.1016/j.cofs.2016.07.001

Newberry SL, Kahmen A, Dennis P, Grant A (2015) *n*-Alkane biosynthetic hydrogen isotope fractionation is not constant throughout the growing season in the riparian tree *Salix viminalis*. Geochim Cosmochim Acta 165:75–85. doi: 10.1016/j.gca.2015.05.001

Prechsl UE, Burri S, Gilgen AK, et al (2015) No shift to a deeper water uptake depth in response to summer drought of two lowland and sub-alpine C3-grasslands in Switzerland. Oecologia 177:97–111. doi:

10.1007/s00442-014-3092-6

PwC, SSAFE (2016) Food fraud vulnerability assessment.

Reuters (2017) Italian police break mafia ring exporting fake olive oil to U.S.

Roden JS, Ehleringer JR (1999a) Hydrogen and oxygen isotope ratios of tree-ring cellulose for riparian trees grown long term under hydroponycally environments. Oecologia 121:467–477.

Roden JS, Ehleringer JR (1999b) Observations of Hydrogen and Oxygen Isotopes in Leaf Water Confirm the Craig-Gordon Model under Wide-Ranging Environmental Conditions. Plant Physiol 120:1165–1173.

Roden JS, Lin G, Ehleringer JR (1999) A mechanistic model for interpretation of hydrogen and oxygen isotope ratios in tree-ring cellulose. Geochim Cosmochim Acta 64:21–35. doi: 10.1016/S0016-7037(99)00195-7

Rossmann A (2001) Determination of Stable Isotope Ratios in Food Analysis. Food Rev Int. doi: 10.1081/FRI-100104704

Rossmann A, Schmidt HL, Reniero F, et al (1996) Stable carbon isotope content in ethanol of EC data bank wines from Italy, France and Germany. Z Lebensm Unters Forsch 203:293–301. doi: 10.1007/BF01192881

Sachse D, Billault I, Bowen GJ, et al (2012) Molecular Paleohydrology: Interpreting the Hydrogen-Isotopic Composition of Lipid Biomarkers from Photosynthesizing Organisms. Annu Rev Earth Planet Sci 40:221–249. doi: 10.1146/annurev-earth-042711-105535

Santato A, Bertoldi D, Perini M, et al (2012) Using elemental profiles and stable isotopes to trace the origin of green coffee beans on the global market. J Mass Spectrom 47:1132–1140. doi: 10.1002/jms.3018

Song X, Loucos KE, Simonin KA, et al (2015) Measurements of transpiration isotopologues and leaf water to assess enrichment models in cotton. New Phytol 1:637–646.

Spink J, Moyer DC (2011) Defining the Public Health Threat of Food Fraud. J Food Sci. doi: 10.1111/j.1750-3841.2011.02417.x

SRF (2016) Grosser Eier-Betrug: Spanische statt Schweizer Wachteleier.

Sternberg L, DeNiro M (1983) Biogeochemical implications of the isotopic equilibrium fractionation factor between the oxygen atoms of acetone and water.

Sternberg L, DeNiro MJ, Savidge RA (1986) Oxygen Isotope Exchange between Metabolites and Water during Biochemical Reactions Leading to Cellulose Synthesis. Plant Physiol 82:423–427. doi:

10.1104/pp.82.2.423

Sternberg L, Ellsworth PFV (2011) Divergent Biochemical Fractionation, Not Convergent Temperature, Explains Cellulose Oxygen Isotope Enrichment across Latitudes. PLoS One 6:e28040. doi: 10.1371/journal.pone.0028040

Tähkäpää S, Maijala R, Korkeala H, Nevas M (2015) Patterns of food frauds and adulterations reported in the EU rapid alarm system for food and feed and in Finland. Food Control 47:175–184. doi: 10.1016/j.foodcont.2014.07.007

Treydte KS, Schleser GH, Helle G, et al (2006) The twentieth century was the wettest period in northern Pakistan over the past millennium. Nature 440:1179–1182. doi: 10.1038/nature04743

U.S. Department of Agriculture (2020) Country of Origin Labeling (COOL). https://www.ams.usda.gov/rules-regulations/cool. Accessed 28 Oct 2020

van Ruth SM, Huisman W, Luning PA (2017) Food fraud vulnerability and its key factors. Trends Food Sci Technol 67:70–75. doi: 10.1016/j.tifs.2017.06.017

Walker CD, Leaney FW, Dighton JC, Allison CS (1989) The influence of transpiration on the equilibration of leaf water with atmospheric water vapour. Plant, Cell Environ 221–234.

West JB, Ehleringer JR, Cerling TE (2007) Geography and vintage predicted by a novel GIS model of wine $\delta^{18}O$. J Agric Food Chem 55:7075–7083. doi: 10.1021/jf071211r

West JB, Kreuzer HW, Ehleringer JR (2010) Approaches to Plant Hydrogen and Oxygen Isoscapes Generation. In: Isoscapes: Understanding Movement, Pattern, and Process on Earth Through Isotope Mapping. pp 161–178

West JB, Sobek A, Ehleringer JR (2008) A Simplified GIS Approach to Modeling Global Leaf Water Isoscapes. PLoS One. doi: 10.1371/journal.pone.0002447

Yakir D (1989) Variation in the natural abundance of oxygen-18 enrichment in leaf water of cotton plants grown under wet and dry conditions: evidence for water compartmentation and its dynamics. Plant, Cell Environ 13:49–56.

Yakir D (1992) Variations in the natural abundance of oxygen-18 and deuterium in plant carbohydrates. Plant, Cell Environ 1005–1020.

Yakir D, Berry JA, Giles L, Osmond CB (1994) Isotopic heterogeneity of water in transpiring ieaves : identification of the component that controls the $\delta^{18}O$ of atmospheric O_2 and CO_2. Plant, Cell Environ 17:73–80.

Yakir D, DeNiro MJ (1990) Oxygen and Hydrogen Isotope Fractionation during Cellulose Metabolism in Lemna gibba L. Plant Physiol 93:325–332. doi: 10.1104/pp.93.1.325

Ziegler H (1989) Hydrogen Isotope Fractionation in Plant Tissues. In: In: Rundel P.W., Ehleringer J.R., Nagy K.A. (eds) Stable Isotopes in Ecological Research. Ecological Studies (Analysis and Synthesis). Springer, New York, pp 105–123

Acknowledgements

During these almost four years of my doctoral studies here in Basel and in Jülich, I have had the chance to meet many people that I am very thankful for. First and foremost, I would like to thank Prof. Ansgar Kahmen and Dr. Markus Boner for giving me the opportunity to do my studies as a part of this amazing project. Your tremendous support and belief in me and my work is cordially appreciated. I gratefully also thank Dr. Daniel Nelson for his analyses in the lab, help with writing, and support with data analysis and interpertation. Moreover, I would also like to take the opportunity to acknowledge Prof. Jason West for agreeing to be the external expert reviewing this thesis.

From the people I worked with here in Basel, I particularly would like to thank the following: Svenja Förster, your unbelievable support in the lab is highly appreciated. Everybody in the PPE Group and the whole botanical institute here in Basel that supported me in any way, shape or form. My long time PhD-study colleagues Maria Vorkauf and Camilo Chiang, who became a really close friends. My office friends Livio, Yating, Jochem and Patrick. Moreover, David Basel and Meisha Holloway-Phillips for the fruitful discussions about stable isotopes and spatial modelling. Georges Grun for the tremendous help running the phytotrons. Sandra Schmid for her help in the field. And last but not least, the whole team of the botanical garden here in Basel, your support and knowledge were more than I could have wished for.

From my stays in Jülich I would like to thank the whole Agroisolab team. With your warm and open "Rheinländer" heart you made me feel at home in Jülich, right from the first day. I especially would like to thank Claudia, Sabine, Lina, and Katy. Moreover, a warm thank you to my flat mates in Jülich: Dieter, Karen, Jochen, Max, and Helena.

I am of course above all very grateful for the support of my family, and my friends outside of work. I especially would like to mention my mum and dad, Beatrice and Marc, and my sisters Raphaela and Selina, who always believed in me and helped me to free my mind.

Finally, I would like to give the biggest "thank you" from the bottom of my heart to Angelika. You are the best partner that I could have ever wished for. You listened to me when I was over excited and kept on talking about stable isotopes, you cheered me up in difficult times, and you

were there during all the adventures with the “Deutsche Bahn” between Basel and Cologne.

The present work was supported by PlantHUB - European Industrial Doctorate funded by the European Commission’s Horizon 2020 research and innovation program under the Marie Skłodowska-Curie grant agreement No 722338. The program is managed by the Zurich-Basel Plant Science Center.